

For Reference

NOT TO BE TAKEN FROM THIS ROOM

For Reference

NOT TO BE TAKEN FROM THIS ROOM

Ex LIBRIS
UNIVERSITATIS
ALBERTAENSIS



Thesis
1966
#273

UNIVERSITY OF ALBERTA

PETROLOGY OF CATACLASTIC ROCKS
OF NORTHEASTERN ALBERTA

A THESIS

SUBMITTED TO THE FACULTY OF GRADUATE STUDIES
IN PARTIAL FULFILMENT OF THE REQUIREMENTS FOR THE DEGREE
OF DOCTOR OF PHILOSOPHY

DEPARTMENT OF GEOLOGY

by

ROY YOSHINOBU WATANABE, B.Sc., M.Sc.

EDMONTON, ALBERTA

November, 1965

UNIVERSITY OF ALBERTA
FACULTY OF GRADUATE STUDIES

The undersigned certify that they have read, and recommend to the Faculty of Graduate Studies for acceptance, a thesis entitled "Petrology of Cataclastic Rocks of Northeastern Alberta", submitted by Roy Yoshinobu Watanabe, B.Sc., M.Sc., in partial fulfilment of the requirements for the degree of Doctor of Philosophy.

ABSTRACT

The Precambrian Shield in northeastern Alberta shows the effects of extensive cataclastic deformation. The cataclastic rocks are distributed along three cataclastic bands that range up to one mile in width and at least 25 miles in length. Seven cataclastic rock-types have been distinguished and classified, a maximum of five occur within a single band. Quantitative data for both the parent and derived rocks are presented in a study of the genesis of this group of rocks.

Metamorphic rocks crystallized under conditions ranging from the upper amphibolite to the hornblende granulite facies during the Hudsonian Orogeny. During the cooling history, cataclastic deformation along confined movement zones gradually dominated over plastic deformation and recrystallization, consequently, cataclastic textures are preserved in these zones.

Early and late phases of paracrystalline cataclasis are recognized; during the early phase, the major cataclastic bands were developed under conditions of upper to middle greenschist facies, and in the late phase of cataclasis movement was localized within the existing cataclastic bands under conditions of the lower greenschist facies. Post-crystalline deformation under essentially non-metamorphic conditions gave rise to longitudinal and transverse faults that locally offset the major cataclastic bands and has produced typical shallow-level ruptural phenomena.

Mineralogical and chemical changes are observed across the transitional contacts from parent to derived rock. The mineralogical changes reflect the pressure-temperature conditions and hydrothermal alteration during cataclasis. Chemical changes are expressed as both systematic and irregular distributions of many components, particularly SiO_2 and K_2O ; potash metasomatism and boron metasomatism were likely effective in some of the cataclastic rocks.

A magnetic susceptibility study shows that regions of high aeromagnetic response are produced by a high magnetite content, and decreased magnetic response is

due to hematization of magnetite.

Individual cataclastic rock-types are shown to be megascopically, microscopically, and chemically homogeneous over widely separated areas. Where two cataclastic rock-types are in juxtaposition, a narrow zone of only slight mechanical mixing separates them. Therefore, careful field mapping permits the use of both parent and cataclastically derived rocks for regional lithologic correlation.

Combined field, petrographic, and chemical study has revealed the sequence of events in the metamorphic history of this part of the Precambrian Shield:

- (i) synkinematic regional granitization and intrusion,
- (ii) early paracrystalline cataclasis,
- (iii) late kinematic intrusion,
- (iv) late paracrystalline cataclasis, and
- (v) post-crystalline cataclasis.

ACKNOWLEDGEMENTS

The writer wishes to thank the staff of the Department of Geology for providing the opportunity of undertaking and completing this study. Special gratitude is expressed to Dr. R.A. Burwash who supervised the preparation and writing of this thesis, for critically reading the manuscript, and for his thoughtfulness throughout the writer's tenure at this university.

The writer is indebted to the Research Council of Alberta for financial support during the summers of 1960 and 1964 inclusive, and for permitting liberal use of their laboratory and drafting facilities. Special thanks are conveyed to Dr. J.D. Godfrey for supervision of the field and laboratory work, many fruitful discussions, advice, and critical reading of the manuscript. His encouragement and enthusiasm was instrumental in the completion of this study. Technical assistance by Max Baaske, who prepared approximately 400 thin sections, and Gary Schmidt, who chemically analysed 27 rock samples is gratefully acknowledged.

The writer is indebted to the University of Alberta for an intersession bursary. X-ray fluorescence analyses were made possible with the aid of a National Research Council Operating Grant A-1042.

Finally, I would like to declare my deepest appreciation to my wife, Nagiko, for her encouragement and the many ways that she helped me.

TABLE OF CONTENTS

	Page
ABSTRACT	i
ACKNOWLEDGEMENTS	iii
CHAPTER ONE - INTRODUCTION	
Location	1
Nature of the problem	1
Field occurrences of mylonite	3
Terminology	4
Miscellaneous terms	5
Mylonite group terms	5
Cataclasite group terms	7
Distribution of cataclastic rocks in northeastern Alberta	7
CHAPTER TWO - DISCUSSION OF MAP-UNITS	
General statement	9
Charles Lake cataclastic band	10
Hornblende cataclasite	11
Foliated hornblende granite	16
Grey hornblende granite	16
Granite gneiss	17
Hornblende granite gneiss	21
Biotite granite gneiss	23
Mylonites K and L	27
Mylonite P	34
Biotite granite F	40
Arch Lake mylonite	44

Arch Lake granite	Page 45
Raisin granite	48
Biotite "q" granite	52
Treasure Loch cataclastic band	54
Mylonite P	54
Granite F	57
Bayonet Lake cataclastic band	60
Mylonites K and L	60
Mylonite M	65
Metasedimentary mylonites	70
Mylonite N	70
Biotite schist	72
Mylonite O	73
Quartzite	75

CHAPTER THREE - MAGNETIC SUSCEPTIBILITY

General comments	78
Regional aeromagnetic study of the thesis area	78
Susceptibility study of area XI, Ashton Lake	79
Sample preparation	80
Measurement of susceptibility	80
Discussion of results	82
Susceptibility study of area III, Charles Lake	87
Discussion of results	89
Susceptibility study of area V, Charles Lake	92
Discussion of results	92
Susceptibility study of area XIV, Charles Lake	95
Discussion of Results	95

CHAPTER FOUR – DETAILED PETROLOGIC STUDIES

General statement	99
Charles Lake studies	
Area I	101
Area II	104
Area III	109
Area IV	115
Area V	118
Area VI	122
Area VII	126
Cornwall Lake studies	
Area VIII	129
Area IX	134
Treasure Loch study	
Area X	137
Ashton Lake study	
Area XI	141
Collins Lake study	
Area XII	145
Bayonet Lake studies	
Area XIII	149
Area XIV	152
Area XV	156

CHAPTER FIVE – STRUCTURE

Faults	160
Paracrystalline faults	160

	Page
Post-crystalline faults	162
Joints	163
Foliation and lineation	164
Folds	165
CHAPTER SIX – DISCUSSION AND SUMMARY	
Faulting	166
Magnetic susceptibility	167
Specific gravity	167
Mineralogical and chemical changes with cataclasis	167
Mineralogical changes	168
Chemical changes	168
Metamorphism	169
Grade of metamorphism	169
Large-Size feldspar megacrysts	170
Massive texture of hornblende cataclasite	171
Lithologic correlation	172
Geologic history	173
REFERENCES CITED	176
APPENDIX A – Tables 25 to 39	180
APPENDIX B – X-ray fluorescence analysis: technique; operating conditions; chemical analyses of calibration standards; standard deviation and precision; comparison of x-ray fluorescence and wet chemical analyses; and calibration curves	201
APPENDIX C – The lower limit of grain size in modal analysis.	217

	Page
Table 1. Cataclastic rocks and their probable parent rocks, Charles Lake area	10
Table 2. Modal and chemical analyses of hornblende cataclasite standard samples, Charles Lake cataclastic band	13
Table 3. Modal and chemical analyses of grey hornblende granite and foliated hornblende granite standard samples, Charles Lake cataclastic band	19
Table 4. Modal analyses of hornblende granite gneiss standard samples, Charles Lake area	22
Table 5. Modal analyses of biotite granite gneiss standard samples, thesis area	25
Table 6. Modal and chemical analyses of mylonites K and L stand- ard samples, Charles Lake cataclastic band	29
Table 7. Average chemical composition of ten biotite granite gneiss samples from map-areas 1 to 4	34
Table 8. Modal and chemical analyses of mylonite P standard samples, Charles Lake cataclastic band	36
Table 9. Modal and chemical analyses of biotite granite F stand- ard samples, Charles Lake cataclastic band	41
Table 10. Modal and chemical analyses of Arch Lake granite stand- ard samples, west of Charles Lake	47
Table 11. Modal and chemical analyses of raising granite standard samples, west of Charles Lake	49
Table 12. Modal and chemical analyses of a biotite "q" granite standard sample, east of Charles Lake	53
Table 13. Modal and chemical analyses of mylonite P standard samples, Treasure Loch cataclastic band	56
Table 14. Modal and chemical analyses of a granite F standard sample, Treasure Loch cataclastic band	59
Table 15. Cataclastic rocks and their probable parent rocks in the Bayonet Lake area	61
Table 16. Modal and chemical analyses of mylonite K and L standard samples, Bayonet Lake cataclastic band	63
Table 17. Modal and chemical analyses of a mylonite M standard sample, Bayonet Lake cataclastic band	68
Table 18. Modal and chemical analyses of a mylonite N standard sample, Bayonet Lake cataclastic band	72

	Page
Table 19. Modal and chemical analyses of mylonite O standard samples, Bayonet Lake cataclastic band	76
Table 20. Susceptibility data of samples from area XI, Ashton Lake	83
Table 21. Susceptibility data of samples from area III, Charles Lake	90
Table 22. Susceptibility data of samples from area V, Charles Lake	93
Table 23. Susceptibility data of samples from area XIV, Bayonet Lake	97
Table 24. Petrogenesis of the cataclastic rocks	175
Table 25. Mineralogy and chemistry of samples from area I, Charles Lake	181
Table 26. Mineralogy and chemistry of samples from area II, Charles Lake	182
Table 27. Mineralogy and chemistry of samples from area III, Charles Lake	184
Table 28. Mineralogy and chemistry of samples from area IV, Charles Lake	186
Table 29. Mineralogy and chemistry of samples from area V, Charles Lake	187
Table 30. Mineralogy and chemistry of samples from area VI, Charles Lake	188
Table 31. Mineralogy and chemistry of samples from area VII, Charles Lake	189
Table 32. Mineralogy and chemistry of samples from area VIII, Cornwall Lake	190
Table 33. Mineralogy and chemistry of samples from area IX, Cornwall Lake	191
Table 34. Mineralogy and chemistry of samples from area X, Treasure Loch	193
Table 35. Mineralogy and chemistry of samples from area XI, Ashton Lake	195
Table 36. Mineralogy and chemistry of samples from area XII, Collins Lake	196
Table 37. Mineralogy and chemistry of samples from area XIII, Bayonet Lake	198
Table 38. Mineralogy and chemistry of samples from area XIV, Bayonet Lake	199

	Page
Table 39. Mineralogy and chemistry of samples from area XV, Bayonet Lake	200
Table 40. Operating conditions for X-ray fluorescence analyses	204
Table 41. Chemical analyses used for calibration curves	205
Table 42. Standard deviation and precision for X-ray fluorescence analyses	206
Table 43. Comparison of X-ray fluorescence data with chemical analyses	207

ILLUSTRATIONS

Map 1. Aeromagnetic map of the study area	In pocket
Map 5. Bayonet Lake	In pocket
Map 9. Charles Lake, North	In pocket
Map 10. Charles Lake, Central	In pocket
Map 11. Charles Lake, South	In pocket
Plate 1. Hornblende cataclasite and grey hornblende granite (Hornblende granodiorite)	Facing page 18
Plate 2. Granite gneiss (biotite quartz monzonite gneiss and hornblende granodiorite gneiss)	Facing page 26
Plate 3. Mylonite K	Facing page 32
Plate 4. Mylonite L	Facing page 33
Plate 5. Mylonite P	Facing page 38
Plate 6. Mylonite P	Facing page 39
Plate 7. Granite F (porphyroblastic granodiorite)	Facing page 43
Plate 8. Arch Lake mylonite (cryptocataclasite) and Arch Lake granite (porphyritic quartz monzonite).	Facing page 46
Plate 9. Raisin granite (flaser granodiorite)	Facing page 50
Plate 10. Mylonite M, and mixed mylonite	Facing page 69
Plate 11. Mylonite N, and mylonite O	Facing page 71

Plate 12.	Arch Lake mylonite (cryptocataclasite) and Arch Lake granite (porphyritic quartz monzonite) . . .	Facing page 131
Figure 1.	Location of map-area	2
Figure 2.	Correction curve for different lengths of core	81
Figure 3.	Aeromagnetic anomaly and sample location map, area XI, Ashton Lake	82
Figure 4.	Aeromagnetic anomaly and sample location map, area III, Charles Lake	88
Figure 5.	Aeromagnetic anomaly and sample location map, area V, Charles Lake	94
Figure 6.	Aeromagnetic anomaly and sample location map, area XIV, Bayonet Lake	98
Figure 7.	Petrologic profiles for samples from area I, Charles Lake	102
Figure 8.	Petrologic profiles for samples from area II, Charles Lake	107
Figure 9.	Petrologic profiles for samples from area III, Charles Lake	113
Figure 10.	Petrologic profiles for samples from area IV, Charles Lake	116
Figure 11.	Petrologic profiles for samples from area V, Charles Lake	120
Figure 12.	Petrologic profiles for samples from area VI, Charles Lake	124
Figure 13.	Petrologic profiles for samples from area VII, Charles Lake	127
Figure 14.	Petrologic profiles for samples from area VIII, Cornwall Lake	132
Figure 15.	Petrologic profiles for samples from area IX, Cornwall Lake	135
Figure 16.	Petrologic profiles for samples from area X, Treasure Loch	139
Figure 17.	Petrologic profiles for samples from area XI, Ashton Lake	143
Figure 18.	Petrologic profiles for samples from area XII, Collins Lake	147
Figure 19.	Petrologic profiles for samples from area XIII, Bayonet Lake	150
Figure 20.	Petrologic profiles for samples from area XIV, Bayonet Lake	153
Figure 21.	Petrologic profiles for samples from area XV, Bayonet Lake	158
Figure 22.	X-ray fluorescence calibration curve for SiO_2	209
Figure 23.	X-ray fluorescence calibration curve for TiO_2	210

Figure 24. X-ray fluorescence calibration curve for Al_2O_3	Page 211
Figure 25. X-ray fluorescence calibration curve for Fe_2O_3	212
Figure 26. X-ray fluorescence calibration curve for MnO	213
Figure 27. X-ray fluorescence calibration curve for MgO	214
Figure 28. X-ray fluorescence calibration curve for CaO	215
Figure 29. X-ray fluorescence calibration curve for K_2O	216

CHAPTER ONE

INTRODUCTION

Location

In 1957 the Research Council of Alberta undertook a long term project to map in detail and to report on various economic and petrologic aspects of an area of the Precambrian Shield in northeastern Alberta. The map-area forms a part of the Churchill geologic province.

The map-area is outlined by the Alberta-Saskatchewan boundary, the Alberta-Northwest Territories boundary, latitude $59^{\circ}30'00''$, and longitude $110^{\circ}37'30''$ (Fig. 1). Excessive muskeg development in the southwest part of the area prohibited completion of mapping of the proposed area.

The area referred to in this thesis consists of portions of map-sheets 5, 6, 9, 10, and 11 (see Fig. 1).

Nature of the Problem

During routine mapping it became obvious that cataclastically-deformed rocks constitute a significant portion of the map-area, and required special attention which then led to the present study.

Cataclastic rocks are mentioned commonly in petrology textbooks and in research papers but they generally present a problem to the field geologist because of the difficulty of correct identification, unless transitional shear contacts can be observed between the parent and derived rocks. Cataclastic textures are readily distinguished where viewed with the petrographic microscope, but a great deal remains to be done in elucidating their petrogenesis.

Cataclastic rocks are typically aphanitic, cherty, streaky or laminated,

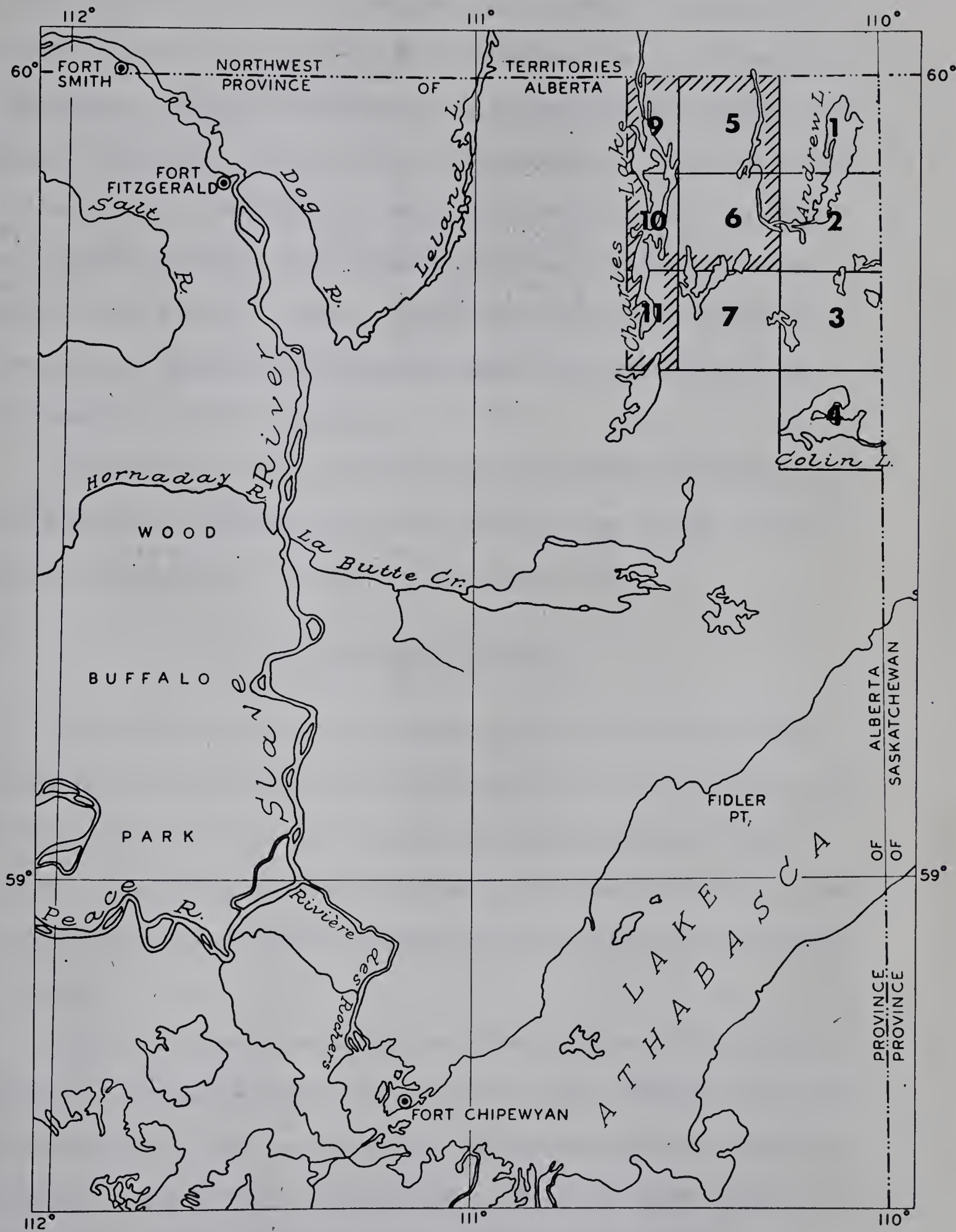
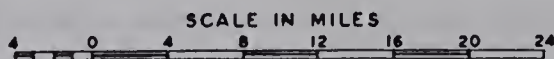


FIGURE 1
LOCATION OF MAP-AREA



and usually enclose elliptical or eye-shaped porphyroclasts* set in an aphanitic groundmass. They are a product of severe cataclasis and their character under the microscope is diagnostic in that the texture and mineralogical changes reflect a history of deformation. A wide variation of cataclastic rock types can be expected from different combinations of the environmental factors such as temperature, hydrostatic pressure, stress, chemical conditions, and the duration and sequence of these factors. Intense crushing followed by thorough recrystallization may produce apparently unsheared, granoblastic rock resembling a fine-grained quartzite or acid igneous rock.

A classification of the cataclastic rocks and quantitative data for the deformed rocks from northeastern Alberta are presented in an attempt to arrive at a better understanding of the genesis of this group of rocks.

Field Occurrences of Mylonite

Areas of intense shearing accompanying transcurrent and thrust faults are characterized by mylonite zones which commonly occur as narrow crush zones several feet thick, but may attain thicknesses of several thousands of feet. The sole of thrust faults is the most commonly observed site of cataclastic rocks, however, examples of mylonite developed along transcurrent faults are described in the literature.

The Moine thrust region of Scotland is the classic area of mylonite associated with thrust fault movements (eg. Peach and Horne, 1930; Christie, 1960; and Johnson, 1961). Other regions of thrust faulting where mylonites have been well studied include Victoria, Australia (Beavis, 1961), the Nepal Himalayas (Scott and Drever, 1953), and the French Alps (Michel-Lévy, 1928).

* Porphyroclast: a large grain surviving in an otherwise granulated or mylonitized rock (Moorhouse, 1959, p. 409).

The San Andreas fault zone in California serves as the classic region for the study of mylonite development in a transcurrent dislocation zone (eg. Waters and Campbell, 1935), and another notable occurrence is found in Tanzania, Africa (Sutton and Watson, 1959).

Terminology

In 1885 Lapworth reported on a group of crushed rocks in the Eireboll district in the Northwest Highlands of Scotland, and proposed the term mylonite (Greek mylon, a mill) for a certain type of crushed rock. Subsequent to Lapworth's work, numerous publications dealing with crushed rocks appeared in the European literature (eg. Sander, 1911; Termier and Boussac, 1911; Quensel, 1916; Shand, 1916; Raguin, 1925; and Hall and Molengraaf, 1925). Later, several papers on this subject appeared in American journals (eg. Knopf, 1931; Waters and Campbell, 1935; Bateman, 1940; and Armstrong, 1941).

Lapworth's precise petrographic definition stipulates that a mylonite must be fine-grained, show well-developed laminations or fluxion structure, and bear the characteristics of mechanical granulation with only minor evidence of recrystallization or neomineralization. Termier and Boussac (1911) in the opposite extreme employ the term mylonite in a general sense and include all material formed by crushing, regardless of their present nature. A reconciliation was reached by Quensel (1916) who recognized two main classes of mylonites: (i) those which show laminated structure were called "mylonitschiefer" (mylonite schist), and (ii) structureless crushed rocks were called "mylonite im engeren Sinn" (mylonite in the restricted sense). Various other attempts have been made to define and classify cataclastic rocks. Confusion and overlap has persisted in the terminology, definitions are ambiguous, and the varied geologic environments under which cataclastic rocks form are not clear due to inadequate communication between English-speaking and other geologists. In the last 10 years, British and

American geologists have intensified their studies on cataclastic rocks and the terminology has been unified to a considerable extent.

In this study, Lapworth's definition of mylonite is essentially retained, with prefixes added where refinement of the term is warranted. The cataclasites, (Hsu, 1955, after Grubenmann and Niggli, 1924) a group of cataclastic rocks which shows no lamination, is advocated to supplement the mylonites of Lapworth. These two groups of cataclastic rocks more or less correspond to Quensel's two-fold breakdown of laminated and unlaminated mylonites. The following summary of terms and definitions is an attempt to group the more commonly used analogous terms under a corresponding single term adopted in this study.

Miscellaneous Terms

Cataclastic rocks: refers to the broad class of rocks formed by the crushing of pre-existing rocks.

Phyllonite or phyllite-mylonite (Knopf, 1931, after Sander, 1911): is fine-grained and phyllitic in appearance, and is produced from a coarser-grained rock by granulation and shearing along existing S-planes. Lenticles are characteristic of phyllonites.

Kakirite (Quensel, 1916): is an unlaminated, megascopic breccia in which slightly displaced cataclastic rock fragments are surrounded by an ultracrushed matrix.

Pseudotachylyte (Shand, 1916): is a dark-coloured, glassy rock of vein-like or dyke-like habit, formed by fusion of finely granulated rock powder and is apparently not related to shear planes.

Mylonite Group Terms (Laminated Cataclastic Rocks)

Protomylonite (Backlund, 1918): is a moderately crushed rock which represents an early stage in the development sequence towards mylonite and cryptomylonite, where

the primary structures of the parental rock are faintly preserved. The granulated matrix constitutes between 20 and 50 per cent of the rock volume.

= Nodular mylonite (Raguin, 1925)

= Flaser rocks (Tyrrell, 1926)

Mylonite (Lapworth, 1885): is a laminated, coherent, microbreccia which shows only minor evidence of recrystallization. The stipulation of minor recrystallization is not rigidly adhered to in this thesis. The granulated matrix constitutes between 50 and 95 per cent of the rock volume (Hsu, 1955). Average matrix grain size (fine-grained phase only if matrix grain size is bimodal) is between 0.03 mm and 0.01 mm.

= Mylonitschiefer (Quensel, 1916)

Ultramylonite (Staub, 1915; Quensel, 1916): is an ultracrushed rock in which porphyroclasts are almost absent and relics of the original structure are virtually undetectable. The granulated matrix comprises more than 95 per cent of the rock volume (Hsu, 1955). Average matrix grain size (fine-grained phase only, if matrix grain size is bimodal) is between 0.03 mm and 0.01 mm.

= Purée parfaite (Termier and Boussac, 1911)

= Hartschiefer (Swedish geologists): is an ultramylonite which possesses sharply defined and parallel laminations.

Cryptomylonite (Scott and Drever, 1954): is an ultracrushed, crystalline rock in which the determination of the mineral constituents is hampered by the relative opacity of the matrix. Average matrix grain size (fine-grained phase only, if matrix grain size is bimodal) is less than 0.01 mm.

Hyalomylonite (Scott and Drever, 1954): is a dark-coloured, glassy rock which is formed by fusion of finely granulated rock powder, and, unlike pseudotachylite, is found along shear planes.

= Flinty crush rock (Clough, 1888)

= Trapshotten gneiss (King and Foote, 1864)

Mylonite gneiss (Quensel, 1916): possesses a combination of cataclastic and recrystallization characteristics. Augen structure is essential, the augen consisting of either single grains or mineral aggregates enclosed in a recrystallized matrix. Average matrix grain size is between 0.03 mm and 0.05 mm.

Blastomylonite (Sander, 1912): is a highly reconstituted rock in which only faint traces of cataclastic structure remain, and even augen are difficult to recognize due to thorough recrystallization. Some of the constituents were formed by synkinematic neomineralization, recrystallization, or both (Hsu, 1955). Average matrix grain size is greater than 0.05 mm.

Metasomatized mylonite (Hsu, 1955): is a crushed rock in which some of the constituents have formed as a result of synkinematic or post-kinematic metasomatism.

Cataclasite Group Terms (Unlaminated Cataclastic Rocks)

The following terms are derived from the mylonite group equivalents.

Protocataclasite (Hsu, 1955)

Cataclasite (Grubenmann and Niggli, 1924)

= Mylonite im engeren Sinn (Quensel, 1916)

Ultracataclasite (Hsu, 1955)

Cryptocataclasite

Blastocataclasite (Hsu, 1955)

Metasomatized cataclasite (Hsu, 1955)

Distribution of Cataclastic Rocks in Northeastern Alberta

Two composite bands of cataclastic rocks at Charles and Bayonet Lakes are of principal interest in this thesis (Map1). These bands were selected for study because of their intensity of deformation, areal extent, variety of parental and derived rock types, excellence of exposures, and the field complexities. A cataclastic band of minor extent at Treasure Loch is also treated in detail.

Other bands and masses of cataclastic rocks have been noted in the course of mapping. However, since they are not as extensive as those rocks included in the present study, and are apparently megascopically similar, they are omitted from further consideration.

CHAPTER TWO

DISCUSSION OF MAP-UNITS

General Statement

This chapter is devoted to the field relations and petrologic character of the parent rock-types and their cataclastic derivatives found in the study area. The rock-types omitted in this discussion are treated in a published report (Godfrey, in press). The petrographic classification of the plutonic rock types is based upon Moorhouse (1959, p. 154) but the alkali feldspar category is restricted to potash feldspars in order to accommodate the problem of irregular albitization of intermediate plagioclase due to retrogressive effects accompanying cataclasis. Petrographic classification of the cataclastic rocks adheres to the textural classification proposed in chapter one.

The description of each rock-type is based upon the examination of numerous outcrops, hand specimens, and thin sections. Standard reference-rock specimens were selected to represent the typical nature of each rock-type, and the number of these samples from each rock-type is proportional to the areal extent of that rock. Large-size thin sections (2 X 3 inches) of standard rock specimens are predominantly used, and the examination of small-size thin sections (1 X 2 inches) of samples scattered throughout each body of rock supplement data from the standard rock specimens. Modal analyses of standard rock specimens were made with a Leitz mechanical stage and involved 2000 to 2500 points with a spacing of 0.5 mm. Chemical analyses are available for 27 standard-rock samples.

The Charles Lake, Treasure Loch, and Bayonet Lake cataclastic bands are treated individually in a west to east sequence, and the discussion of each cataclastic rock-type is followed directly by a discussion of the probable parent rock-type. The mylonite group rock-types from each band are discussed in alphabetical

sequence (K, L, M, N, O, P). Cataclastic rocks that do not fall into this scheme are discussed either before or after the mylonite group rock-types.

Charles Lake Cataclastic Band

The Charles Lake cataclastic band comprises one main band and several parallel, smaller bands, all of which trend northerly and form a major part of map-areas 9, 10, 11, and the western margin of map-area 5. The main band trends northerly along Charles Lake, with a branch along Selwyn Lake, forming an upright Y-shape. This crush zone is striking in the field by virtue of the various types of mylonites developed, and the great longitudinal extent - mapping shows that it is continuous for at least 25.5 miles, and extends both to the north and south for undetermined distances. The maximum unbroken width of the band is about 5,000 feet.

TABLE 1. CATACLASTIC ROCKS AND THEIR PROBABLE PARENT ROCKS, CHARLES LAKE AREA

Cataclastic rock*	Probable parent rock*
Recrystallized hornblende cataclasite**	Foliated hornblende granite, grey hornblende granite, or hornblende granite gneiss.
Recrystallized mylonite K**	Biotite granite gneiss
Recrystallized mylonite L**	Biotite granite gneiss
Recrystallized mylonite M**	Hornblende granite gneiss and/ or biotite granite gneiss
Recrystallized mylonite P**	Biotite granite F***
Arch Lake mylonite	Arch Lake granite
Raison granite	Biotite "q" granite

* Field classification.

** "Recrystallized" is omitted in the text.

*** "Biotite" is omitted in the text.

Hornblende Cataclasite

The term cataclasite is applied to crushed rocks which lack a megascopic, laminar flow texture (Plate 1,b). Indistinct mineral and colour layering may be common, but smearing of the constituent minerals is not obvious in hand specimens. Localized late-kinematic mylonitization may smear the minerals to produce a mylonitized cataclasite (Plate 1,c).

Hornblende cataclasite is the unique unlaminated crush rock in the study area, limited in outcrop to map-areas 9, 10, and 11. In map-area 9, hornblende cataclasite is found as narrow bands up to 600 feet wide and 6,500 feet long on the east side of the peninsulas in the north-central region, and as a small lens in the largest island south of the northernmost peninsula. In map-area 10, hornblende cataclasite forms a band up to 1,400 feet wide and at least 4,500 feet long in the north-central area about one mile east of Arch Lake. In map-area 11, hornblende cataclasite forms sporadic, narrow bands and lenses near the east and west shoreline of Charles Lake, and a small mass near the western shoreline of Cornwall Lake.

Weathered outcrops are commonly littered with rectangular, slabby, fracture blocks (Plate 1,a), and in map-area 9, the fracture blocks form talus slopes along the east side of two peninsulas. Weathered surfaces are buff-grey to pinkish grey, whereas fresh surfaces are medium grey, and both surfaces show reticulate thin lines of bright, reddish orange iron oxide discoloration. Fracture surfaces are commonly coated with dark brown iron oxide. Abundant

spherical to elliptical, 2 to 3 mm mafic megacrysts* and minor 2 to 12 mm feldspar megacrysts are set in a saccharoidal, foliated to granoblastic felsic matrix.

The petrographic description of the general properties of the cataclasite rock-type is based upon the examination of 18 thin sections. Quantitative data for most of these 18 samples, and correlation of different bodies are treated in chapter four. Modal and chemical analyses of three standard cataclasite samples (Table 2) are used to define the general properties of the cataclasite rock-type.

Cataclasite comprises megacrysts of plagioclase, hornblende or actinolite, or both, and rare microcline, set in a matrix of plagioclase, quartz, microcline, epidote, biotite, and chlorite. Mosaic texture (Plate 1,e) is produced by interlocking, equidimensional grains and indicates thorough recrystallization under hydrostatic pressure conditions. The cataclastic character of the rock in thin section is recognized by the presence of rounded and rolled hornblende porphyroclasts. Granoblastic, relatively unstrained quartz lenticles and polycrystalline aggregates with straight grain margins are common, and probably formed when thermal effects outlasted dynamic effects. Microcline forms rare, stretched megacrysts and abundant interstitial grains in the matrix.

Hornblende, or actinolite, or both, are common constituents of cataclasites from the two peninsulas near the north end of Charles Lake in map-area 9. Rejuvenated movement along the fault zone cutting the island south of the northernmost peninsula of Charles Lake has caused extensive retrogressive alteration of amphibole to biotite, chlorite, and epidote, and the production of mylonite from cataclasite.

* Megacryst: a large grain of undetermined or mixed origin in a finer-grained matrix (Research Council of Alberta). This term embraces phenocryst, porphyroblast, and porphyroclast.

TABLE 2. MODAL AND CHEMICAL ANALYSES OF HORNBLENDE CATACLASITE
STANDARD SAMPLES, CHARLES LAKE CATACLASTIC BAND

	94	120	144	Average
Q	17.3	15.5	25.8	19.5
KFp	11.6	21.6	10.4	14.5
Pl	59.1	48.0	58.6	55.2
Hbl, Act	0.4	0.4	-	0.3
Bio	4.4	-	1.4	1.9
Chl	1.5	6.2	1.5	3.1
Mu	-	0.1	1.2	0.1
Ep	4.7	7.2	1.6	4.5
Cal	0.1	0.2	tr	0.1
Zr	tr	-	-	tr
Ap	0.5	0.2	0.2	0.3
Sph	tr	0.2	0.1	0.1
Lx	-	0.1	1	tr
Mag	0.5	0.5	0.5	0.5
Hem	-	-	tr	tr
No. of Points	2500	2500	2500	-
SiO ₂	66.95	65.74	69.16	67.28
TiO ₂	0.21	0.24	0.16	0.20
Al ₂ O ₃	17.28	17.58	16.38	17.08
Fe ₂ O ₃	2.26	2.57	1.61	2.15
MnO	0.08	0.09	0.06	0.08
MgO	1.09	1.34	0.98	1.14
CaO	3.84	3.45	2.38	3.22
Na ₂ O	5.09	5.19	4.55	4.94
K ₂ O	2.41	2.83	3.49	2.91
L.O.I.	0.69	0.91	0.53	0.71
P ₂ O ₅	0.09	0.12	0.06	0.09
Total	99.99	100.06	99.36	99.80

(Chemical analyses by G. Schmitz.)

Key for abbreviations used in this thesis

Minerals

Rocks

Q	Quartz
KFp	Potash feldspar
Pl	Plagioclase
Di	Diopside
Hbl	Hornblende
Act	Actinolite
Bio	Biotite
Chl	Chlorite
Mu	White mica
Ep	Epidote
Cal	Calcite
Ct	Cordierite
Gt	Garnet

Gr	Granite
Gr Gn	Granite gneiss
Myl	Mylonite

Chemistry

Zr	Zircon
Ap	Apatite
Al	Allanite
Sph	Sphene
Lx	Leucosene
Tl	Tourmaline
Mag*	Magnetite
Hem	Hematite
Py	Pyrite

Fe ₂ O ₃	total iron reported as Fe ₂ O ₃
L.O.I.	loss on ignition

Miscellaneous

shr	sheared
tr	trace
mm	millimetre
ppm	parts per million
No.	Number

* includes Ilmenite

Amphibole in the cataclasites of map-areas 10 and 11 are commonly pseudomorphed by biotite, chlorite, and epidote. Hornblende and actinolite megacrysts (Plate 1, e and f) are generally rounded, spherical to elliptical, and form up to 20 per cent of the rock. Actinolite is pale green, fresh, and highly poikiloblastic with numerous quartz inclusions, whereas hornblende is medium green to dark greenish brown, and partly to completely altered. Where partly altered, hornblende is also commonly pseudomorphed by a polycrystalline aggregate of biotite and chlorite surrounded by epidote (Plate 1, g). Commonly, hornblende is partly pseudomorphed by actinolite. Evidently, hornblende grains are relict porphyroclasts, whereas actinolite forms porphyroblasts* that originated during the terminal phase of cataclasis. The coexistence of hornblende, actinolite, biotite, chlorite, and epidote in the cataclasites of map-area 9 suggests the metamorphic grade as intermediate between the quartz-albite-epidote-biotite subfacies and quartz-albite-epidote-almandine subfacies of the greenschist facies (Turner and Verhoogen, 1960). The assemblage chlorite-epidote in map-area 10 indicates the quartz-albite-muscovite-chlorite subfacies of the greenschist facies; and in map-area 11, the assemblage biotite, chlorite, and epidote suggests the quartz-albite-epidote-biotite subfacies of the greenschist facies.

Modal and chemical analyses of the standard cataclasite samples (Table 2) indicate the mineralogical and chemical homogeneity of the rock-type; sample 94 is from map-area 9, sample 120 is from map-area 10, and sample 144 is from map-area 11. The absence of biotite and presence of relict islands of hornblende in sample 120 indicates that the biotite grade of metamorphism was absent, resulting in direct alteration from hornblende to chlorite. The absence of amphibole, and the smaller quantity of biotite and epidote in sample 144 may be explained by the

* Porphyroblast (=metacryst): A large crystal that has grown in a finer-grained rock during metamorphism or metasomatism (Moorhouse, 1959, p. 409).

lower metamorphic grade, and relatively lower calcium and iron content compared to standard samples 94 and 120.

Average matrix grain size of the cataclasite rock-type ranges from 0.03 mm to 0.09 mm, and leads to a petrographic classification extending from cataclasite into blastocataclasite.

Foliated Hornblende Granite

This rock-type forms a major part of the second peninsula south of the Northwest Territories boundary in map area 9 and is absent from the remainder of the thesis area. Foliated hornblende granite is homogeneous, equigranular, medium- to coarse-grained, coarsely foliated with lenticular clots of hornblende and biotite, and pink to pinkish grey on fresh and weathered surfaces. Massive phases and pegmatites are uncommon. The proximity of foliated hornblende granite to hornblende cataclasite suggests a possible genetic relationship. However, comparison of the modal and chemical analyses of foliated hornblende granite (Table 3) with analyses of hornblende cataclasite (Table 2) readily demonstrates the dissimilarity of the two rock-types, and further discussion of foliated hornblende granite becomes unnecessary in this chapter.

Grey Hornblende Granite

Grey hornblende granite is commonly associated with hornblende cataclasite in the field. The contact between these rocks is transitional wherever observed, and the field distinction is based upon matrix grain size. Samples with an aphanitic to fine-grained matrix are classified as hornblende cataclasite, whereas samples with fine- to medium-grained matrix are classified as hornblende granite. Thin section study demonstrates that the field classification is valid; average matrix grain size of samples from the cataclasite rock-type is invariably 0.1 mm or less, whereas the average matrix grain size of samples from the grey hornblende granite rock-type is greater than 0.1 mm. In map-area 9, grey hornblende granite forms

rare, small lenses along the east side of the second peninsula south from the Northwest Territories boundary, Charles Lake; a small mass in the north-central region of map-area 10; and relatively large masses along the east and west sides of Charles Lake, and along the west side of Cornwall Lake in map-area 11.

Grey hornblende granite is inequigranular, massive, light to medium grey on fresh surfaces with a common pinkish tinge due to hematization of plagioclase. Weathered surfaces are buff-grey to pink, and pitted due to differential weathering of mafic clots.

Thin section examination shows that grey hornblende granite has a fine-grained matrix ranging from 0.4 to 0.8 mm and rounded megacrysts with indented grain margins (Plate 1,h) which suggests that hornblende granite is a highly recrystallized phase of hornblende cataclasite. The matrix is composed of equant plagioclase, microcline, quartz, biotite, hornblende, and epidote, with sutured grain margins (Plate 1,h).

Comparison of the average modal and chemical analyses for grey hornblende granite (Table 3) and hornblende cataclasite (Table 2) illustrates the close similarity and probable genetic relationship of the two rock-types. Mineralogical differences are slight and insignificant. The most diagnostic features are a high alumina, lime, and soda content, and a soda to potash ratio of two to one.

Comparison of modal and chemical analyses of grey hornblende granite with Johannsen's (1932) compilation of granodiorite analyses indicates a close resemblance to Johannsen's sample 22 (pages 334,341), in the basic granodiorites (Family 2278). The modal and chemical analyses of Johannsen's sample 22, which was classified in the field as soda hornblende granite, are given in Table 3.

Granite Gneiss

Granite gneiss is the most extensive map-unit in the thesis area, and is the probable parent rock for several cataclastic rock-types, including hornblende

PLATE I

HORNBLENDE CATACLASITE AND GREY HORNBLENDE GRANITE

(HORNBLENDE GRANODIORITE)

- a. Hornblende cataclasite. Field photograph. Typical flagstone-like fracturing.
- b. Hornblende blastocataclasite. Sample I-1, hand specimen. Elliptical mafic mineral clots in a granoblastic matrix.
- c. Ultramylonite. Sample II-k, hand specimen. Rare feldspar porphyroclasts in a finely laminated, aphanitic matrix. Wide grey band in mylonitized epidote. This rock represents hornblende cataclasite that has undergone secondary mylonitization.
- d. Hornblende granodiorite. Sample III-p, hand specimen. Abundant, equant, hornblende porphyroclasts in a fine-grained, granoblastic matrix. Note the lens-shaped concentration of mafic minerals.
- e. Hornblende blastocataclasite. Standard sample 94, photomicrograph. Elliptical hornblende porphyroclast in a highly recrystallized, granoblastic matrix. Crossed nicols, x 10.
- f. Hornblende blastocataclasite. Standard sample 94, photomicrograph. Pear-shaped hornblende porphyroclast sheathed by biotite, chlorite, epidote, and magnetite. Plane light, x 10.
- g. Blastocataclasite. Standard sample 144, photomicrograph. Biotite pseudomorph, after hornblende. Note the rim of epidote. Plane light, x 25.
- h. Hornblende granodiorite. Standard sample 150, photomicrograph. Large, spherical megacryst of rod perthite with many inclusions of quartz, biotite and epidote. Note the fine- to medium-grained, granoblastic matrix. Crossed nicols, x 10.

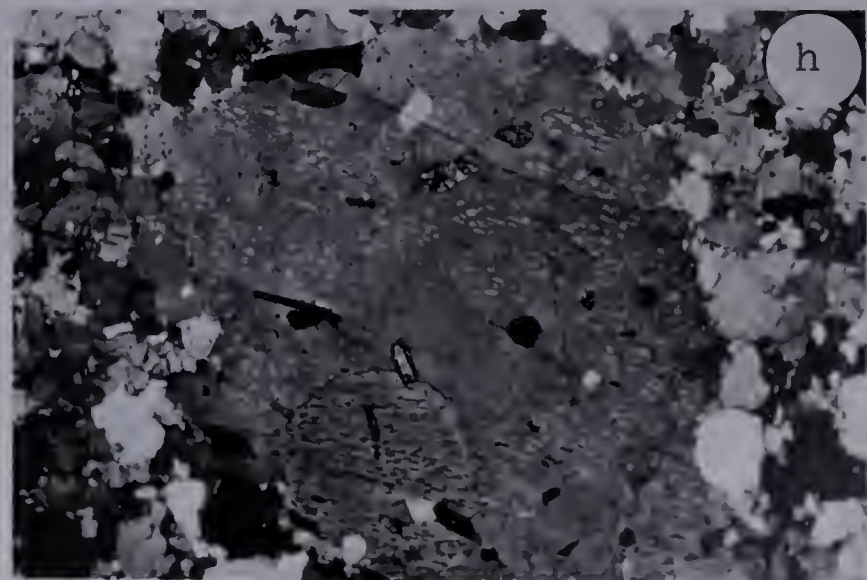
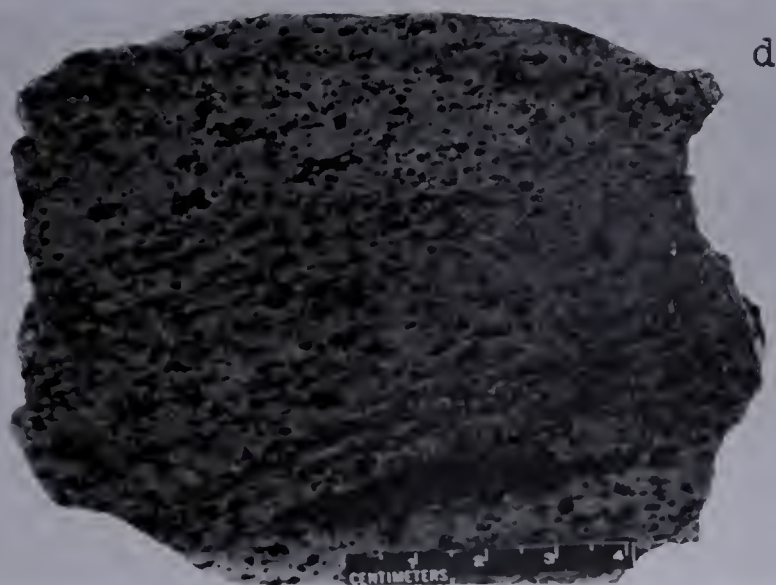
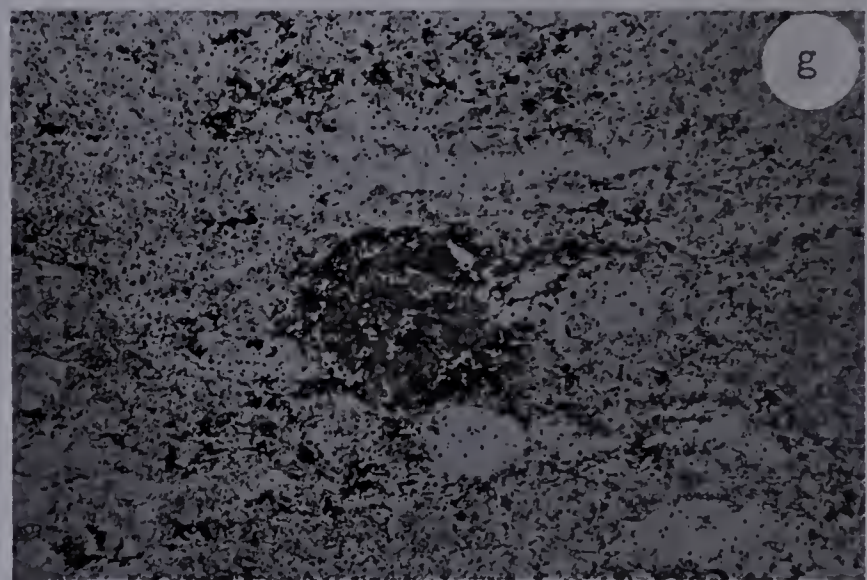
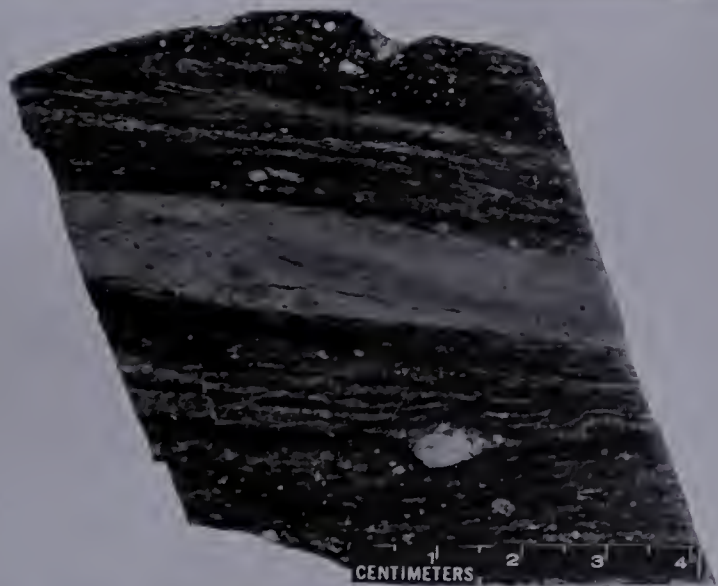
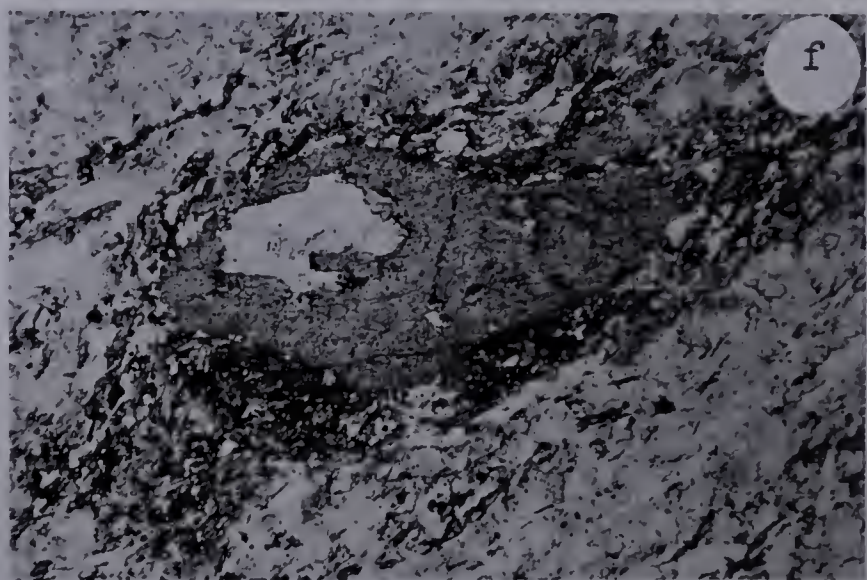
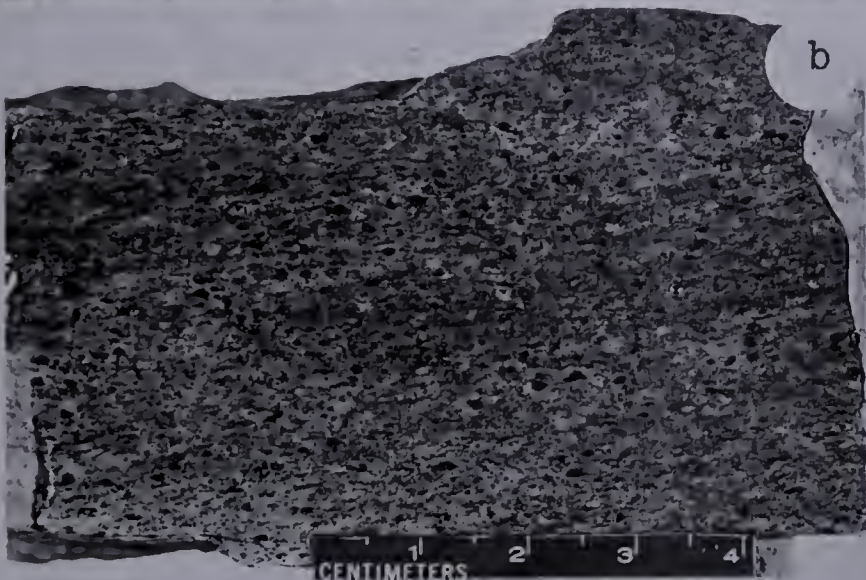
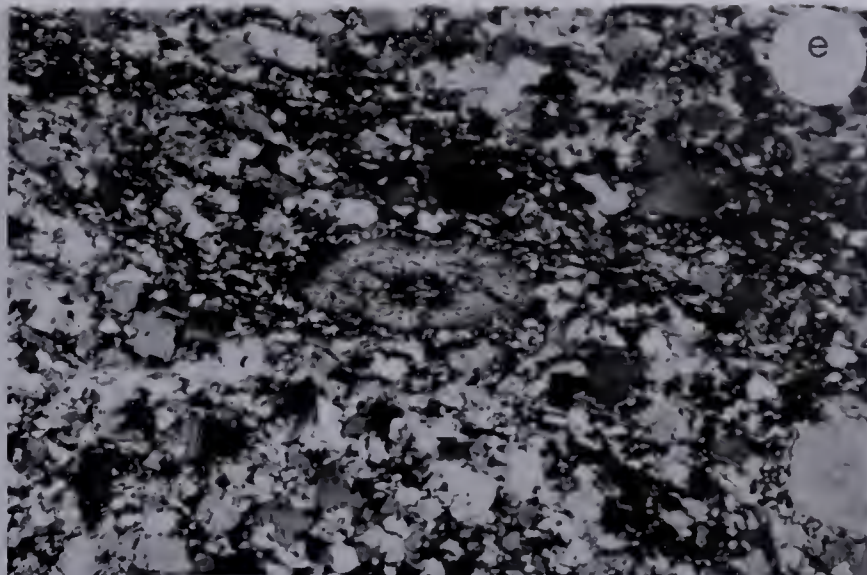


TABLE 3. MODAL AND CHEMICAL ANALYSES OF FOLIATED HORNBLENDE
GRANITE AND GREY HORNBLENDE GRANITE STANDARD SAMPLES,
CHARLES LAKE CATACLASTIC BAND

Foliated Hornblende Granite			Grey Hornblende Granite			Soda Hornblende Granite (Johannsen)*
87	89	Average	150	156	Average	
Q	22.6	42.1	32.4	13.8	24.4	19.1
KFp	44.7	37.4	41.1	22.9	18.0	20.5
Pl	14.7	7.6	11.2	54.4	54.2	54.3
Hbl	14.1	7.4	10.8	3.9	-	1.9
Bio	3.6	5.3	4.5	1.4	1.6	1.5
Chl	-	-	-	-	tr	tr
Mu	-	-	-	-	0.5	0.3
Ep	-	-	-	1.5	0.8	1.2
Zr	0.1	0.1	0.1	-	-	-
Ap	0.3	-	0.2	0.3	tr	0.2
Al	-	-	-	0.3	-	0.2
Sph	-	0.3	0.2	-	tr	tr
Mag	0.2	0.1	0.2	0.7	0.7	0.7
Hem	-	-	-	-	-	-
Py	-	-	-	-	-	-
No. of Points	2,000	2,500	-	2,500	2,500	-
SiO ₂		74.37	74.37	66.16		66.16
TiO ₂		0.26	0.26	0.23		0.23
Al ₂ O ₃		11.42	11.42	17.14		17.14
Fe ₂ O ₃		3.98	3.98	2.26		2.26
MnO		0.05	0.05	0.09		0.09
MgO		0.30	0.30	1.06		1.06
CaO		1.43	1.43	3.60		3.60
Na ₂ O		2.51	2.51	5.29		5.29
K ₂ O		4.55	4.55	2.53		2.53
L.O.I.		0.26	0.26	0.37		0.37
P ₂ O ₅		-	-	0.11		0.11
Total		99.13	99.13	98.84		98.84

(Chemical analyses by G. Schmitz).

* Johannsen, 1932, pages 334 and 341.

x Indicates the mineral is present.

cataclasite, and mylonites K, L, and M. The map representation of granite gneiss shows a breakdown into biotite granite gneiss and hornblende granite gneiss which are discussed in some detail separately. The granite gneiss terrain contains numerous lenses and bands of amphibolite and metasedimentary rocks on the outcrop and regional scale of observation. Masses and bands of massive to foliated granitic rocks, and pegmatite, are also common in granite gneiss areas. Granite gneiss is regarded as the fundamental basement complex (Godfrey, 1962) upon which later events of sedimentation, metamorphism, deformation, and intrusion have been superimposed.

The Bayonet Lake and Potts Lake map-areas consist of about 80 per cent outcrop-area of granite gneiss, whereas the three Charles Lake map-areas show a north to south decrease in granite gneiss from about 60 per cent in Charles Lake, North, 40 per cent in Charles Lake, Central, and 30 per cent in Charles Lake, South. Biotite granite gneiss is prevalent and hornblende granite gneiss is irregularly distributed throughout the thesis area, although two large masses of hornblende granite gneiss are located in the north-central region of the Bayonet Lake map-area, and east of Charles Lake to Selwyn Lake in the Charles Lake, North, map-area.

Granite gneiss is typically layered, with alternating 1/2 to 6 inches wide felsic and mafic layers that are commonly continuous for many feet, or 1/16 to 1/4 inch discontinuous folia, or both. Individual layers are fine- to medium-grained, and equigranular to porphyroblastic. The foliation is generally wavy, commonly highly contorted, and shows plastic flow effects (Plate 2, a).

The presence or absence of visible hornblende is the criterion for the field distinction between hornblende granite gneiss and biotite granite gneiss: hornblende granite gneiss contains biotite and visible hornblende, which commonly forms 5 to 10 per cent of the rock, and with increase of hornblende grades into amphibolite gneiss. Biotite granite gneiss generally contains 5 to 15 per cent biotite and lacks significant amounts of visible hornblende.

Hornblende Granite Gneiss. The discussion of hornblende granite gneiss is confined to those masses that enclose or are adjacent to grey hornblende granite and hornblende cataclasite bodies in the Charles Lake map-areas. The main masses include a large, bulbous body east of Charles Lake in the Charles Lake, North, map-area, a narrow band east of Arch Lake in the Charles Lake, Central, map-area, and a continuous mass along the east and west sides of Charles Lake in the Charles Lake, South, map-area.

Two types of hornblende granite gneiss are distinguished: (i) felsic, pink to grey gneiss with indistinct layering and wavy, discontinuous folia; and (ii) mafic gneiss with sharply-defined dark green layers alternating with felsic layers. These varieties of hornblende granite gneiss are present in about equal amounts, and are irregularly distributed.

In thin section, the rock is subequigranular, with a grain size between 0.5 and 2 mm. The foliation is defined by discontinuous, wavy mafic lenticles, and continuous, mafic-rich and mafic-poor layers; the mafic minerals consist of intergrown biotite and hornblende, rare diopside, and accessory apatite, magnetite, and sphene. Biotite tends to be oriented parallel to the foliation, and the sharp contact with hornblende indicates that hornblende and biotite are coeval. Rarely, biotite is partly altered to chlorite. Identification of the pyroxene variety is difficult due to the prevalence of relict grains, but the 90° intersection of cleavage traces on basal sections, pale green to colorless grains, $2V$ angle of about 60 degrees, positive optic sign, and extinction angle $Z_{\wedge c} = 44$ degrees indicate diopside with about 40 per cent hedenbergite solid solution (Winchell and Winchell, 1951). Diopside is altered to a fibrous mat of pale green uraltite surrounding the grains. The presence of relict diopside indicates that parts of the hornblende granite gneiss terraine must have reached the granulite facies of metamorphism prior to diaphthoresis. Potash feldspar is always xenoblastic microcline commonly rimmed with myrmekite and slightly sericitized plagioclase. Quartz forms elon-

TABLE 4. MODAL ANALYSES OF HORNBLENDE GRANITE GNEISS STANDARD
SAMPLES, CHARLES LAKE AREA

	93	119	152	Average
Q	8.6	16.4	21.3	15.4
KFp	13.7	13.2	0.1	9.0
Pl	48.7	53.4	56.0	52.7
Di	-	-	2.9	1.0
Hbl	3.2	1.9	7.8	4.3
Bio	15.5	7.7	8.5	10.6
Chl	-	3.8	2.1	2.0
Ep	4.1	1.9	0.7	2.2
Zr	0.1	-	tr	tr
Ap	1.5	0.1	0.3	0.6
Al	0.2	0.1	-	0.1
Sph	1.3	0.6	-	0.6
Mag	3.3	0.8	0.7	1.6
Hem	0.1	-	-	tr
No. of Points	2000	2000	2000	-

gated blebs, and small, rounded inclusions in microcline and plagioclase. Quartz grains in the polycrystalline blebs commonly show sutured margins, and are moderately strained, but not granulated.

Petrographic classification of hornblende granite gneiss indicates a predominance of granodiorite ranging to quartz diorite.

Comparison of the average mineralogical composition of hornblende granite gneiss (Table 4) and hornblende cataclasite (Table 2) shows a close similarity and a possible genetic connection. Though the mafic mineral content in the two rocks differs appreciably, the differences may be explained on the basis of hydrothermal alteration of the mafic minerals during cataclasis. Chemical analyses of the hornblende granite gneiss samples are not available. It is feasible that hornblende granite gneiss gives rise to hornblende cataclasite, and this aspect is investigated and elucidated in chapter four.

Biotite Granite Gneiss. Biotite granite gneiss is the predominant rock-type in the study area, and is the probable parent rock for mylonites K, L, and possibly mylonite M, which together constitute about 70 per cent of the mylonite area. The discussion of biotite granite gneiss is not restricted to those standard samples proximal to the crush zones by virtue of the widespread distribution of mylonites K and L in biotite granite gneiss.

Biotite granite gneiss is pink to red, and rarely grey on fresh and weathered surfaces. Two types of biotite granite gneiss are recognized by the character of the layering: (i) biotite granite gneiss with sharply-defined, continuous, 1/2 to 10 inch-wide mafic layers regularly alternating with fine- to medium-grained, granoblastic to foliated, felsic interlayers (Plate 2, d); and (ii) biotite granite gneiss with less distinct layering defined by mafic streaks and dispersed, oriented biotite flakes (Plate 2, c). The former variety is reminiscent of sedimentary layering which suggests that much of the granite gneiss terrain is derived from metasedimentary rocks.

In thin section, biotite granite gneiss is equigranular to prophyroblastic, well foliated, and composed of interlocking 0.3 to 2 mm grains of plagioclase, quartz, potash feldspar, biotite, chlorite, and epidote. Plagioclase is abundant, slightly sericitized or saussuritized, commonly forms anhedral to subhedral porphyroblasts 2 to 4 mm in diameter, and is rarely antiperthitic. Chessboard albite (Plate 2, h) is rare, and myrmekite is present in most samples. Microcline, or microcline perthite, or both, is abundant as elliptical to augen-shaped porphyroblasts 2 to 5 mm in diameter, which tend to be corroded and indented and enclosed by myrmekite and fine-grained plagioclase. Quartz forms polycrystalline lenticles, rounded inclusions in plagioclase and microcline porphyroblasts, and bulbous, lenticular porphyroblasts. Biotite flakes are generally dark brown, commonly chloritized along cleavage planes, and are concentrated and oriented in planes to produce the characteristic gneissic structure of the rocks. Small amounts of hornblende are present in several samples as small, dispersed grains within mafic clots, and as relict grains enclosed by chlorite. The irregular distribution of hornblende in parts of the granite gneiss terrain is regarded as a function of differences in original rock composition primarily, and to a less extent on the grade of metamorphism. One sample contains about 2 per cent hornblende and 1 per cent cordierite, a mineral association indicative of the hornblende granulite facies (Fyfe, Turner, and Verhoogen, 1958, p. 235). Accessory minerals make up to 1.5 per cent of the rock, and mainly consist of apatite, sphene and magnetite. Allanite is common in several samples as metamict, anhedral to euhedral grains with an epidote rim.

The modal analyses of 13 samples are given in Table 5. The variation in composition is relatively small for a rock which is apparently inhomogeneous in the field, and petrographic classification places biotite granite gneiss in the quartz monzonite field ranging to granodiorite. Chemical analyses are not available.

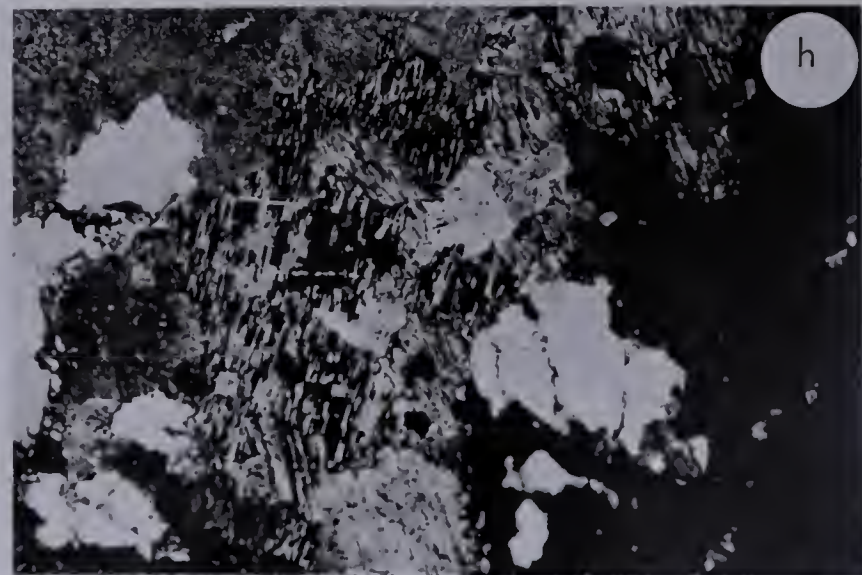
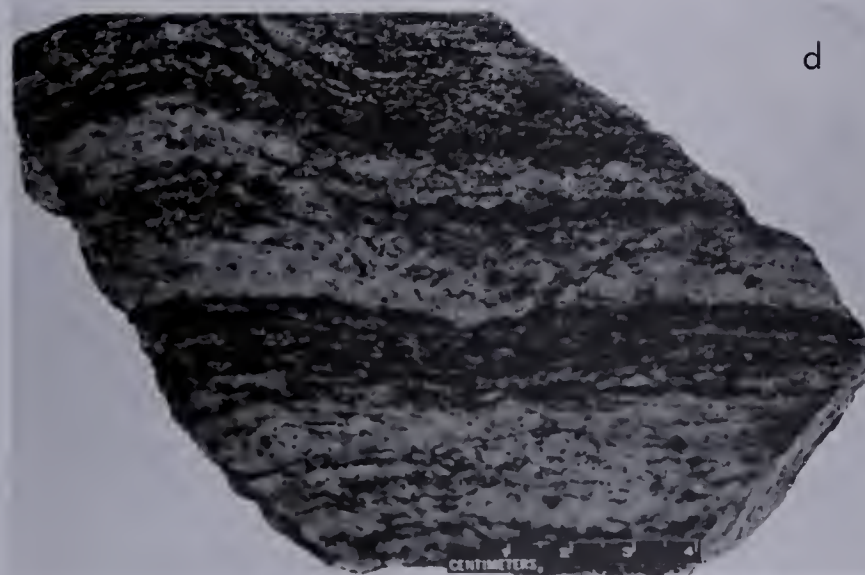
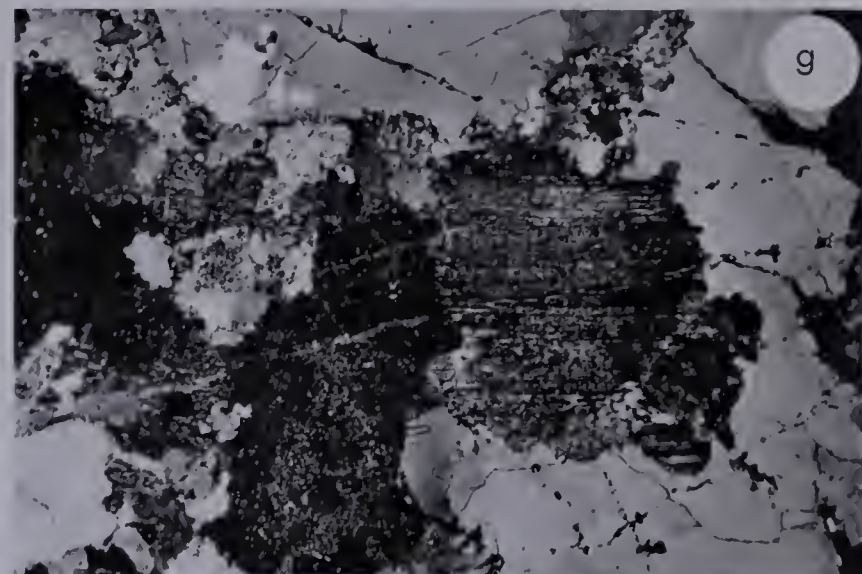
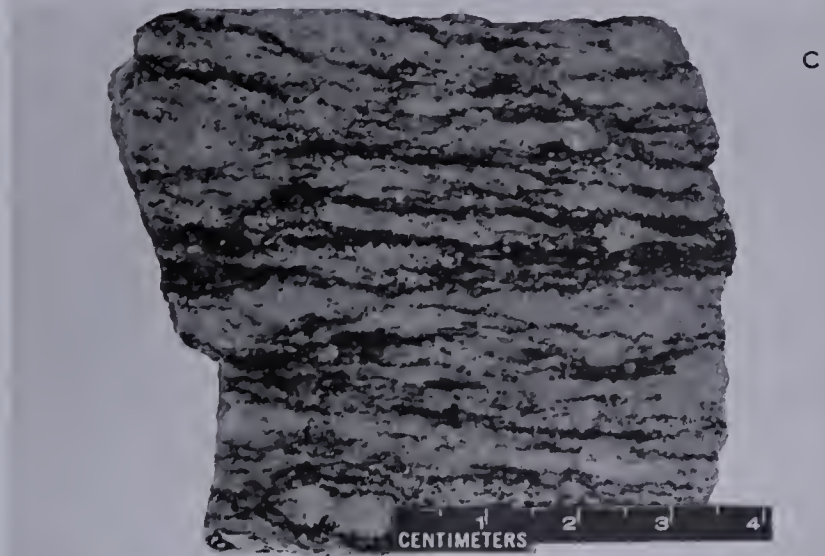
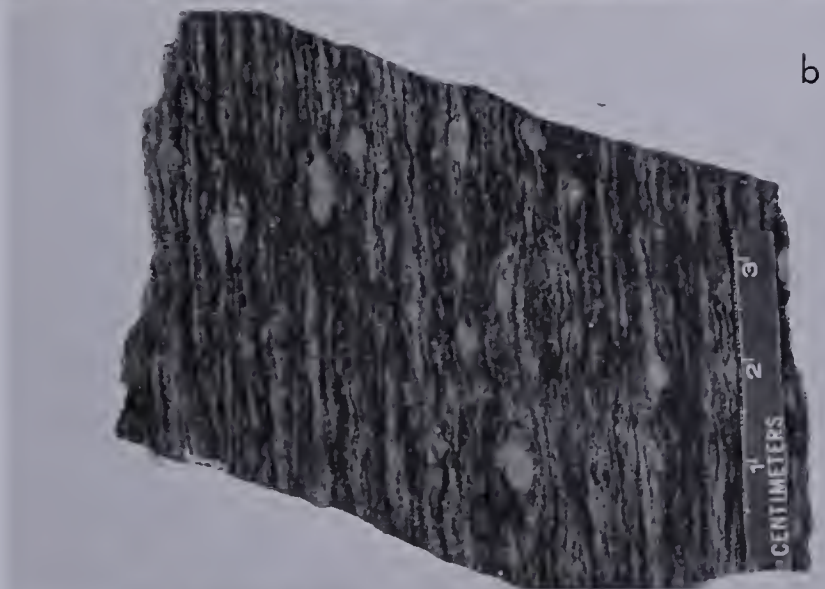
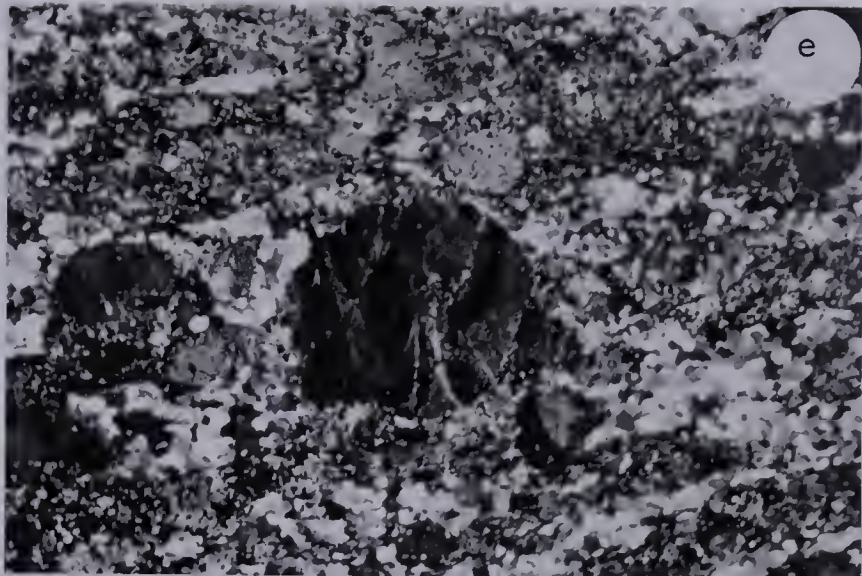
TABLE 5. MODAL ANALYSES OF BIOTITE GRANITE GNEISS STANDARD SAMPLES, THESIS AREA

	80	83	90	102	103	105	107	110	112	117	122	128	151	Average
Q	24.9	27.3	29.9	18.0	28.1	29.3	30.3	26.9	29.1	19.8	27.5	24.4	24.7	26.3
KFp	22.1	28.5	24.4	25.1	32.7	33.9	13.3	24.7	26.7	10.3	30.2	11.2	34.3	24.4
Pl	44.3	34.8	36.4	40.0	31.7	32.5	39.6	35.3	35.1	48.3	29.9	97.0	33.5	37.6
Hbl	-	-	-	-	-	-	1.8	0.7	-	-	0.6	-	0.5	0.3
Bio	5.2	6.6	5.4	13.7	4.1	0.7	13.6	10.9	7.8	13.9	5.2	13.9	2.7	8.0
Chl	2.7	1.0	0.4	-	0.4	1.7	0.1	0.4	0.3	2.4	1.3	0.2	2.7	1.1
Mu	0.1	-	0.2	-	1.2	0.8	-	-	0.1	-	0.1	0.6	-	0.2
Ep	0.6	0.7	2.7	0.1	0.3	0.1	0.3	1.3	0.3	2.2	3.1	0.9	1.1	1.1
Cal	-	-	0.1	0.1	0.2	0.3	-	tr	-	tr	0.2	-	0.1	0.1
Ct	-	-	-	-	-	-	0.8	-	-	-	-	-	-	0.1
Zr	-	0.1	tr	0.1	-	tr	-	-	-	tr	0.1	0.1	tr	tr
Ap	0.2	0.2	0.1	0.4	0.1	-	0.1	tr	0.2	1.0	0.1	0.4	0.2	0.2
Al	0.2	0.1	-	0.4	0.4	tr	-	-	-	0.1	0.1	0.1	0.3	0.1
Sph	tr	-	0.3	0.4	0.6	-	-	-	-	0.4	0.4	0.3	-	0.2
Lx	-	-	-	0.4	-	-	-	-	-	0.1	0.2	-	-	0.1
Mag	0.2	0.8	0.3	1.0	0.4	0.2	0.2	0.4	0.4	1.5	1.2	0.9	0.4	0.6
Hem	-	-	-	-	-	-	-	-	-	-	-	-	tr	tr
No. of Points	2,500	2,500	2,500	2,000	2,500	2,500	2,000	2,500	2,000	2,500	2,000	2,000	2,000	-

PLATE 2

GRANITE GNEISS (BIOTITE QUARTZ MONZONITE GNEISS
AND HORNBLENDE GRANODIORITE GNEISS)

- a. Migmatitic hornblende granodiorite gneiss. Field photograph. Felsic layers are highly contorted and boudinaged. Adjacent to mylonite P.
- b. "Pencil" biotite quartz monzonite gneiss. Sample 61-434-5, hand specimen. Fine mafic laminations are reminiscent of pencil lines. Small feldspar augen are common. Adjacent to mylonite P bands.
- c. Biotite quartz monzonite gneiss. Standard sample 90, hand specimen. Alternating, thin, mafic and felsic layers with indistinct, small, feldspar porphyroblasts.
- d. Biotite quartz monzonite gneiss. Standard sample 107, hand specimen. Alternating, coarse mafic and felsic layers.
- e. Blastomylonite. Sample XI-d, photomicrograph. A spherical, plagioclase porphyroclast with undulatory extinction, in a typical blastomylonite matrix. Mapped as mylonitic biotite granite gneiss. Crossed nicols, x 10.
- f. Blastomylonite. Sample XI-c, photomicrograph. Randomly oriented microcline fragments which were part of a large microcline megacryst. Note the deformation lamellae in the quartz grain at the top-center. Mapped as mylonitic biotite granite gneiss. Crossed nicols, x10.
- g. Hornblende granodiorite gneiss. Sample XI-g, photomicrograph. Typical texture of unsheared granite gneiss. Note the thin fracture that transects the rock subparallel to the twin lamellae of the large plagioclase grain in the center and is healed successively by new growth of the host grains. Cross nicols, x 10.
- h. Cheessboard albite in granodiorite gneiss. Sample XI-g, photomicrograph. Note the small, altered plagioclase inclusions. Crossed nicols, x10.



Mylonites K and L

Mylonites K and L are commonly interlayered and gradational and where both rocks are represented in a single outcrop, only the predominant rock-type is shown on the map. Field mapping on this basis indicates that both rock-types commonly form large masses. However, mylonites K and L are discussed together because of their intimate field association and megascopic similarity.

Mylonite K bands are found throughout the length of the Charles Lake crush zone, whereas mylonite L bands and masses are restricted to the northern one-third of this cataclastic zone. Mylonite K is predominant and commonly encloses isolated bodies of mylonite L. The maximum unbroken length of mylonite K in the Charles Lake area is 8.5 miles, from the southern tip of the peninsula in the southeast corner of map-area 9, to Selwyn Lake and the Northwest Territories boundary; the maximum thickness is about one mile, just west of the second peninsula south of the Northwest Territories boundary. The maximum length of mylonite L is about one and one-half miles, along the core of the second peninsula south of the Northwest Territories boundary, and the maximum width is about 1,500 feet, south-southwest of the northern-most peninsula of Charles Lake.

The distinction between mylonites K and L in the field is based upon the differences in size and amount of feldspar megacrysts – megacrysts in mylonite K are rarely more than 5 mm long, and form less than 5 per cent of the rock volume (Plate 3, a,b,c,d), whereas mylonite L has two generations of megacrysts, 1 to 5 mm and 10 to 15 mm long, that comprise about 5 to 8 per cent of the rock (Plate 4, a,b,c,d). Otherwise, mylonites K and L are similar: fresh surfaces are greyish red to reddish black, and weathered surfaces are generally pink, and the matrix is aphanitic, felsic, finely-laminated, with elliptical to spherical and augen-shaped feldspar megacrysts. Most specimens possess mineralogical and colour layering (Plate 4,d) which is reminiscent of the probable parent rock, biotite granite gneiss.

Mathematics 101

Mathematics 101 is a course that covers the basics of algebra, geometry, and trigonometry. It is designed for students who are new to the subject and provides a solid foundation for more advanced studies. The course includes a variety of topics, from basic arithmetic to more complex concepts like functions and trigonometric identities. Students will learn how to solve problems and apply mathematical principles in real-world situations.

Mathematics 101 is a course that covers the basics of algebra, geometry, and trigonometry. It is designed for students who are new to the subject and provides a solid foundation for more advanced studies. The course includes a variety of topics, from basic arithmetic to more complex concepts like functions and trigonometric identities. Students will learn how to solve problems and apply mathematical principles in real-world situations. The course is divided into several units, each focusing on a specific area of mathematics. The first unit covers basic arithmetic and algebra, including operations with numbers and solving linear equations. The second unit covers geometry, focusing on the properties of shapes and the calculation of area and volume. The third unit covers trigonometry, introducing the concepts of sine, cosine, and tangent. The fourth unit covers functions, including linear, quadratic, and exponential functions. The fifth unit covers probability and statistics, including the calculation of probabilities and the interpretation of data. The course is taught by a qualified teacher who will provide guidance and support throughout the learning process. Students are encouraged to participate actively in class and to work on problems independently. The course is assessed through a combination of quizzes, tests, and a final exam. Students who complete the course successfully will receive a certificate of completion.

The course is designed to be a comprehensive introduction to mathematics. It covers a wide range of topics, from basic arithmetic to more complex concepts like functions and trigonometric identities. Students will learn how to solve problems and apply mathematical principles in real-world situations. The course is divided into several units, each focusing on a specific area of mathematics. The first unit covers basic arithmetic and algebra, including operations with numbers and solving linear equations. The second unit covers geometry, focusing on the properties of shapes and the calculation of area and volume. The third unit covers trigonometry, introducing the concepts of sine, cosine, and tangent. The fourth unit covers functions, including linear, quadratic, and exponential functions. The fifth unit covers probability and statistics, including the calculation of probabilities and the interpretation of data. The course is taught by a qualified teacher who will provide guidance and support throughout the learning process. Students are encouraged to participate actively in class and to work on problems independently. The course is assessed through a combination of quizzes, tests, and a final exam. Students who complete the course successfully will receive a certificate of completion.

In thin section, mylonites K and L are composed of spherical to elliptical plagioclase megacrysts (Plate 3, e, f, h; Plate 4, g), polycrystalline "eyes" of microcline and microcline perthite, and rounded rock fragments set in a finely-laminated matrix of plagioclase, quartz, microcline, epidote, chlorite, white mica, and biotite, with an average matrix grain size ranging between 0.005 to 0.04 mm. Both mylonites are relatively deficient in mafic minerals (Table 6) with 2 to 10 per cent combined biotite, chlorite, and epidote. Plagioclase megacrysts are probably relics from the parent rock which have undergone various degrees of alteration to white mica, and thorough peripheral abrasion; grains remain intact, and no evidence of secondary growth is noted. Rare rock fragments are internally granulated, and contain rounded, and corroded microcline megacrysts. Potash feldspar megacrysts appear to have a complex history: many of the small single-crystal augen and rare spherical to elliptical megacrysts may have formed early in the metamorphic history prior to the main cataclastic event, whereas polycrystalline megacrysts chiefly seen in mylonite L, may have crystallized late in the deformational history, resulting in lenticular, polycrystalline aggregates. The largest single-crystal megacrysts in mylonites K and L are exclusively microcline. Potash diffusion from the matrix, or potash metasomatism is responsible for the prolific amounts of replacement antiperthite megacrysts. The amount of K_2O in mylonite K (Table 6) falls within the reported range of potash (Godfrey, in preparation) in biotite granite gneiss samples adjacent to the thesis area, and therefore it seems unlikely that potash metasomatism has affected mylonite K. However, mylonite L is highly enriched in K_2O compared with mylonite K, and correspondingly stretched, boudinaged microcline megacrysts are abundant in mylonite L (Plate 4, a, g) and are rare in mylonite K. Several microcline megacrysts in mylonite L show helicitic texture formed by strings of quartz, plagioclase, and biotite, which suggest that potash was introduced, producing microcline porphyroblasts in mylonite. Corroded megacryst margins and the presence of myrmekite along the periphery of the larger

TABLE 6. MODAL AND CHEMICAL ANALYSES OF MYLONITES K AND L
STANDARD SAMPLES, CHARLES LAKE CATACLASTIC BAND

	MYLONITE K							MYLONITE L
	65	71	72	95	98	149	Average	85
Q	10	21.8	15	32.0	29.1	15	20.5	15
KFp	40	1.8	20	25.8	23.3	14	20.8	15
Pl	40	69.1	45	35.3	37.9	65	48.7	50
Bio	-	-	-	2.7	-	-	0.5	2
Chl	5	3.3	-	1.0	6.1	2	3.0	0.5
Mu	0.5	0.3	15	1.0	0.6	1	2.9	17
Ep	5	3.1	4	1.7	1.7	3	3.1	tr
Cal	-	-	-	0.1	0.2	-	0.1	0.5
Zr	tr	tr	tr	tr	tr	tr	tr	tr
Ap	0.2	0.3	-	-	0.2	-	0.1	-
Al	tr	-	-	tr	0.6	-	0.1	-
Sph	-	0.3	-	-	-	-	0.1	-
Lx	-	-	-	-	-	tr	tr	-
Mag	-	0.4	-	0.6	0.7	-	0.3	tr
Hem	0.2	-	1	-	-	0.2	0.2	0.5
Py	-	-	tr	-	-	-	tr	-
No. of Points	Estimate	2,500	Estimate	2,500	2,500	Estimate	-	Estimate
SiO ₂		68.74	71.31		68.35	74.93	70.83	71.87
TiO ₂		0.24	0.12		0.42	0.16	0.24	0.31
Al ₂ O ₃		16.71	15.26		14.88	13.08	14.95	14.39
Fe ₂ O ₃		2.37	1.32		3.66	1.48	2.21	1.91
MnO		0.04	0.04		0.05	0.03	0.04	0.03
MgO		0.99	0.55		1.77	0.78	1.02	0.82
CaO		2.35	2.24		1.40	1.54	1.88	1.37
Na ₂ O		7.48	4.61		3.85	3.22	4.79	2.91
K ₂ O		0.70	3.14		4.01	3.71	2.89	5.22
L.O.I.		0.75	0.76		1.09	1.69	1.07	1.07
P ₂ O ₅		0.10	0.04		0.11	0.02	0.07	0.13
Total		100.47	99.39		99.59	100.64	99.99	100.03

(Chemical analyses by G. Schmitz)

microcline megacrysts is the result of recrystallization of the matrix. Hairlike laminations of quartz (Plate 3,e), that are commonly composed of granoblastic and relatively unstrained grains, form by post-deformational diffusion of quartz into loci of easiest growth which correspond to foliation planes. Quartz also forms within pressure shadows at the ends of megacrysts. White mica and chlorite plates are oriented within flow planes and are largely responsible for the finely laminated fabric. White mica as finely divided muscovite or sericite, is derived by shearing and hydrothermal alteration of potash feldspar and plagioclase and commonly sheathes these minerals. Chlorite is a product of hydrothermal alteration of biotite. In mylonite K, chlorite and epidote are common and biotite is rare, contrasted with mylonite L where biotite is common, chlorite is in moderate amounts, and epidote is rare. These features, plus abundant microcline megacrysts, suggest mylonite L formed (i) at higher temperature than mylonite K, and (ii) where potash was introduced.

The distinction between mylonites K and L is thus based upon:

	<u>Mylonite K</u>	<u>Mylonite L</u>
(i) megacrysts in hand specimen	1 to 5 mm diameter, less than 3 per cent of rock	1 to 5 mm, and 10 to 15 mm diameter, 5 to 8 per cent of rock
(ii) megacrysts in thin section	small, spherical to elliptical plagioclase; small, lenticular to elliptical microcline	same type of megacrysts occur with the addition of large, lenticular to elliptical microcline megacrysts.
(iii) mineralogical differences	chlorite, and epidote common, biotite rare	biotite common, chlorite less common, epidote rare
(iv) chemical differences	$\text{Na}_2\text{O}:\text{K}_2\text{O}$ approximately equals 5:3	$\text{Na}_2:\text{K}_2\text{O}$ approximately equals 3:5

It is suggested that both mylonites K and L were derived from the same rock-type, but mylonite L was situated in "hot spots" where relatively less biotite was chloritized, and where K_2O was concentrated either in the parent rock, or introduced into the crushed rock.

The effects of reactivated fault movement are noted in the western two-thirds of the largest island south of the northernmost peninsula in Charles Lake. All the rock-types on the island were affected, and secondary cataclastic rocks have been produced (Plate 6,c). Repeated cataclasis has involved

- (i) extensive granulation of the matrix producing cryptomylonite (Plate 3,g),
- (ii) introduction and subsequent smearing of epidote,
- (iii) rupture of feldspar porphyroclasts and displacement of the broken fragments (Plate 3,h), and
- (iv) the development of rare cryptomylonite veins of the same composition as the host mylonite (Plate 3,d).

The rock retained its coherence during this later phase of mylonitization, consequently cataclasis took place at considerable depth. Reactivated fault movement probably occurred at the late-kinematic stage, under conditions of high confining pressure which prohibited the formation of open fractures, and of sufficiently high temperature to allow plastic flow (Plate 4,h), and likely to cause partial fusion and intrusion of secondary cryptomylonite veins.

The last cataclastic effect seen in some mylonitic rocks is the development of open fractures and subsequent filling by comb quartz, adularia, vermicular chlorite, and euhedral epidote. These open fractures formed during the post-kinematic history of the mylonites after the rocks had been uplifted to a high level in the earth's crust.

Thin section study establishes mylonites K and L as predominantly cryptomylonite to mylonite, and rarely mylonite gneiss.

Chemical analyses of biotite granite gneiss samples in the study area are unavailable, but the average chemical analysis of 10 biotite granite gneiss samples from the adjoining map-areas is given in Table 7. Comparison of the average chemical compositions of mylonites K and L (Table 6) with biotite granite gneiss indicates a close similarity, with appreciable differences in only Na_2O and K_2O which may

PLATE 3

MYLONITE K

- a. Cryptomylonite. Standard sample 72, hand specimen. Leucocratic, aphanitic matrix with an indistinct, single agglomeroporphyroclast in the lower left. Note the small-scale fold near the top.
- b. Mylonite. Sample 63-579-8, hand specimen. Leucocratic, finely laminated matrix, with broken feldspar porphyroclasts. Post-kinematic shears cut the rock into slightly displaced segments.
- c. Secondary cryptomylonite. Sample II-d, hand specimen. Megascopic breccia fragments of primary mylonite enclosed by secondary cryptomylonite.
- d. Cryptomylonite in mylonite. Sample II-e, hand specimen. Cryptomylonite veins form an inverted V-shape in mylonite.
- e. Cryptomylonite. Standard sample 72, photomicrograph. Typical laminated, highly crushed matrix, with many uncrushed, angular fragments. Note the three small microcline augen (dark patches). Crossed nicols, x10.
- f. Mylonite. Standard sample 95, photomicrograph. Typical laminated, highly crushed matrix, with many elliptical feldspar megacrysts. Note the large, rotated heterogeneous megacrysts; the upper one-half is microcline, and the lower one-half is highly sericitized plagioclase. Plane light, x10.
- g. Secondary cryptomylonite. Sample II-f, photomicrograph. Highly fragmented, microcline porphyroclast, in a pulverized, poorly laminated matrix. Crossed nicols, x10.
- h. Mylonite gneiss. Sample XIV-c, photomicrograph. A microcline megacryst broken into three slightly displaced segments. The interstices are partly filled by mylonitic matrix. Crossed nicols, x 10.

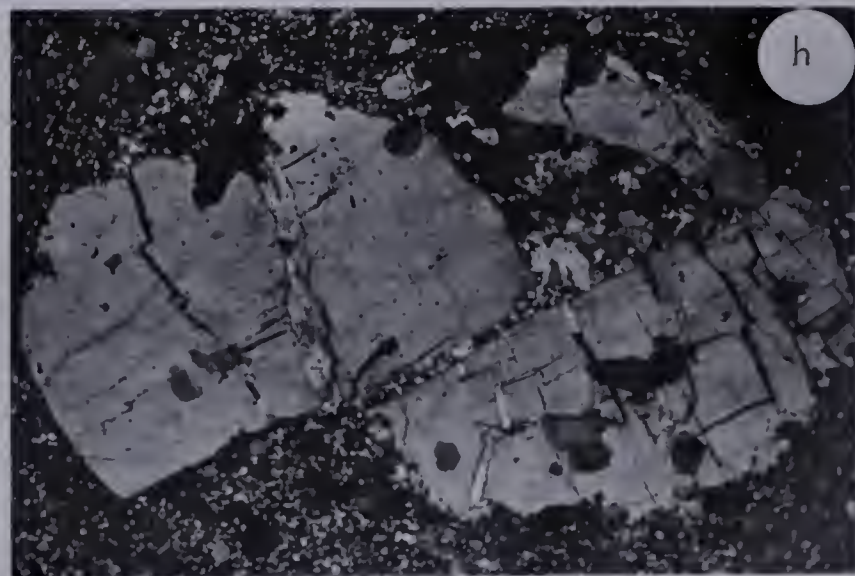
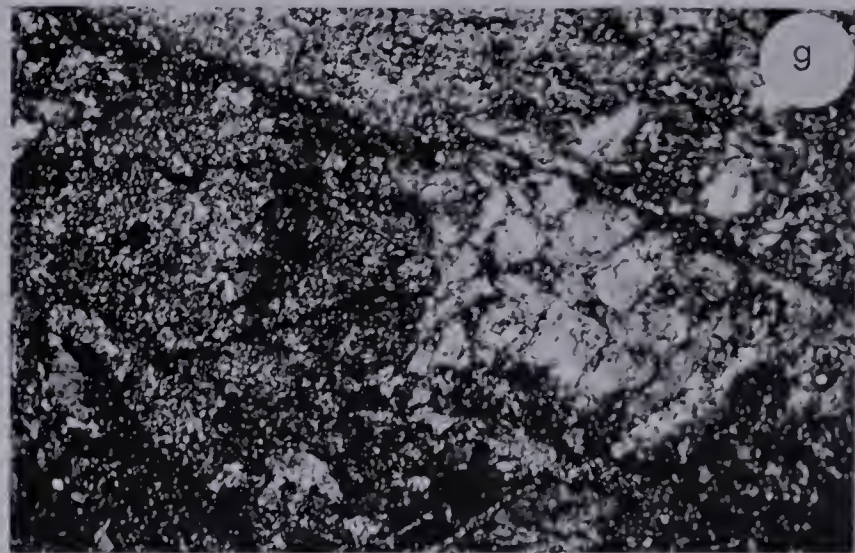
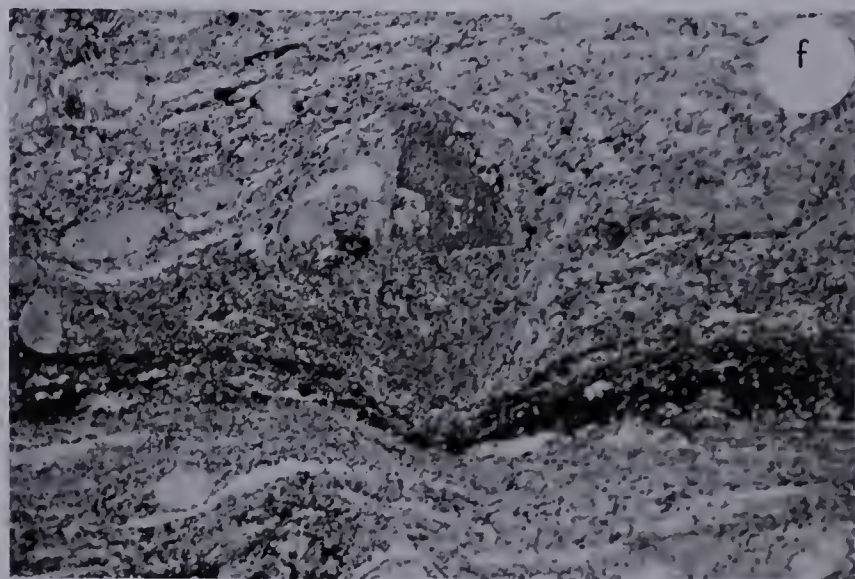
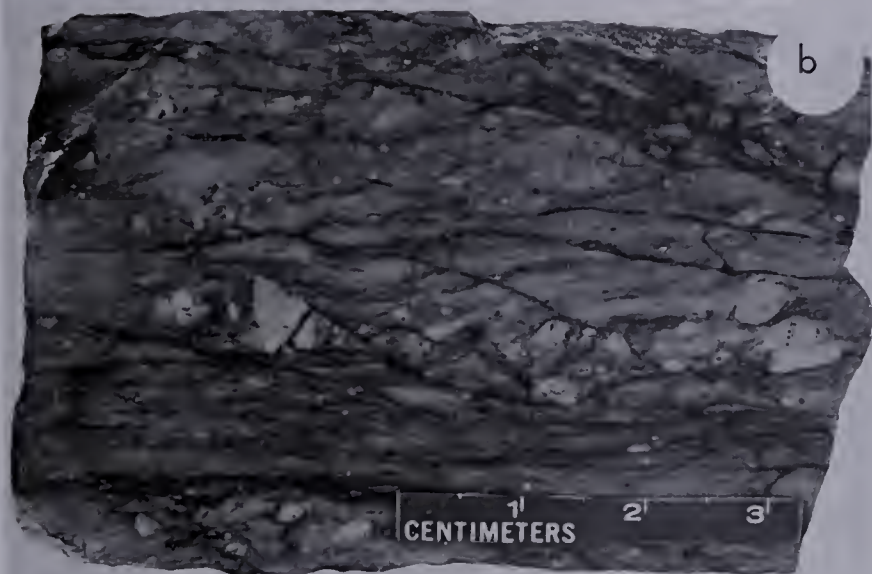
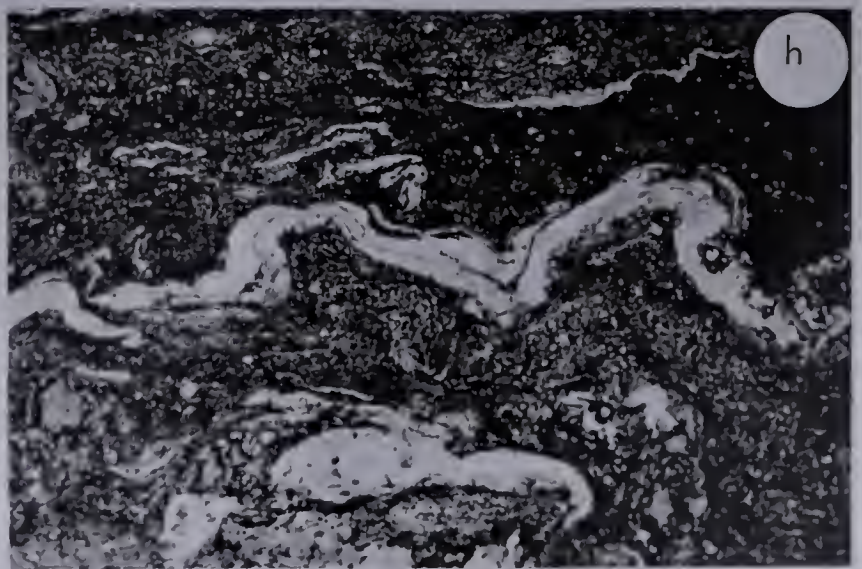
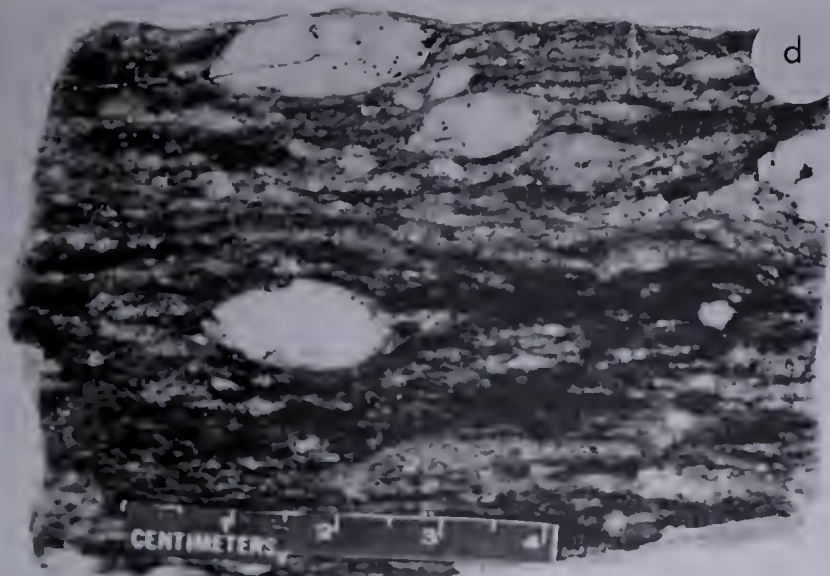
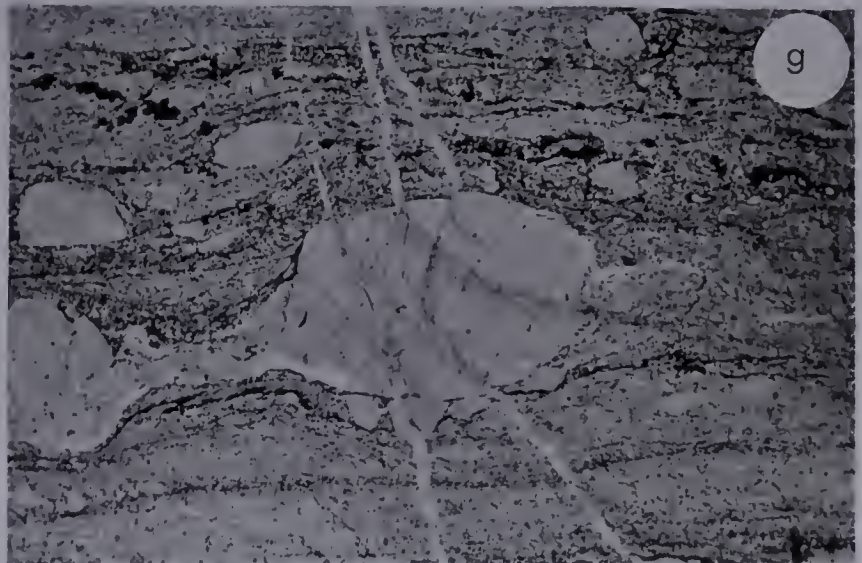
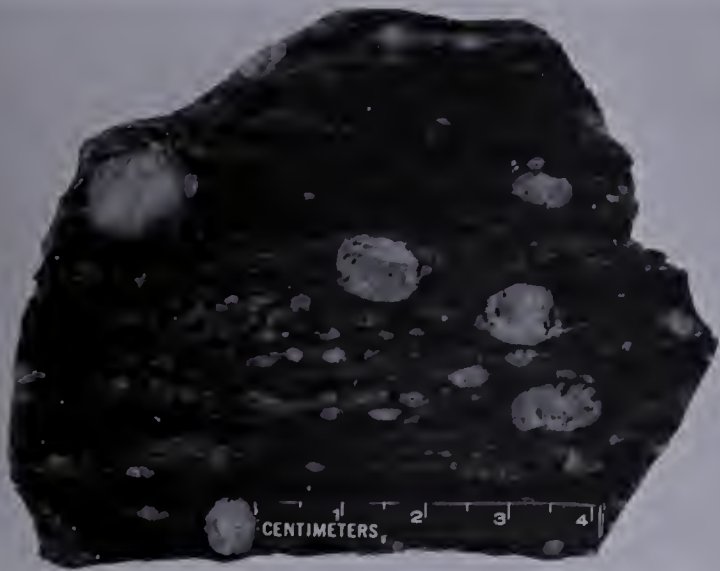
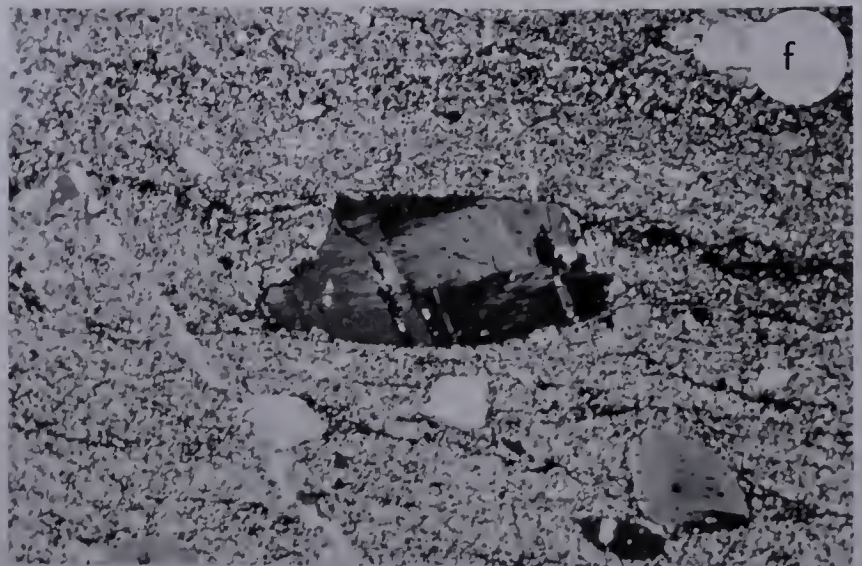
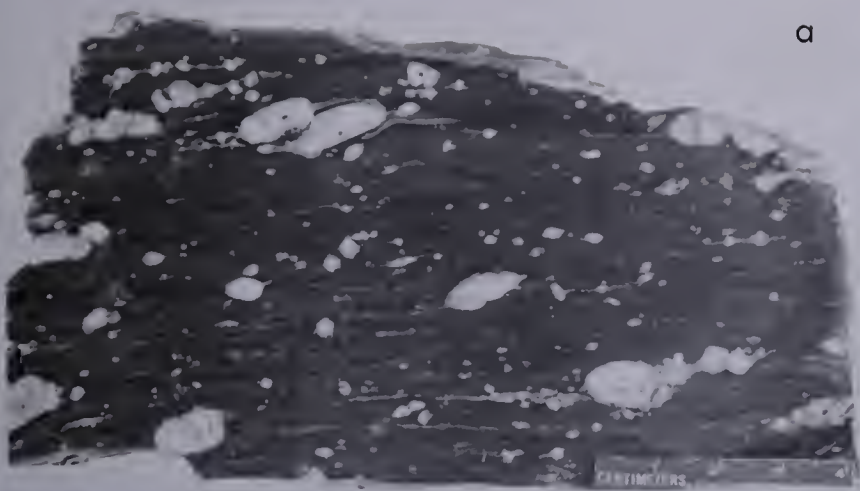


PLATE 4

MYLONITE L

- a. Mylonite. Standard sample 85, hand specimen. Numerous elliptical feldspar megacrysts in an aphanitic, finely laminated matrix.
- b. Mylonite. Sample 11-m, hand specimen. Elliptical feldspar megacrysts in a fine-grained, laminated matrix. Note the small-scale fold in the center.
- c. Mylonite. Sample 61-464-9, hand specimen. Spherical to elliptical megacrysts in a fine-grained matrix showing flow structure. Note the Carlsbad twinning in the center megacryst, with the plane (010) subparallel to the foliation.
- d. Mylonite gneiss. Sample 61-464-7, hand specimen. Feldspar augen in a moderately crushed matrix retaining relict gneissic layering. Note the Carlsbad twinning in the uppermost megacryst, with the twin plane (010) subparallel to the foliation.
- e. Cryptomylonite. Standard sample 78, photomicrograph. Microcline megacryst in the upper half, in a highly crushed matrix. Plagioclase along the periphery of the megacryst shows highly deformed twin lamellae. A vein of unstrained quartz grains cuts the matrix and megacryst. Plane light, $\times 10$.
- f. Cryptomylonite. Standard sample 78, photomicrograph. Microcline porphyroclast with corroded ends, in a highly crushed, laminated matrix. Crossed nicols, $\times 10$.
- g. Cryptomylonite. Standard sample 78, photomicrograph. A microcline porphyroclast is distended and forms two elliptical porphyroclasts joined by a trail of microcline. Fractures in the matrix are filled with quartz, but the same fractures are healed by potash feldspar where they cut the largest microcline porphyroclast. Plane light, $\times 10$.
- h. Mylonite. Sample 11-g, photomicrograph. Microfolds of microcrystalline quartz layers, in a highly crushed, finely laminated matrix. Crossed nicols, $\times 10$.



reflect their high mobility in metamorphic rocks.

Chemical data indicate that mylonites K and L may be derived from biotite granite gneiss, and examination of this probable genetic relationship is made in chapter four.

TABLE 7. AVERAGE CHEMICAL COMPOSITION OF TEN BIOTITE GRANITE GNEISS STANDARD SAMPLES FROM MAP-AREAS 1 TO 4

SiO ₂	70.83
TiO ₂	0.32
Al ₂ O ₃	14.50
Fe ₂ O ₃	3.02
MnO	0.05
MgO	0.87
CaO	1.44
Na ₂ O	3.45
K ₂ O	4.90
L.O.I.	0.54
P ₂ O ₅	0.09
Total	100.01

(Chemical analyses by H.A. Wagenbauer).

Mylonite P

Mylonite P is the major rock-type of the Charles Lake crush zone and is the principal cataclastic rock in map-areas 10 and 11. The main band of mylonite P extends continuously for 16 miles along the east side of Charles Lake to Alexander Lake, and continues beyond the southern margin of the map-area. The maximum

width of the main mylonite P band is about 4,000 feet, located north of Ellis Lake. Smaller, parallel bands up to 4 miles long and 1,600 feet wide are located west of the main band.

Mylonite P is distinctive and uniform in the field, and typically contains megacrysts with bimodal size distribution in an aphanitic to fine-grained, greyish black to greenish black matrix. The larger-size megacrysts are augen and subhedra up to 100 mm long (Plate 5) and oriented within the foliation, whereas the smaller-size megacrysts are spherical to elliptical and rarely truncate the foliation. The larger megacrysts contain numerous biotite and plagioclase inclusions, and some megacrysts show zonal arrangement of both biotite (Plate 5,f) and plagioclase. The groundmass is rich in biotite or chlorite, or both, and is well-laminated. Matrix grain size ranges from aphanitic to fine-grained, and with increasing grain size, notably biotite, quartz and feldspar, grades into granite F (Plate 5, e).

Under the microscope, mylonite P exhibits mortar texture (Plate 6, c, e), with rounded, rotated, and strained microcline and plagioclase megacrysts and rock fragments (Plate 6, a, b) which form 20 to 30 per cent of the rock volume. The matrix is finely laminated, and consists of plagioclase, quartz, biotite, microcline, muscovite, and chlorite. Six modal analyses (Table 8) of standard samples give approximate mean values of 43 per cent plagioclase, 24 per cent quartz, 12 per cent biotite, 11 per cent microcline and microcline perthite, 5 per cent white mica, 4 per cent chlorite, and 1 per cent epidote. Average matrix grain size ranges from about 0.01 mm to about 0.03 mm. Microcline forms megacrysts of two generations, the larger tend to be subhedral with rare, marginal myrmekite, and the smaller tend to be elliptical- to augen-shape. Many microcline megacrysts show simple twinning on the Carlsbad law, with the 010 twin plane parallel to the foliation plane. Plagioclase and rock porphyroclasts are rounded, augen - to spherical - or elliptical-shape and range from 0.5 to 5 mm, whereas quartz forms irregular to

TABLE 8. MODAL AND CHEMICAL ANALYSES OF MYLONITE P STANDARD
SAMPLES, CHARLES LAKE CATACLASTIC BAND

	99	130	132	133	145	153	Average
Q	23.9	25	17.3	27.9	25	22.9	23.7
KFp	7.0	5	11.1	13.3	20	8.6	10.8
PL	52.3	40	38.0	40.3	40	46.6	42.9
Bio	0.2	20	30.5	13.0	tr	6.5	11.2
Chl	9.7	3	0.9	0.3	5	6.9	4.3
Mu	6.0	1	1.0	40	10	7.5	4.9
Ep	0.4	3	0.8	0.5	tr	0.4	0.9
Cal	0.1	-	0.1	0.4	0.2	tr	0.1
Zr	0.1	tr	0.2	tr	tr	tr	0.1
Ap	0.1	-	0.4	0.1	-	0.2	0.1
Al	-	tr	-	-	-	-	tr
Sph	-	-	-	0.1	-	0.8	0.2
Lx	0.6	-	-	-	-	0.2	0.1
Mag	tr	-	0.1	0.3	tr	0.1	0.1
Hem	tr	0.1	-	-	tr	-	tr
No. of Points	2500	Estimate	2500	2500	Estimate	2500	-
SiO ₂	67.74				71.50		69.62
TiO ₂	0.51			0.44	6.28		0.41
Al ₂ O ₃	15.68				13.27		14.48
Fe ₂ O ₃	3.59			3.35	2.43		3.12
MnO	0.07			0.05	0.07		0.06
MgO	1.97				1.66		1.82
CaO	2.07				1.40		1.74
Na ₂ O	3.47			3.01	2.11		2.85
K ₂ O	3.25			3.82	4.88		3.98
L.O.I.	1.61			0.78	1.50		1.30
P ₂ O ₅	0.20			0.16	0.05		0.14
Total	100.11			-	99.15		99.52

(Chemical analyses by G. Schmitz)

bulbous porphyroblasts. Plagioclase porphyroclasts exhibit bent twin lamellae, and commonly are highly sericitized. The presence of medium-grained, granitic, inequigranular rock fragments attests to the character of the parent rock. Replacement antiperthite porphyroclasts and discordant microcline veinlets are effects of potash metasomatism or mobilization of potash initially present in the rock.

Deformation must have continued into the late growth history of the large microcline porphyroblasts as indicated by their abraded and stretched character, and some broken, displaced fragments. Quartz is metamorphically differentiated into single crystal porphyroblasts and monomineralic lenticles which probably formed during the late thermal history of the rocks after shearing had terminated. Sericite slip surfaces around plagioclase porphyroclasts (Plate 6,e) give indirect evidence of cataclasis.

The textural classification establishes mylonite P as a true mylonite, though sample 133 contains abundant rock-fragment augen, and may be classified as flaser gneiss (Tyrell, 1926).

Thin section evidence of late-kinematic deformation is seen in standard sample 153 which shows synchronous folding of a quartz band and plagioclase porphyroclast (Plate 6,f) and has a narrow vein of cryptomylonite with angular microbreccia fragments. Post-kinematic fractures in mylonite P are filled with epidote, chlorite, quartz and calcite.

Inclusions of granite gneiss, metasedimentary rocks, and amphibolite are uncommon in mylonite P and never exceed outcrop dimensions. Concordant pegmatite and aplite layers one half inch to 2 feet thick are rare, and tend to be near the margins of mylonite P masses.

The contact between mylonite P and granite F is completely gradational with the transition taking place over a distance of approximately 200 feet.

PLATE 5

MYLONITE P

- a. Mylonite. Field photograph. Numerous large, irregularly distributed, microcline megacrysts with all gradations in shape from anhedral to euhedral. Note the thin, feldspathic stringers in the matrix, and the feldspar "tails" extending from the ends of many porphyroblasts.
- b. Mylonite. Sample 63-563-1, hand specimen. Weathered surface, showing a large, subhedral microcline porphyroblast in a finely laminated matrix.
- c. Mylonite. Sample 63-563-4, hand specimen. Weathered surface, showing large microcline porphyroblast with displacement along a fracture, and a "tail" extending from the end of the crystal. Note the generation of smaller feldspar megacrysts in the laminated matrix.
- d. Mylonite. Sample 63-579-8, hand specimen. Part of a large, highly fragmented microcline porphyroblast. Note the straight mineralogical banding in the matrix.
- e. Flaser gneiss. Standard sample 133, hand specimen. Abundant elliptical to augen-shaped feldspar megacrysts and rock fragments in a well laminated, highly recrystallized matrix.
- f. Mylonite. Sample 63-86-7, hand specimen. Euhedral, poikiloblastic microcline with zonal arrangement of biotite inclusions.
- g. Mylonite. Sample 63-86-16, hand specimen. Rounded microcline megacrysts with numerous biotite inclusions. Feldspathic streaks are bulged by late growth of a porphyroblast.
- h. Mylonite. Sample 63-578-15, hand specimen. Rotated microcline porphyroblast with a minimum of 150 degrees rotation is indicated.

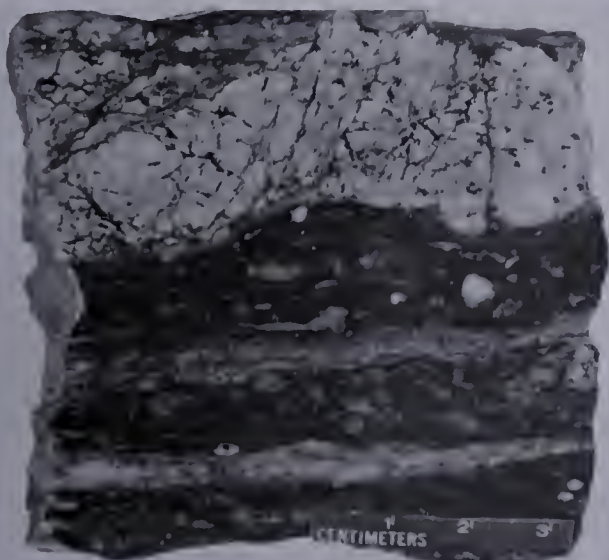
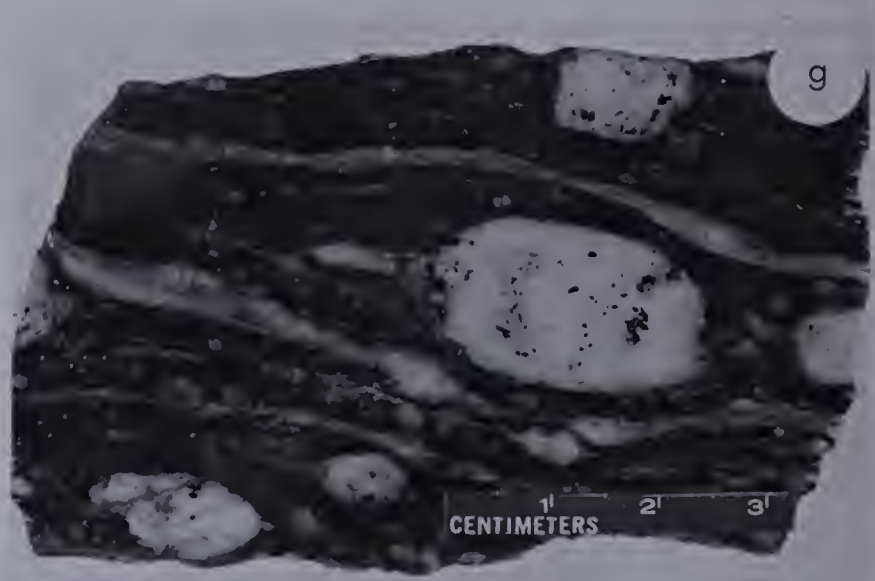
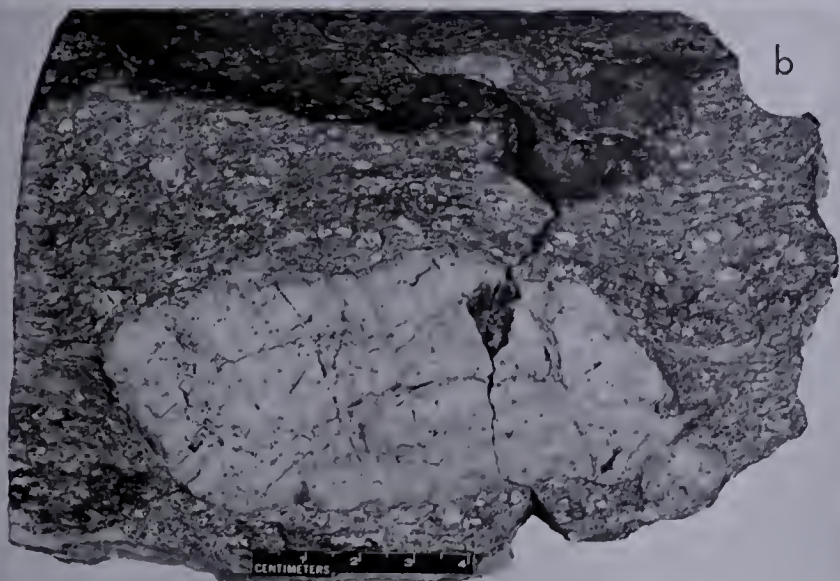
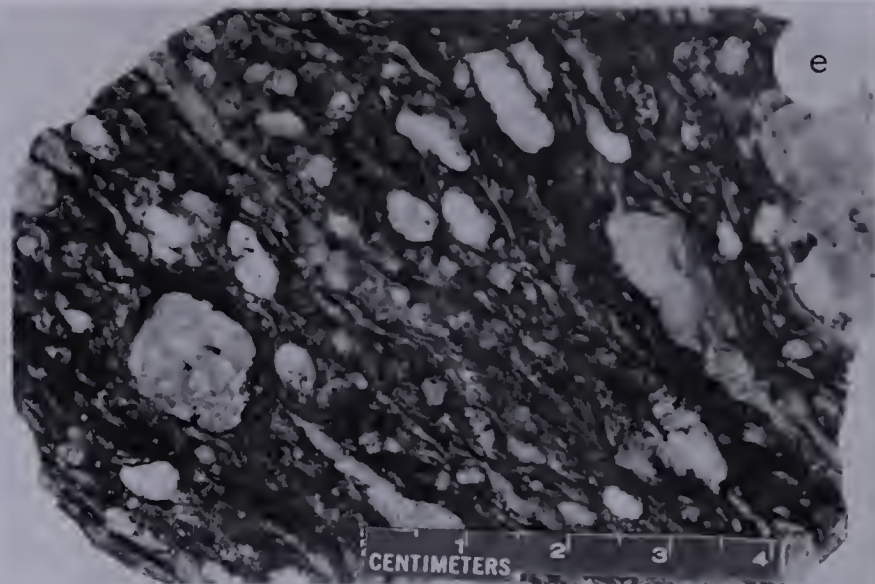
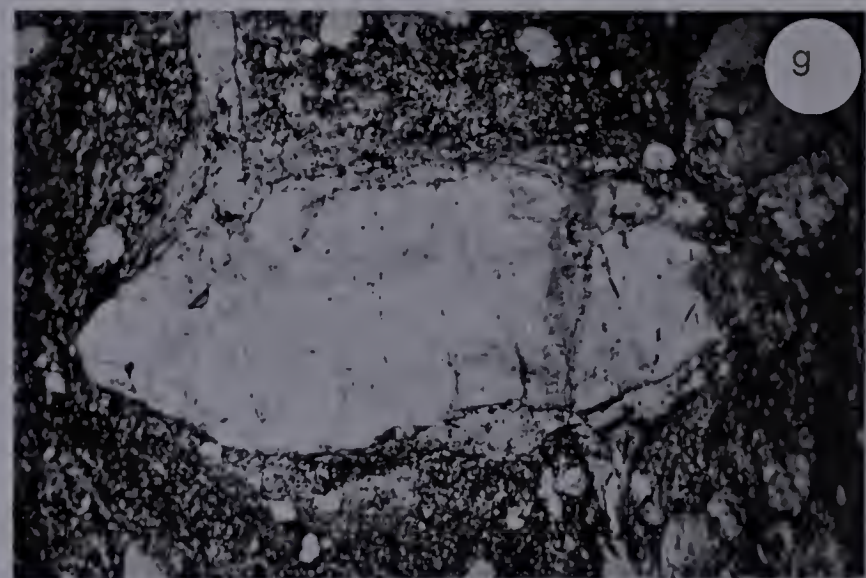
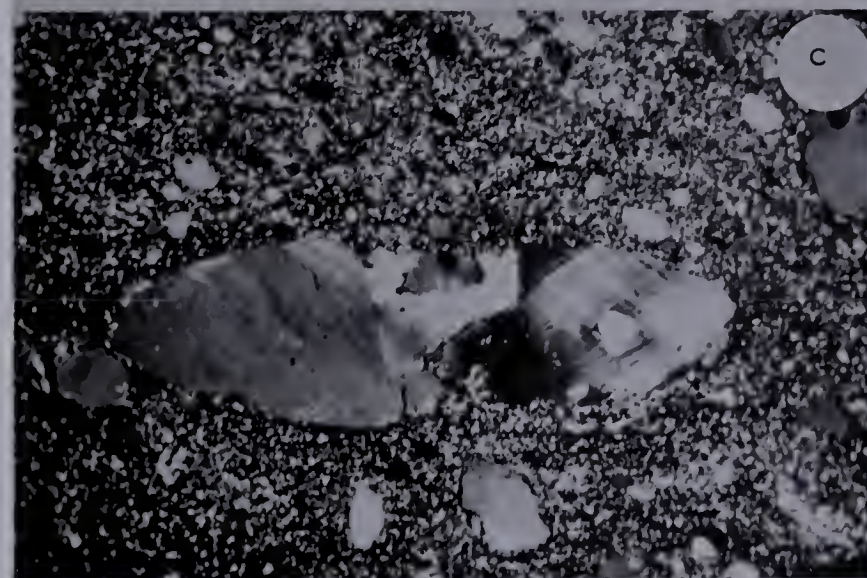
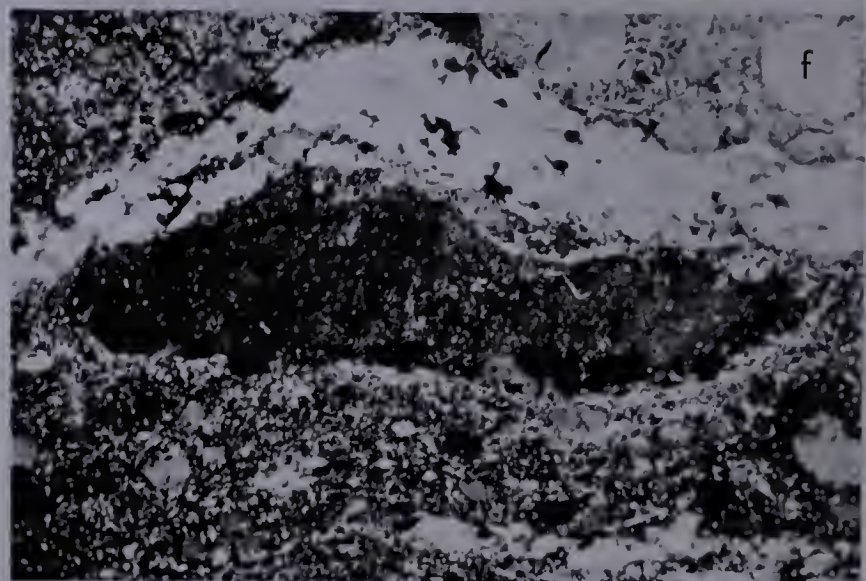
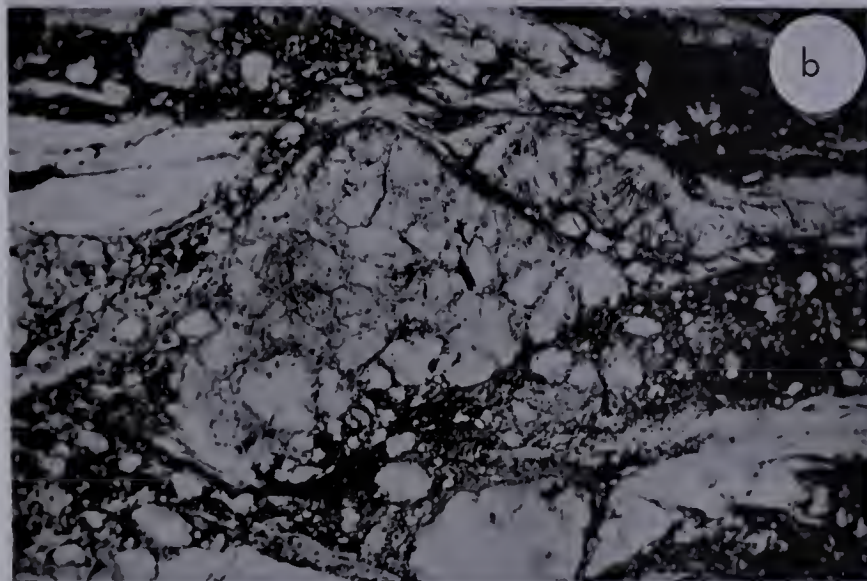
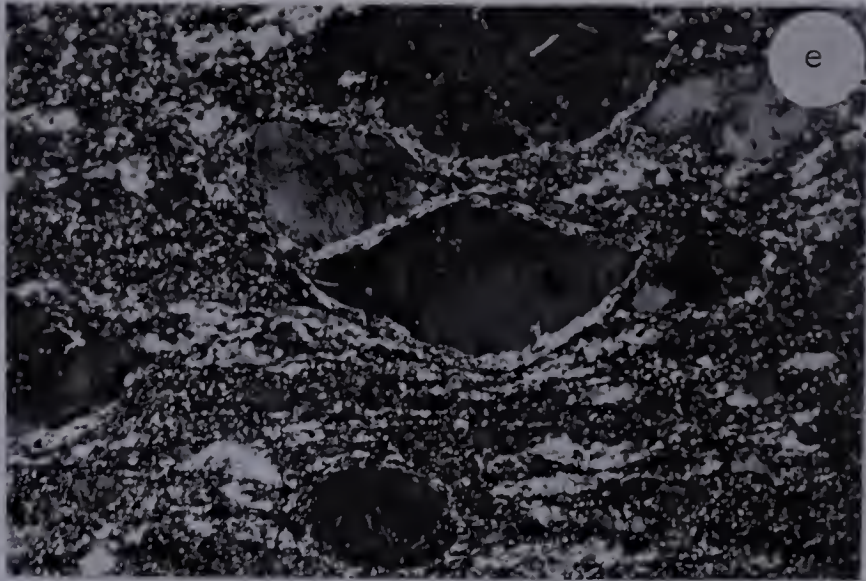
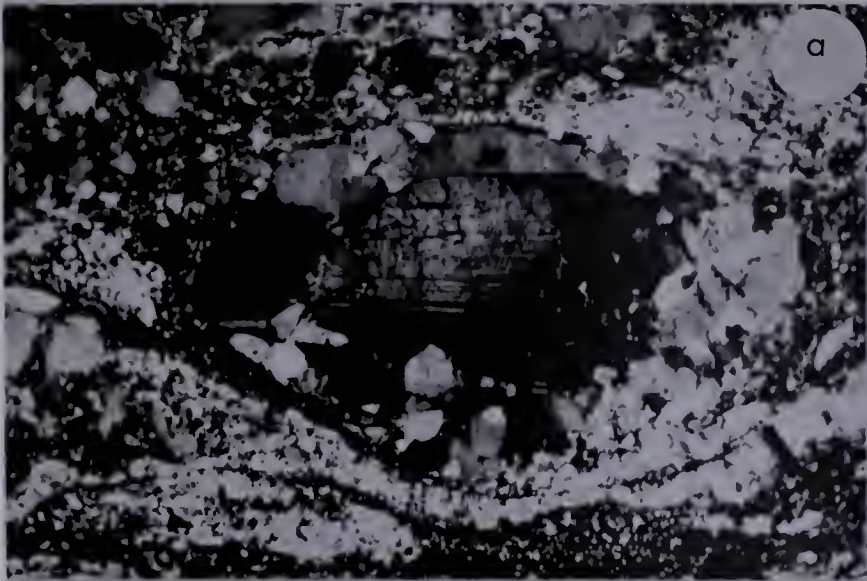


PLATE 6

MYLONITE P

- a. Flaser gneiss. Standard sample 133, photomicrograph. Augen-shaped, granitic rock porphyroclast with a slightly strained plagioclase megacryst. Crossed nicols, $\times 10$.
- b. Flaser gneiss. Standard sample 133, photomicrograph. Distorted, lens-shaped, equigranular, granitic rock porphyroclast. White bands are microcrystalline quartz. Note the tightly folded quartz band at the lower right. Crossed nicols, $\times 10$.
- c. Mylonite. Standard sample 132, photomicrograph. Elliptical microcline porphyroclast with quartz inclusions and quartz indentation, in a typical mylonitic matrix. Crossed nicols, $\times 10$.
- d. Mylonite. Sample VI-a, photomicrograph. Small, elliptical, microcline porphyroclast is derived by shearing of the megacryst. The upper one-half of the photograph is microcline, except for a segment in upper right; in plane light, no apparent granulation is detected. Crossed nicols, $\times 10$.
- e. Mylonite. Sample IX-n, photomicrograph. Augen structure with white mica enclosing plagioclase. White mica is derived from the plagioclase porphyroclast. Crossed nicols, $\times 10$.
- f. Mylonite. Standard sample 153, photomicrograph. Folded plagioclase porphyroclast conforms to the shape of the adjacent, folded quartz band. Crossed nicols, $\times 10$.
- g. Mylonite. Standard sample 132, photomicrograph. Euhedral plagioclase megacryst with slight marginal granulation. The megacryst has probably been rotated 90 degrees. Crossed nicols, $\times 10$.
- h. Mylonite gneiss. Sample IX-m, photomicrograph. The microcline porphyroclast in the upper right shows marginal granulation. The small microcline fragments are incorporated into a quartzose layer, and show relative displacement to the left. Plane light, $\times 10$.



Biotite Granite F

The distinction between mylonite P and granite F in the field is based upon texture, matrix grain size, and megacryst size and shape. Granite F is foliated to granoblastic, with a fine- to medium-grained matrix, and subhedral feldspar porphyroblasts mainly 50 mm long (Plate 5,a,b). Extreme development of granite F consists of a porphyroblastic rock with euhedral porphyroblasts up to 150 mm long set in a granoblastic, medium- to coarse-grained groundmass. Granite F has maximum thickness of 4,500 feet in the east-central region of map-area 10.

Granite F is almost invariably associated with mylonite P, however, a notable exception is the isolated body of granite F west of Selwyn Lake.

Thin section examination of granite F standard samples reveals a massive, porphyroblastic texture. The matrix consists of interlocking 0.5 to 1 mm grains of plagioclase, quartz, and microcline, and poorly oriented muscovite, biotite, and chlorite. Porphyroblasts of microcline are mainly subhedral, from 5 to 50 mm long, containing plagioclase and biotite inclusions, and myrmekite is found commonly along the corroded margins. Plagioclase grains are commonly from 2 to 3 mm in diameter, and are included with the matrix. Modal analyses (Table 9) of three standard samples give approximate values of 42 per cent plagioclase, 31 per cent quartz, 11 per cent biotite, 9 per cent microcline, 4 per cent chlorite, 2 per cent garnet, 0.6 per cent white mica, and 0.1 per cent accessory minerals. Cataclastic effects in granite F consist of highly strained quartz blebs with slightly sutured grain boundaries, bent twin lamellae in plagioclase porphyroblasts, and locally a slightly granulated matrix. Diaphoretic effects include the partial alteration of biotite to chlorite, alteration of garnet to sericite, chlorite and for biotite (Plate 7,d,e,f), and the slight sericitization of feldspar. Petrographic classification establishes granite F as porphyroblastic granodiorite.

Comparison of granite F and mylonite P characteristics establishes their genetic relationship. Field mapping indicates granite F is the parent rock of mylonite P,

TABLE 9. MODAL AND CHEMICAL ANALYSES OF BIOTITE GRANITE F
STANDARD SAMPLES, CHARLES LAKE CATACLASTIC BAND

	127	129	146	Average
Q	30.4	34.4	29.5	31.4
KFp	13.0	10.7	4.5	9.4
Pl	37.7	40.4	47.0	41.7
Bio	5.7	11.0	16.8	11.2
Chl	7.2	3.0	0.2	3.5
Mu	1.8	-	-	0.6
Cal	0.1	-	-	tr
Gt	4.3	-	2.2	2.2
Zr	tr	tr	-	tr
Ap	-	0.2	-	0.1
Mag	-	-	0.1	tr
No. of Points	2500	2500	2500	-
SiO ₂	67.95		65.21	66.58
TiO ₂	0.50		0.76	0.63
Al ₂ O ₃	15.51		16.13	15.82
Fe ₂ O ₃	4.28		4.99	4.64
MnO	0.07		0.06	0.07
MgO	1.39		2.48	1.94
CaO	2.30		3.22	2.76
Na ₂ O	3.05		2.81	2.93
K ₂ O	2.93		3.20	3.07
L.O.I.	1.16		0.76	0.96
P ₂ O ₅	0.12		0.17	0.15
Total	99.28		99.79	99.55

(Chemical analysis by G. Schmitz)

and a systematic gradation is observed. The modal analyses of mylonite P and granite F (Tables 8 and 9) indicate a similarity of the essential minerals microcline, plagioclase, and biotite, although quartz is appreciably more abundant in granite F. White mica, mainly in the form of sericite, is relatively more abundant in mylonite P, but is simply a function of the degree of shearing affecting feldspar. Garnet is common as fresh to highly altered porphyroblasts in two of the three standard samples of granite F, and the lack of garnet in mylonite P is explained by diaphoresis during mylonitization of the granite F parent rock. Finally, the presence of epidote in mylonite P and absence in granite F is evidence of retrogressive effects whereby lime was likely released from the plagioclase during cataclasis.

Megacrysts in mylonite P hand specimens are mainly feldspar augen that denote syntectonic origin, but rare subhedral porphyroblasts imply continuous growth until deformation subsided. Thin section examination reveals extensive development of replacement antiperthite in mylonite P. The average values of two chemical analyses of granite F (Table 9) compared with two complete and one partial analysis of mylonite P (Table 8) indicate that K_2O is enriched and about the same amount of CaO is lost in the transition from granite F to mylonite P. Na_2O is essentially the same in both rocks.

Thus, field observations, microscopic examination, and chemical analyses indicate a complex history for the feldspar megacrysts in granite F and mylonite P. A syntectonic, porphyroblastic granite, produced by granitization of a sequence of sedimentary rocks was crushed along a north-trending shear zone to produce mylonite P. Under conditions of relaxed stress, reactivated growth of microcline megacrysts and potash migration into the mylonite zone resulted in subhedral to euhedral microcline growth and replacement antiperthite in mylonite P.

Minor rock constituents in granite F include lenses and layers of amphibolite, impure, thin quartzo-feldspathic layers. The impure quartzite remnants in the main band of granite F are commonly in the form of digitations from the continuous band

PLATE 7

GRANITE F (PORPHYROBLASTIC GRANODIORITE)

- a. Porphyroblastic granodiorite. Field photograph. Anhedral to subhedral microcline porphyroblasts in a foliated matrix.
- b. Porphyroblastic granodiorite. Standard sample 127, hand specimen. Anhedral to subhedral, small-size feldspar porphyroblasts in a medium-grained, foliated matrix.
- c. Porphyroblastic granodiorite. Sample V-g, photomicrograph. A plagioclase porphyroblast with deformation twinning in a medium-grained matrix which is partly granulated. Note the highly sutured boundaries between quartz grains in the upper left. Crossed nicols, $\times 10$.
- d. Porphyroblastic granodiorite. Standard sample 127, photomicrograph. Garnet porphyroblasts in a moderately granulated matrix. Sericite alteration is developed along the fractures. Crossed nicols, $\times 10$.
- e. Porphyroblastic granodiorite. Standard sample 127, photomicrograph. Highly poikiloblastic garnet shows alteration to biotite and sericite. Quartz (white) and feldspar (grey) enclose garnet. Plane light, $\times 10$.
- f. Porphyroblastic granodiorite. Standard sample 127, photomicrograph. Relict garnet islands (high relief grains, to the left of centre) in a sericite mat. Quartz, plagioclase, and biotite are other prominent minerals in the photomicrograph. Plane light, $\times 10$.

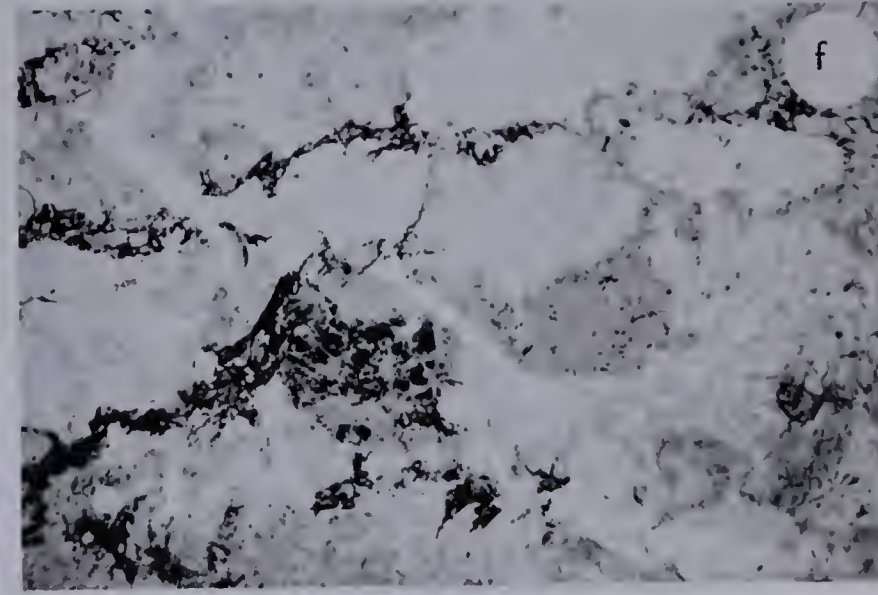
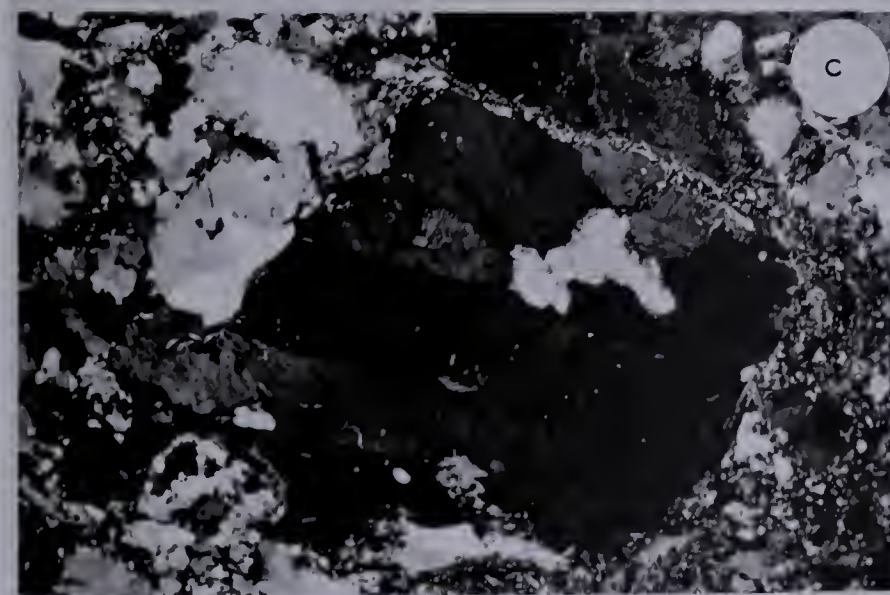
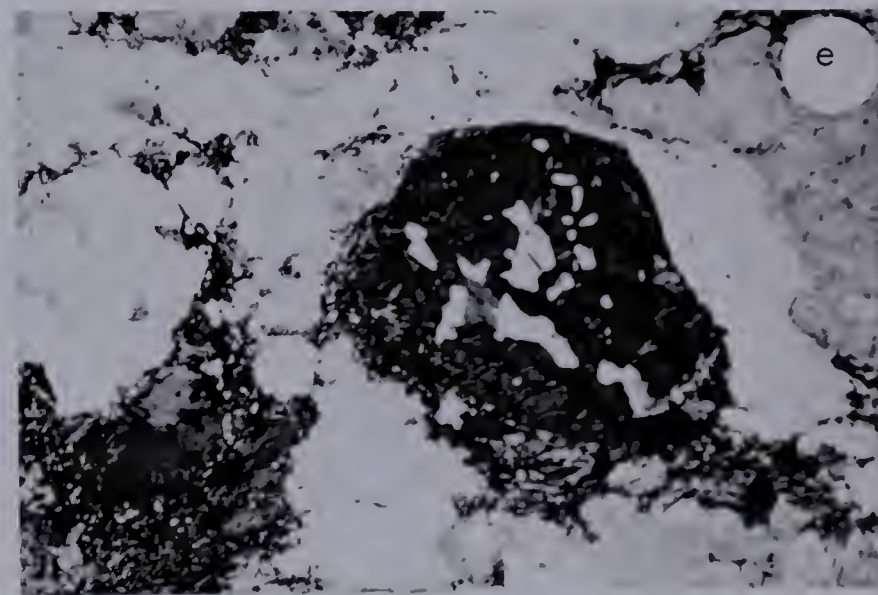
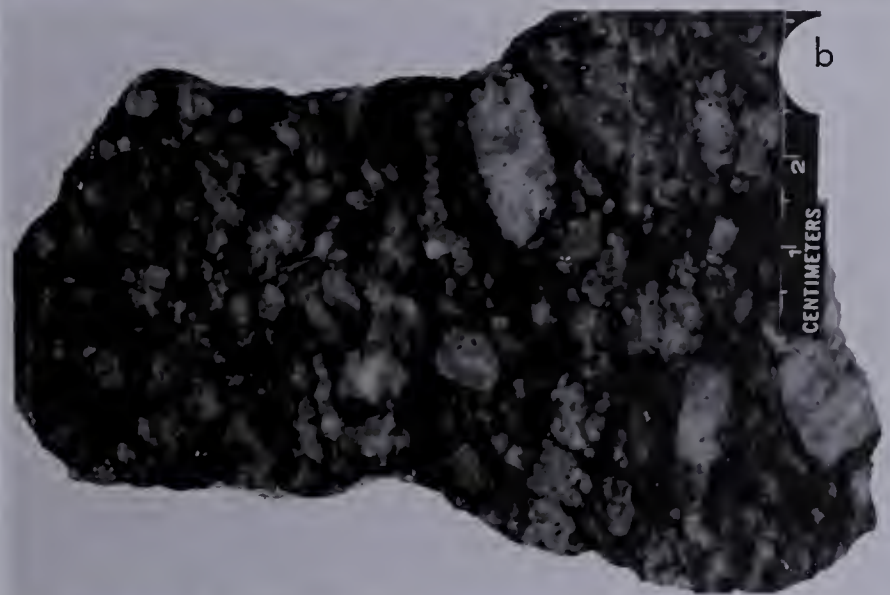
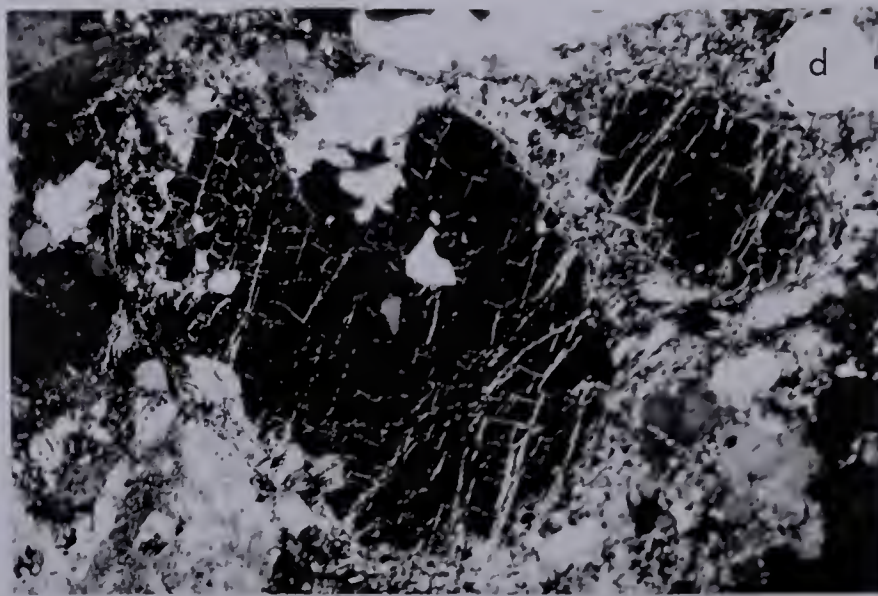


PLATE 7

of impure quartzite along the eastern contact of granite F. Metasedimentary rocks are absent along the western contact between the sheared equivalents of granite F and granite gneiss. Metasedimentary rocks were conceivably located along the western contact before granite F and granite gneiss were deformed to mylonite P and mylonite K respectively, and were incorporated into the shear zone. Alternatively, granite gneiss and granite F were in contact prior to deformation, and faulting with crushing resulted in a mylonite K - mylonite P contact.

Arch Lake Mylonite

Felsic mylonite within Arch Lake granite forms two lenses, one near Arch Lake in map-area 10, and another west of Cornwall Lake in map-area 11. The map-legend for maps 10 and 11 designates these mylonite lenses as mylonite L, but the term Arch Lake mylonite is adopted in this thesis to emphasize the genetic relationship with Arch Lake granite.

Arch Lake mylonite hand specimens resemble rhyolite or chert, and conchoidal fracture surfaces are light green. Texturally, the mylonite is aphanitic, faintly laminated, and slightly to highly porphyroclastic. Under the microscope, the mylonite comprises angular to subrounded, anhedral porphyroclasts of microcline, plagioclase, quartz, and glomeroporphyroclasts of partly crushed parent rock, set in a cryptocrystalline matrix (Plate 8,g) of quartz, microcline, plagioclase, chlorite, and muscovite. No standard sample of Arch Lake mylonite exists, consequently no chemical analysis is available. However, mineralogical and X-ray fluorescence data of Arch Lake mylonite samples are given in chapter four. The matrix is unlaminated with average grain size less than 0.01 mm which petrographically classifies Arch Lake mylonite as cryptocataclasite.

Arch Lake mylonite grades into sheared Arch Lake granite through a cross-strike distance of about 20 feet.

Arch Lake Granite

Arch Lake granite is named after Arch Lake located in the northern part of the granite body which forms a continuous mass along the western margin of map-areas 9, 10, and 11. The granite extends southerly from the southwest corner of map-area 9 for 19 miles and continues for an unknown distance beyond the southern margin of the thesis area. The eastern boundary is defined by the contact with granite gneiss, whereas the westward extent of the body is uncertain as indicated by Riley (1960) who mapped the Arch Lake granite as a phase of the large plutonic mass located predominantly west of the thesis area.

Arch Lake granite is texturally distinctive, with elongate, subhedral to euhedral feldspar megacrysts that are commonly aligned in a foliated, medium-grained, felsic matrix (Plate 8,a). Dark red plagioclase grains in the matrix are dusted by hematite. The granite tends to be subequigranular and massive in the interior of the mapped body. The weathered surface is pink, whereas the fresh surface is dark reddish grey. In thin section, Arch Lake granite comprises abraded, anhedral to subhedral, stretched microcline megacrysts set in a foliated, sheared matrix of plagioclase, quartz, microcline, biotite, chlorite, muscovite, and epidote (Plate 8,b,c,d,e,f). Examination of five standard samples from throughout the granite body indicates that deformation has played an important role in the history of Arch Lake granite. Microcline megacrysts are elongate-subhedral (Plate 8,c), to rounded, ovoid (Plate 8,d), and lens shaped (Plate 8,e) with shadowy extinction, and bent composition planes of Carlsbad twin crystals. The matrix is subequigranular (Plate 8,b) to highly inequigranular (Plate 8,c), depending upon the degree of cataclasis, and average matrix grain size ranges from 0.1 to 1 mm. The matrix in all standard samples exhibit shear phenomena, and the amount of crushed matrix ranges from about 10 to 50 per cent. Thorough recrystallization of the matrix results in equigranular, fine-grained crystals, with grain size ranging from 0.1 to 0.3 mm, surrounding the coarse-grained (1 to 2 mm) crystals and megacrysts.

Five modal and two chemical analyses of Arch Lake granite standard samples

PLATE 8

ARCH LAKE MYLONITE (CRYPTOCATACLASITE) AND
ARCH LAKE GRANITE (PORPHYRITIC QUARTZ MONZONITE)

- a. Arch Lake granite. Standard sample 100, hand specimen. Euhedral to subhedral, tabular, microcline megacrysts showing lineation.
- b. Porphyritic quartz monzonite. Standard sample 121, photomicrograph. Typical texture. Crossed nicols, x 10.
- c. Porphyritic quartz monzonite, sheared. Standard sample 155, photomicrograph. Large microcline megacryst with simple twinning, granulated grain margin. Crossed nicols, x 10.
- d. Porphyritic quartz monzonite, sheared. Standard sample 155, photomicrograph. Large, elliptical microcline crystal with selvage of polycrystalline plagioclase. Plane light, x 10.
- e. Porphyritic quartz monzonite, sheared. Standard sample 155, photomicrograph. Large, lenticular, polycrystalline microcline megacryst in the centre. Plane light, x 10.
- f. Porphyritic quartz monzonite, sheared. Sample VIII-b, photomicrograph. Large, strained, and fractured plagioclase and microcline megacrysts. Crossed nicols, x 10.
- g. Cryptocataclasite. Sample VIII-e, photomicrograph. Unstrained, granoblastic quartz vein cuts the cryptocrystalline ground-mass. Crossed nicols, x 10.
- h. Cryptocataclasite. Sample VIII-f, photomicrograph. Large, angular, cryptocataclasite breccia fragment in cryptocataclasite. Note the cryptocataclasite vein in the centre of the photomicrograph. Plane light, x 10.

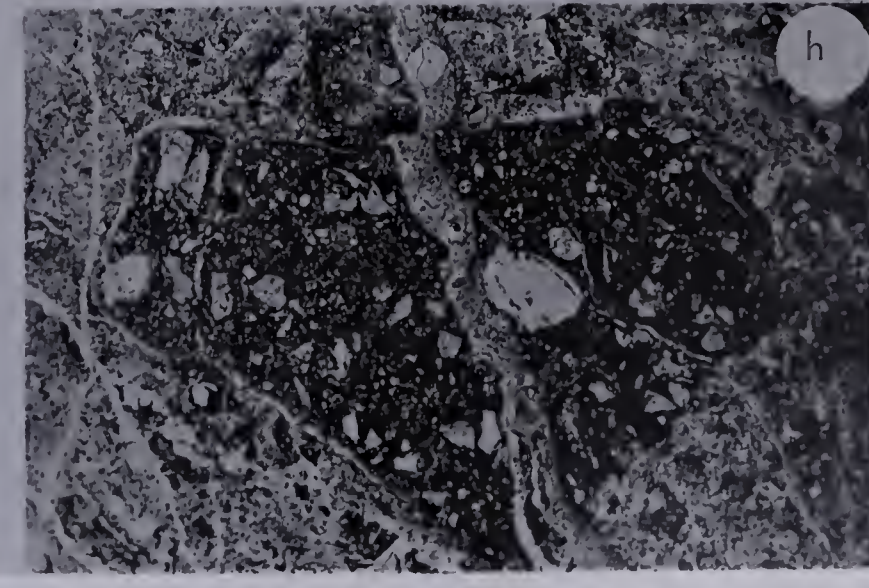
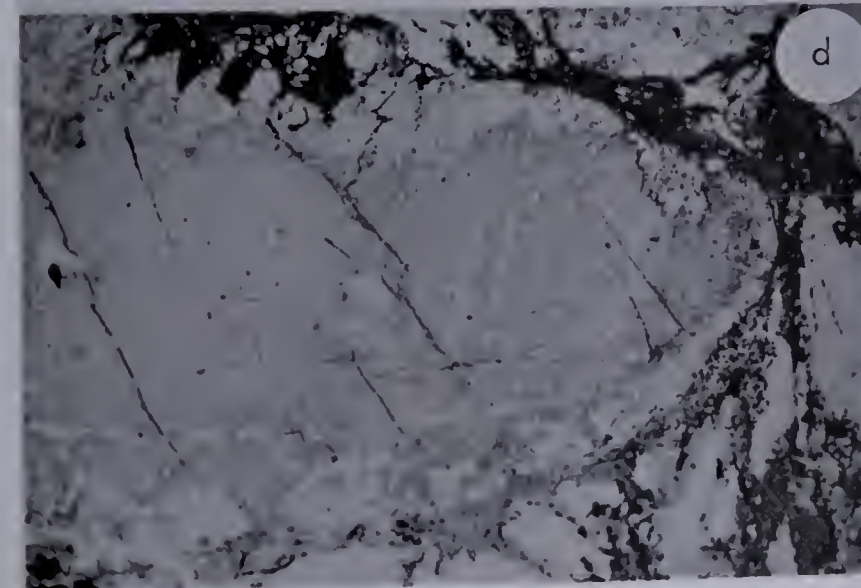
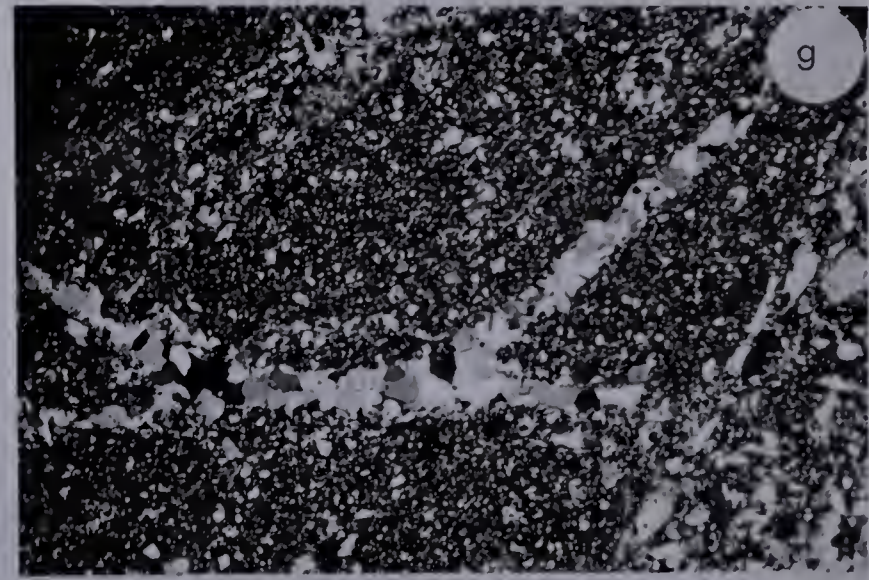
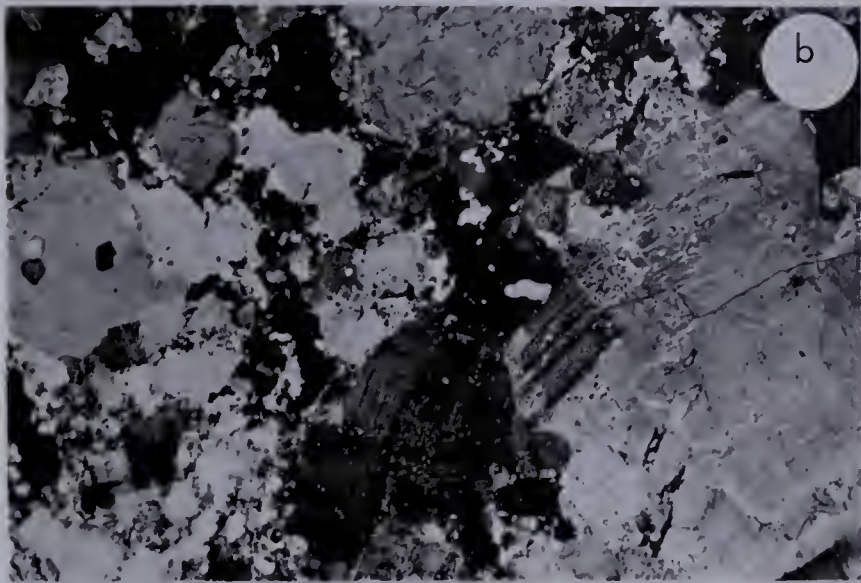
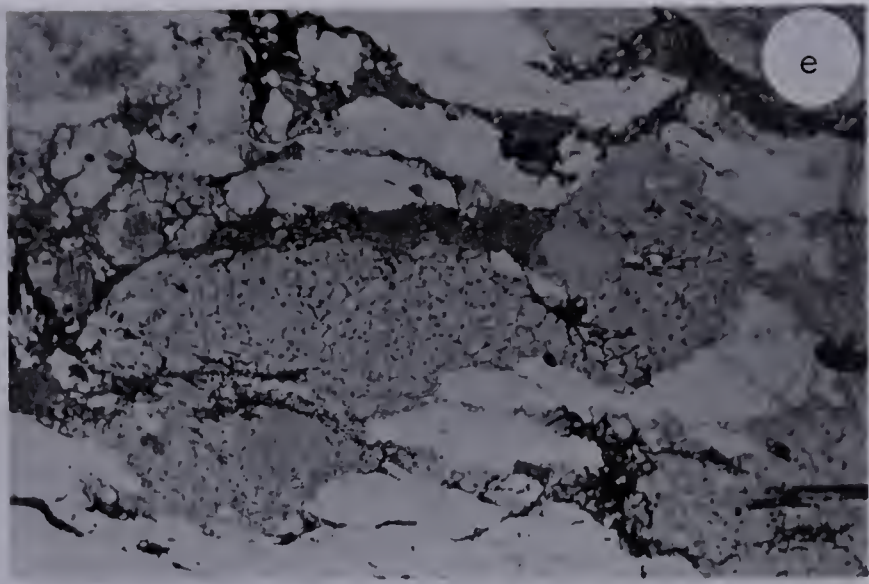
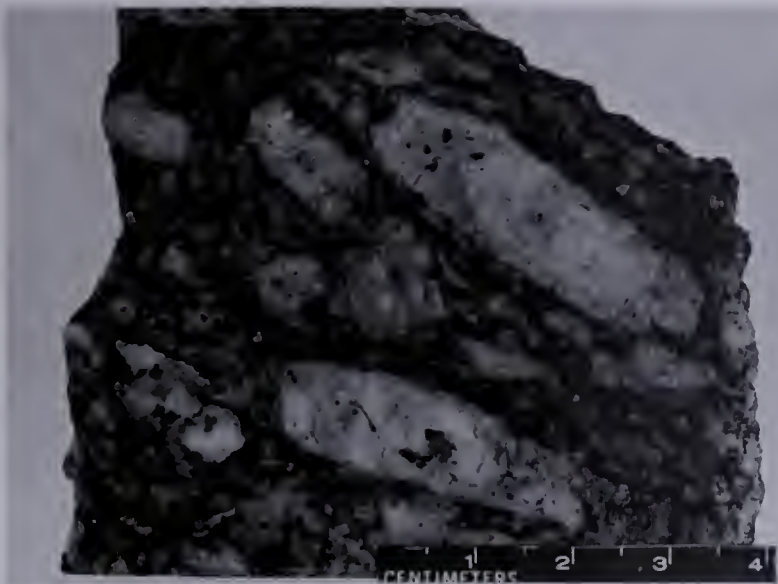


TABLE 10. MODAL AND CHEMICAL ANALYSES OF ARCH LAKE GRANITE
STANDARD SAMPLES, WEST OF CHARLES LAKE

	100	121	131	148	155	Average		
Q	21.9	19.4	44.9	22.8	33.6	28.5		
KFp	45.6	42.0	16.8	37.4	26.4	33.6		
Pl	25.6	32.5	29.1	30.8	26.5	29.1		
Bio	1.9	3.3	3.6	5.0	6.9	4.1		
Chl	1.7	0.9	0.7	1.0	0.6	1.0		
Mu	2.0	0.9	3.5	1.7	5.9	2.8		
Ep	0.1	0.3	1.4	0.6	tr	0.5		
Cal	0.1	-	0.2	0.1	-	0.1		
Ar	0.1	-	tr	-	tr	tr		
Ap	-	-	-	0.2	-	tr		
Al	-	-	tr	tr	tr	tr		
Sph	-	0.2	0.1	-	0.2	0.1		
Lx	-	-	0.1	0.1	-	tr		
Mag	0.2	0.1	0.1	0.5	tr	0.2		
Hem	x	x	x	x	x	x		
Gt	-	-	-	-	tr	tr		
No. of points	2,500	2,500	2,500	2,500	2,500	-	*	**
SiO ₂				67.80	70.87	69.34	69.35	72.31
TiO ₂				0.48	0.10	0.29	0.35	0.33
Al ₂ O ₃				15.26	15.26	15.26	14.27	12.67
Fe ₂ O ₃				3.18	1.60	2.39	3.55	4.16
MnO				0.04	0.02	0.03	0.07	0.11
MgO				1.28	0.58	0.93	1.13	0.40
CaO				1.77	1.15	1.46	2.18	1.65
Na ₂ O				3.26	2.86	3.06	2.95	3.27
K ₂ O				5.61	5.61	5.61	5.36	4.42
L.O.I.				0.87	0.70	0.79	0.55	0.75
P ₂ O ₅				0.29	0.10	0.20	0.17	0.07
Total				99.75	98.33	99.36	99.94	100.14

(Chemical analyses by G. Schmitz)

* Average of 23 granites. Johannsen, 1932, p. 193. The term "granites" includes granites and quartz monzonites.

** Average of 11 rapakivi granites. Johannsen, 1932, p. 247.

x Mineral present.

are given in Table 10. The wide range of modal quartz and microcline may be explained by the coarse grain-size and the irregular distribution of quartz blebs and microcline megacrysts, so that the mineralogical differences may not represent marked changes in bulk chemical composition. The average mineralogical composition comprises about 34 per cent microcline, 29 per cent quartz, 29 per cent plagioclase, 4 per cent biotite, 3 per cent white mica, and 1 per cent chlorite, which classifies the rock as quartz monzonite. The average chemical composition compares favourably to Johannsen's (1932, p. 193) average of 23 granites and quartz monzonites.

Rapakivi-type texture is developed (Plate 8,d) where ovoid microcline megacrysts are mantled with polycrystalline plagioclase grains. The absence of euhedral quartz, evidence of cataclasis, and the presence of megacryst alignment disqualifies the classification of Arch Lake granite as a rapakivi granite (Turner and Verhoogen, 1960, pp. 368-370; Johannsen, 1932, pp. 243-248. However, the position of Arch Lake granite as a marginal phase of a large plutonic mass lying to the west is in accord with some occurrences of rapakivi granite (Turner and Verhoogen, 1960, p. 368).

Raisin Granite

An elongate mass of raisin granite in the northwest part of the Charles Lake, North map-area is the northernmost phase of a continuous, composite granitic band along the western margin of the Charles Lake, North, Central, and South map-areas.

The presence of numerous, isolated feldspar porphyroclasts in a green, finely-laminated, chloritic matrix is typical (Plate 9,a), and the texture is reminiscent of raisins spilled onto a flat surface. The feldspar porphyroclasts are spherical to augen-shaped, and chiefly range from 2 to 6 mm in size. Remnants of the porphyritic, medium-grained parent rock are present, and fresh surfaces are dark grey due to abundant biotite.

Thin section study of two raisin granite standard samples and additional samp-

TABLE 11. MODAL AND CHEMICAL ANALYSES OF RAISIN
GRANITE STANDARD SAMPLES, WEST OF CHARLES LAKE

	84	91	Average	
Q	25.7	24.5	25.1	
KFp	9.2	2.7	6.0	
Pl	49.8	64.3	57.1	
Bio	-	2.9	1.5	
Chl	9.3	1.4	5.4	
Mu	2.2	3.6	2.9	
Cal	0.1	0.6	0.4	
Zr	0.1	-	0.1	
Ap	0.3	-	0.2	
Al	-	tr	tr	
Sph	0.1	-	0.1	
Lx	-	0.2	0.1	
Mag	-	0.2	0.1	
No. of Points	2,500	2,500	-	
				*
SiO ₂	66.61		66.61	67.86
TiO ₂	0.61		0.61	0.51
Al ₂ O ₃	15.26		15.26	14.97
Fe ₂ O ₃	5.09		5.09	3.93
MnO	0.03		0.03	0.05
MgO	2.01		2.01	1.38
CaO	2.30		2.30	2.82
Na ₂ O	3.03		3.03	3.29
K ₂ O	3.12		3.12	3.58
L.O.I.	1.86		1.86	0.90
P ₂ O ₅	0.12		0.12	0.17
Total	100.04		100.04	99.46

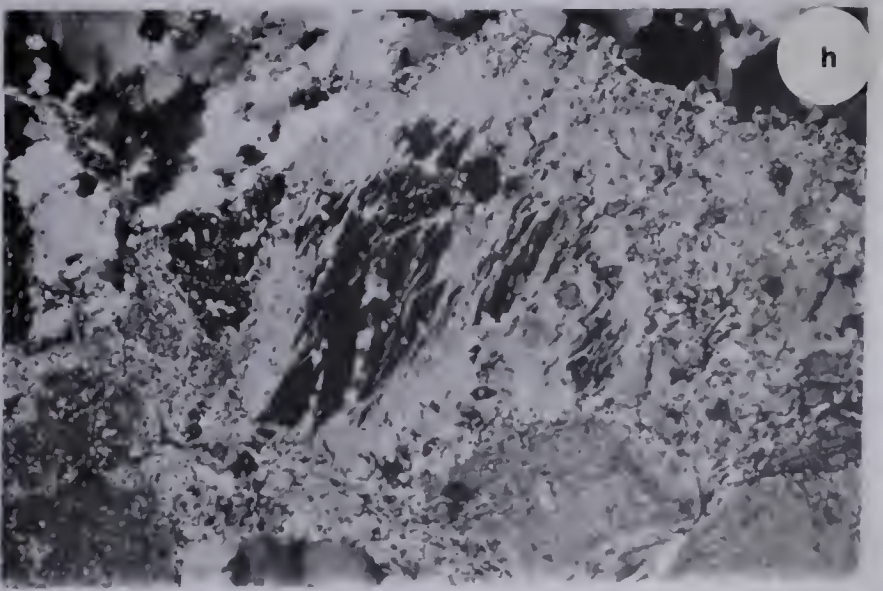
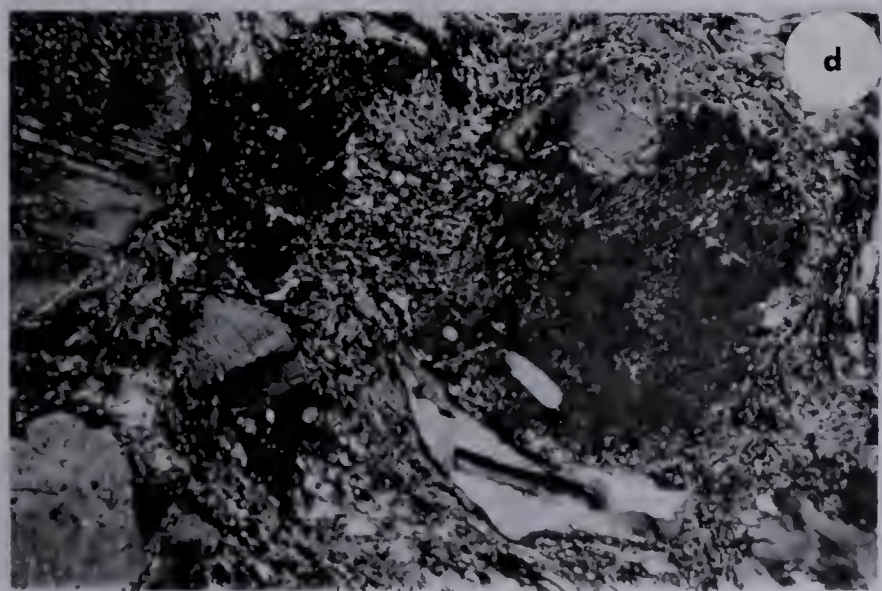
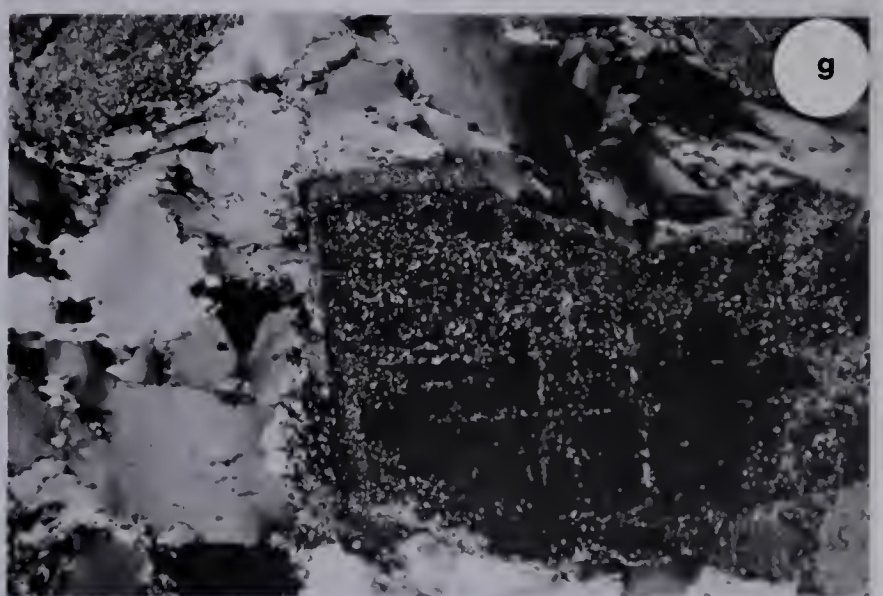
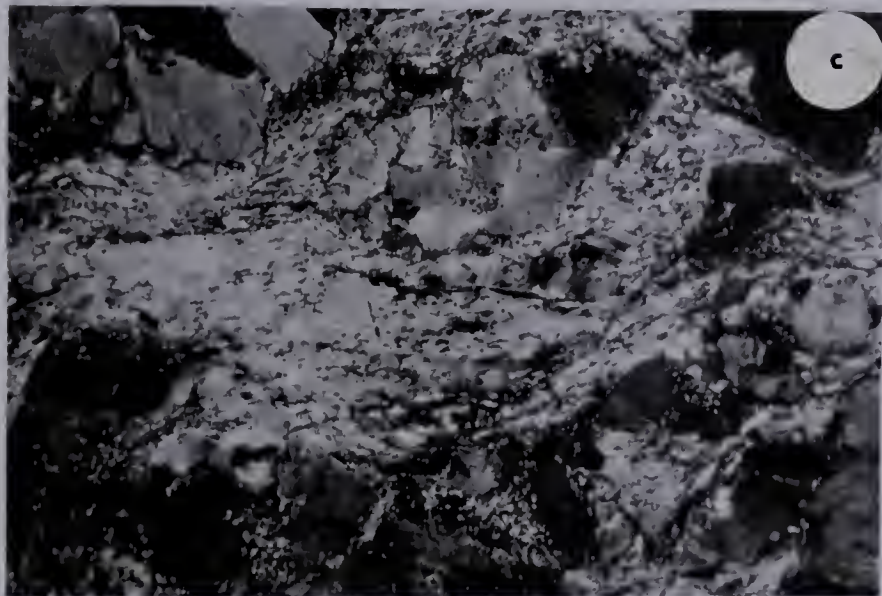
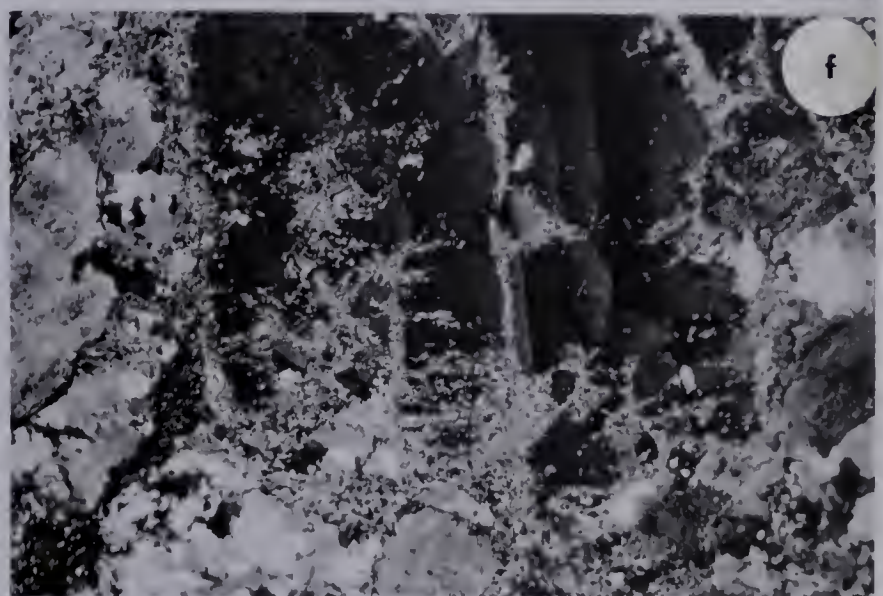
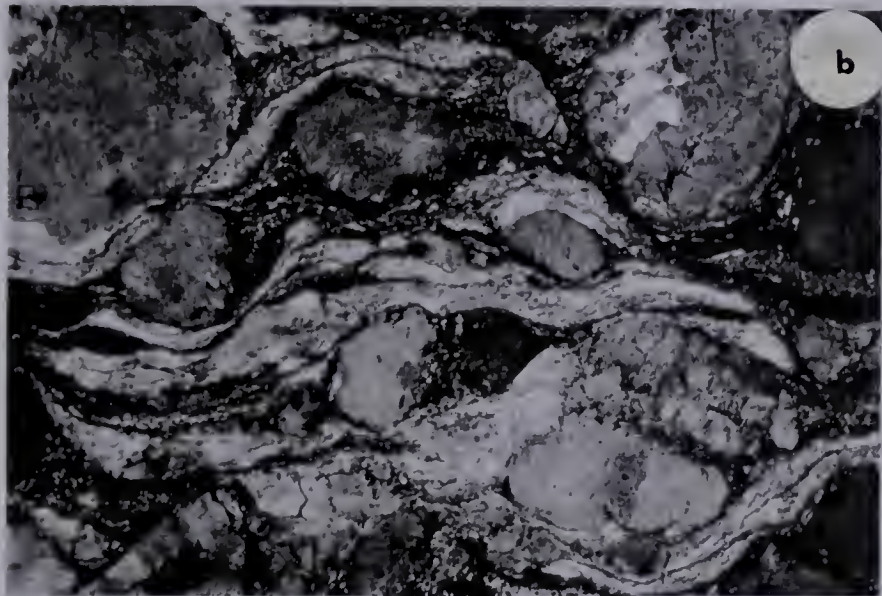
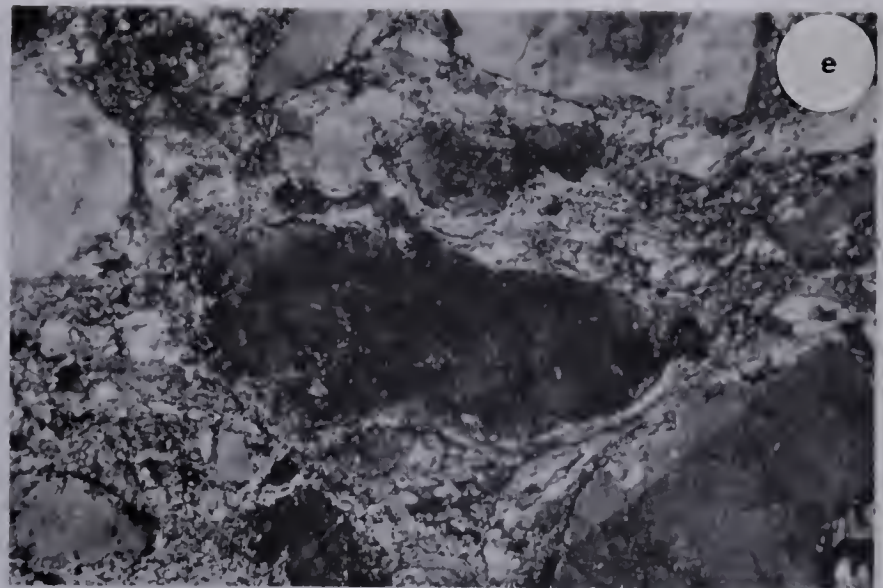
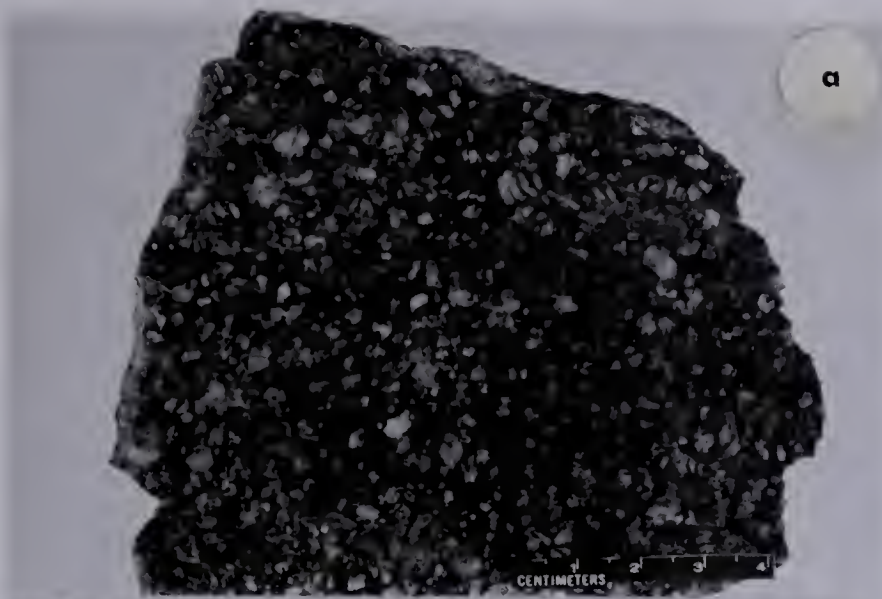
(Chemical analyses by G. Schmitz)

* Average granodiorite. Johannsen, 1932, p. 331. Average of 24 samples.

PLATE 9

RAISIN GRANITE (FLASER GRANODIORITE)

- a. Raisin granite (Flaser granodiorite). Standard sample 84, hand specimen. Abundant 2 to 6 mm feldspar porphyroclasts and rock fragments in a laminated, chloritic matrix.
- b. Flaser granodiorite. Standard sample 84, photomicrograph. Elliptical to augen-shaped plagioclase and microcline porphyroclasts in a highly crushed matrix with wavy, microcrystalline quartz bands (light) and chlorite-rich bands (dark). Crossed nicols, $\times 10$.
- c. Flaser granodiorite. Sample IV-a, photomicrograph. An augen-shaped, uncrushed rock fragment (top-center) enclosed in a quartzose, highly crushed matrix. The matrix shows less cataclasis than the previous sample. Crossed nicols, $\times 10$.
- d. Flaser granodiorite. Sample IV-b, photomicrograph. Two strained, bent biotite books (left of center, and top-right of center) in a highly crushed matrix consisting of quartz, plagioclase, biotite, chlorite, and white mica. Note deformation twinning in the quartz grain in the bottom center. Crossed nicols, $\times 25$.
- e. Flaser granodiorite. Sample IV-b, photomicrograph. A rounded plagioclase porphyroclast with bent twin lamellae, in a highly crushed matrix. Note simple twinning in the plagioclase porphyroclast at the bottom right. Crossed nicols, $\times 10$.
- f. Garnetiferous porphyroclastic granodiorite. Sample IV-c, photomicrograph. A large-size microcline porphyroclast shows development of white mica along the periphery and fractures. The matrix shows moderate crushing. Crossed nicols, $\times 10$.
- g. Porphyritic quartz diorite. Standard sample 91, photomicrograph. A euhedral, zoned, plagioclase phenocryst with quartz embayments along the top and bottom of the crystal is enclosed in a polycrystalline aggregate of quartz showing highly sutured grain margins. Crossed nicols, $\times 25$.
- h. Porphyritic quartz diorite. Standard sample 91, photomicrograph. A microcline perthite megacryst (in the center) is largely replaced by plagioclase (light) leaving irregular blebs and wisps of unreplaced material (dark). Note the development of fine-grained white mica along the periphery of the megacryst. Crossed nicols, $\times 25$.



les from scattered locations shows that a complete textural gradation exists from massive, unsheared, porphyritic granodiorite (Plate 9,g,h) to laminated, highly sheared, flaser granodiorite (Plate 9,b). The massive, unsheared phase has about 60 per cent subhedral to euhedral phenocrysts* (Plate 9,g) comprising plagioclase and microcline about 4 mm in diameter, in a medium-grained, granitic matrix with numerous, irregular, polycrystalline, medium-grained quartz blebs. Progressive shearing causes rounding and decrease in size and quantity of the feldspar megacrysts. The most intensely sheared phase contains about 35 per cent porphyroclasts with an average diameter of 2 mm, in a crushed matrix that constitutes about 50 per cent of the rock and has an average grain size of 0.02 mm. Microcline megacrysts are commonly highly albitized (Plate 9,h), and sericitized in both unsheared and sheared phases. The irregular quartz blebs of the unsheared phase show the most pronounced cataclastic effect, with comminution and recrystallization giving rise to "shoestring" quartz that bends around feldspar porphyroclasts (Plate 9,b). Biotite is unstrained in porphyritic granodiorite, strained and contorted in moderately sheared, flaser granodiorite (Plate 9,d), and pulverized and chloritized in flaser granodiorite.

Sample IV-c has about 2 per cent garnet enclosed by sericite and biotite mats. The proximity of this sample to a lens of impure quartzite (see Charles Lake, North map-sheet) suggests that partial assimilation of metasedimentary rock by granitic magma has resulted in a contaminated zone around the inclusion, and has crystallized garnet. Harker (1950, p. 300) states that garnet is a characteristic constituent of granitic rocks crystallized or recrystallized under high pressure and stress; however, the presence of garnet in only one sample of raisin granite is not explained by Harker's observation.

Two modal analyses and one chemical analysis of raisin granite standard sam-

* Phenocryst: a large crystal in a finer-grained igneous rock.

ples are given in Table 11. Modal analyses classify raisin granite as granodiorite, and the similarity of the chemical analysis of sample 84 and Johannsen's average granodiorite (Johannsen, 1932, p. 331) confirms this classification.

Biotite "q" Granite

Biotite "q" granite is present as narrow layers, lenses, and bulbous masses in map-areas 5, 6, and 7, and is most common in map-area 5, where numerous, isolated masses are restricted to the area west of a line through Logan Lake, Treasure Loch, and Ashton Lake. Biotite "q" granite is intrusive into most of the major lithologies and contains inclusions of these rocks. Continuous layers several feet thick are commonly interlayered with granite gneiss which indicates the granite was intruded in a mobile, liquid state. Apparently, biotite "q" granite is one of the youngest major rock-types in the thesis area, and evidence of mylonitization is lacking in this rock.

Biotite "q" granite is texturally distinctive, with abundant, equant, anhedral to subhedral feldspar phenocrysts, mainly 6 mm in size, in a medium-grained, massive to foliated matrix consisting of quartz, feldspar, biotite, and muscovite. Hand specimens of biotite "q" granite and unsheared phases of raisin granite are similar, but mapping shows no apparent evidence of a genetic association.

Modal analysis of a single sample (Table 12) from map-area 5 shows that the rock may be petrographically classified as quartz monzonite, and the chemical analysis is similar to Nockolds' (1954, p. 1014) biotite adamellite (quartz monzonite). Comparison of biotite "q" granite with raisin granite shows that in the modal analyses the former is distinctly more acid, with more quartz and potash feldspar, and less plagioclase than in raisin granite, whereas chemical data discloses appreciably higher SiO_2 and K_2O , and less Al_2O_3 , Fe_2O_3 , MgO , and CaO than in raisin granite.

Field and laboratory criteria indicate no obvious genetic relationship between biotite "q" granite and raisin granite. However, both rocks have crystallized from

TABLE 12. MODAL AND CHEMICAL ANALYSES OF A BIOTITE "Q"
GRANITE STANDARD SAMPLE, EAST OF CHARLES LAKE

76		
Q	31.2	
KFp	34.8	
Pl	24.1	
Bio	5.8	
Chl	0.7	
Mu	1.0	
Ep	0.2	
Zr	tr	
Ap	0.2	
Al	0.5	
Sph	1.2	
Mag	0.5	
No. of Points	2,500	
		*
SiO ₂	71.02	71.03
TiO ₂	0.50	0.39
Al ₂ O ₃	13.58	14.31
Fe ₂ O ₃	3.25	2.91
MnO	-	0.06
MgO	0.65	0.75
CaO	1.68	1.89
Na ₂ O	2.83	3.33
K ₂ O	5.60	4.66
L.O.I.	0.50	0.50
P ₂ O ₅	0.18	0.17
Total	99.79	100.00

(Chemical analyses by G. Schmitz)

* Biotite adamellite (quartz monzonite). Nockolds, 1954, p. 1014.

magma, and the difference in composition of raisin granite (granodiorite) and biotite "q" granite (quartz monzonite) may be due to magmatic differentiation, where satellitic intrusions of biotite "q" granite have been derived from separation of a quartz monzonite magma from a granodiorite magma. The coexistence of large, primary biotite and muscovite flakes in both granitic rocks indicates that crystallization took place between 650 to 825°C, and at about 1,700 to 4,000 atmospheres of water-vapour pressure (Yoder and Eugster, 1954) which implies considerable depth of burial at the time of crystallization.

In summary, biotite "q" granite and raisin granite have distinctly different compositions, and are physically separated, but are possibly genetically related to a common magmatic source. Post-crystalline cataclasis has produced "raisin" texture in the latter granitic mass, whereas the former granitic rock is virtually un-sheared.

Treasure Loch Cataclastic Band

Cataclastic rocks in the Treasure Loch area are confined to several narrow, north-trending, en echelon bands that have a composite mapped length of 6 miles and a maximum width of 2,500 feet. This cataclastic zone is located in the north-central part of map-area 5 and extends northerly for an unknown extent, beyond the Northwest Territories boundary. Mylonite P is the only cataclastic rock-type represented in the Treasure Loch cataclastic band.

Mylonite P

The presence of megacrysts from 40 to 50 mm and 5 to 20 mm in a well-laminated, aphanitic to fine-grained, greyish black to greenish black matrix denote the similarity of mylonite P in the Treasure Loch and Charles Lake areas. The textural transition to granite F, and sheaths of metasedimentary rock duplicate the field setting of mylonite P in the Charles Lake area. Two general megascopic features

distinguish mylonite P in the Treasure Loch area and Charles Lake area: in the Treasure Loch area mylonite P has a relatively coarser average grain size of individual hand specimens, and a larger proportion of subhedral to euhedral porphyroblasts. The difference in average grain size depends upon the abundance of large and small megacrysts - 20 to 30 per cent in samples from Treasure Loch (Plate 5, e) as compared with 15 to 20 per cent in samples from Charles Lake - and is not a function of the matrix grain size.

Thin section examination of Treasure Loch samples discloses large and small, rounded and stretched plagioclase megacrysts commonly with bent twin lamellae and biotite inclusions. Also, large and small augen and subhedra of microcline with biotite and subhedral to euhedral plagioclase inclusions are seen in a well-laminated matrix with average grain size ranging from 0.02 to 0.05 mm. The mylonite P standard samples from the Treasure Loch area have similar modal and chemical compositions (Table 13) that substantiate the noted homogeneity of the rock-type in the field. The approximate mineralogical composition based on the two standard samples follows: 49 per cent plagioclase; 28 per cent quartz; 7 per cent microcline; 7 per cent biotite; 7 per cent chlorite; 2 per cent sericite; and less than 1 per cent accessory minerals. Rare fractures are filled with adularia, quartz, vermicular chlorite, and epidote. Highly strained quartz is well differentiated into distinct, fine-grained laminations and lenses. Microcline is common as larger-size porphyroblasts, patches in antiperthite, and as interstitial grains in the matrix; these features are probably potash metasomatic effects. Chemical data of the two mylonite P standard samples from two adjacent bands at Treasure Loch disclose their similarity and suggest a general homogeneity.

Comparison of average modal and chemical analyses for standard samples from the Treasure Loch (Table 13) and Charles Lake (Table 8) bands indicates a close similarity. Slight mineralogic differences are apparent but interpretation is complicated by megacrysts in coarse texture matrix and the limited size and number of

TABLE 13. MODAL AND CHEMICAL ANALYSES OF MYLONITE P STANDARD
SAMPLES, TREASURE LOCH CATACLASTIC BAND

	73	75	Average
Q	27.1	29.0	28.0
KFp	7.3	7.5	7.4
Pl	47.3	50.7	49.0
Bio	3.1	10.8	7.0
Chl	12.8	0.2	6.5
Mu	2.1	1.5	1.8
Ep	0.1	0.1	0.1
Cal	-	0.1	0.1
Zr	tr	tr	tr
Ap	0.2	0.3	0.3
Sph	0.1		0.1
Mag	0.2	0.2	0.2
No. of Points	2,500	2,500	-
SiO ₂	67.32	69.06	68.19
TiO ₂	0.59	0.44	0.52
Al ₂ O ₃	15.63	15.22	15.43
Fe ₂ O ₃	3.68	3.20	3.44
MnO	0.04	0.05	0.05
MgO	1.90	1.61	1.76
CaO	3.59	2.55	3.07
Na ₂ O	3.68	3.44	3.56
K ₂ O	2.94	3.51	3.23
L.O.I.	1.02	0.64	0.83
P ₂ O ₅	0.22	0.14	0.18
Total	100.61	99.86	100.26

(Chemical analyses by G. Schmitz)

thin sections. These sampling problems, however, are minimized by counting 2,500 points on each 3 by 2 inches thin section, and by selection of a rock slice with typical amounts of megacrysts. Representative chemical analyses of the samples is made possible by the preparation of about 400 grams of crushed-rock powder. Comparison of the average chemical analyses indicates a slightly more basic composition of mylonite P in the Treasure Loch band demonstrated by slightly less silica and potash, and slightly more lime and soda. These slight chemical differences may be attributed to the presence of large-size plagioclase megacrysts in the Treasure Loch band, and their virtual absence in the Charles Lake band. The chemical and mineralogical differences are slight and these widely separated bands of mylonite P are considered to be essentially of the same composition. The similarity of mylonite P in the Charles Lake and Treasure Loch areas is demonstrated by the

- (i) megascopic and microscopic fabric,
- (ii) mineralogy,
- (iii) chemical composition,
- (iv) contact relationship with granite F, and
- (v) metasedimentary rock association.

Granite F

Small, elliptical masses of granite F are located within some en echelon bands of mylonite P in the Treasure Loch area. A transitional shear contact exists between mylonite P and granite F, the transition taking place within a narrow zone of several tens of feet. Granite F masses in the Treasure Loch area are considered to be relatively massive remnants of formerly large, elongate masses.

In hand specimen, granite F typically has large, anhedral to subhedral, 15 to 75 mm feldspar porphyroblasts in a foliated, fine- to medium-grained, greyish black matrix. Megascopic evidence of crushing are denoted by feldspar augen and an irregular development of a fine-grained matrix. The critical basis for distinction

between granite F and mylonite P is (i) the matrix grain size – phaneritic for granite F, and aphanitic for mylonite P, and (ii) massive versus foliated to sheared, for granite F and mylonite P respectively. Granite F has irregular, discontinuous biotite folia but tends to be unlaminate.

Under the microscope, granite F is distinctly inequigranular with rounded, spherical to elliptical 0.5 to 5 mm rock fragments and plagioclase porphyroclasts, and larger-size augen and subhedra of microcline in a partly crushed matrix. Other typical features include granulated grain boundaries, bent plagioclase twin lamellae, and from 10 to 30 per cent crushed matrix. One granite F standard sample from the Treasure Loch band contains approximately 30 per cent crushed matrix, which classifies the rock as a protomylonite. Quartz forms lenticles and irregular to polygonal blebs formed by metamorphic differentiation. Subsequent deformation of the rock has given rise to partial granulation and sutured grain margins in the quartz blebs. Garnet is found as relict fragments within fine-grained, equidimensional blebs of sericite and biotite which have developed by diaphoresis of garnet.

Modal and chemical analyses of the granite F standard sample from the Treasure Loch cataclastic band are listed in Table 14. Granite F samples from the Treasure Loch and Charles Lake (Table 7) areas have only slight mineral and chemical differences and evidently represent petrologically similar rocks. Modal analyses of samples from the Treasure Loch and Charles Lake areas petrologically classify granite F as a porphyroblastic granodiorite.

The correlation of granite F from the Treasure Loch and Charles Lake areas based on hand specimen features is thus confirmed by

- (i) association with metasedimentary rocks,
- (ii) transitional shear contact to mylonite P,
- (iii) mineralogical composition, and
- (iv) chemical composition.

TABLE 14. MODAL AND CHEMICAL ANALYSES OF A GRANITE F STANDARD
SAMPLE, TREASURE LOCH CATACLASTIC BAND

	74
Q	24.5
KFp	6.7
Pl	44.4
Bio	20.0
Chl	0.4
Mu	3.7
Ep	0.2
Cal	0.1
Gt	0.2
Ap	0.2
Mt	tr
No. of Points	2,500
SiO ₂	66.96
TiO ₂	0.59
Al ₂ O ₃	15.42
Fe ₂ O ₃	4.15
MgO	2.03
CaO	3.45
Na ₂ O	3.62
K ₂ O	2.71
L.O.I.	0.70
P ₂ O ₅	0.23
MnO	0.04
Total	99.90

(Chemical analyses by G. Schmitz).

Bayonet Lake Cataclastic Band

The Bayonet Lake mylonite zone consists of a major band on the east side of Bayonet Lake, and a smaller band that extends northward from Collins Lake and continues beyond the Northwest Territories boundary. Several smaller bands are also mapped in the vicinity of Bayonet Lake. The major band trends northerly, having a known length of 15 miles and an unbroken maximum width of 3,000 feet. It extends south from Bayonet Lake, along the east side of One Week Lake and Mylonite Lake, to Pans Lake, and north for an unknown extent beyond the Northwest Territories boundary. The northern part of the major mylonite band is offset by the northwest-trending Bonny fault but there is no difficulty in tracing the northward extension. The Bayonet Lake cataclastic band forms about 10 per cent of map-area 5, and about 5 per cent of map-area 6 to the south.

Mylonites K and L

Mylonites K and L are discussed together because of their intimate field association, similar hand-specimen characteristics, and apparent common derivation from biotite granite gneiss.

Mylonites K and L together form about 90 per cent of the cataclastic rocks of the Bayonet Lake crush zone. Mylonite K predominates in the northern and southern extremes of the Bayonet Lake cataclastic band in map-area 5 whereas mylonites K and L form about equal amounts in the intermediate region.

Mylonite K and L bands are enclosed by biotite granite gneiss, and contain or are adjacent to several narrow bands of mylonite M, numerous lenses of mylonite N, and rare lenses of sheared, impure quartzite.

The field distinction of mylonite K from mylonite L is based upon the size and quantity of rounded feldspar megacrysts: mylonite K contains less than 5 per cent feldspar megacrysts that range in size from 2 to 5 mm whereas mylonite L has 5 to 8

TABLE 15. CATACLASTIC ROCKS AND THEIR PROBABLE PARENT ROCKS
IN THE BAYONET LAKE AREA

Cataclastic rock*	Probable parent rock*
Recrystallized mylonite K**	Biotite granite gneiss
Recrystallized mylonite L**	Biotite granite gneiss
Recrystallized mylonite M**	Hornblende and / or biotite granite gneiss
Recrystallized mylonite N**	Metasedimentary rocks, predominantly biotite schist
Recrystallized mylonite O**	Metasedimentary rocks, predominantly impure quartzite

* Field classification

** "Recrystallized" is omitted in the text

per cent feldspar megacrysts that range from 2 to 20 mm. Otherwise, both mylonites are characterized by greyish pink to red weathered surfaces, greenish red to dark greyish red fresh surfaces, and distinct mineral and colour layering probably inherited from biotite granite gneiss.

Under the microscope, mylonites K and L contain plagioclase and microcline megacrysts that form 3 to 20 per cent of the rock, in a matrix with average grain size predominantly 0.03 to 0.05 mm but ranging from 0.01 to 0.1 mm, and comprising plagioclase, quartz, microcline, chlorite, biotite, white mica, epidote, authigenic euhedra of allanite, and composite magnetite-sphene euhedra. Modal analyses of mylonite K and L standard samples are given in Table 16. Plagioclase megacrysts, including anhedral and subhedral of chessboard albite, are spherical to elliptical, commonly rotated, moderately to highly sericitized, and have highly sutured margins due to thorough recrystallization of the matrix. Inclusions of biotite, chlorite, quartz, and subhedral of plagioclase are common. Microcline forms large (5 to 15 mm) and small (0.5 to 2 mm) megacrysts. Large microcline megacrysts are commoner in mylonite L, are highly fractured and disrupted, and contain inclusions of biotite, chlorite, quartz, and subhedral to euhedral plagioclase. Small megacrysts generally form augen with highly sutured margins and distinct "tails", and with decreasing grain size, grade imperceptibly into the matrix. With rare exception, the matrix is thoroughly recrystallized, and the felsic grains form an equigranular, interlocking network, with quartz commonly forming relatively unstrained, polycrystalline lenticles and bulbous lenses with straight internal grain boundaries. Along the periphery of large-size microcline megacrysts, myrmekite becomes common with increasing degree of recrystallization. Evidently, recrystallization and quartz differentiation in the matrix are late-kinematic thermal effects.

Averages of modal and chemical analyses of mylonites K and L standard samples are given in Table 16. Chemical analyses of samples 111 and 109 are similar, and quartz plus feldspar, and the combined mafic minerals, biotite, chlorite, and epidote

TABLE 16. MODAL AND CHEMICAL ANALYSES OF MYLONITE K AND L
STANDARD SAMPLES, BAYONET LAKE CATACLASTIC BAND

MYLONITE K						MYLONITE L		
	77	101	104	111	Average	78	109	Average
Q	21.0	19.2	29.4	24.1	23.4	20	21.8	20.9
KFp	24.5	tr	4.9	15.4	11.2	30	25.4	27.7
Pl	38.7	75.1	60.1	41.5	53.9	40	33.2	36.6
Bio	5.8	-	-	0.9	1.7	-	10.5	5.3
Chl	1.5	5.3	4.6	12.5	6.0	3	3.3	3.2
Mu	1.9	-	-	1.2	0.8	6	0.4	3.2
Ep	4.5	-	0.6	2.6	1.9	-	3.5	1.8
Cal	0.1	-	-	0.3	0.1	-	0.5	0.3
Zr	0.1	-	-	tr	tr	tr	0.1	0.1
Ap	0.4	-	0.2	0.7	0.3	-	0.5	0.3
Al	0.3	0.5	-	0.3	0.3	-	0.6	0.3
Sph	1.1	-	-	0.2	0.3	-	0.5	0.3
Lx	-	-	-	-	-	-	0.2	0.1
Mag	0.5	tr	0.2	0.4	0.2	tr	tr	tr
Hem	-	0.1	0.1	0.2	0.1	1	tr	tr
No. of Points	2,500	2,500	2,500	2,500	-	Estimate	2,500	-
SiO ₂				66.75	66.75	72.96	68.06	70.51
TiO ₂				0.59	0.59	0.25	0.45	0.35
Al ₂ O ₃				14.83	14.83	13.79	14.65	14.22
Fe ₂ O ₃				4.49	4.49	2.08	3.68	2.87
MnO				0.07	0.07	0.04	0.08	0.06
MgO				2.38	2.38	1.07	1.75	1.41
CaO				1.51	1.51	0.90	2.62	1.76
Na ₂ O				3.21	3.21	3.89	3.38	3.64
K ₂ O				3.81	3.81	4.01	3.88	3.95
L.O.I.				1.76	1.76	0.86	0.95	0.91
P ₂ O ₅				0.17	0.17	0.06	0.14	0.10
Total				99.57	99.57	99.91	99.64	99.78

(Chemical analyses by G. Schmitz)

compare favourably. But the most significant petrogenetic difference between mylonites K and L is shown by the feldspar: both mylonites have about 65 per cent total feldspar, but mylonite L contains about 28 per cent microcline whereas mylonite K contains about 11 per cent microcline. However, mylonites K and L have virtually the same amounts of Na_2O and K_2O , and thus it seems feasible that metamorphic conditions for mylonite L particularly promoted K_2O migration from the matrix and diadochy for CaO and Na_2O , in plagioclase megacrysts.

Local reactivated movement along the Bayonet Lake crush zone after crystallization of the larger microcline megacrysts is indicated by the disrupted state of the microcline megacrysts and secondary mylonitization of part of the matrix in many samples of mylonites K and L. Shoestring quartz tends to be homogenized into the matrix in these secondary mylonites. Some of the reactivated movement was absorbed by plastic flow of the matrix where the matrix has penetrated between slightly displaced megacryst fragments. The feature of large, fractured megacrysts set in a secondary mylonitic matrix which shows plastic flow indicates multiple dynamothermal metamorphism.

In summary, initial mylonitization of biotite granite gneiss was followed by relaxation of stress and concurrent growth of large potash feldspar crystals under conditions of continued high temperature; a second, less severe dynamothermal event took place at the late-kinematic stage, with the development of secondary mylonites, fragmented and displaced megacrysts, and plastic flowage of the secondary mylonite matrix. The last dynamic effect is the production of post-kinematic fractures and subsequent filling by granoblastic quartz.

Petrographic classification establishes mylonites K and L as predominantly mylonite gneiss to blastomylonite, and rarely cryptomylonite.

Mylonites K and L from Bayonet Lake are similar to the corresponding mylonites from Charles Lake. Differences apparently arise, however, in the late metamorphic history of the two areas. A higher degree of recrystallization is observed in

the Bayonet Lake mylonites, with development of predominantly mylonite gneiss and blastomylonite compared with chiefly cryptomylonite to mylonite in the Charles Lake area. Large-size microcline megacrysts in mylonite L from the Bayonet Lake band probably formed from K_2O in the matrix, whereas the large-size microcline megacrysts in mylonite L from the Charles Lake band likely formed by an equivalent gain of K_2O and loss of Na_2O with mylonite K. Otherwise, differences are minor, and mylonites K and L from the Bayonet Lake band are correlated with the corresponding mylonites of the Charles Lake band.

The similarity of chemical analyses of mylonites K and L from the Charles Lake cataclastic band with the average chemical analysis of 10 biotite granite gneiss samples from an adjoining area has been noted. The correlation of mylonites K and L from the Bayonet Lake and Charles Lake bands thus implies that biotite granite gneiss is the parent rock of mylonites K and L in both cataclastic bands.

Mylonite M

Mylonite M is intimately associated with mylonites K and L; the field identification and map representation of these mylonites is complicated by their mutually nebulous, and interlayered contacts. Map representation based upon the predominant rock-type allows the delineation of distinct mylonite M bands. Several northerly trending mylonite M bands up to 1/8 mile wide and 2 1/2 miles long are found along the east side of Bayonet Lake, and a larger band 1/4 mile wide and at least 1 1/2 miles long trends northerly from Collins Lake and continues beyond the Northwest Territories boundary.

Mylonite M is distinguished by a dark and apparently more basic character compared to the felsic appearance of mylonites K and L. Fresh surfaces of mylonite M are dark reddish green to dark reddish black, compared to the red, greenish red, and dark greyish red colours of mylonites K and L. Otherwise, mylonite M has megascopic features common to both mylonites K and L, with indistinct to well-defined mineral

The first part of the paper is devoted to the study of the asymptotic behavior of the sequence of functions $f_n(x)$ defined by the recurrence relation $f_{n+1}(x) = f_n(x) + \frac{1}{n} f_n'(x)$. It is shown that $f_n(x)$ converges to a function $f(x)$ which satisfies the differential equation $f'(x) = f(x)$. The second part of the paper is devoted to the study of the asymptotic behavior of the sequence of functions $g_n(x)$ defined by the recurrence relation $g_{n+1}(x) = g_n(x) + \frac{1}{n} g_n'(x) + \frac{1}{n^2} g_n''(x)$. It is shown that $g_n(x)$ converges to a function $g(x)$ which satisfies the differential equation $g'(x) = g(x) + g''(x)$.

The third part of the paper is devoted to the study of the asymptotic behavior of the sequence of functions $h_n(x)$ defined by the recurrence relation $h_{n+1}(x) = h_n(x) + \frac{1}{n} h_n'(x) + \frac{1}{n^2} h_n''(x) + \frac{1}{n^3} h_n'''(x)$. It is shown that $h_n(x)$ converges to a function $h(x)$ which satisfies the differential equation $h'(x) = h(x) + h''(x) + h'''(x)$. The fourth part of the paper is devoted to the study of the asymptotic behavior of the sequence of functions $k_n(x)$ defined by the recurrence relation $k_{n+1}(x) = k_n(x) + \frac{1}{n} k_n'(x) + \frac{1}{n^2} k_n''(x) + \frac{1}{n^3} k_n'''(x) + \frac{1}{n^4} k_n^{(4)}(x)$. It is shown that $k_n(x)$ converges to a function $k(x)$ which satisfies the differential equation $k'(x) = k(x) + k''(x) + k'''(x) + k^{(4)}(x)$.

References

1. E. T. Whittaker, *A Treatise on the Theory of Functions*, 2nd ed., Cambridge University Press, 1927.
2. E. T. Whittaker, *A Treatise on the Theory of Functions*, 2nd ed., Cambridge University Press, 1927.
3. E. T. Whittaker, *A Treatise on the Theory of Functions*, 2nd ed., Cambridge University Press, 1927.
4. E. T. Whittaker, *A Treatise on the Theory of Functions*, 2nd ed., Cambridge University Press, 1927.
5. E. T. Whittaker, *A Treatise on the Theory of Functions*, 2nd ed., Cambridge University Press, 1927.
6. E. T. Whittaker, *A Treatise on the Theory of Functions*, 2nd ed., Cambridge University Press, 1927.
7. E. T. Whittaker, *A Treatise on the Theory of Functions*, 2nd ed., Cambridge University Press, 1927.
8. E. T. Whittaker, *A Treatise on the Theory of Functions*, 2nd ed., Cambridge University Press, 1927.
9. E. T. Whittaker, *A Treatise on the Theory of Functions*, 2nd ed., Cambridge University Press, 1927.
10. E. T. Whittaker, *A Treatise on the Theory of Functions*, 2nd ed., Cambridge University Press, 1927.

The fifth part of the paper is devoted to the study of the asymptotic behavior of the sequence of functions $l_n(x)$ defined by the recurrence relation $l_{n+1}(x) = l_n(x) + \frac{1}{n} l_n'(x) + \frac{1}{n^2} l_n''(x) + \frac{1}{n^3} l_n'''(x) + \frac{1}{n^4} l_n^{(4)}(x) + \frac{1}{n^5} l_n^{(5)}(x)$. It is shown that $l_n(x)$ converges to a function $l(x)$ which satisfies the differential equation $l'(x) = l(x) + l''(x) + l'''(x) + l^{(4)}(x) + l^{(5)}(x)$. The sixth part of the paper is devoted to the study of the asymptotic behavior of the sequence of functions $m_n(x)$ defined by the recurrence relation $m_{n+1}(x) = m_n(x) + \frac{1}{n} m_n'(x) + \frac{1}{n^2} m_n''(x) + \frac{1}{n^3} m_n'''(x) + \frac{1}{n^4} m_n^{(4)}(x) + \frac{1}{n^5} m_n^{(5)}(x) + \frac{1}{n^6} m_n^{(6)}(x)$. It is shown that $m_n(x)$ converges to a function $m(x)$ which satisfies the differential equation $m'(x) = m(x) + m''(x) + m'''(x) + m^{(4)}(x) + m^{(5)}(x) + m^{(6)}(x)$.

and colour layering inherited from granite gneiss, and 3 to 8 per cent rounded megacrysts which range from 2 to 5 mm in diameter. The apparent relatively basic nature of mylonite M suggests that hornblende granite gneiss may be the parent rock. However, mylonite M is rarely in contact with hornblende granite gneiss and the dark colour of mylonite M is probably mainly a function of extreme cataclasis, and only to a secondary extent depends upon the mafic mineral content.

In thin section, mylonite M has about 3 to 15 per cent feldspar megacrysts in a finely laminated matrix of plagioclase, quartz, microcline, biotite, chlorite, white mica, and epidote, with an average matrix grain size predominantly 0.01 to 0.02 mm but ranging from about 0.005 to 0.03 mm. which texturally classifies mylonite M as cryptomylonite to mylonite. Pyrite cubes with a selvedge of hematite, authigenic, composite, euhedral grains of sphene and leucoxene, and euhedral allanite rimmed with epidote are dispersed in many samples. Mafic aggregates of chlorite, magnetite, hematite, and calcite likely represent pseudomorphism of biotite or hornblende. Plagioclase megacrysts from 0.05 to 2 mm in size are spherical to elliptical, contain a few inclusions of quartz and biotite, and are commonly highly sericitized. Microcline forms large and small megacrysts, containing a few inclusions of quartz, plagioclase, and biotite, and are generally augen- to lens-shaped. Larger microcline megacrysts are rare, range in size from 2 to 10 mm and are commonly fractured. The fractures in microcline are commonly healed with granoblastic quartz, and carbonate. In several samples the mylonitic matrix partially fills the fractures and more rarely completely fills the space between slightly displaced segments. Microcline megacrysts in a few samples are rimmed by a later generation of microcline which is probably more sodic than the core as indicated by the more intense stain of the core compared to the shell after sodium cobaltinitrite treatment. The flow structure of the matrix is defined by fine, continuous mica laminations which curve around megacrysts. Quartz is dispersed throughout the matrix as fine, polycrystalline lenticles which tend to be incipient, discontinuous, and wavy. Unstrained quartz in these lenticles indicates

that metamorphic differentiation of quartz occurred under static pressure conditions, and mimetic crystallization gives rise to lenticle formation parallel to the rock foliation. Microcline in the matrix tends to be concentrated in narrow, discontinuous, polycrystalline folia and streaks which commonly form "tails" extending from the ends of microcline megacrysts.

Mylonite M samples commonly show complex late-kinematic metamorphic effects. In summary, many of the large-size microcline megacrysts apparently formed during the terminal phases of early paracrystalline cataclasis. Local renewed growth followed and gave rise to zoned microcline megacrysts. Rejuvenated cataclasis locally produced secondary cryptomylonite and kakirite (Plate 10,a), and ruptured the large microcline megacrysts (Plate 10,c). The temperature and pressure were sufficiently high to allow plastic flowage of the mylonitic matrix between the slightly displaced megacryst fragments (Plate 10,d). In the Collins Lake area, mylonite M was permeated by K_2O which resulted in the development of potash feldspar veins and partial to complete replacement of plagioclase by microcline in both the matrix and megacrysts. Post-kinematic rupture, and fracture-fillings by quartz and calcite are the last deformational effects noted in mylonite M.

The chemical analysis of mylonite M standard sample 79 is given in Table 17. Comparison of this analysis with analyses of mylonites K and L (Table 16) shows that mylonite M is chemically similar, and, in fact, is intermediate between the two analyses, and is therefore also likely derived from biotite granite gneiss.

In summary, the hand specimen colour difference - dark reddish green to dark reddish black colour of mylonite M compared with red, greenish red, and dark greyish red colour of mylonites K and L - forms the basis of distinguishing mylonite M from mylonites K and L, and is a function primarily of finer matrix grain size in mylonite M, and in some samples, greater mafic mineral content, or both.

TABLE 17. MODAL AND CHEMICAL ANALYSES OF A MYLONITE M STANDARD
SAMPLE, BAYONET LAKE CATACLASTIC BAND

79	
Q	25
KFp	10
Pl	35
Bio	20
Chl	1
Mu	8
Ep	0.2
Cal	0.1
Zr	tr
Mag	tr
Hem	1
No. of Points	Estimate
SiO ₂	67.69
TiO ₂	0.47
Al ₂ O ₃	14.93
Fe ₂ O ₃	4.43
MnO	0.08
MgO	1.92
CaO	2.27
Na ₂ O	3.26
K ₂ O	3.49
L.O.I.	1.10
P ₂ O ₅	0.11
Total	99.75

(Chemical analysis by G. Schmitz)

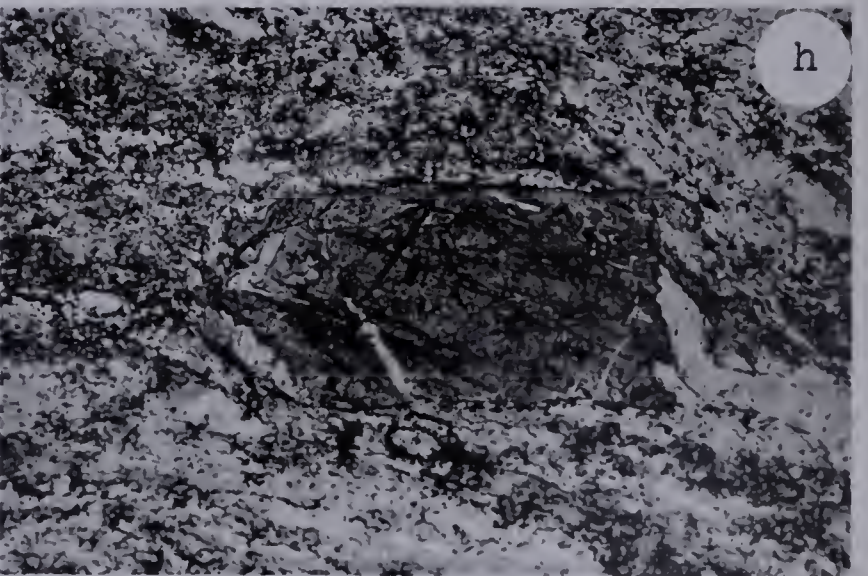
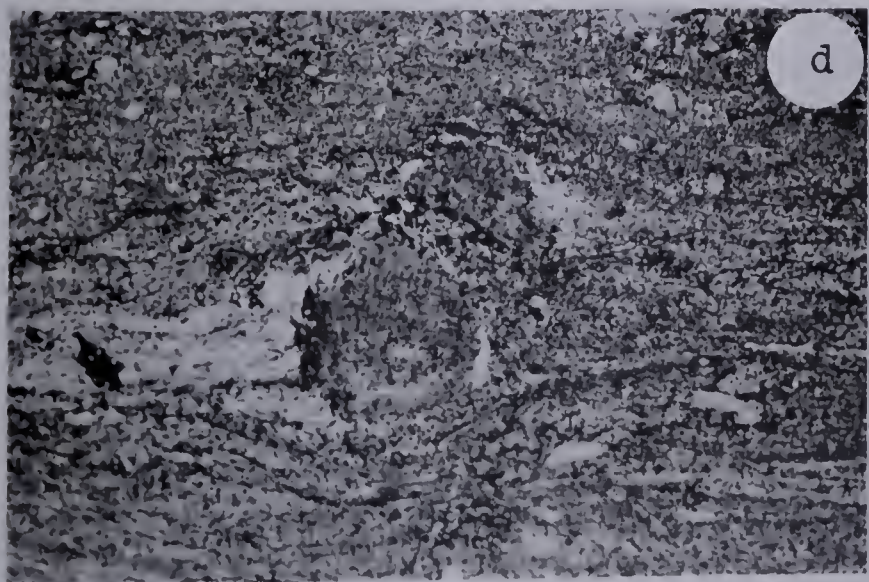
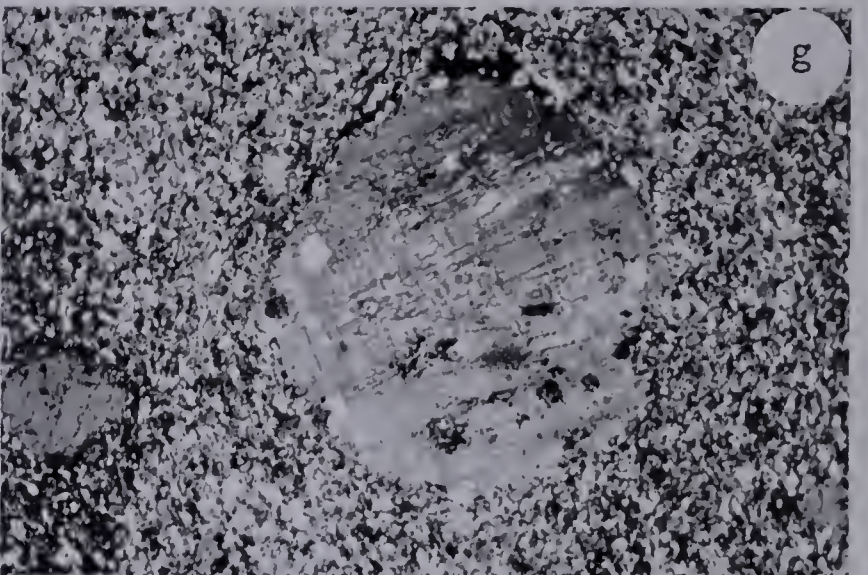
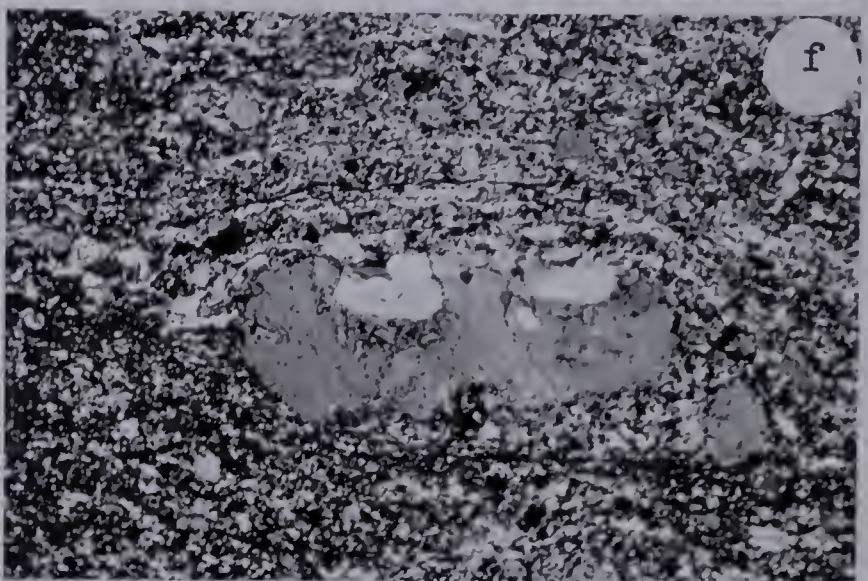
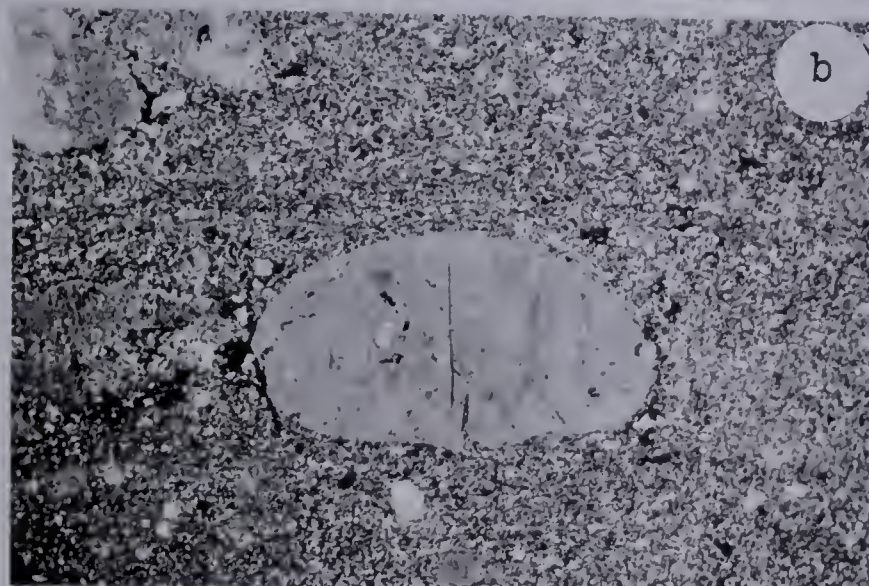
PLATE 10

MYLONITE M

- a. Mylonite. Sample XII-d, hand specimen. Dark-coloured rock with many small feldspar porphyroclasts in a finely laminated matrix. Note the narrow kakirite band with numerous breccia fragments which are derived from the enclosing mylonite and cryptomylonite. Kakirite is developed along the right side of the cryptomylonite layer.
- b. Ultramylonite. Standard sample 79, photomicrograph. Elliptical microcline porphyroclast with plagioclase and quartz inclusions, in a typical ultramylonite matrix. Crossed nicols, x 10.
- c. Mylonite gneiss. Sample XV-e, photomicrograph. Large-size elliptical microcline porphyroclast with fractures filled with granoblastic quartz and calcite. Crossed nicols, x 10.
- d. Mylonite. Sample XV-d, photomicrograph. A highly sericitized plagioclase porphyroclast in a pulverized, well-laminated matrix. The porphyroclast grades imperceptibly into the matrix. Note that the porphyroclast is broken and the matrix flows between the 2 segments. Plane light, x 10.

MIXED MYLONITE

- e. Blastomylonite. Sample III-j, photomicrograph. A large-size elliptical microcline megacryst with quartz inclusions. The spotted appearance of the megacryst is due to imperfect staining. Crossed nicols, x 10.
- f. Hornblende blastomylonite. Sample III-f, photomicrograph. Microcline porphyroclast with irregular margins and deep indentations filled with quartz. This porphyroclast is likely a rock fragment. Crossed nicols, x 10.
- g. Mylonite. Sample III-g, photomicrograph. A spherical megacryst of rod perthite with quartz inclusions. Crossed nicols, x 10.
- h. Mylonite gneiss. Sample IX-j, photomicrograph. A euhedral porphyroblast of metamict allanite with a small apatite inclusion at the left end. The matrix is well laminated and thoroughly recrystallized. Plane light, x 25.



Metasedimentary Mylonites

Considerable difficulty is experienced in the field distinction of many metasedimentary mylonite hand specimens from mylonite M by virtue of the dark colour, but the common schistose and siliceous character, and rusty weathered surfaces make many metasedimentary mylonites distinctive. A two-fold subdivision into mylonites N and O corresponds to the biotite schist and quartzite rock-units, respectively. However, a complete textural and mineralogical gradation exists between biotite schist and quartzite, which is carried over into the derived mylonites.

Mylonite N

Several north-trending bands and lenses of mylonite N are mapped adjacent to or within mylonite K, north of Bayonet Lake, and the largest band measures 2,000 feet by 1 mile and extends beyond the Northwest Territories boundary. Scattered lenses of mylonite N are found east of Bayonet Lake, enclosed in mylonite K or L.

Mylonite N is slaty to schistose with few feldspar megacrysts and quartz augen. Slaty fragments broken perpendicular to the foliation are aphanitic and flint-like. In thin section, the matrix is too fine-grained for quantitative study, and qualitative study only is possible. Small, elliptical to augen-shaped plagioclase, quartz and microcline porphyroclasts are enclosed in a finely laminated matrix (Plate 11,b) of white mica, quartz, biotite, chlorite, pyrite, and presumably feldspar. The white mica in parallel orientation and continuous layers is recrystallized to give a uniform interference colour within each layer. One chemical analysis of mylonite N is given in Table 18, and for comparative purposes, the modal and chemical analyses of chlorite schist from a fault zone along the axis of Waugh Lake (Watanabe, 1961) is also presented. The chemical analyses are similar, and the mineralogy of chlorite schist is qualitatively similar to mylonite N; thus, it is likely that

PLATE 11

MYLONITE N

- a. Cryptomylonite. Field photograph. Finely laminated weathered surface, with bulbous quartz megacryst.
- b. Cryptomylonite. Standard sample 66, photomicrograph. Note the highly micaceous matrix with small quartz porphyroclasts. Crossed nicols, x 10.

MYLONITE O

- c. Mylonite. Sample XII-i, photomicrograph. Typical mylonite texture. Note the elliptical mylonite porphyroclast in the right-center. Potash feldspar veins are concordant and discordant with the foliation in the left one-half of the photomicrograph. Crossed nicols, x 10.
- d. Kakirite. Standard sample 70, photomicrograph. Angular, microscopic and megascopic quartz and feldspar fragments in a pulverized, unlaminated matrix. Quartz fragments are predominantly microcrystalline aggregates. Crossed nicols, x 10.
- e. Cryptomylonite breccia. Sample XII-j, photomicrograph. Angular, megascopic breccia fragments cemented by vein quartz. Note the finely laminated, porphyroclastic nature of the breccia fragments. Plane light, x 10.
- f. Cryptomylonite breccia. Sample XII-j, photomicrograph. Angular cryptomylonite breccia fragments cemented by vein quartz. Note the former presence of a cavity, successively filled by a drusy lining of inward projecting comb quartz crystals and then calcite. Plane light, x 10.
- g. Mylonite gneiss. Sample XII-m, photomicrograph. Euhedral tourmaline crystal broken into four segments by flowage of the matrix. Plane light, x 25.
- h. Mulonite. Sample XII-0, photomicrograph. Tourmaline porphyroblast showing extensive sericite pseudomorphism. Plane light, x 25.

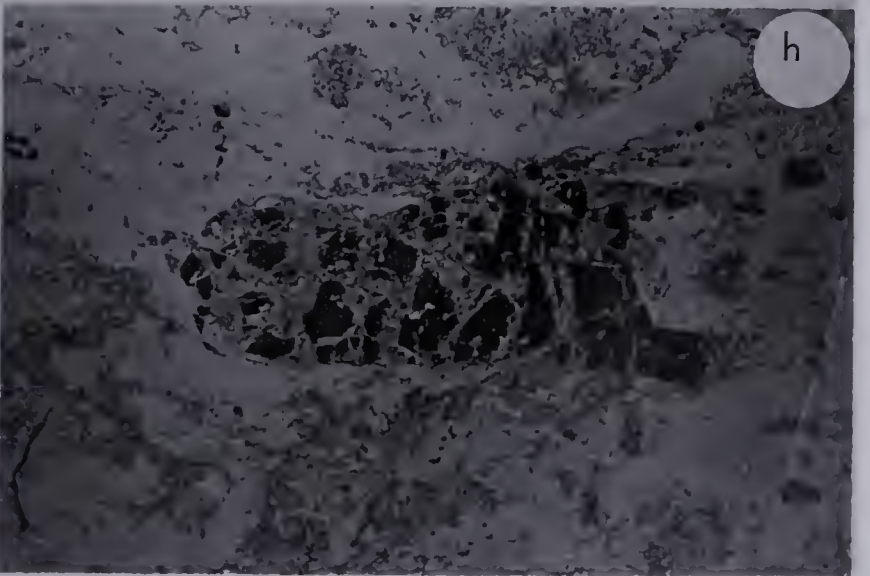
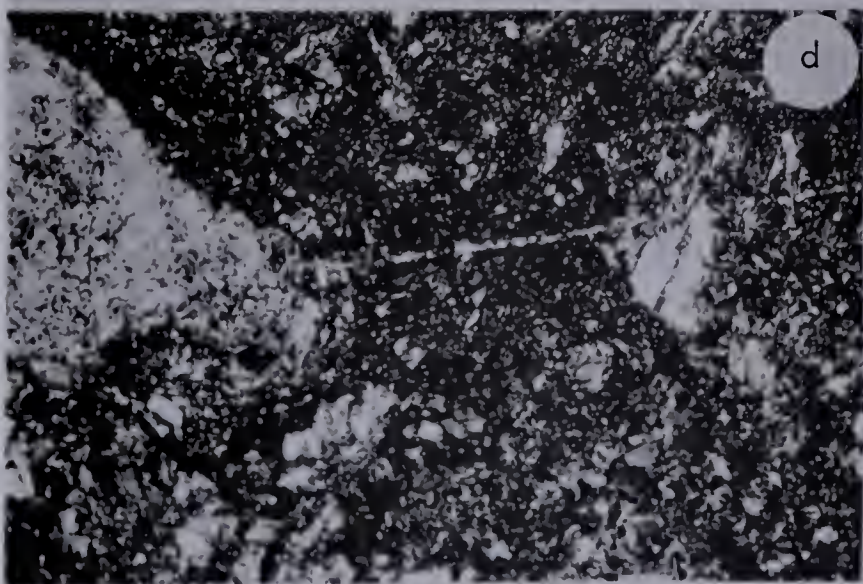
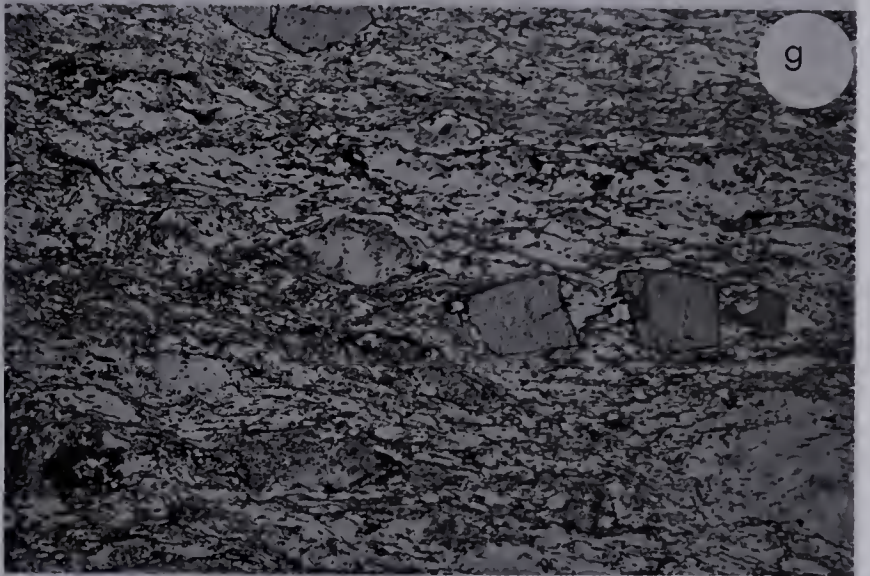
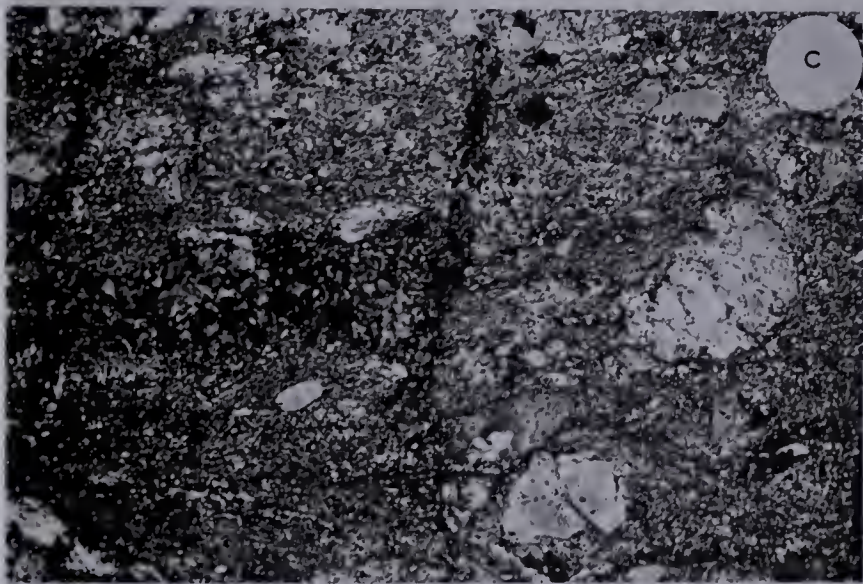
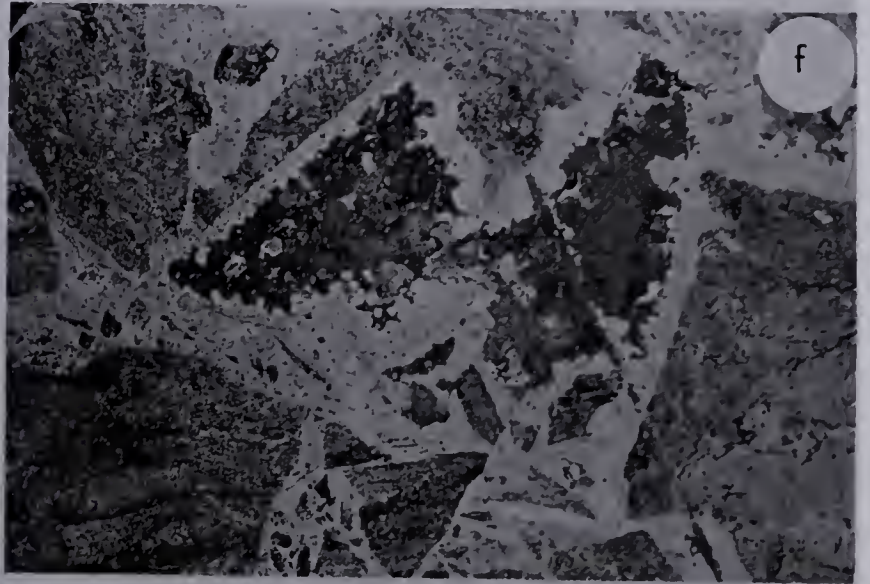
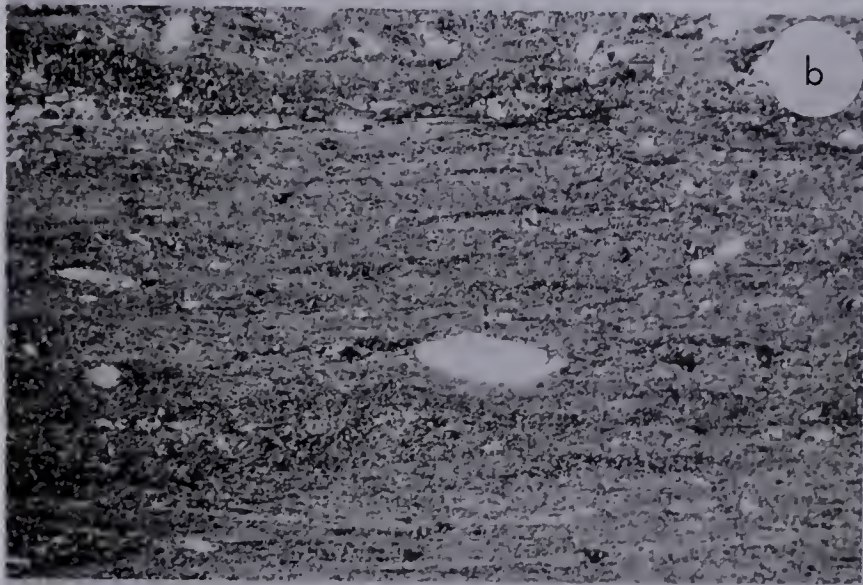
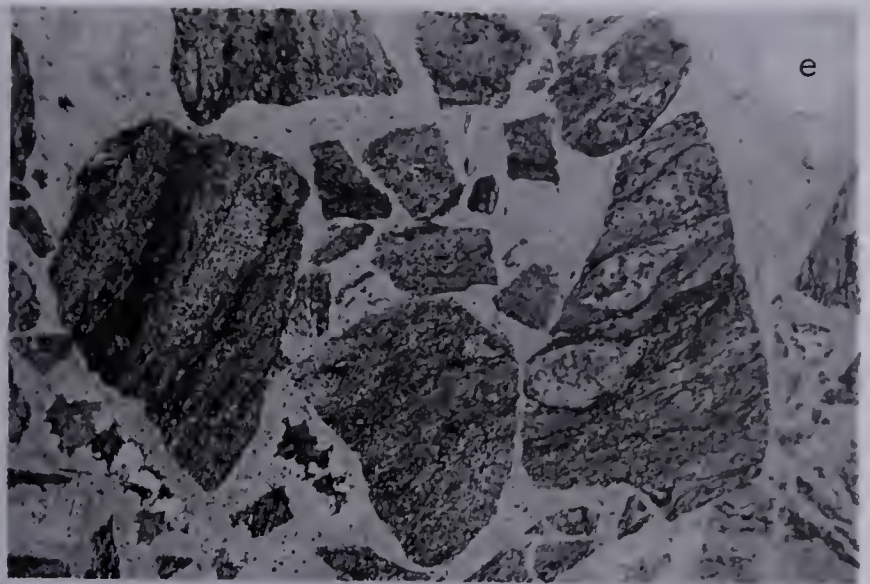


TABLE 18. MODAL AND CHEMICAL ANALYSES OF A MYLONITE N STANDARD
SAMPLE, BAYONET LAKE CATACLASTIC BAND

66		*
Q	x	36.8
Pl	x	0.5
Chl	x	8.7
Mu	x	50.8
Mag	-	3.4
Hem	x	-
Py	x	-
No. of Points	-	1,000
SiO ₂	68.75	67.93
TiO ₂	0.65	0.46
Al ₂ O ₃	15.44	16.10
Fe ₂ O ₃	4.61	6.43
MnO	0.02	0.05
MgO	1.73	1.66
CaO	0.50	0.25
Na ₂ O	0.20	0.56
K ₂ O	4.72	3.67
L.O.I.	2.79	2.89
P ₂ O ₅	0.08	0.08
Total		

(Chemical analysis by G. Schmitz)

x mineral present

* Chlorite schist, Waugh Lake (Watanabe, 1961).
Sample number 60-717-4. Chemical analysis by
H.A. Wagenbauer.

the modes would be similar.

Biotite schist. Few layers and lenses of biotite schist are found in the Bayonet Lake area, and the two main lenticular bodies are located about 1 mile east of Bayonet Lake. Biotite schist and mylonite N form isolated bodies, and thus no transitional contacts were observed.

Biotite schist may be interlayered with pure and impure quartzite, phyllite, phyllonite, sericite schist, hornblende schist, and amphibolite. Feldspathic stringers are common, and parallel the foliation of the enclosing rocks. Mapping is based on the predominant lithology in single outcrops, but the scale of mapping prohibits a refined breakdown of the metasedimentary rocks, and a two-fold grouping into quartzite and biotite schist has been adopted. The predominance of phyllitic and schistose rocks designates a biotite schist lithology, and large amounts of siliceous to feldspathic rocks determine the quartzite lithology.

Garnet is uncommonly developed in biotite schist, and mixed metasedimentary rocks comprising the bands in the adjoining Andrew Lake, North map-area, just to the east contain appreciable muscovite, garnet, cordierite, sillimanite, and rare andalusite, a mineral assemblage which is transitional between the sillimanite-almandine subfacies of the almandine amphibolite facies, and the hornblende hornfels facies (Fyfe, Turner, and Verhoogen, 1958, p. 211). The assemblage muscovite - cordierite-andalusite is diagnostic of the hornblende hornfels facies, whereas the sillimanite-garnet association is characteristic of the sillimanite-almandine subfacies of the almandine amphibolite facies.

Mylonite O

Three northerly-trending mylonite O bands up to 2,000 feet wide and more than 1 mile long are found north of Bayonet Lake. Two of the three bands grade into quartzite, and the third is enclosed by mylonite M.

The cataclastic character of equigranular, highly siliceous metasedimentary

rocks may be readily missed in the absence of schistosity and stretched feldspar porphyroclasts. Impure quartzite north of Bayonet Lake tends to be biotitic and feldspathic, and the derived mylonite is typically porphyroclastic, with elliptical to lenticular feldspar porphyroclasts in an aphanitic matrix which is dark grey to black, or green on fresh surfaces. Wavy, micaceous laminations and indistinct colour banding are present in most samples.

In thin section, mylonite 0 is composed of 0.5 to 3 mm plagioclase and potash feldspar megacrysts, and rock fragments in a finely laminated matrix (Plate 11, c) with average grain size from 0.005 to 0.03 mm and comprising plagioclase, quartz, microcline, white mica, biotite, chlorite, and epidote. Microcline is restricted to megacrysts in many samples. Plagioclase porphyroclasts are spherical to elliptical, contain few biotite and quartz inclusions, and are rarely found among the largest feldspar megacrysts. Microcline and microcline perthite form elliptical to augen-shaped megacrysts with sutured grain margins, and contain numerous inclusions of biotite, quartz, and plagioclase. Rock fragments have a fine-grained matrix with feldspar porphyroclasts, and some represent highly recrystallized mylonite (Plate 11, c). White mica aggregates in fine laminations show uniform extinction. Tourmaline forms up to 8 per cent of several samples from the band that extends north from Collins Lake, and appears as bluish green, zoned, euhedral crystals 0.3 to 1 mm in diameter, with one rounded porphyroblast 4 mm in diameter. The pleochroic formula is $O = \text{bluish green}$, and $E = \text{brownish yellow}$ which corresponds to either schorl or chromium tourmaline (Winchell and Winchell, 1951, p. 467). Rarely, sericite is pseudomorphous after tourmaline (Plate 11, h). Single grains are commonly fragmented and displaced (Plate 11, g), or rarely sheared, which indicate that tourmaline crystallized under conditions of plastic flowage of the matrix and abated shearing stress. Calcite is commonly intermingled with tourmaline grains and fills pressure shadows at the ends of feldspar megacrysts, which suggest that calcite and tourmaline are coeval and were introduced during the late-kinematic stage

of metamorphism.

Local development of kakirite in mylonite 0 bands is demonstrated by standard sample 70 located 1 mile north of Bayonet Lake. Thin section study reveals a breccia consisting of angular plagioclase partly replaced by potash feldspar, microcline, and polycrystalline quartz fragments enclosed in a cryptocrystalline matrix of quartz, plagioclase, chlorite and abundant interstitial potash feldspar (Plate 11, d). The chemical analysis (Table 19) indicates abnormally high K_2O for a rock which is obviously siliceous in hand specimen, and potash metasomatism is likely responsible for the features observed under the microscope. Kakirite probably results from rapid oscillatory movements in an environment of high hydrostatic pressure, which in the above sample is accompanied by potash metasomatism.

Post-kinematic deformation has brecciated the rocks in the central part of the mylonite 0 band north of Collins Lake. Breccia fragments are not apparent in hand specimen, but cut and polished rock slabs, and thin sections show the true character of the rock: felsic, porphyroclastic, finely laminated mylonite fragments up to 20 mm in diameter are randomly oriented and enclosed in fine-grained quartz and sparry calcite (Plate 11, e, f). The openings within brecciated mylonite 0 were incompletely filled by vein quartz, and the remaining cavities were successively filled by comb quartz and sparry calcite. These features are indicative of local, post-kinematic, reactivated movement in rocks at a high level in the crust.

Chemical analyses of two mylonite 0 samples are given in Table 19. Comparison of mylonite 0 and quartzite analyses is not practical by virtue of the highly inhomogeneous nature of these rock-types and by the lack of analyses of quartzite from the study area.

Quartzite. Quartzite is a major rock-type in the study area, and forms major bands and lenses in the Bayonet Lake area. Two of the quartzite bands north of Bayonet Lake are adjacent and grade into mylonite N.

TABLE 19. MODAL AND CHEMICAL ANALYSES OF MYLONITE O STANDARD
SAMPLES, BAYONET LAKE CATACLASTIC BAND

	67	68	70	Average
Q		20	25	23
KFp		8	35	22
Pl		35	35	35
Bio		10	-	5
Chl		0.5	5	3
Mu		25	-	13
Ep		0.5	0.5	0.5
Cal		0.2	-	0.1
Zr		tr	-	tr
Sph		0.3	-	0.2
Lx		0.1	0.5	0.3
Hem		tr	2	1
Py		0.5	2	1
No. of Points		Estimate	Estimate	-
SiO ₂	70.26		69.07	69.67
TiO ₂	0.31		0.44	0.38
Al ₂ O ₃	14.86		13.27	14.07
Fe ₂ O ₃	2.11		3.37	2.74
MnO	0.04		0.04	0.04
MgO	0.88		3.01	1.95
CaO	1.57		2.02	1.80
Na ₂ O	3.94		1.33	2.64
K ₂ O	3.69		7.28	5.49
L.O.I.	1.05		1.08	1.07
P ₂ O ₅	0.11		0.05	0.08
Total	98.82		100.96	99.93

(Chemical analyses by G. Schmitz)

Garnetiferous, feldspathic, and biotitic quartzite, and smaller amounts of biotite schist are the major lithologies in the quartzite bands; minor rock constituents comprise pure quartzite, sericite schist, hornblende schist, phyllite, phyllonite, and amphibolite. Iron-stained weathered surfaces are typical of the metasedimentary band. Granitic (quartzo-feldspathic) material is common as stringers, lenses and bands that parallel the foliation. Feldspar porphyroblasts are common and generally range from 5 to 20 mm.

The metamorphic minerals in the metasedimentary rocks, and the facies classification are discussed under the biotite schist section.

CHAPTER THREE

MAGNETIC SUSCEPTIBILITY

General Comments

The exposed Precambrian Shield in northeastern Alberta has been aeromagnetically surveyed, and aeromagnetic maps (Geological Survey of Canada, 1964) are available on the scale of one inch to one mile.

Godfrey (Godfrey and Baadsgaard, 1962) has outlined the structural and geologic history of the Precambrian rocks in northeastern Alberta, and a broad correlation has been demonstrated between the structural - lithologic framework and aeromagnetic patterns in the Andrew and Bayonet Lake areas.

Regional Aeromagnetic Study

Parts of four aeromagnetic maps (Geophysics maps 2892G, 2893G, 2903G, and 2904G) are used in the compilation of aeromagnetic data for the thesis area (Map 1). Cataclastic rock bands and faults are superimposed on the simplified aeromagnetic map.

Aeromagnetic relief ranges from about 61,300 gammas to about 62,700 gammas. High aeromagnetic response (greater than 62,000 gammas) generally corresponds to regions of relatively unsheared biotite and hornblende granite gneiss. Three main regions of low aeromagnetic response are noted: (i) The extreme southwest to west aeromagnetic low corresponds to Arch Lake granite; (ii) the Charles Lake-Alexander Lake anomaly corresponds to the main region of the Charles Lake crush zone; and (iii) the northeast anomaly corresponds to the Bayonet Lake mylonite band. In general, the cataclastic rocks correlate with regions of low to intermediate aeromagnetic response regardless of the nature of parental rocks. In the region from Bayonet Lake to Pans Lake, the configuration of a mylonite band along the west side

of the elongate, aeromagnetic trough suggests that the mylonite zone has a steep easterly dip; however, a wide, continuous metasedimentary-rock band immediately east of the mylonite band (map-sheet 5) accounts for the observed aeromagnetic phenomenon, and dip estimation of the mylonite zone is not feasible.

In principle, aeromagnetic response is a function of both magnetic susceptibility and residual magnetism. However, Watkins (1961) has shown that the aeromagnetic response of rocks in the Bayonet Lake area is essentially a function of magnetic susceptibility since the contribution of residual magnetism is negligible. Thus, the laboratory determination of magnetic response on rock samples from north-eastern Alberta becomes much simpler in that only magnetic susceptibility need be measured. This approach is employed in detailed magnetic susceptibility studies of rocks in the Ashton Lake, Bayonet Lake, and Charles Lake areas.

Susceptibility Study of Area XI, Ashton Lake

In the Ashton Lake area, two northeast trending major faults are defined on the basis of lithology, air photo interpretation, and contoured aeromagnetic maps. The granite gneiss region cut by these faults in the northeast section of Ashton Lake was selected for detailed study (Fig. 3). Brecciation, silicification, and local mylonitization are notable in the immediate region of the fault zone.

The contoured aeromagnetic map shows an abrupt break in the northerly trending aeromagnetic high and indicates a "demagnetization" effect of the granite gneiss in the region of the fault zone. A continuous, wide metasedimentary rock band east of Ashton Lake contributes to the width of the aeromagnetic trough created by the fault zone.

Demonstration of "demagnetization" was attempted by measuring magnetic susceptibility on a suite of rock specimens located along the crest of the aeromagnetic highs and through the aeromagnetic trough (Fig. 3). A certain amount of lithologic uniformity is achieved by the selection of rock samples from a relatively

narrow band of granite gneiss. Supplementary petrologic effects in the region of faulting are noted in the mineralogy and fabric of thin sections of the cored samples.

Sample Preparation

A 2.5 inch long core was obtained, wherever possible, from fifteen samples of the granite gneiss band which included - eleven biotite and hornblende granite gneisses, three feldspathic amphibolite gneisses, and one mylonite. The rocks were clamped in a jaw vice and cored with a one inch diamond core bit mounted on a drill press. Varying resistance to the diamond bit was encountered, the highly siliceous rocks offering the most resistance.

Measurement of Susceptibility

The MS-3 Susceptibility Bridge, manufactured by the Geophysical Specialties Company of Hopkins, Minnesota was used to make the measurements. The rock core is inserted into an open coil, causing a change of inductance which disturbs the balance of the bridge. Restoration of the balance provides a measure of the susceptibility. The reading obtained is then corrected for variations in diameter and length of the specimen.

The graph for determining susceptibility is provided with the instrument and is stated to be applicable to specimens of the same diameter as the open coil, and at least 4 inches in length.

For specimens of smaller diameter than that of the open coil, the correction is:

$$K_U \times \frac{1.413}{D^2}$$

where K_U = uncorrected susceptibility

D = diameter of specimen in inches.

Since all cores are one inch in diameter, the diameter correction is $K_U \times 1.413$.

For specimens less than 2.5 inches in length, Watkins (1961) constructed a length-correction curve (Fig. 2) employing data from two long cores of samples coll-

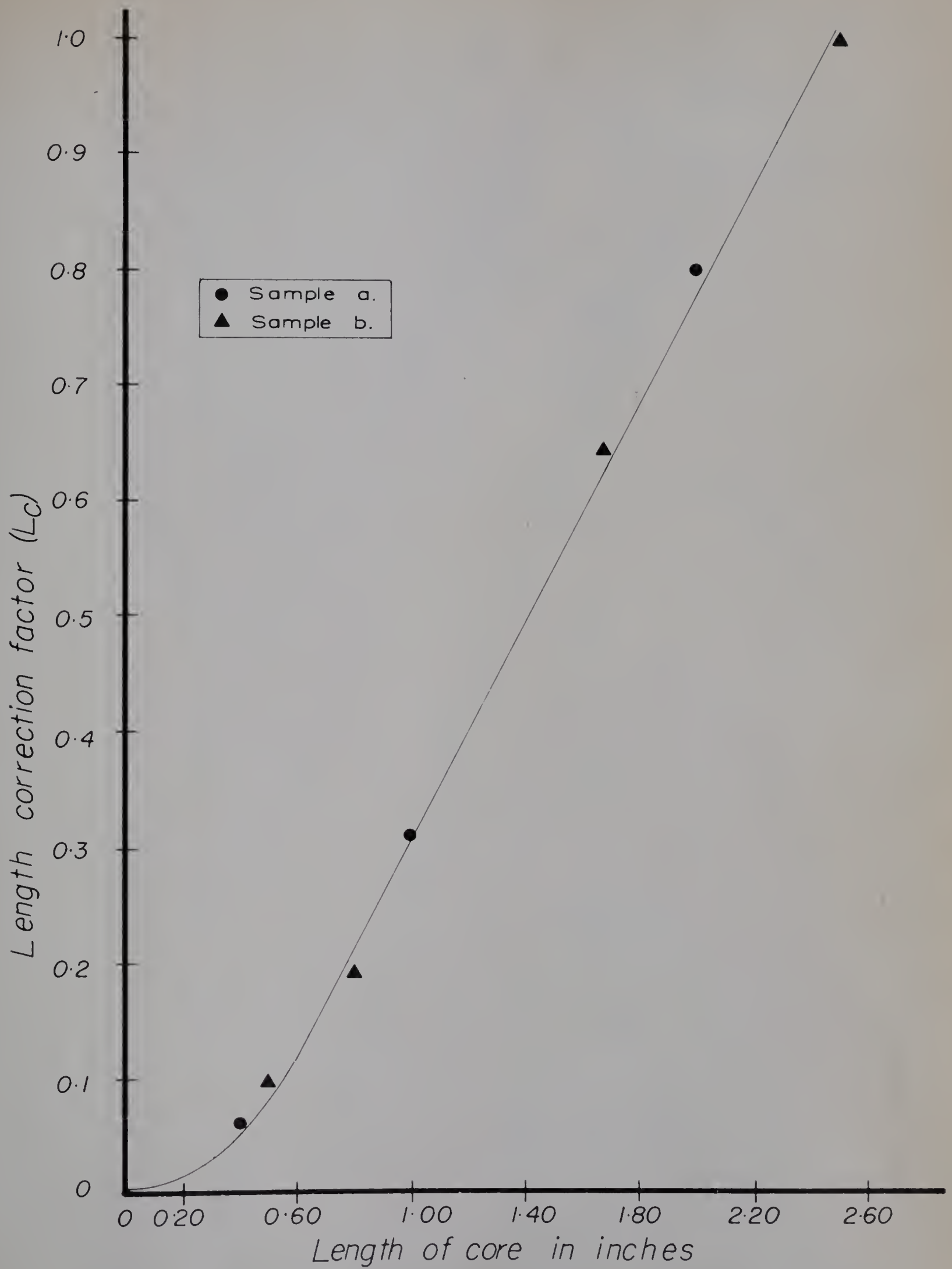
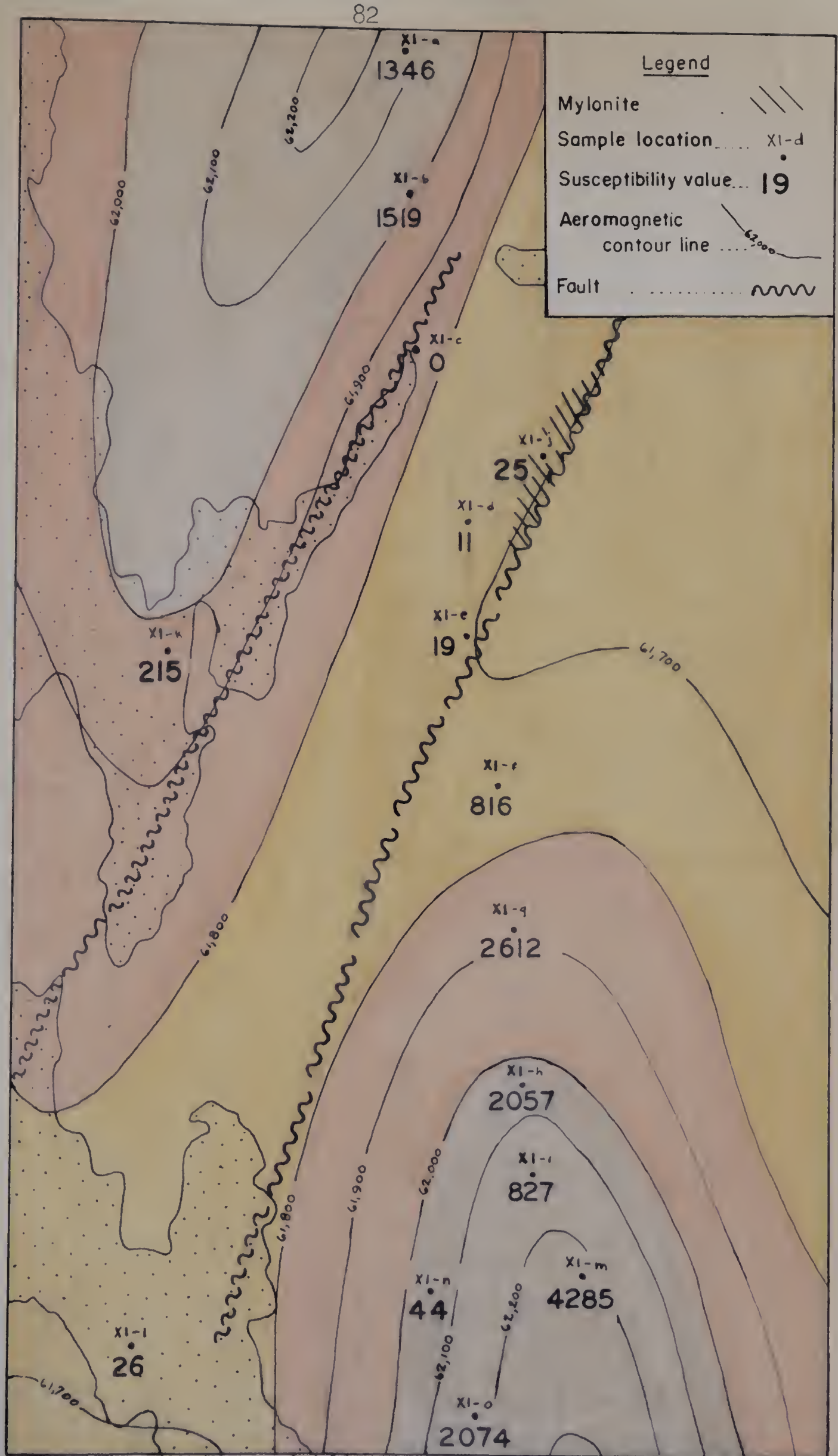


Fig.2. Correction curve for different lengths of core



Scale: 4 inches to 1 mile

Figure 3. Aeromagnetic anomaly and sample location map, area XI, Ashton Lake.

TABLE 20. SUSCEPTIBILITY DATA OF SAMPLES FROM AREA XI, ASHTON LAKE

Sample Number and Field Classification	ΔR	K_u-6 $\times 10^{-6}$ c.g.s.		L_c L_c and D_c		K_c-6 $\times 10^{-6}$ c.g.s.	Opaque Minerals			Thin Section Examination	
							Mag	Heml	Py		Lx
XI-a Biotite Granite Gneiss	276	922	2.40	0.97	1.46	1346	1	tr	tr	-	Fine-grained, strained quartz blebs, highly altered.
XI-b Biotite Granite Gneiss	332	1,109	2.53	1.03	1.37	1519	1	tr	tr	-	Fine-grained, highly altered.
XI-c Biotite Granite Gneiss, Mylonitic	0	0	2.06	0.82	1.72	0	tr	1	tr	-	Fine-grained, recrystallized mylonite, quartz lenticles, highly altered.
XI-d Biotite Granite Gneiss, Mylonitic	2	5.68	2.09	0.83	1.71	11	-	1	-	-	Fine-grained, recrystallized mylonite, quartz lenticles, highly altered.
XI-e Biotite Granite Gneiss	4	13.4	2.44	0.99	1.43	19	tr	1	-	-	Fine-grained, quartz lenticles moderate alter- ation.
XI-f Biotite Granite Gneiss	138	461	2.03	0.80	1.77	816	1	1	-	-	Fine-grained, moderate alteration.
XI-g Biotite Granite Gneiss	432	1,443	2.00	0.78	1.81	2612	1	tr	tr	-	Medium-grained, highly altered.

TABLE 20. (CONTINUED)

Sample Number and Field Classification	ΔR			$K_u \times 10^{-6}$ c.g.s.			Combined L_c L_c and D_c			$K_c \times 10^{-6}$ c.g.s.	Opaque Minerals			Thin Section Examination
XI-h Granite Gneiss	296	989	1.78	0.68	2.08	2057	1	1	-	-	-	-	-	Fine-grained, highly altered.
XI-i Hornblende Granite Gneiss	163	544	2.31	0.93	1.52	827	1	0.5	0.5	-	-	-	-	Fine-grained, moderately altered.
XI-j Felsic Ultramylonite	2	6.68	1.16	0.38	3.72	25	-	tr	-	-	-	-	-	Very fine-grained, highly crushed, quartz lenticles, highly altered.
XI-k Hornblende Granite Gneiss	45	150	2.44d	0.99	1.43	215	0.3	0.2	0.5	-	-	-	-	Fine-grained, incipient shearing, quartz lenticles, highly altered.
XI-l Biotite Granite Gneiss	4	13.4	1.89	0.73	1.94	26	tr	tr	0.5	-	-	-	-	Fine-grained, highly altered.
XI-m Feldspathic Amphibolite Gneiss	844	2,819	2.31	0.93	1.52	4285	2	tr	0.5	-	-	-	-	Fine-grained.
XI-n Feldspathic Amphibolite Gneiss	9	30.1	2.38	0.97	1.46	44	-	0.5	1	-	-	-	-	Fine-grained.
XI-o Feldspathic Amphibolite Gneiss	434	1,450	2.44	0.99	1.43	2074	1	-	tr	-	-	-	-	Fine-grained, moderate alteration.

Legend for Tables 1, 2, 3, 4

ΔR --- difference in readings on the susceptibility bridge when the coil is empty and when it is occupied by a rock core.

K_u --- uncorrected susceptibility

K_c --- corrected susceptibility

L --- length of sample in inches

L_c --- length correction factor

D_c --- diameter correction factor

Mag --- Magnetite in per cent

Hem --- Hematite in per cent

Py --- Pyrite in per cent

Lx --- Leucoxene in per cent

tr --- trace

ected in the Bayonet Lake area, and this curve is used for all specimens from the Precambrian Shield in northeastern Alberta.

$$\text{Thus, } K_c = K_u \times \frac{1.413}{\text{length correction factor}} \quad \text{where } K_c = \text{corrected susceptibility for different length and diameter}$$

Discussion of Results

The susceptibility readings show a general trend from high to low values as the fault zone (marked by two faults) is approached from the aeromagnetic high regions (Fig. 3). Five samples lie within the fault zone and have susceptibility values ranging from 0 to 26. Eleven samples outside of the fault zone have susceptibility values ranging from 44 to 4280. One of these samples has an anomalously low-susceptibility value that is explained on the basis of petrographic data. Omitting the one anomalous value, the range of susceptibility for samples outside the fault zone becomes 215 to 4280.

Thin sections of all cored specimens were studied and the petrography of the samples is presented in chapter four. Only the opaque minerals and brief textural data are reported in this geophysical section.

The high susceptibility rocks are fine- to medium-grained and are relatively unsheared. They usually contain one per cent or more of magnetite, rarely contain pyrite, and hematization is slight to moderate.

Low-susceptibility rocks within the fault zone are very fine to fine-grained, with evidence of intense shearing. Magnetite is absent or occurs in trace amounts only, and hematite is the predominant opaque mineral.

It is apparent that a significant magnetite content in rocks produces high susceptibility, and relatively increasing amounts of pyrite and hematite is associated with the low-susceptibility rocks. Hematization is commonly noted in faults of this region and the fault-zone rocks of the Ashton Lake area show this phenomenon distinctly.

Amongst the three amphibolites, sample XI-n has a very low susceptibility which is explained by the absence of magnetite. Further, the presence of actinolite along with pale green hornblende reflects the bulk chemistry of the parental rock which was most likely a calcareous, impure sedimentary rock.

Extensive alteration is common in most of the samples, and cataclasis is slight to absent except for the fault-zone rocks which in general are moderately to highly crushed. The crush-zone rocks show the effects of silicification as evidenced by quartz veinlets and lenses on both macro and micro scales.

Notable features of the Ashton Lake fault zone are the brecciation, minor development of mylonite, hematization, silicification, and extensive hydrothermal alteration.

Susceptibility Study of Area III, Charles Lake

Two peninsulas located in the northern part of Charles Lake are underlain by crushed rocks. The excellence of exposures, stratigraphic control, the variety of rock types, and detailed sample coverage of the southern peninsula make it suitable for detailed study.

The two cataclastic rock types, hornblende cataclasite and mylonite L form a composite crush zone (Fig. 4). Foliated hornblende granite and minor hornblende granite gneiss lie along the western margin of the crush zone. Biotite granite gneiss lies to the north and hornblende granite gneiss lies to the east of the crush zone. This cataclastic rock band has minimum dimensions of 900 feet by 8,000 feet and contrasts markedly with the small-scale cataclastic effects associated with faulting in area XI, Ashton Lake.

The contoured aeromagnetic map (Fig. 4) shows only a slight indication of decreased aeromagnetic response in the region of the crush zone. A finger-shaped northward extension of the 62,100 gamma contour line suggests a decreased aeromagnetic response due to shearing. However, the presumed limited extent of the cata-

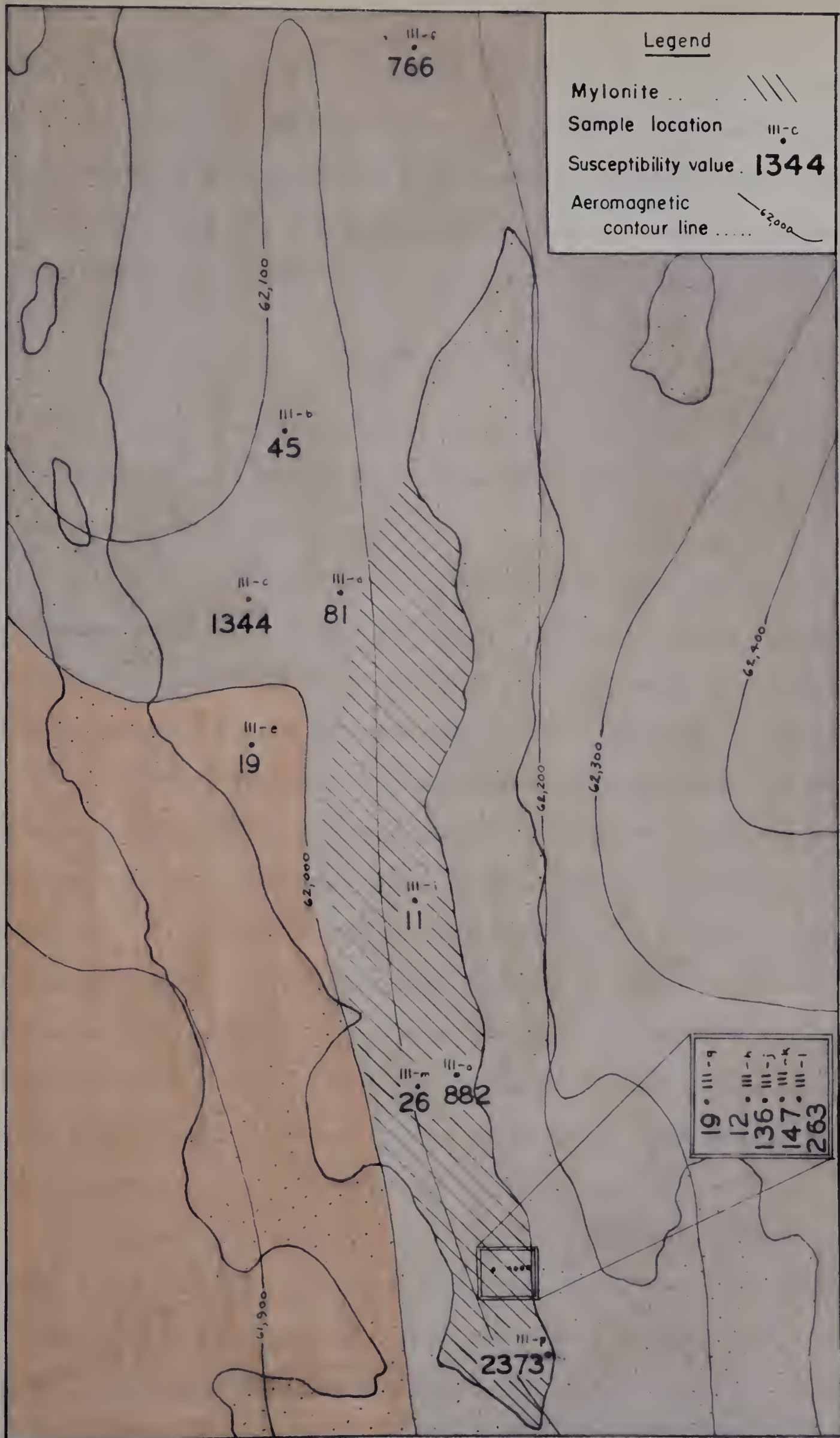


Figure 4. Aeromagnetic anomaly and sample location map, area III, Charles Lake.

clastic band produces only gentle aeromagnetic relief, and the abrupt change of rock type through a short distance does not permit effective interpretation and understanding of aeromagnetic data of the peninsula and adjacent area. Therefore, the aim of this study has resolved into a determination of susceptibility values of each of the rock types and an examination of their relationship to geologic events.

Discussion of Results

On the basis of megascopic and microscopic examination, the geophysical samples can be arranged into five distinct rock groups (Table 21), of which three groups represent crushed rocks.

The foliated hornblende granite samples occur within a large, relatively homogeneous rock body. The susceptibility of five foliated hornblende granite samples have a wide range of values some of which could be expected from the difference in mafic mineral content in hand specimen. However, thin section data explains susceptibility values on the basis of degree of cataclasis and the opaque mineral constituents. Shearing has played an important role in the history of the foliated hornblende granite and transitional stages of crushing are detected from a fabric study. Sample III-b is relatively unsheared but has a very low susceptibility which is accounted for by the negligible amount of magnetite. High susceptibility values of samples III-c and III-f are explained by the significant amounts of magnetite, negligible hematization, and an intermediate degree of shearing. Low susceptibility values of samples III-d and III-e are due to the negligible amount of magnetite, an advanced stage of hematization, and intense shearing.

The hornblende cataclasite rock-type is most notable for a nearly massive fabric and hornblende porphyroclasts. Four hornblende cataclasite specimens of different grain size were selected to examine the effect of grain size on susceptibility. The results indicate that susceptibility decreases with grain size. Thin section study reveals that magnetite is common in high-susceptibility samples, and the

TABLE 21. SUSCEPTIBILITY DATA OF SAMPLES FROM AREA III, CHARLES LAKE

Sample Number and Field Classification	ΔR			$K_u \times 10^{-6}$ c.g.s.			Combined L_c and D_c		$K_c \times 10^{-6}$ c.g.s.	Opaque Minerals			Thin Section Examination
III-b Foliated Hornblende Granite	8	26.7	2.13	0.84	1.69	45				tr		-	Medium-grained, very slightly sheared, moderately altered.
III-c Foliated Hornblende Granite	230	7.68	2.06	0.81	1.75	1344				0.3	-	-	Fine- to medium-grained, moderately granulated.
III-d Foliated Hornblende Granite, Sheared	15	50.1	2.22	0.88	1.61	81				tr	tr	tr	Very fine-grained, highly crushed.
III-e Foliated Hornblende Granite, Sheared	2	6.68	1.44	0.51	2.77	19				tr	tr	-	Very fine-grained, quartz lenticles, highly crushed.
III-f Foliated Hornblende Granite	156	521	2.38	0.96	1.47	766				0.5	tr	-	Fine-grained, moderately granulated.
III-g Mylonite L	4	13.4	2.44	0.98	1.44	19				-	-	-	Very fine-grained, highly crushed.
III-h Mylonite L	2	6.68	2.00	0.78	1.81	12				-	0.4	-	Very fine-grained, quartz lenticles, highly crushed.
III-i Mylonite L	2	2.68	2.25	0.90	1.57	11				-	0.2	-	Very fine-grained, highly crushed.

TABLE 21. (CONTINUED)

Sample Number and Field Classification	K _u -6 x 10 ⁻⁶			Combined L _c and D _c		K _c -6 x 10 ⁻⁶ c.g.s.	Opaque Minerals			Thin Section Examination
	ΔR	L	L _c	L _c	L _c		Mag	Hem	Py	
III-j Mixed Mylonite	25	83.5	2.19	0.87	1.63	136	tr	-	0.5	Very-fine grained, highly crushed.
III-k Mixed Mylonite	208	695	2.16	0.86	1.65	1147	0.7	0.2	0.1	Very fine-grained, moderately crushed, moderately altered.
III-l Hornblende Cata- clasite	54	180	2.38	0.97	1.46	263	0.5	1	-	Very fine-grained, highly recrystallized then crushed again, moderately altered.
III-m Hornblende Cata- clasite	5	16.7	2.25	0.90	1.57	26	tr	0.1	0.1	Very fine-grained, slightly recrystallized, slightly altered.
III-o Hornblende Cata- clasite	151	5.04	2.06	0.81	1.75	882	1	-	-	Fine-grained, highly re-crystallized, slightly altered.
III-p Grey Hornblende Granite	4.8	1396	2.09	0.83	1.70	2373	1	tr	-	Very fine-grained, highly recrystallized.

degree of hematization increases in lower-susceptibility rocks. Extensive hematization and chloritization of samples III-m and III-l indicate that hydrothermal solutions were active along reactivated movement zones in the hornblende cataclasite. Hematization of these two hand specimens is quite evident by their red coloration.

Amongst the three crush-rock types of area III, Charles Lake, mylonite L is least recrystallized. Samples from this rock-type have a uniformly low susceptibility and thin sections show extensive chloritization and hematization effects which are related to the demagnetization process.

Samples III-j and III-k are from the narrow transitional zone between mylonite L and hornblende cataclasite and apparently result from the mixing of these two adjacent rock types with subsequent recrystallization. Susceptibility values are intermediate between the uniformly low values of mylonite L and the high values of hornblende cataclasite. Abundant magnetite in sample III-k is responsible for the high susceptibility value, whereas the lower susceptibility of sample III-j is the result of magnetite oxidation to hematite.

Susceptibility Study of Area V, Charles Lake

The elongate aeromagnetic trough (less than 61,600 gammas) on the east side of Charles Lake (Map 1) corresponds to the combined areas of granite F and mylonite P. Whether the aeromagnetic low is a function of crushing or is due to similar low-aeromagnetic responses of both rock types needs to be tested by susceptibility determinations.

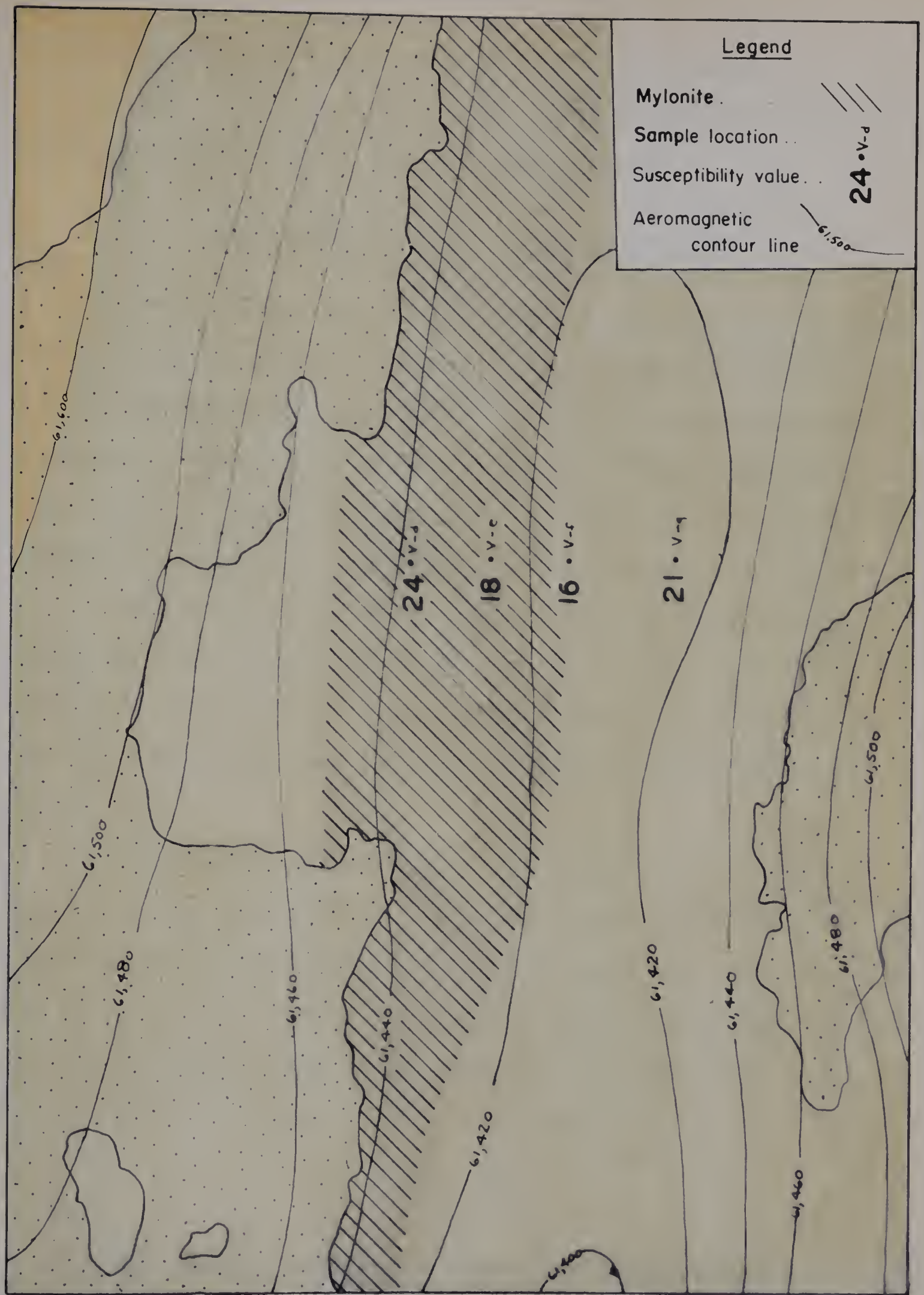
Four samples which grade from granite F to mylonite P were selected for study (see Fig. 5).

Discussion of Results

All samples have very low-susceptibility values which indicates that the aeromagnetic trough is unquestionably due to the uniformly low-aeromagnetic response of

TABLE 22. SUSCEPTIBILITY DATA OF SAMPLES FROM AREA V, CHARLES LAKE

Sample Number and Field Classification	ΔR	$K_u \times 10^{-6}$ c.g.s.			Combined L_c and D_c		$K_c \times 10^{-6}$ c.g.s.	Opaque Minerals			Thin Section Examination
		L	L_c	L_c	L_c	D_c		Mag	Hem	Py	
V-d Mylonite P	3	10.0	1.58	0.58	2.44		24	-	tr	tr	Very fine-grained, highly crushed, moderate alteration.
V-e Mylonite P	2	6.68	1.44	0.53	2.67		18	-	tr	tr	Very fine-grained, highly crushed, moderate alteration.
V-f Mylonite P	2	6.68	1.59	0.59	2.39		16	-	tr	tr	Very fine-grained, highly crushed, quartz lenticles, moderate alteration.
V-g Granite F	3	10	1.75	0.66	2.14		21	tr	tr	-	Fine-grained, crushed grain margins, moderate alteration.



Scale: 4 inches to 1 mile

Figure 5. Aeromagnetic anomaly and sample location map, area V, Charles Lake.

both map-units and is not a function of the degree of mylonitization.

Study of the opaque minerals in thin section indicates trace amounts of hematite and leucoxene, whereas magnetite is virtually absent.

Susceptibility Study of Area XIV, Bayonet Lake

Areas underlain by granite gneiss typically correspond to areas of relatively high aeromagnetic response. The Bayonet Lake area is underlain predominantly by granite gneisses within which a major mylonitic band is developed along the east side of the lake, extending to both the north and south. The regional aeromagnetic map (Map 1) indicates a broad aeromagnetic trough coincident with the mapped extent of mylonites, and aeromagnetic relief increases rapidly away from the disturbed zone.

In this area XIV, an attempt is made to examine the change in magnetic susceptibility that accompanies mylonitization of granite gneiss. The mylonite band parallels the regional strike of the enclosing granite gneiss, and the study samples represent a cross section through the band of mylonite and enclosing granite gneiss (Fig. 6).

Watkins (1961) studied the magnetic properties of a suite of rocks in the Bayonet Lake area and demonstrated that the total measured magnetic intensities correlate closely with values derived from the aeromagnetic map. The present study area XIV makes use of five samples and magnetic susceptibility data from the Bayonet Lake mylonite band studied by Watkins. Sample XIV-e is added to give a more complete coverage of this wide mylonite band in the present study.

Discussion of Results

The six samples illustrate moderately well the demagnetization accompanying fault activity in granite gneiss. Petrographic analyses indicate that all the samples have been highly crushed with the exception of sample IV-f. Hydrothermal solutions have thoroughly altered both the mafic minerals and feldspar. Abundant hematite

results from both alteration of magnetite and the introduction of iron-rich solutions along fractures. Extensive fault activity across the entire width of the sampled area is responsible for low susceptibility values.

Three samples adjacent or within the mylonite zone have susceptibility values ranging from 16 to 38 c.g.s. units. Two of these samples (XIV-c, XIV-e) are well-developed mylonites, whereas the third (XIV-d) is thoroughly recrystallized. It appears that recurrent crushing of a pre-existing recrystallized mylonite without subsequent pronounced recrystallization has left lenses of uncrushed recrystallized rock (eg. XIV-d) within the mylonite band.

Three granite gneiss samples outside the mylonite zone have susceptibilities ranging from 76 to 882 c.g.s. units. The two samples west of the fault zone appear to be highly recrystallized mylonites which were later subjected to minor crushing as evidenced by slight granulation along grain margins. The sample east of the mylonite zone shows no granulation effects and is the only sample in this group containing trace amounts of hematite, whereas concentrations of hematite in other samples range from 0.2 to 4 per cent.

TABLE 23. SUSCEPTIBILITY DATA OF SAMPLES FROM AREA XIV, BAYONET LAKE

Sample Number and Field Classification	K _u × 10 ⁻⁶ R c.g.s. L L _c			K _c -6 x 10 ⁻⁶ c.g.s.	Combined L _c and D _c			Opaque Minerals				Thin Section Examination
								Mag	Hem	Py	Lx	
XIV-a Chlorite Granite Gneiss, Sheared	4	13.4	0.88	0.25	5.65	76		0.2	2	-	-	Very fine-grained, crushed then highly recrystallized, highly altered.
XIV-b Chlorite Granite Gneiss, Sheared	14	46.8	1.0	0.30	4.71	220		0.2	2	tr	-	Very fine-grained, highly crushed but highly recrystallized, moderately altered.
XIV-c Chlorite Granite Gneiss	2	6.68	0.88	0.25	5.65	38		tr	4	-	-	Very fine-grained, highly crushed, highly altered.
XIV-d Porphyroblastic Chlorite Granite Gneiss, Sheared	3	10.0	2.28	0.91	1.55	16		tr	tr	0.2	0.3	Very fine-grained, crushed but lightly recrystallized, highly altered.
XIV-e Mylonite M	6	20.0	2.65	1.10	1.28	26		tr	0.3	0.1	-	Very fine-grained, highly crushed, highly altered.
XIV-f Biotite Granite Gneiss, Sheared	176	588	2.34	0.94	1.50	882		0.5	tr	-	-	Fine-grained, strained, highly altered.

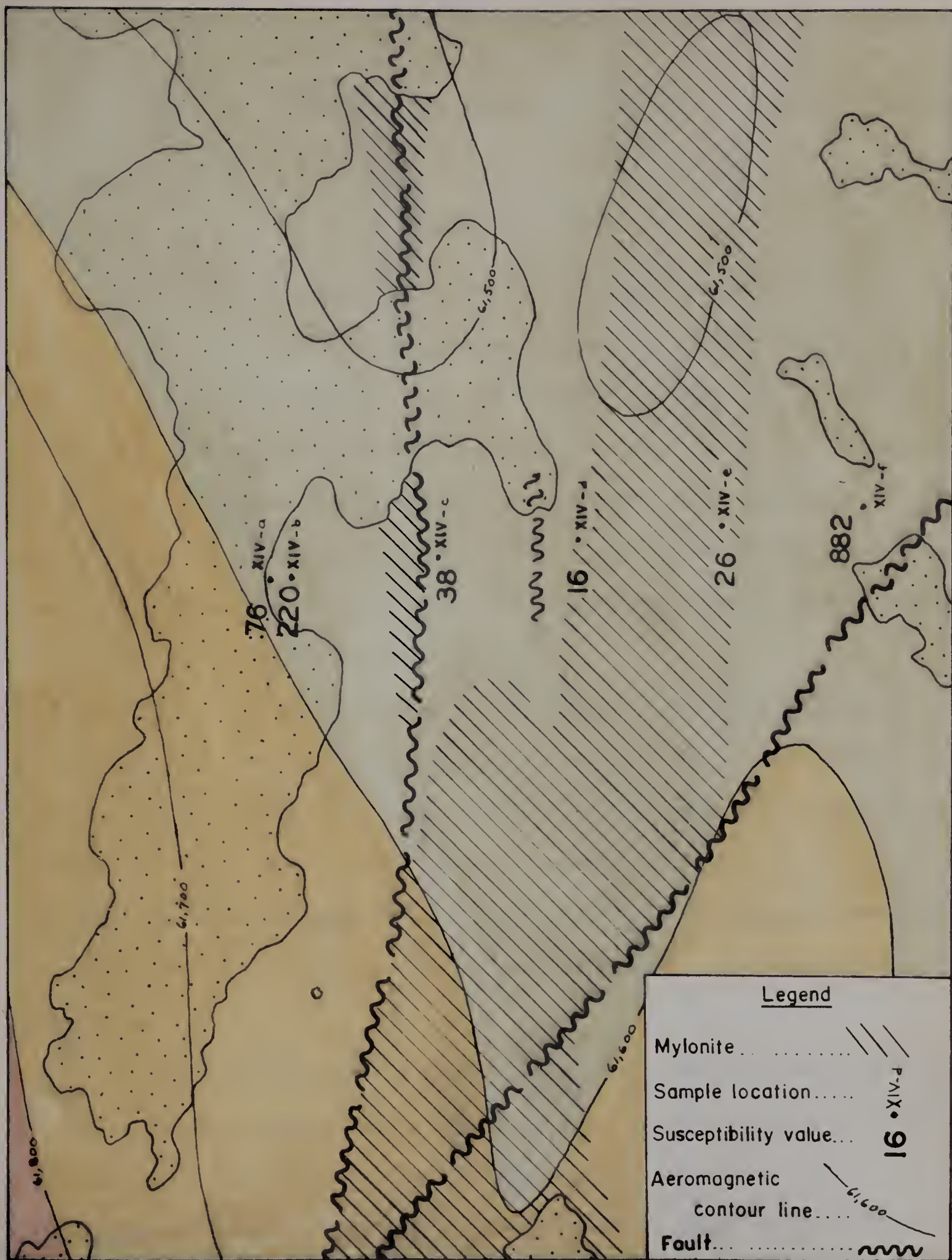


Figure 6. Aeromagnetic anomaly and sample location map, area XIV, Bayonet Lake.

CHAPTER FOUR

DETAILED PETROLOGIC STUDIES

General Statement

Rock sample suites were collected at closely spaced intervals along selected traverses through the cataclastic rocks. Many of these sample suites and a few groups of irregularly distributed samples are used for detailed examination of various petrologic aspects. Fifteen detailed study areas are located and numbered on the map-sheets, and are successively examined in a north to south and west to east sequence. The location of samples from each study area is not given on the map-sheets by virtue of the close spacing of samples, but the stratigraphic sequence and relative distance between samples are shown on graphs for each study area.

The main purpose of this chapter is to describe the changes that arise in passing from parent to cataclastically-derived rock, and attempt to confirm parent-daughter relationships where petrogenesis remains doubtful. Other aspects investigated include: the amount of mixing of adjacent mylonites in complex mylonite zones; the fate of magnetite with increasing degree of cataclasis; and change of metamorphic grade with cataclasis. Various techniques are used in these studies and a brief description of each follows.

The fine-grained matrix of crushed rocks makes quantitative modal analysis difficult and commonly impossible; as the matrix grain size approaches the thickness of the rock slice in thin section (0.03 mm) or smaller, the volume estimation of the constituent minerals become increasingly unreliable* (Chayes, 1956; Elliott, 1952). Errors

* Thorough discussion of the lower limit of thin section analysis is made in Appendix C.

in quantitative estimates are primarily due to two factors: overlap of adjoining grains with dissimilar relief; and difficulty in restricting observations to the upper surface of the rock slice. In this study, the two sources of error are subdued by the use of thin sections about 0.02 mm thick which decreases the overlap effect of adjacent grains, strong hydrofluoric acid etch which frosts the feldspars and helps to restrict observations to the upper surface of the rock section, and sodium cobaltinitrite staining of potash feldspar which also is a surface feature that aids in restricting observations to the upper plane of the rock slice. Modal analyses in this chapter represent visual estimates, unless otherwise specified, made on treated thin sections, and operator bias is effectively eliminated by obscuring the sample number of thin sections from each study area, and analysing thin sections in a random sequence. The volume estimate of minerals is presented in tables (Appendix A) and graphs (Figures 7 to 21). In the graphs, hornblende plus biotite, and chlorite plus epidote form natural pairs by virtue of their mutual association in rocks, and provide indicators of metamorphic grade.

Chemical data are based on X-ray fluorescence analyses^{**}. Only Na_2O , P_2O_5 , and loss on ignition are lacking for a complete normal silicate rock analysis. Wet chemical analyses (Chapter Two) indicate a general range of 4.5 to 6.5 per cent for $\text{Na}_2\text{O} + \text{P}_2\text{O}_5 + \text{loss on ignition}$, which, if added to the X-ray fluorescence analyses gives approximate totals of 100 ± 3 per cent for virtually all samples analysed. The cationic oxides, Fe_2O_3 , TiO_2 , MnO , MgO , and CaO , are grouped and represented as one line on the graphs by virtue of their generally sympathetic concentration; CaO is found mainly in plagioclase and epidote, whereas the other oxides are found either as components in individual mafic minerals such as hornblende,

^{**} Details of the method employed, discussion of the limitations, statistical assessment of reliability, and comparison with chemical analyses are treated in Appendix B.

biotite, chlorite, garnet, magnetite, and ilmenite, or are diadochic in these minerals.

Theoretically, a systematic change in plagioclase composition from parent to the cataclastically-derived rock would likely be observed, and would be most pronounced where basic rocks are affected. However, mylonitization is relatively rapid, and probably produces a mixture of plagioclase derived by cataclasis and neomineralization. In addition, hydrothermal and metasomatic activity tends to be irregular, and varied degrees of alteration are noted in the plagioclase within each study area. A thorough, statistical study of plagioclase composition in cataclastic rocks is required, but is beyond the scope of this thesis.

Specific gravity measurements were made on 51 samples from 5 detailed study areas. The samples were pre-wetted in distilled water to reduce the formation of air bubbles which may adhere to the rocks, and specific gravity values are corrected for variation in water temperature.

Charles Lake Studies

Area I

Thirteen samples were collected along an easterly traverse through the eastern one-half of the northernmost peninsula of Charles Lake. The rock-types encountered were hornblende granite gneiss, mylonite L, and hornblende cataclasite. The contact between hornblende granite gneiss and mylonite L is obscured by a linear, wooded trough that likely corresponds to the trace of a strike fault, whereas mylonite L grades into hornblende cataclasite through a mixed zone about 10 feet wide.

Mylonite L is distinctive in area I by virtue of the high content of potash feldspar and white mica, small amounts of mafic minerals, high SiO_2 and K_2O , and low calcemic oxides. Hornblende cataclasite typically has abundant plagioclase, small amounts of potash feldspar and hornblende, low SiO_2 and K_2O , high Al_2O_3 and calcemic oxides, and an extremely high Sr content.

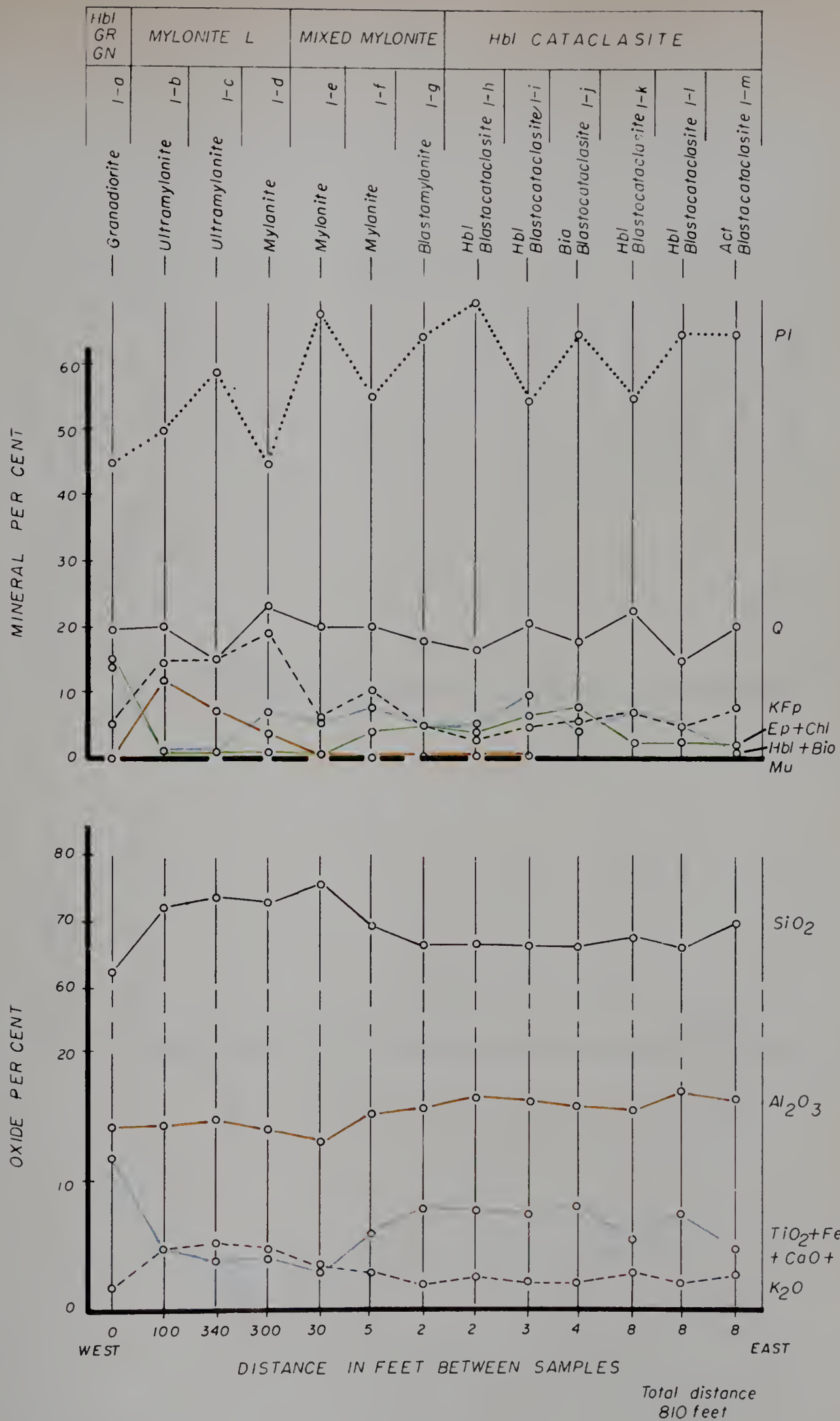


Figure 7. Petrologic profiles for samples from area I,
Charles Lake.

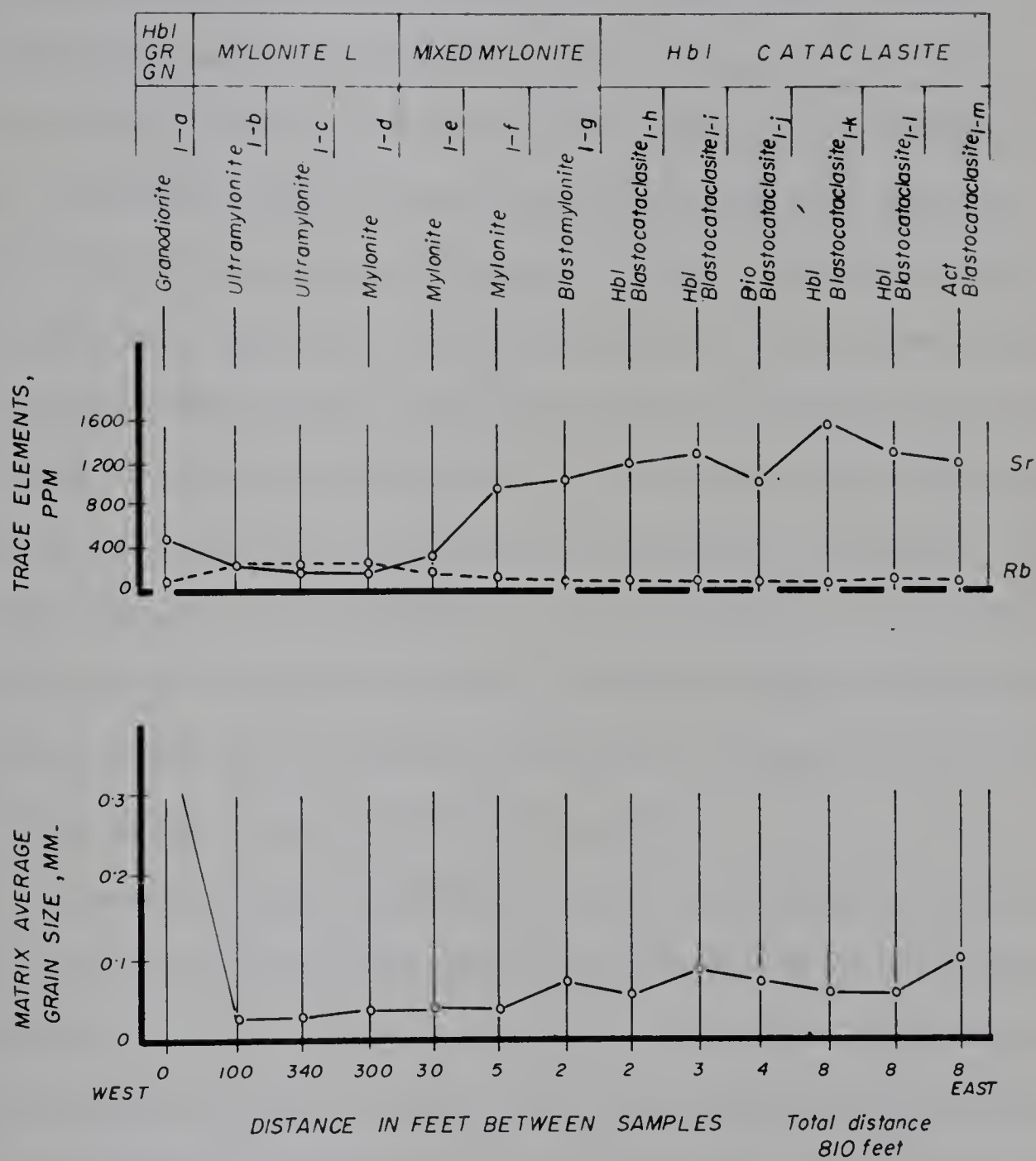


Figure 7. (Continued)

The matrix average grain size increases gradually from 0.01 to 0.02 mm in passing from mylonite L to hornblende cataclasite.

The probable derivation of mylonite L from biotite granite gneiss, and hornblende cataclasite from hornblende granite gneiss is demonstrated in chapter two. Biotite granite gneiss and hornblende granite gneiss are appreciably dissimilar, and the derived cataclastic rocks possess features that correspond to the differences in the parent rock. Hornblende granite gneiss is genetically unrelated to mylonite L, and the juxtaposition of the two rocks is attributed to faulting. Mineralogical and chemical trends, and grain size measurements indicate a gradational contact zone between mylonite L and hornblende cataclasite. The mixed zone of cataclastic rocks has an intermediate composition, and the width of the zone is an indication of the amount of intermingling of mylonite L with hornblende cataclasite during deformation. The massive, inequigranular, and crystalloblastic nature of hornblende cataclasite contrasted with the pulverized matrix, fractured and displaced porphyroclasts, and laminated structure of mylonite L indicate that hornblende cataclasite remained undeformed during a late phase of cataclasis that affected mylonite L.

The sequence of events disclosed and implied by evidence in the samples from area I may be stated: major deep-seated cataclasis during the synkinematic phase of metamorphism produced crushed rocks derived from biotite granite gneiss and hornblende granite gneiss; relaxation of stress and continued high temperature promoted the growth of feldspar porphyroblasts in mylonite L; late-kinematic dynamothermal activity ensued but was confined to mylonite L, perhaps under the influence of lubricating fluids in mylonite L.

Area II

The four islands south of the northernmost peninsula of Charles Lake are underlain by cataclastic rocks. The largest island was selected for close examination by virtue of its variety of crushed rocks and excellence of exposures. Fifteen samples were

collected at irregular intervals on an easterly traverse, and the rock-types successively encountered were mylonite K, mylonite L, hornblende cataclasite, and mylonite L. Mylonite K grades into mylonite L with increase of feldspar megacrysts, and hornblende cataclasite forms a well-delineated lens that trends northerly and measures 30 feet by 100 feet, and has a sharp contact with mylonite L.

A second phase of paracrystalline cataclasis and post-crystalline deformation have produced secondary cataclastic rocks through part of the island, and matrix grains of the western bodies of mylonite K and L are sufficiently comminuted to make quantitative estimates of the minerals virtually impossible. The renewed mylonitization has produced abundant secondary cryptomylonite and kakirite from mylonite K, and the graphs showing the chemical data for this rock-type have an irregular pattern. SiO_2 in mylonite K is exceedingly low (about 60 per cent) compared to mylonite K standard samples (about 70 per cent) and may be due to mobilization of silica during secondary mylonitization; SiO_2 increases rapidly towards the contact with mylonite L and attains a normal amount (about 73 per cent) for mylonite L. Al_2O_3 in mylonite K has an irregular distribution with a range from about 13 to 18 per cent. K_2O shows a highly irregular distribution in mylonite K with a range from 0.5 to 6 per cent, and it is likely that potash has been locally leached, and enriched in adjacent rocks. The cationic oxides curve shows considerable increase in several mylonite K samples, a feature predominantly due to high CaO which was introduced into the rock in the form of numerous epidote veins. The element Sr is exceedingly concentrated in one mylonite K sample (about two times more abundant than other mylonite K samples). The enrichment may be attributed to excessive local epidotization with consequent enrichment of Ca and geochemically similar Sr. It may be significant that the highest enrichment of Sr is found in the single kakirite sample with abundant mylonitized epidote, compared to adjacent samples of cryptomylonite with undeformed to partly sheared epidote veins.

Hornblende cataclasite and mylonite L on the east side of the island are only slightly affected by secondary mylonitization and are sufficiently coarse-grained for modal analysis. Hornblende cataclasite has undergone partial crushing during secondary mylonitization, with the development of distinct laminations in three or the four hornblende cataclasite samples resulting in secondary mylonites. Modal and chemical analyses of hornblende cataclasite samples show good correlation with data of the standard-rock specimens (chapter two), the most diagnostic features being: abundant plagioclase, minor microcline, and scattered hornblende porphyroclasts; low SiO_2 (66 per cent), low K_2O (2 per cent), high calcemic oxides (9 per cent), and extremely high Sr (1,400 ppm). Examination of the graphs shows that samples between hornblende cataclasite and mylonite L are intermediate in mineral and chemical composition. Physical mixing of these two dissimilar rocks or homogenization by ionic diffusion (or both) may have been operative through several inches to one foot. However, ionic diffusion is favoured due to the relatively abrupt contact between the two rock-units in outcrop. The survival of a small lens of hornblende cataclasite within a wide mylonite band that has experienced three episodes of cataclasis is evidence of limited mixing of adjacent rock-types during cataclasis and lends support to the validity of multiple speciation of cataclastic rocks comprising complex mylonite zones. An important stratigraphic implication is that a single distinctive parent rock-type gives rise to a correspondingly distinctive cataclastic rock-type, and either parent rock or derived rock may be used for regional correlation.

Mylonite L and hornblende cataclasite of area II are similar to the corresponding rocks of area I and represent the on-strike continuation of the cataclastic band. Two major and one minor episode of cataclasis are evident: phase 1, synkinematic deformation produced a wide band of cataclastic rocks from biotite and hornblende granite gneiss, followed by a period of subdued shearing and continued high temperature which induced the formation of microcline porphyroblasts and partial recrystallization of the matrix; phase 2, late-kinematic rejuvenation of shearing stress, combined with waning

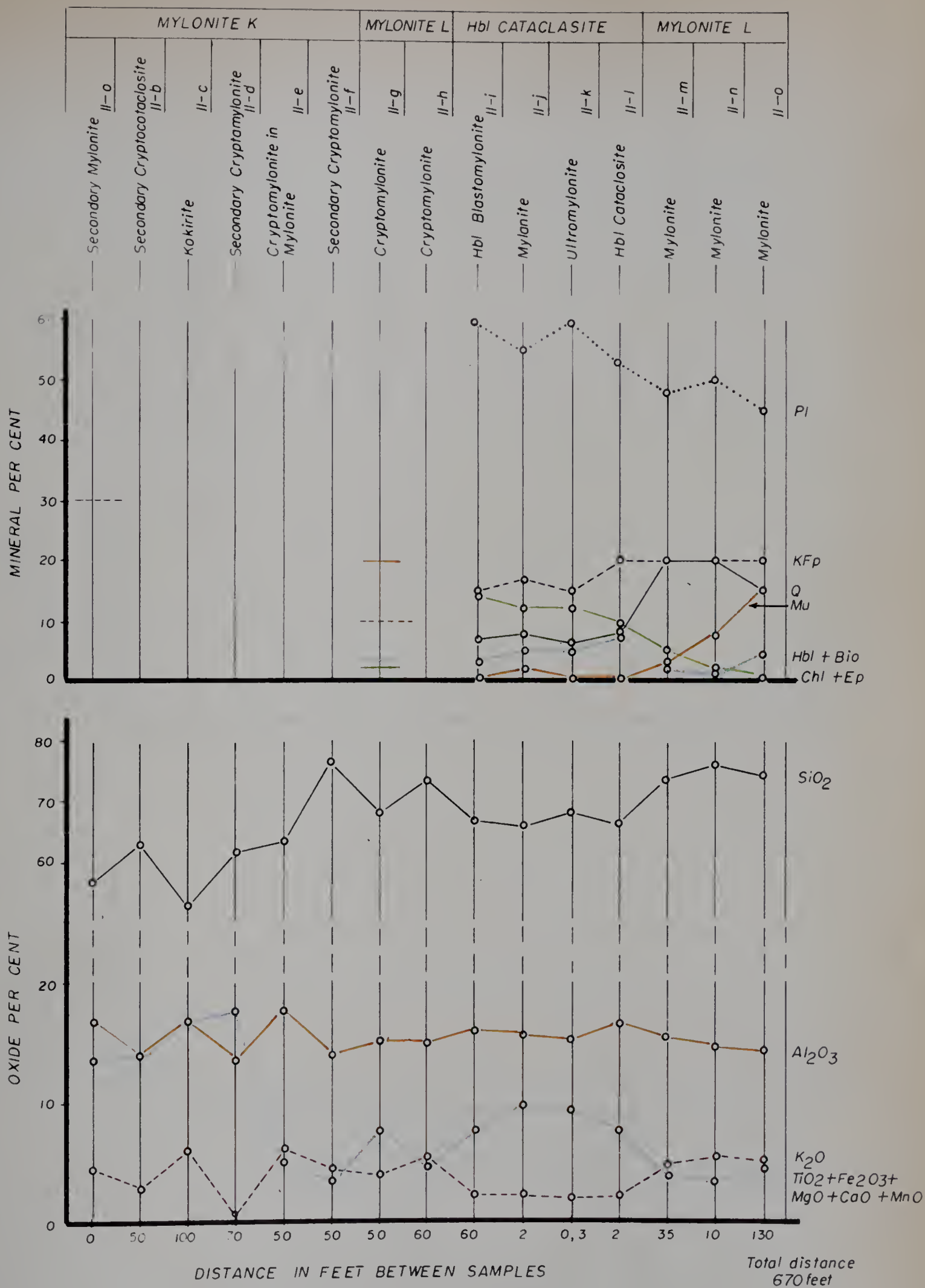


Figure 8. Petrologic profiles for samples from area II,

Charles Lake.

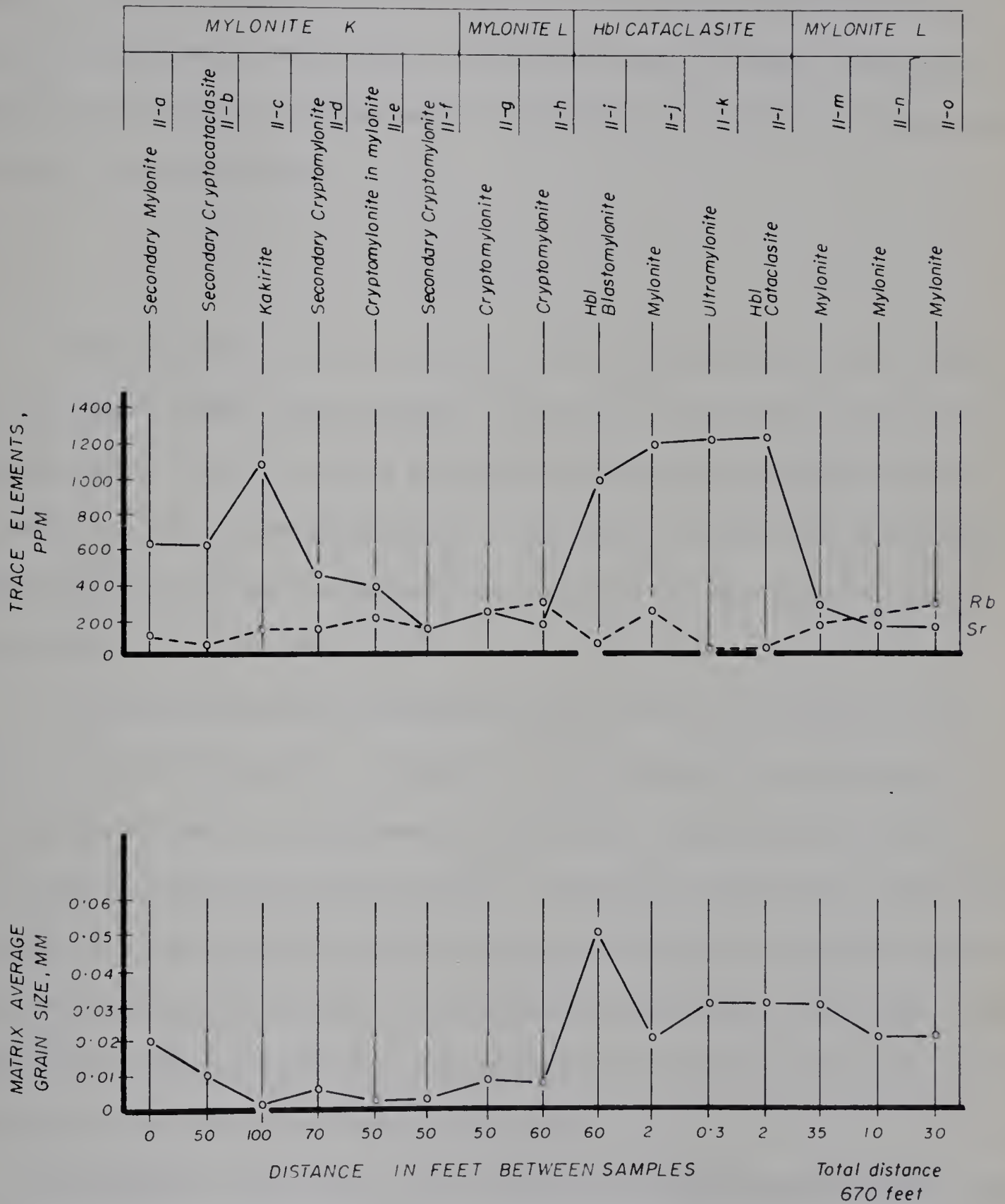


Figure 8. (Continued)

temperatures produced secondary cryptomylonite with fractured and displaced porphyroclasts that were partly filled by crushed material, with only slight recrystallization of the matrix; uplift of the rocks to a relatively shallow level was followed by the formation of open fractures later filled with epidote; phase 3, locally intense post-crystalline fault activity developed kikirite and tertiary cryptomylonite which were mobile and intrusive in places.

Area III

The second peninsula south of areas I and II, Charles Lake is partly underlain by cataclastic rocks. The remainder is composed of a minor mass of hornblende granite gneiss and a broad, elongate body of foliated hornblende granite which encloses small lenses of biotite granite gneiss. This body of foliated hornblende granite probably represents a granite syntectonically intruded concordant with the northerly structural trend of the enclosing rocks.

The general sequence of cataclastic rocks in area III is similar to that in area I: in an easterly direction, - mylonite L, mixed mylonite, and hornblende cataclasite are successively encountered. Westerly from the cataclastic band foliated hornblende granite becomes less sheared. The eastern margin of the cataclastic band is formed by the shoreline of Charles Lake, but patches of grey hornblende granite (locally developed along this eastern margin) are too small to show on the map. Hornblende granite gneiss is the prevalent rock in the terrain east of the cataclastic band but an intervening elongate bay obscures the contact.

The eighteen samples used in this study (Fig. 4) are scattered throughout the length of the peninsula. Most of the samples selected for measurement of magnetic susceptibility showed different degrees of cataclasis within each rock-type. Two hornblende granite gneiss samples from the area east of the cataclastic band have been included to examine the genetic relationship between hornblende granite gneiss and hornblende cataclasite. The different types of data derived from these samples

are plotted on graphs in which each rock-type is placed in its proper field setting, and the samples from each rock-type are generally arranged according to average matrix grain size.

The possibility that foliated hornblende granite is the parent rock of hornblende cataclasite was dispelled in chapter two, and the dissimilarity of the two rocks is unquestionably demonstrated by the configuration of the graphs: foliated hornblende granite has abundant potash feldspar and quartz, and small amounts of plagioclase, whereas hornblende cataclasite has abundant plagioclase and relatively small amounts of potash feldspar and quartz; chemically, foliated hornblende granite has 10 per cent more silica, 5 per cent less alumina, 3 per cent more potash, and about 3 per cent less ferromagnetic oxides than hornblende cataclasite; Rb and Sr are low in foliated hornblende granite, compared with prolific Sr and low Rb in hornblende cataclasite. Progressive cataclastic effects in foliated hornblende granite are noted as the contact with mylonite L is approached: the rocks become more crushed, with the development of protomylonite and mylonite; potash feldspar and quartz diminishes, and plagioclase increases; chemical changes appear to be insignificant, although a slight decrease in SiO_2 and slight increase in Al_2O_3 are indicated; Sr increases; and the specific gravity increases. Obvious changes in mineralogy are not accompanied by corresponding changes in chemistry. It is likely that the foliated hornblende granite body behaved as a closed system, and changes in mineralogy are accommodated by changes in the composition and proportion of the constituent minerals. The increase of specific gravity with increasing degree of cataclasis is likely due to the reduction of pore space; sample III-f is highly recrystallized (blastomylonite) and may have contributed to a greater specific gravity by further elimination of pore space under considerable load pressure.

Mylonite L possesses several mineral and chemical features that are intermediate between foliated hornblende granite and hornblende cataclasite. However, distinctive characteristics of mylonite L consist of negligible biotite, abundant white mica, low basic oxides, and low specific gravity (which may be deduced from the

felsic appearance of the hand specimens). Mylonite L in area III is similar to the same rocks in areas I and II.

A narrow zone of mixed mylonite is intermediate in mineral and chemical composition (particularly SiO_2 and K_2O) between mylonite L and hornblende cataclasite. A tendency to be enriched in mafic minerals, and Fe_2O_3 is reflected in the high magnetic susceptibility and high specific gravity. In addition, mixed mylonite is more readily recrystallized, resulting in coarser grain size than the adjacent cataclastic rocks. It seems feasible that mixed mylonite is the product of reaction between highly dissimilar mylonite L and hornblende cataclasite. The general features and rock association of mixed mylonite in areas I and III are similar, although the basic character is not as well developed in the former area. Incipient development of mixed mylonite is observed in area II.

Hornblende cataclasite is sufficiently recrystallized locally along the eastern margin of the band to warrant classification as grey hornblende granite. Grey hornblende granite is fine grained (0.4 mm average matrix grain size), massive, and inequigranular, with spherical to elliptical hornblende and plagioclase megacrysts. Matrix grains show highly sutured grain margins, and the plagioclase megacrysts have indented boundaries, which are the effects of thorough recrystallization. The contact with hornblende granite gneiss is obscured by the lake, but an attempt is made to demonstrate the genetic affinity of hornblende granite gneiss, grey hornblende granite, and cataclasite. Two hornblende granite gneiss samples are added to the original samples that were selected for magnetic susceptibility measurements: sample III-q is located near the tip of the deep bay, and standard-rock sample 93 is located about one mile east of the bay. Both samples are well foliated, banded, and pinkish grey in colour, and the microscope reveals an equigranular, fine- to medium-grained texture. The graphs show many systematic mineral and chemical changes in the sequence from hornblende cataclasite to grey hornblende granite and hornblende granite gneiss: decrease in plagioclase and quartz, and erratic increase of potash feldspar, and increase

of hornblende + biotite at the expense of epidote + chlorite; SiO_2 decreases markedly, Al_2O_3 decreases slightly, basic oxides increase markedly, and K_2O increases slightly; Sr is exceedingly abundant in hornblende cataclasite and related rocks, and shows a regular increase with grain size to grey hornblende granite, then decreases substantially in hornblende granite gneiss. Thus, the field association, and many characteristics of the mineral, chemical, and textural features indicate a gradational relationship among hornblende cataclasite, grey hornblende granite, and hornblende granite to gneiss. Cataclasis, therefore, has been accompanied by chemical adjustment; particularly enrichment of SiO_2 , Al_2O_3 , and Sr in the cataclasite, with some removal of calcic oxides to the mixed mylonite zone. Hornblende cataclasite and grey hornblende granite show an apparent increase in specific gravity with decrease in grain size. However, the specific gravity is related to the distribution of basic oxides, and perhaps to a lesser degree, to the average matrix grain size.

Many systematic mineral and chemical trends are noted throughout area III. These systematic changes are accounted for by a west to east sequence of three distinctive chemical groups of rocks - from highly acidic foliated hornblende granite, to acidic mylonite L, and to intermediate hornblende cataclasite and related rock-types. Also, near the interface of dissimilar rock-types cataclasis and thermodynamic disequilibrium has likely promoted mechanical mixing and ionic diffusion respectively. Nevertheless, the megascopic distinctiveness of each rock-type and their mutual contacts remain well-defined.

The tectonic history of area III may be outlined as follows: cataclasis produced mylonite L and hornblende cataclasite from biotite granite gneiss and hornblende granite gneiss, respectively. Subsequent relaxation of stress during the syntectonic stage permitted foliated hornblende granite to be intruded along the interface between mylonite L and biotite granite gneiss. Reactivated movement in the late-kinematic stage was chiefly restricted to the east side of the foliated hornblende granite body. No evidence of post-crystalline fault activity is seen in area III.

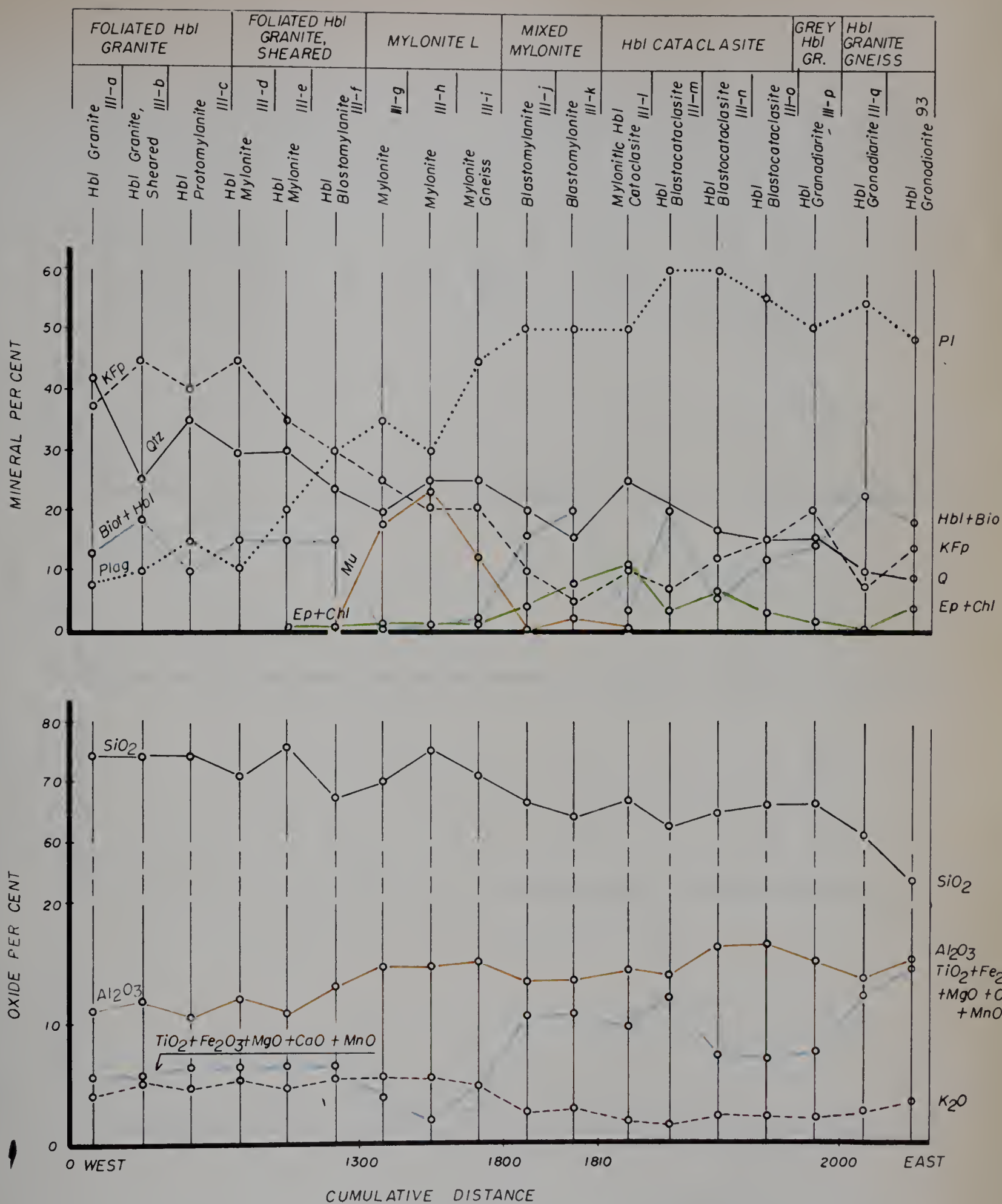
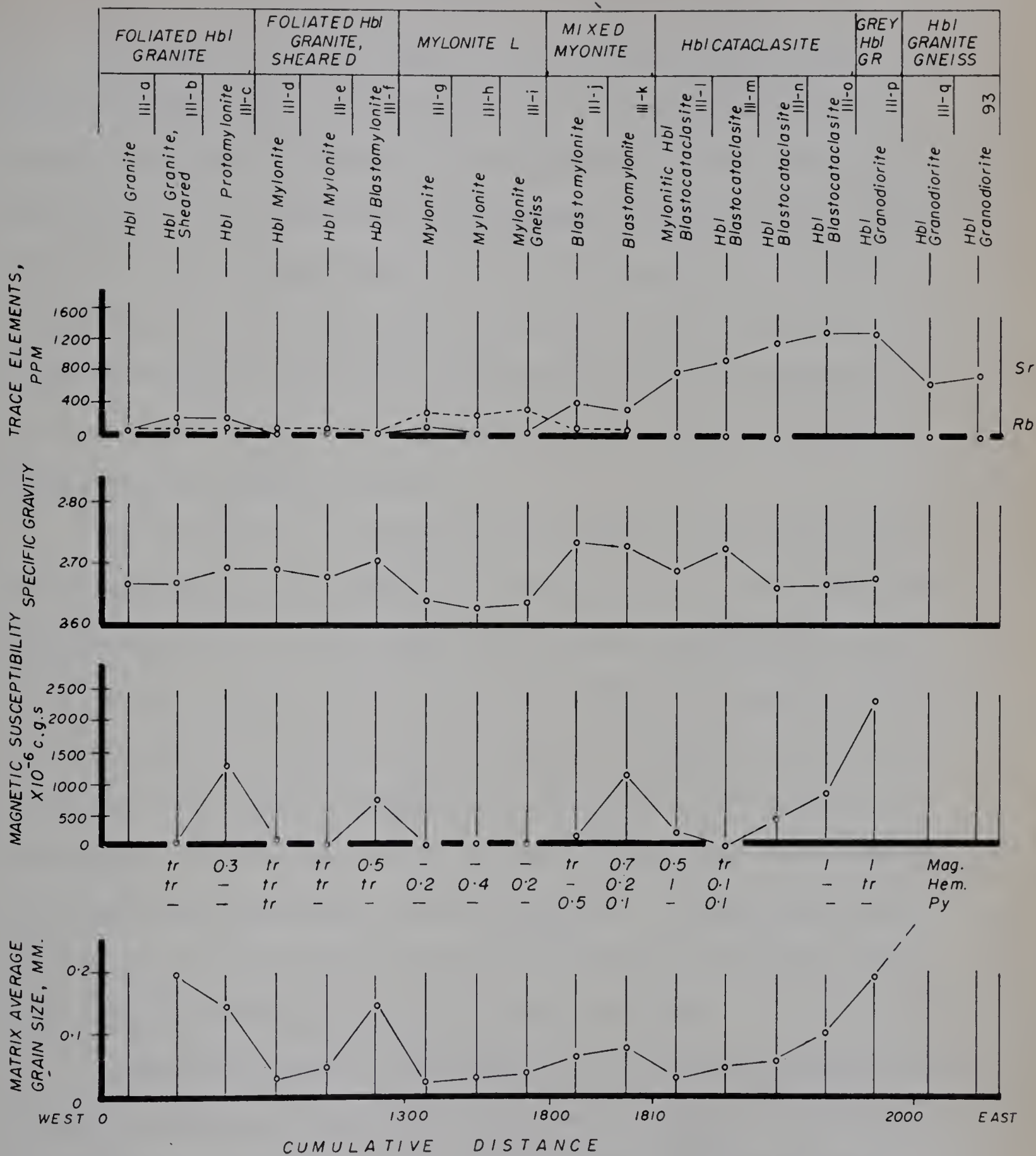


Figure 9. Petrologic profiles for samples from area III, Charles Lake.



Refer to text for explanation
of sample arrangement

Figure 9. (Continued)

Area IV

Raisin granite forms an elongate, continuous mass in the northwestern part of the Charles Lake, North map-area, and typically has numerous, 2 to 5 mm, rounded feldspar porphyroclasts that are loosely-packed in a finely-laminated, wavy chloritic matrix. The examination of hand specimens, polished rock slabs, and thin sections shows that unsheared remnants of the porphyritic parent rock and all textural gradations to typical raisin granite are present. Six samples are used to show the textural variation and the mineral and chemical changes that accompany progressive shearing. The arrangement of samples from left to right on the graphs corresponds to decreasing shear effects.

Thin sections show a continuous textural gradation from unsheared, porphyritic granodiorite to flaser granodiorite (Plate 9, f, e, c, b) with plagioclase and microcline megacrysts, and rare, sheared polycrystalline fragments persisting into the sheared phases as augen-shaped porphyroclasts. Microcline megacrysts are highly albitized (Plate 9, h). The sparsity of rock fragments in flaser granodiorite is not unexpected, as the numerous megacrysts act as mechanically stable units that individually comminute the enclosing matrix upon shearing, and leave only remnants of the matrix along the periphery of some porphyroclasts. Progressive cataclasis in the matrix is accompanied by the development of "shoestring" quartz from quartz blebs, and by comminution of quartz, plagioclase, and biotite.

Appreciable mineralogic inhomogeneity of raisin granite is demonstrated by the irregular distribution of plagioclase, quartz, and microcline. Increasing degree of cataclasis increases chlorite at the expense of biotite. The virtual absence of shear effects in sample 91 may be partly explained by its relative resistance to shearing due to low content of mica. The presence of 2 per cent garnet in sample IV-c may be due to assimilation of metasedimentary inclusions.

The chemical analysis of standard sample 84 presented in chapter two is not

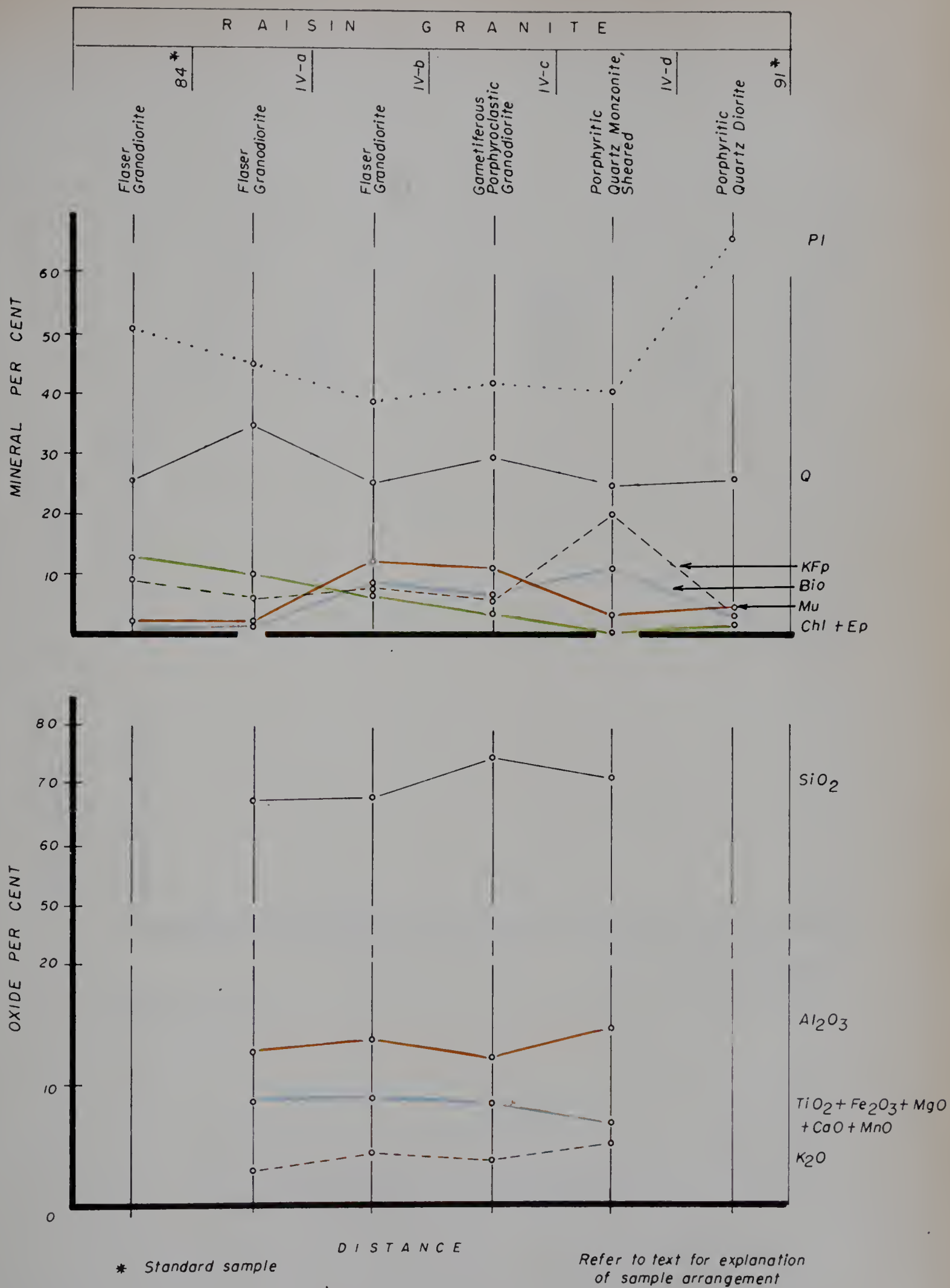


Figure 10. Petrologic profiles for samples from area IV,

Charles Lake.

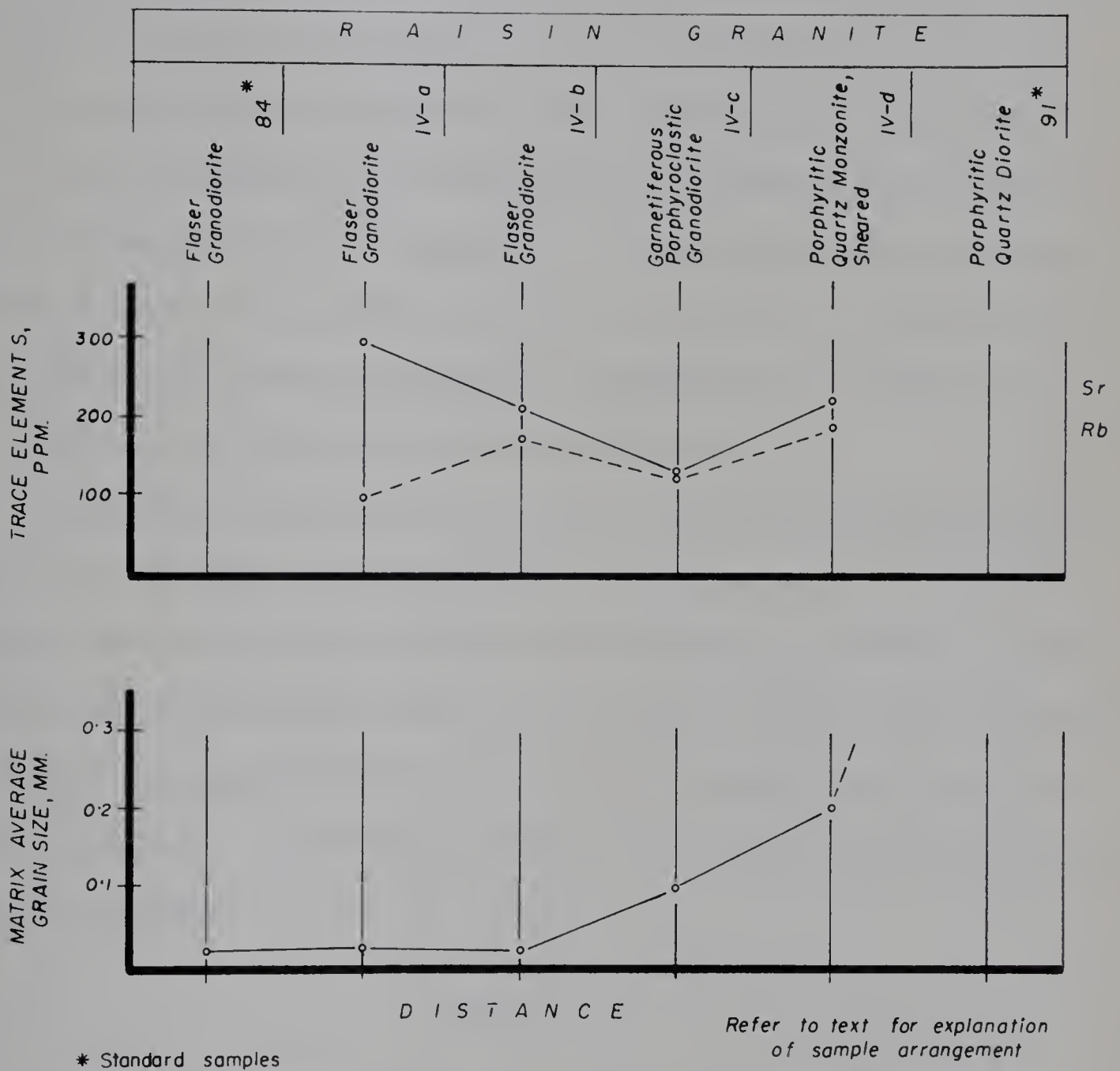


Figure 10. (Continued)

used in this detailed study, and chemical analysis of standard sample 91 is not available. The graphs show chemical variations that are unrelated to increasing degree of cataclasis, except for an apparent loss of SiO_2 , and increase in Sr. Table 28 (Appendix A) shows that CaO content in samples IV-a and IV-b is twice as high as the less-sheared parent rocks, and may reflect pre-deformation chemical differences in the granitic mass, or Ca and Sr may have migrated into highly sheared phases during cataclasis.

Mylonitized phases of raisin granite may be classified as either flaser granodiorite or protomylonite, but the former name is deemed more appropriate due to the prevalence of augen-structure which is cited by Tyrrell (1926) as a characteristic feature of flaser rocks. The rock composition is predominantly granodiorite, but ranges into the quartz diorite and quartz monzonite fields.

Raisin granite likely represents one phase of multiple synkinematic magma intrusion along the western margin of the Charles Lake map-areas. Cataclasis has rounded and stretched the phenocrysts, and comminuted much of the matrix. Quartz blebs have yielded both by brittle fracture which results in microcrystalline aggregates, and by flow during recrystallization which produced "shoestring" quartz that curves around porphyroclasts. Increasing degree of cataclasis was accompanied by progressive chloritization of biotite.

Area V

A broad, composite mylonite P - granite F band along the east shoreline of Charles Lake extends the length of map-area 10. Mylonite P is developed along the western part of granite F, and is in contact commonly with mylonite K. Samples from area V represent a section through the cataclastic rocks and the corresponding parent rocks. The sequence of rocks encountered on an easterly traverse comprises sheared, chlorite granite gneiss, mylonite K, mixed mylonite, mylonite P, sheared granite F, and granite F. The main purpose of this study is to determine the mineral and chemical changes that accompany cataclasis of medium- to coarse-grained granite F, and a sec-

ondary aim is to describe the nature of a mixed zone of mylonite.

Transitional contacts are seen where mylonite P and granite F are associated, and general megascopic features of the two rock-types unequivocally establishes a parent-daughter relationship. Five samples from area V show a gradational change from a fine-grained to aphanitic matrix, and massive to finely laminated structure, and are used to demonstrate the mineral and chemical changes that accompany cataclasis of a homogeneous rock. Microcline porphyroblasts 25 to 50 mm in length cannot be accommodated on small thin sections, but 5 to 20 mm megacrysts can be included in thin sections used for systematic detailed analysis. Rock slices representative of large samples were crushed for X-ray fluorescence analysis.

Mineralogical changes accompanying granulation of granite F are slight and irregular, and only quartz shows a systematic decrease with increasing degree of cataclasis. The westernmost sample of mylonite P appears anomalous and may be due to mechanical mixing of granite gneiss or metaseds - typically peripheral to granite F - during cataclasis. Decrease in SiO_2 with increasing degree of cataclasis is the single chemical trend.

Mixed mylonite is texturally classified as cryptomylonite and is too fine-grained for modal estimation, but chemical data reveals a highly acidic composition that cannot be correlated with the adjacent rocks and may be the product of basic oxide leaching and silicification. Mylonite K, which is derived from biotite granite gneiss, is not represented in this study. The mineralogy of sheared chlorite granite gneiss differs considerably from mylonite P, but the chemical composition is comparable; this apparent peculiarity is due to a fortuitous circumstance whereby different proportions of the same minerals in two different rocks give a comparable bulk chemical composition.

The graph showing specific gravity of the samples from area V is identical to the graph showing the distribution of basic oxides, and the two parameters can be directly related. The variation of SiO_2 and degree of crushing may also contribute appreciably to changes in specific gravity.

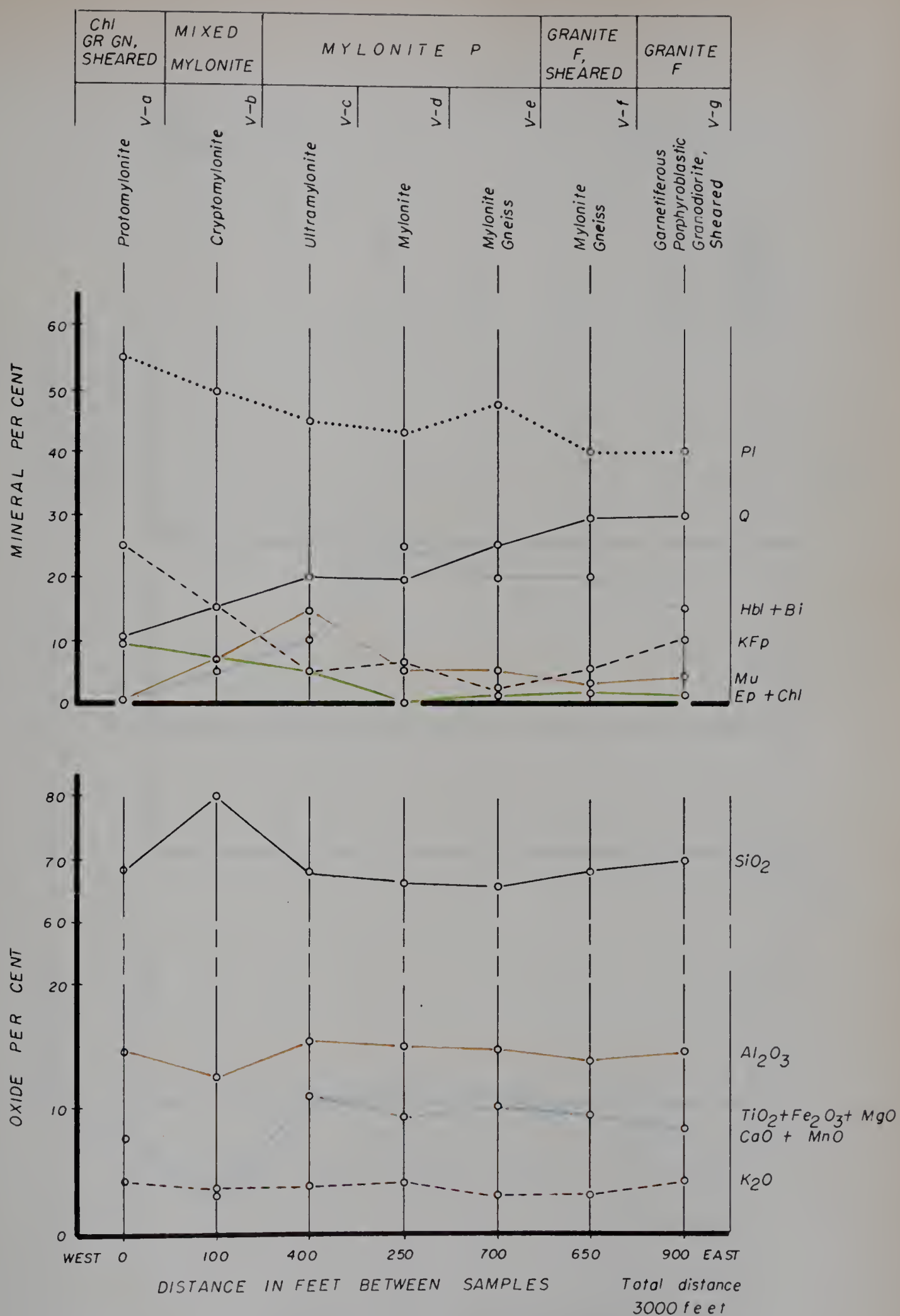


Figure 11. Petrologic profiles for samples from area V,
 Charles Lake.

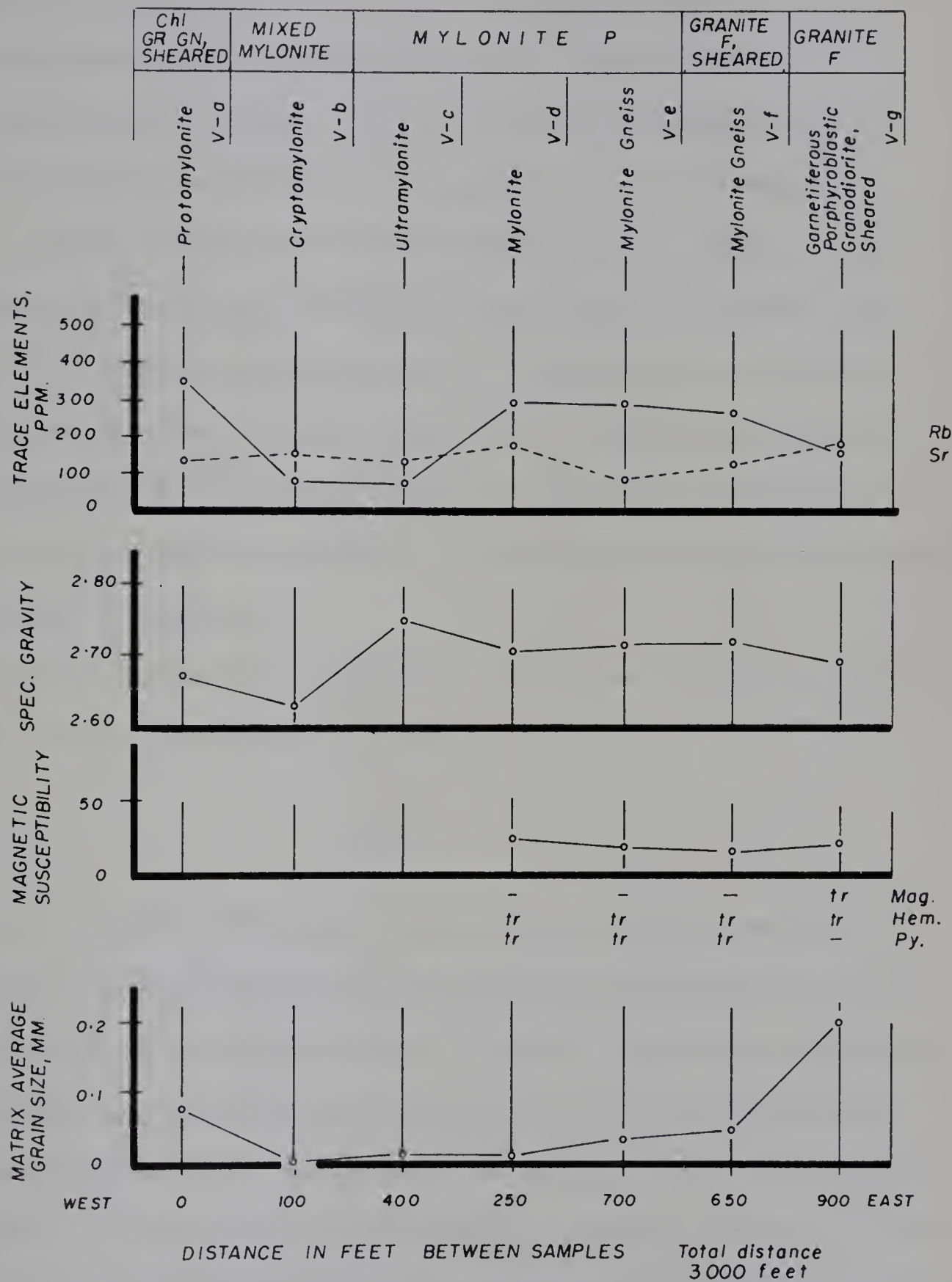


Figure 11. (Continued)

Magnetic susceptibility of mylonite P and granite F samples is uniformly low and shows no significant trend, and is due to the virtual absence of magnetite.

Metasomatism likely took place during a late stage of cataclasis as evidenced by the presence of abundant 1 to 2 inch microcline megacrysts with all gradations from augen to euhedral shapes. Apparently, part of the large-size microcline megacrysts in mylonite P are inherited from the parent rock, but most of the megacrysts initiated growth during the terminal phase of cataclasis. They grew under the influence of moderate temperature and progressively relaxed stress until deformation had virtually ceased. The presence of mobile potash during the late history of mylonite P is seen by the extensive development of replacement antiperthite, and potash feldspar folia and veins. The genesis of the large feldspar megacrysts is discussed in chapter six.

The biotite granite gneiss - granite F contact acted as a locus for faulting, and mylonites are derived from both wall rocks.

Area VI

Area VI is about 4 miles south from area V, and samples of mylonite P, granite F, granitic metasedimentary rocks, and hornblende granite gneiss were successively collected along an easterly traverse. This study is an attempt to elucidate chiefly the genetic relationship between granite F and granitic metasedimentary rocks, and to provide additional data to define the changes that accompany cataclasis of granite F. Peripheral bands and inclusions of quartzose and granitic metasedimentary rocks are found with most granite F bodies, and are regarded as ungranitized remnants.

The graphs show the two samples of granite F have dissimilar mineral compositions but a similar chemical composition. Close examination of the mineral pairs plagioclase-muscovite, and biotite-chlorite (supplemented with details from Table 30, Appendix A) suggests that plagioclase is increasingly sericitized and biotite is corr-

espondingly chloritized with decrease in grain size as mylonite P is approached. Mineralogical data for the single mylonite P sample (VI-a) is unavailable due to the fine-grain size of the rock, however, chemical data indicate a significant decrease in SiO_2 and increase in K_2O in mylonite P compared to granite F, analogous to the mylonite P-granite F transition in area V.

The metasedimentary rocks of area VI have a dissimilar mineral assemblage compared to granite F, and include cordierite, diopside, hornblende, and actinolite, in addition to garnet which is common to both rock-types. Sample VI-d contains 3 per cent garnet and 2 per cent cordierite besides numerous sharply outlined sericite knots that are indicative of prolific cordierite prior to diaphoresis. Sample VI-e contains 17 per cent diopside and 8 per cent combined hornblende and actinolite but contains neither garnet nor cordierite. The argillaceous nature of sample VI-d is indicated by about 17 per cent Al_2O_3 , whereas the marly nature of sample VI-e is shown by about 11 per cent combined CaO and MgO . Retrogressive metamorphic effects are seen in the sericitization of cordierite and garnet, alteration of hornblende to actinolite, and chloritization of biotite. They are attributed to hydrothermal solutions moving from the fault zone into the adjacent region of upper amphibolite and lower granulite facies rocks. The presence of numerous, thin, granitic veins inter-layered with metasedimentary rock on a fine scale likely represents metamorphic differentiation of felsic constituents from the metasedimentary rocks under anatectic conditions. The abundance of pale green hornblende and actinolite in adjacent metasedimentary and granite gneiss samples suggests a genetic association, and mineral and chemical data for the single hornblende granite gneiss sample indicates a composition that is intermediate between the two metasedimentary rock analyses.

The contacts between adjacent rock-types in the study area are chiefly gradational, and the smooth chemical trends suggest that the four rock-types are genetically related. Cataclasis of granite F has produced mylonite P, and details of this transition are treated in the study of area V. The granite F - metasedimentary rock

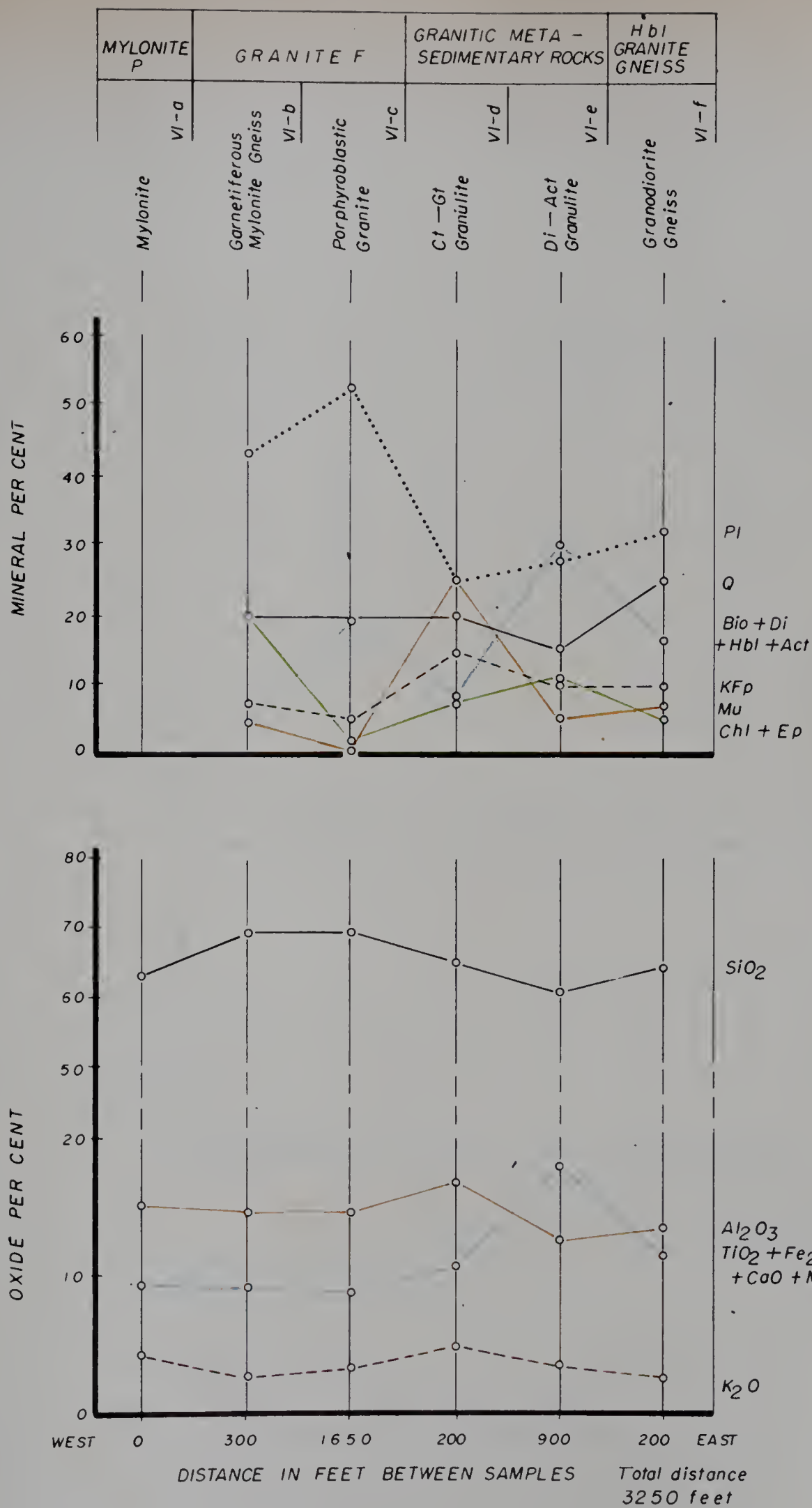


Figure 12. Petrologic profiles for samples from area VI,
Charles Lake.

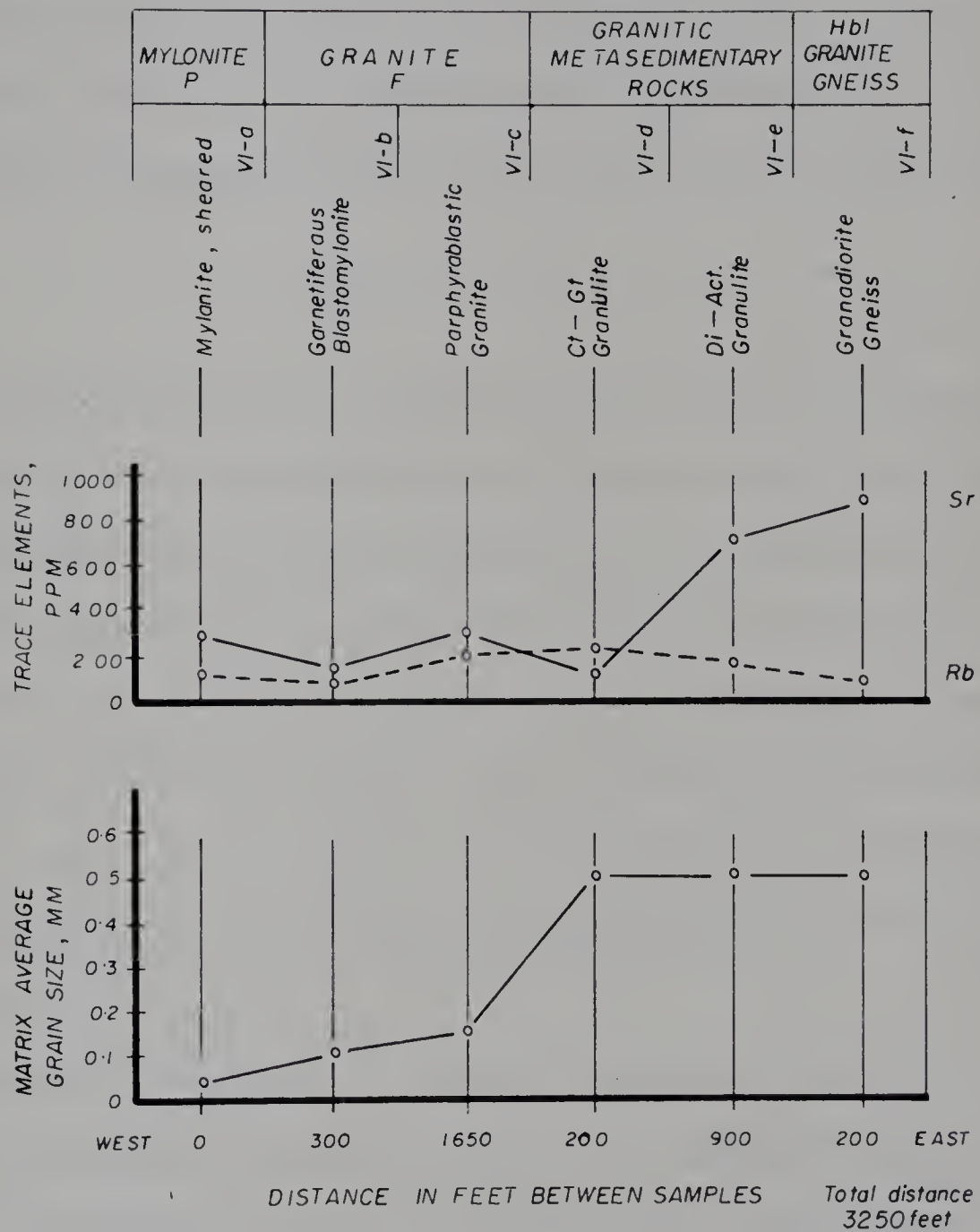


Figure 12. (Continued)

contact is both gradational and interfingering, and it seems likely that the observed features are due to the combined effects of granitization of the metasedimentary rocks and upward migration of the anatectic granite. The metasedimentary rocks to hornblende granite gneiss transition is an effect of granitization whereby the marginal part of the metasedimentary band has been incorporated into the granite gneiss terrain.

Post-crystalline fault activity was confined to the westernmost part of mylonite P, and has produced megascopic breccia with epidote filling the interstices.

Area VII

Several small bands and lenses of hornblende cataclasite are located near the shorelines of Charles Lake, in the Charles Lake, South map-area. Hornblende cataclasite is always associated with grey hornblende granite, and both rock-types are enclosed by hornblende granite gneiss. This setting provides the necessary field association for a study of the genetic relationships of these three rock-types, and is comparable to a similar study made in area III. The five samples used for detailed analysis are located along a curved, southerly-trending line that joins standard-rock samples 144 (hornblende cataclasite), 150 (grey hornblende granite), and 152 (hornblende granite gneiss).

The north to south arrangement of samples corresponds to an increase in grain size except for the hornblende granite gneiss sample. The single hornblende cataclasite sample is typical of this rock-type with abundant quartz, plagioclase, and low potash feldspar and mafic minerals; about 68 per cent SiO_2 , 15 per cent Al_2O_3 , and 6 per cent calcemic oxides. Increase in grain size within grey hornblende granite and on into hornblende granite gneiss is accompanied by several distinct trends: increase in amount of plagioclase, and decrease in quartz; decrease in SiO_2 and K_2O , and increase in basic oxides; Sr increases with grain size in grey hornblende granite, then decreases markedly in hornblende granite gneiss. The plagioclase and K_2O trends are opposite to a similar study in area III, but the differences are minor in comparison to

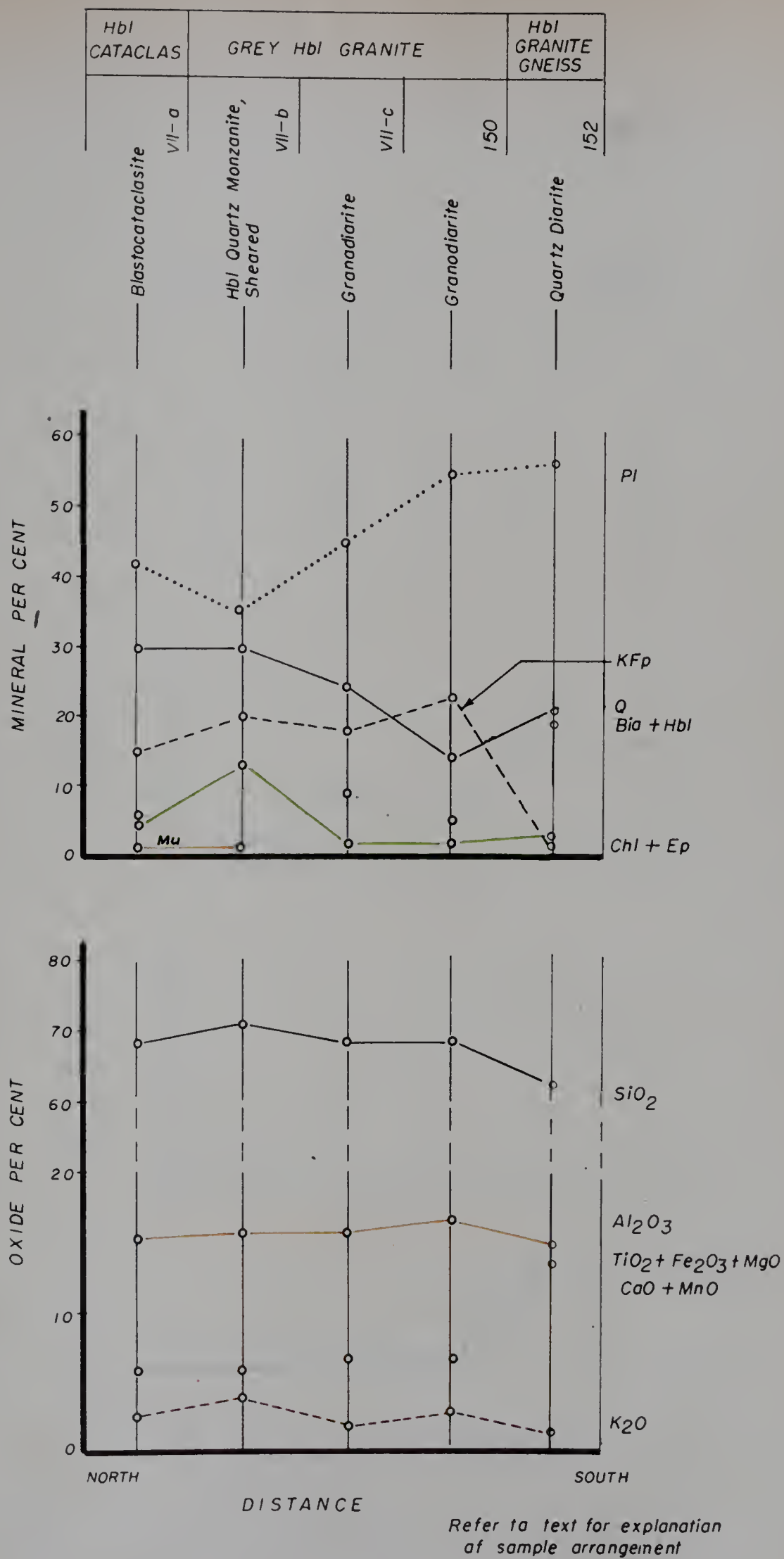


Figure 13. Petrologic profiles for samples from area VII,
Charles Lake.

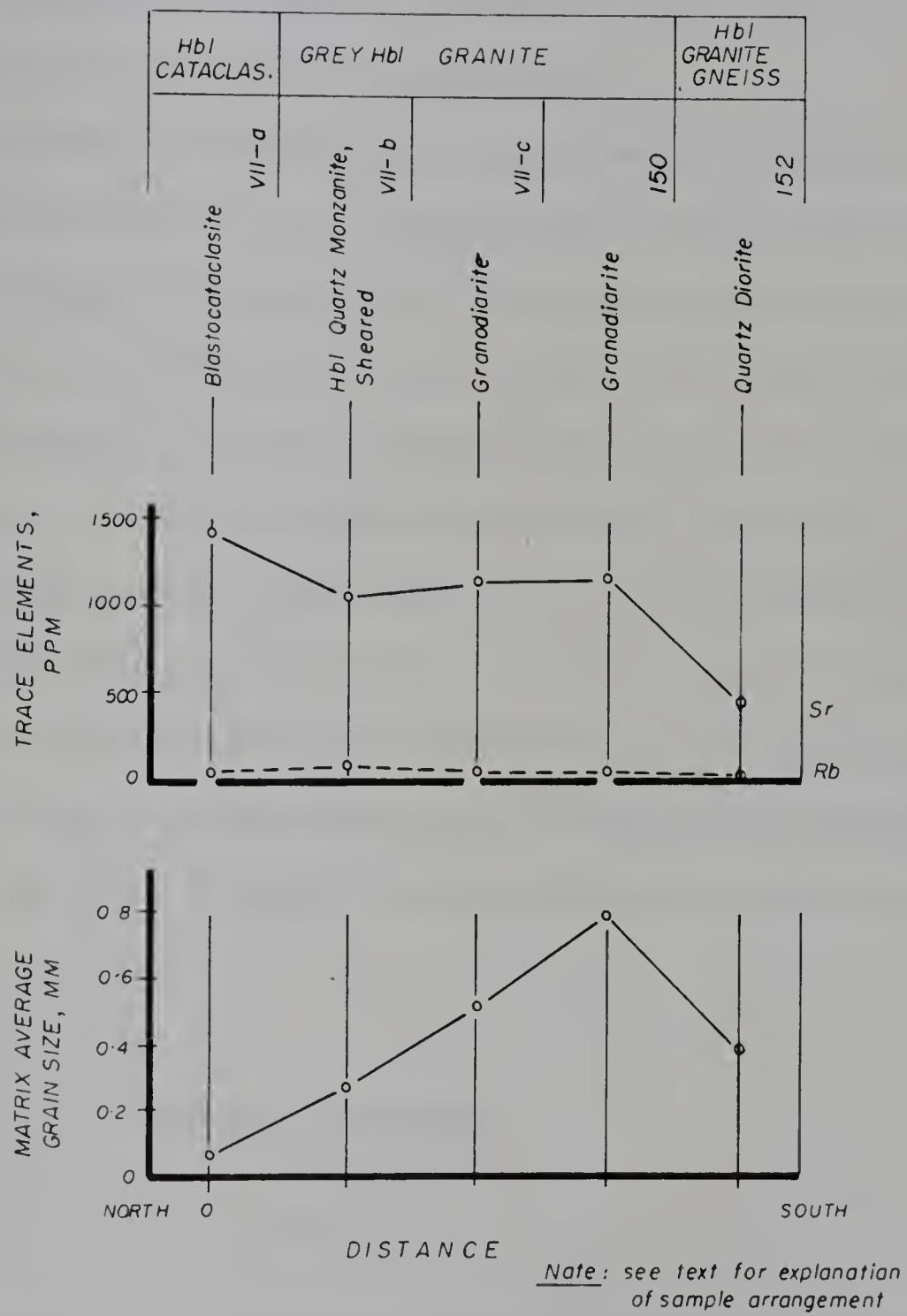


Figure 13. (Continued)

the major trends common to both study areas, and similar conclusions may be drawn. Field, textural, mineralogical, and chemical criteria (p. 134) indicate that hornblende cataclasite, grey hornblende granite, and hornblende granite gneiss are genetically related, and differences in megascopic appearance among these rock-types are due to a combination of cataclasis and recrystallization.

Extensive cataclasis of hornblende granite gneiss resulted in appreciable chemical adjustments in the derived rock - increase in SiO_2 and K_2O , and a decrease in calcemic oxides; the amount of chemical change being related to the degree of cataclasis. Subsequent recrystallization in an environment of continued high temperature and hydrostatic pressure produced a massive, inequigranular rock with interlocking, sutured grains in the matrix and spherical plagioclase porphyroclasts with irregular margins. Where relatively higher temperature conditions prevailed, or where relatively less cataclasis occurred, or both, a massive fine-grained, grey hornblende granite was produced. The effects of hydrothermal alteration that accompanied cataclasis are seen in abundant spherical to elliptical biotite and chlorite pseudomorphs after hornblende. Post-crystalline deformation has not affected the rocks in area VII.

Cornwall Lake Studies

Area VIII

Arch Lake granite forms a continuous mass along the west margin of the Charles Lake, North, Central, and South map-areas. Cataclastic rocks are rarely developed, but one lens 2.5 miles west of the north tip of Cornwall Lake shows a striking gradation from aphanitic, equigranular, cherty cryptocataclasite to moderately sheared Arch Lake granite through a zone 20 feet wide. This gradation observed in the field and the corresponding thin section study is illustrated in Plate 12. A relatively unshaped sample of Arch Lake granite, located about 1 mile west of Arch Lake is included to complete

the sequence.

Close examination of polished-rock slabs shows that aphanitic material, represented by sample VIII-f, is intrusive into phaneritic rock as seen in sample VIII-e. The fine- and coarse-grained phases of sample VIII-e have been separated for individual analysis with the intention of demonstrating the similarity of fine-grained vein material in sample VIII-e with the bulk of sample VIII-f. The vein material is texturally classified as cryptocataclasite, and not pseudotachylyte, by virtue of the anisotropic matrix (Plate 12, b). Modal analysis of cryptocataclasite is virtually impossible with the petrographic microscope.

The samples are arranged in a west to east sequence that corresponds to increasing degree of cataclasis, and the profiles show many systematic trends: (i) increase in quartz and plagioclase; (ii) decrease in potash feldspar, chlorite + epidote, white mica, and biotite; (iii) increase in SiO_2 ; (iv) decrease in Al_2O_3 , basic oxides, and K_2O ; and (v) decrease in Rb and Sr in the early stage of cataclasis. The net result is silicification, accompanied by a decrease in other major oxides. It is suggested that hydrous solutions migrated through the rocks during cataclasis to promote chloritization of biotite, preferential leaching of chlorite, epidote, white mica, and potash feldspar, and resulting in the relative enrichment of plagioclase and quartz. The leaching effects are more pronounced with increasing degree of cataclasis due to greater effective surface area available for reaction. An intergranular film of water may have acted as a lubricant for intrusion of cryptocataclasite into protomylonite; however, the presence of abundant, angular cryptocataclasite fragments in cryptocataclasite matrix suggests a more likely mechanism for the intrusive nature of cryptocataclasite – initial cataclasis of coarse-grained Arch Lake granite produced a continuous sequence from unsheared rock to cryptocataclasite, followed by a second cataclastic event that chiefly affected cryptocataclasite, causing brecciation, and migration of pulverized material into fractures developed in protomylonite. Post-kinematic fractures are filled by granoblastic, unstrained quartz.

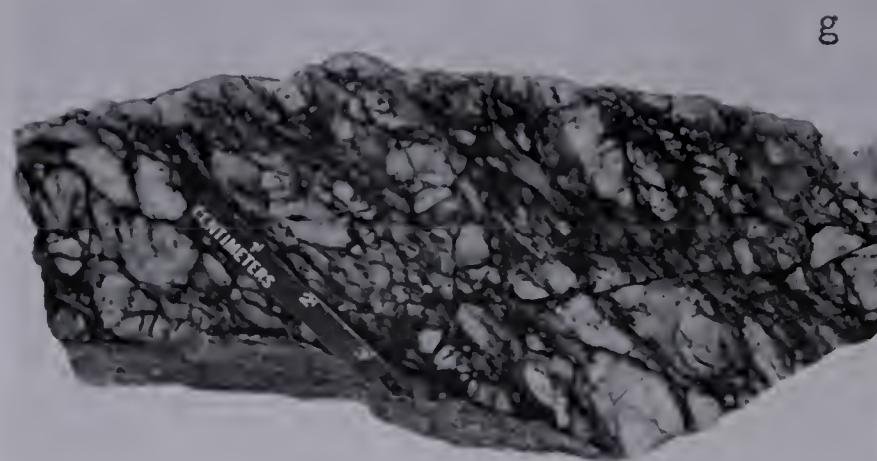
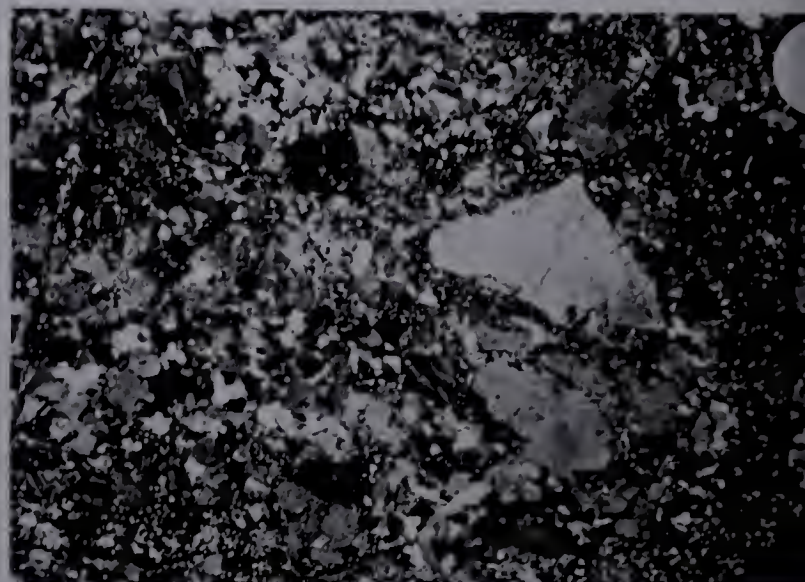
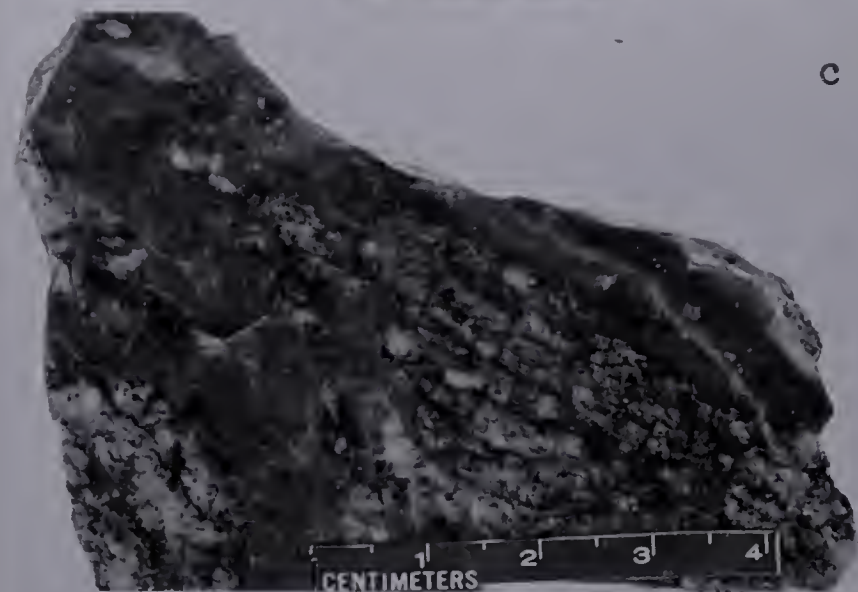
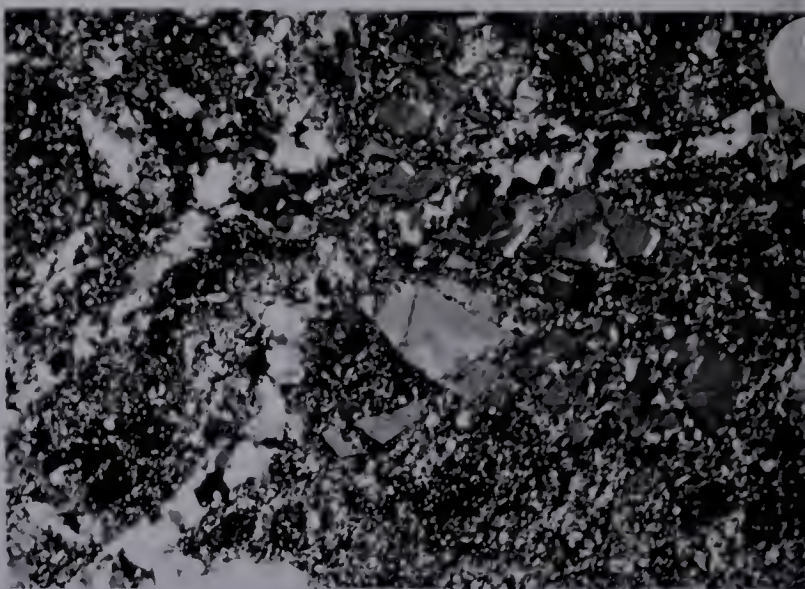


PLATE 12

ARCH LAKE MYLONITE (CRYPTOCATACLASITE) AND
ARCH LAKE GRANITE (PORPHYRITIC QUARTZ MONZONITE)

- a. Cryptocataclasite. Sample VIII-f, hand specimen. Aphanitic, cherty rock with quartz veins.
- b. Cryptocataclasite. Sample VIII-f, photomicrograph. Fragmented microcline porphyroclast invaded by cryptocrystalline matrix. Unstrained, granoblastic quartz in veins. Crossed nicols, $\times 10$.
- c. Protomylonite. Sample VIII-d, hand specimen. Cryptomylonite surrounds protomylonite.
- d. Protomylonite. Sample VIII-d, photomicrograph. Angular porphyroclasts in partly mylonitized matrix. Cryptomylonite vein along the right side of the photomicrograph. Crossed nicols, $\times 10$.
- e. Porphyritic quartz monzonite, sheared. Sample VIII-c, hand specimen. Highly fragmented feldspars in a partly crushed matrix.
- f. Porphyritic quartz monzonite, sheared. Sample VIII-b, photomicrograph. Fragmented microcline with simple twinning, invaded by mylonitic matrix. Crossed nicols, $\times 10$.
- g. Porphyritic quartz monzonite, sheared. Sample VIII-b, hand specimen. Highly fragmented feldspars, in a partly crushed matrix.
- h. Porphyritic quartz monzonite, sheared. Standard sample 155, photomicrograph. Partly granulated matrix. Note the quartz grain with grid pattern strain shadows in the center of the photomicrograph. Crossed nicols, $\times 10$.

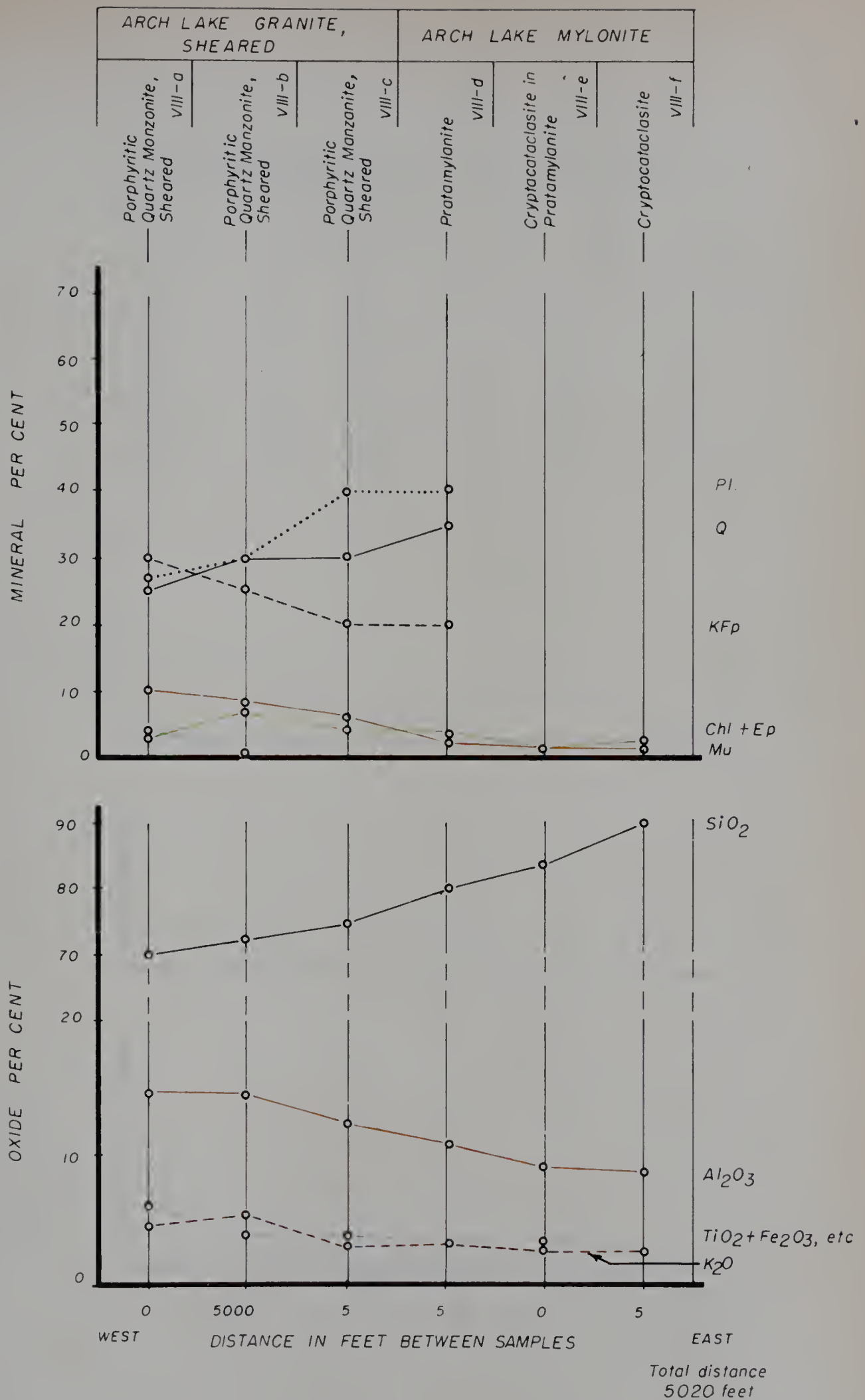


Figure 14. Petrologic profiles for samples from area VIII,
Cornwall Lake.

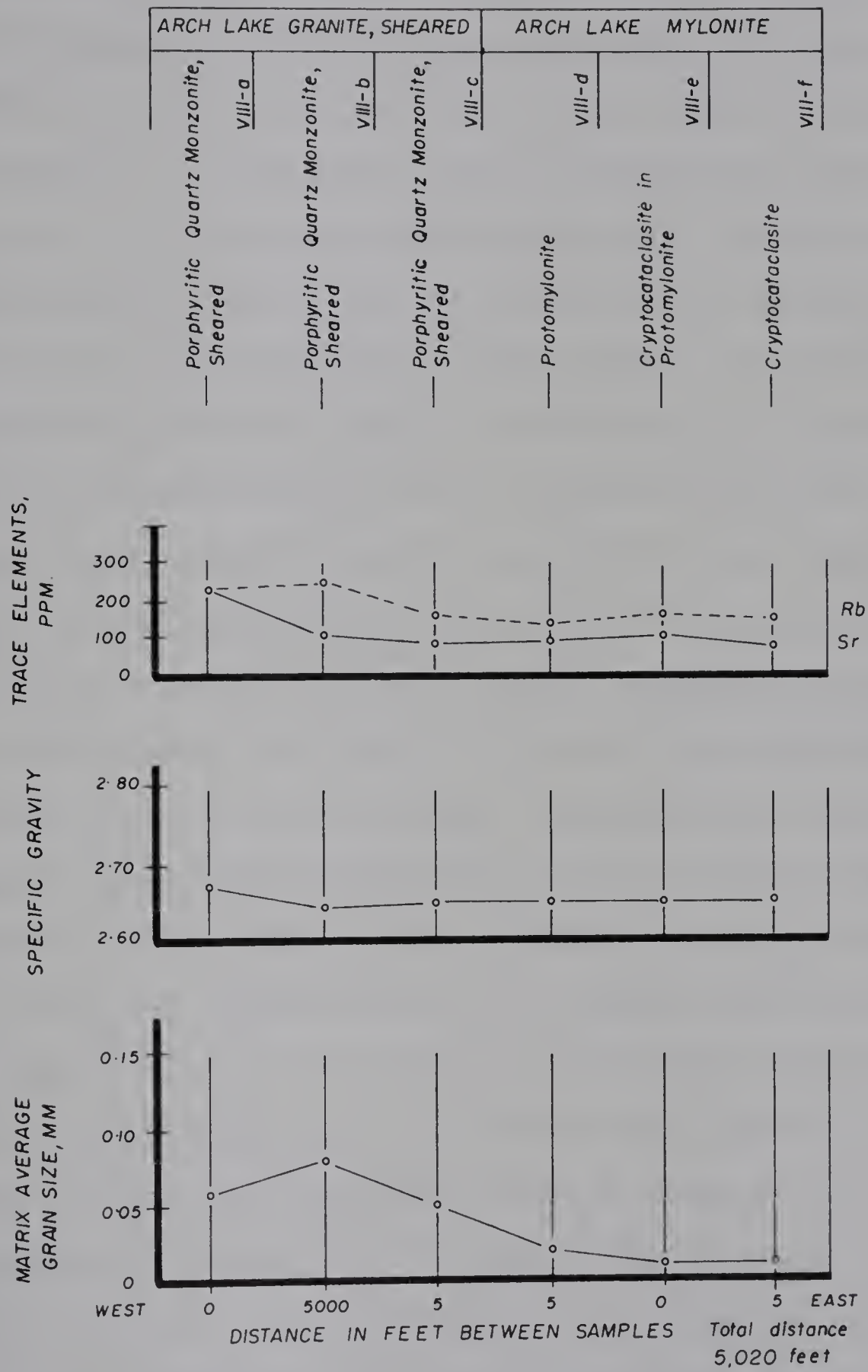


Figure 14. (Continued)

Area IX

In map-area 11, mylonite P forms major bands east of Charles Lake, which extend southerly between Cornwall and Alexander Lakes, and continue beyond the southern margin of the thesis area for an unknown distance. Mylonite P and granite F are not associated with metasedimentary rocks in the Charles Lake, South map-area in contrast to occurrences in other parts of the map-area. East of Cornwall Lake, hornblende granite gneiss and biotite granite gneiss enclose mylonite P; hornblende granite gneiss becomes migmatitic and highly sheared as the mylonite P contact is approached from the west, whereas biotite granite gneiss becomes finely laminated and sheared as the mylonite P contact is approached from the east. A detailed rock suite was collected through the western contact zone to study primarily the relationship of hornblende granite gneiss and mylonite P. The sequence of rock types encountered in an easterly direction is - sheared, hornblende granite gneiss, mylonite M, mixed mylonite, and mylonite P. The scale of map representation prohibits placing mylonite M on the printed map. The single sample collected in the hornblende granite gneiss band is a sheared phase in which hornblende is absent.

Examination of the profiles indicates a relatively uniform composition through the contact zone. Neither mylonite M nor mylonite P show distinctive mineral and chemical features. It is interesting to note that K_2O is relatively constant in both mylonite M and mylonite P, and if these two mylonites are genetically related, the presence of large feldspar megacrysts in mylonite P and their absence in mylonite M indicates that K_2O for the microcline megacrysts was derived from the matrix of mylonite P. The definition of the two mylonite types is based upon thin section, hand specimen and outcrop features where relict gneissic layering and 5 to 15 mm feldspar porphyroclasts in mylonite M compare with thin feldspar stringers and microcline megacrysts from 20 to 100 mm in size in mylonite P.

The relatively coarse average grain size of the matrix through the entire

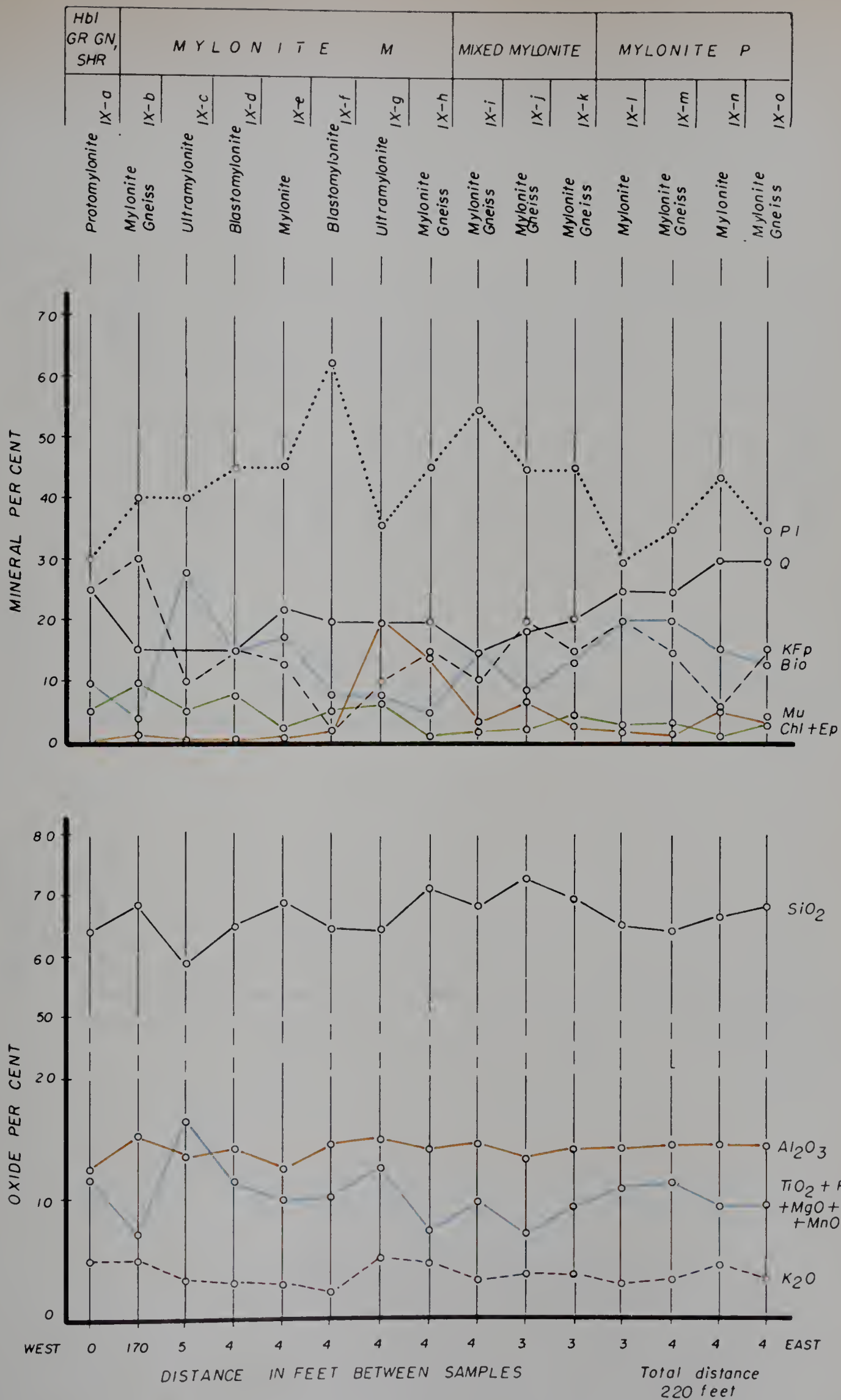


Figure 15. Petrologic profiles for samples from area IX, Cornwall Lake.

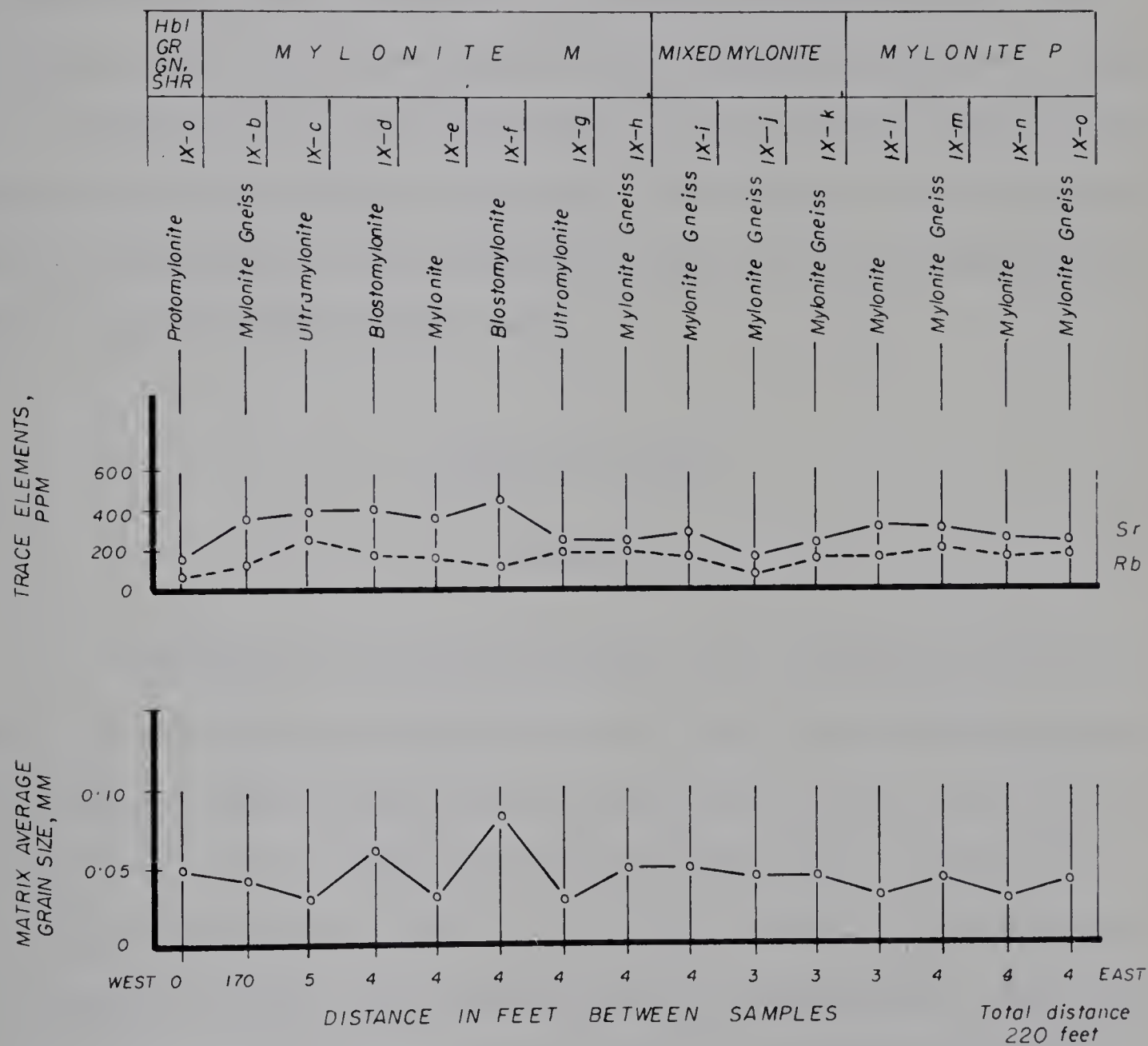


Figure 15. (Continued)

suite of samples can be attributed to uniform recrystallization of the composite mylonite band.

The tectonic history of the rocks in area IX is not clear, but an interpretation based primarily upon field observations is attempted. Extensive granitization of metasedimentary rocks was likely accompanied by infolding of metasedimentary rocks into the granite gneiss. Major cataclasis probably was initiated in the synkinematic stage and though mainly confined to granite F bodies, granite gneiss was also mylonitized to a lesser extent. Late-kinematic potash metasomatism may have developed microcline megacrysts. High but declining temperature thoroughly recrystallized the mylonitic rocks.

Treasure Loch Study

Area X

Mylonite P is the prevalent cataclastic rock in the Treasure Loch mylonite band. Mylonite K forms rare bands a few tens of feet wide, but these are too small for map representation. Slightly-sheared cores of granite F are enclosed by mylonite P which in turn is sheathed with metasedimentary rock. A small mass of mylonite P in the northeast region of Treasure Loch is selected for detailed study by virtue of the complex inter-relationships shown by the associated rocks: mylonite P encloses and grades into granite F in one direction and grades transitionally into impure metasedimentary rocks in another direction; a narrow zone of mixed mylonite and mylonite K separate sheared, biotite granite gneiss from the metasedimentary band.

The granite F - mylonite P - metasedimentary rock sequence is examined, and the relationship of these rocks to the adjacent mylonite K and sheared, biotite granite gneiss is investigated. The granite F - mylonite P relationship has been studied also in areas V and VI.

A moderate degree of cataclasis produced protomylonite and rare mylonite

from granite F, and subsequent recrystallization resulted in an increase in grain size of the crushed matrix. Several trends are noted in the profiles with decrease in grain size: plagioclase and biotite increases, quartz and potash feldspar decreases, and calcemic oxides increase. These trends are also seen in area V, and where information is available, in area VI. Thus, it is apparent that systematic mineral and chemical changes accompany mylonitization of granite F masses.

Thin sections show that metasedimentary rocks are moderately mylonitized, and from 5 to 50 per cent of the rock is crushed. Relict garnets in white-mica mats and thorough sericitization of many plagioclase grains are diaphoretic effects that accompanied cataclasis. The transition from mylonite P to impure metasedimentary rocks is accompanied by a large increase in quartz, white mica, and chlorite, and a marked decrease in plagioclase. These changes take place through a contact zone of several feet, which implies that mylonite P and impure metasedimentary rock have not been appreciably mixed during mylonitization, and that the pre-cataclastic stratigraphy is preserved. The major and minor oxides show an irregular distribution through the metasedimentary rock band and differences with mylonite P are obvious. However, examination of data from Table 34 (Appendix A) indicates that high Fe_2O_3 (about 8 per cent) and low CaO (about 1 per cent) are distinctive features of the metasedimentary rock band. The Sr content is low in the metasedimentary rock band compared to mylonite P and approximately corresponds to the CaO distribution between the two rocks.

Mylonitization along the metasedimentary rocks - biotite granite gneiss contact has produced mylonite from both rocks, and a mixed mylonite. Subsequent recrystallization has obliterated many of the mylonitic features of the matrix, and has given rise to mylonite gneiss and blastomylonite. The mineralogy and chemistry of mylonite K and biotite granite gneiss are appreciably different from those of the metasedimentary rocks; mixed mylonite has a composition appropriately intermediate between these rock types.

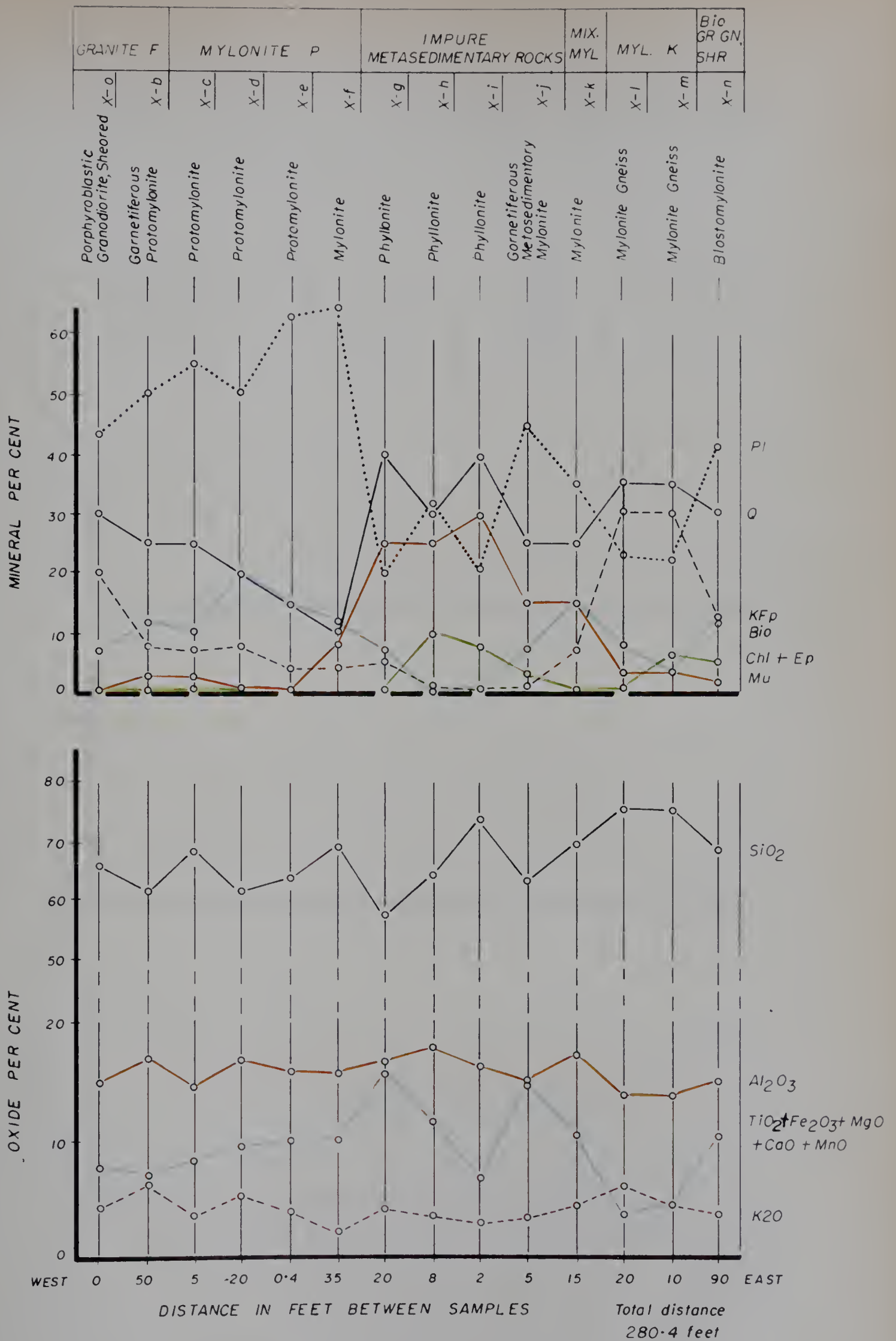


Figure 16. Petrologic profiles for samples from area X,

Treasure Loch.

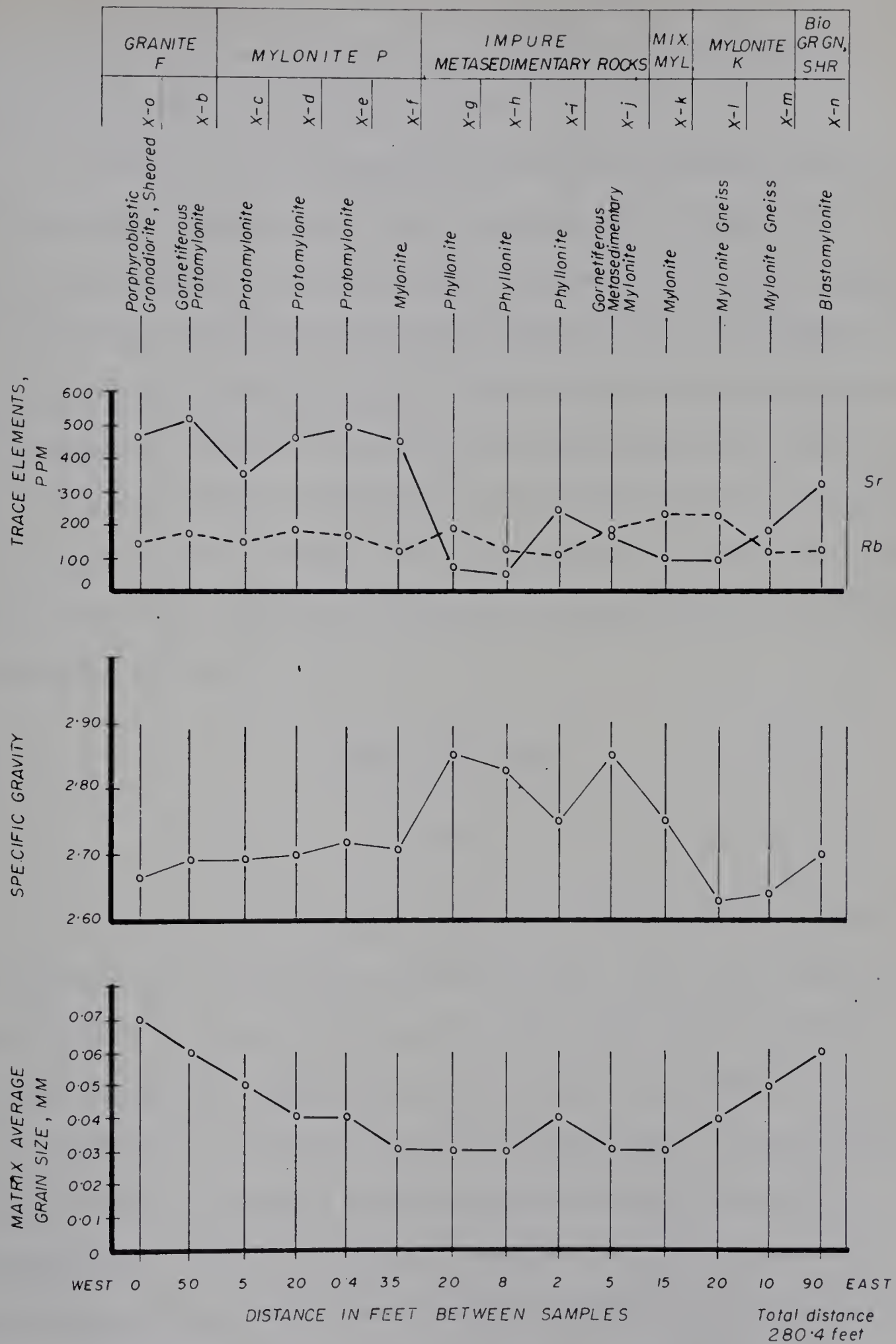


Figure 16. (Continued)

The curves for specific gravity and the basic oxides are virtually the same shape and grain size apparently has no appreciable affect on the specific gravity. The same relationship has been shown in area V.

In summary, a moderate degree of cataclasis in the Treasure Loch area has affected granite F, metasedimentary rocks, and biotite granite gneiss, and subsequent recrystallization has destroyed many of the cataclastic features. Mineral and chemical data indicate that negligible mechanical mixing of the different adjacent rocks has accompanied cataclasis. Progressive basification accompanies increasing degree of cataclasis in granite F, and similar changes in mineralogy and chemistry are noted in area V. Moderate cataclasis and thorough recrystallization in the Treasure Loch area contrasts with severe cataclasis and moderate recrystallization in the Charles Lake area, and explains the coarser grain size of mylonite P in the Treasure Loch area.

Ashton Lake Study

Area XI

A wide band of granite gneiss trending northerly along the east side of Ashton Lake is cut by two parallel, northeasterly faults. Brecciation, and local mylonitization in the region of the faults are shallow-level phenomena which are in contrast with the wide, deep-seated mylonite zones in the Charles Lake and Bayonet Lake areas. The contoured aeromagnetic map (Map 1, in pocket) shows a distinct break in the northerly trending aeromagnetic high and indicates a "demagnetization" effect in the region of the faults. Magnetic susceptibility measurements on fifteen samples show a general trend from high to low values as the fault zone is approached from the aeromagnetic high regions to the north and south (Fig. 3). Nine of these samples, located along a northerly line, are used in this study to demonstrate the petrologic changes that take place within a band of gneissic

rocks cut by faults.

The graphs show many systematic trends that are apparently related to changes in average matrix grain size. Minerals have an irregular distribution except potash feldspar which is enriched in the four northernmost samples, comprising three blastomylonites and a single quartz monzonite gneiss. Samples bounded by the two faults show a considerable increase in SiO_2 , and a corresponding decrease in Al_2O_3 , cafermic oxides, and Sr. These chemical changes are due to concomitant silicification and leaching of mafic minerals in the fault zone. However, the irregular quartz profile contrasts with the SiO_2 profile, and the SiO_2 distribution may be complicated by an event that pre-dates the observed faults. An earlier, deep-seated cataclastic event produced abundant mylonite from biotite granite gneiss in a zone approximated by the position of the two observed faults and locally outside of this zone. Silicification and leaching of the mafic minerals are effects from this early cataclastic event. Thorough recrystallization of the mylonites produced fine-grained, leucocratic rocks with only faint cataclastic nature (blastomylonites), accompanied by metamorphic differentiation of quartz into lenticles and porphyroblasts. Post-crystalline shearing stress produced faults near the boundary of the pre-existing zone of cataclastic rocks, and local mylonitization and brecciation along the faults. Post-crystalline thermal conditions were insufficient to cause appreciable recrystallization.

The specific gravity profile shows a rapid decrease from sample XI-f to XI-c that is explained by the pronounced increase in potash feldspar (S.G. = 2.54 to 2.57) and decrease in biotite (S.G. = 2.7 to 3.1) in a south to north direction through the fault zone. The overall specific gravity profile shows a similarity to the cafermic oxides profile.

The magnetic susceptibility and average matrix grain size profiles are similar, but changes in susceptibility cannot be adequately explained only by changes in grain size. The amounts of magnetite, hematite, and pyrite in individual samples are given, and susceptibility may be shown to be directly related to the magnetite content. Sam-

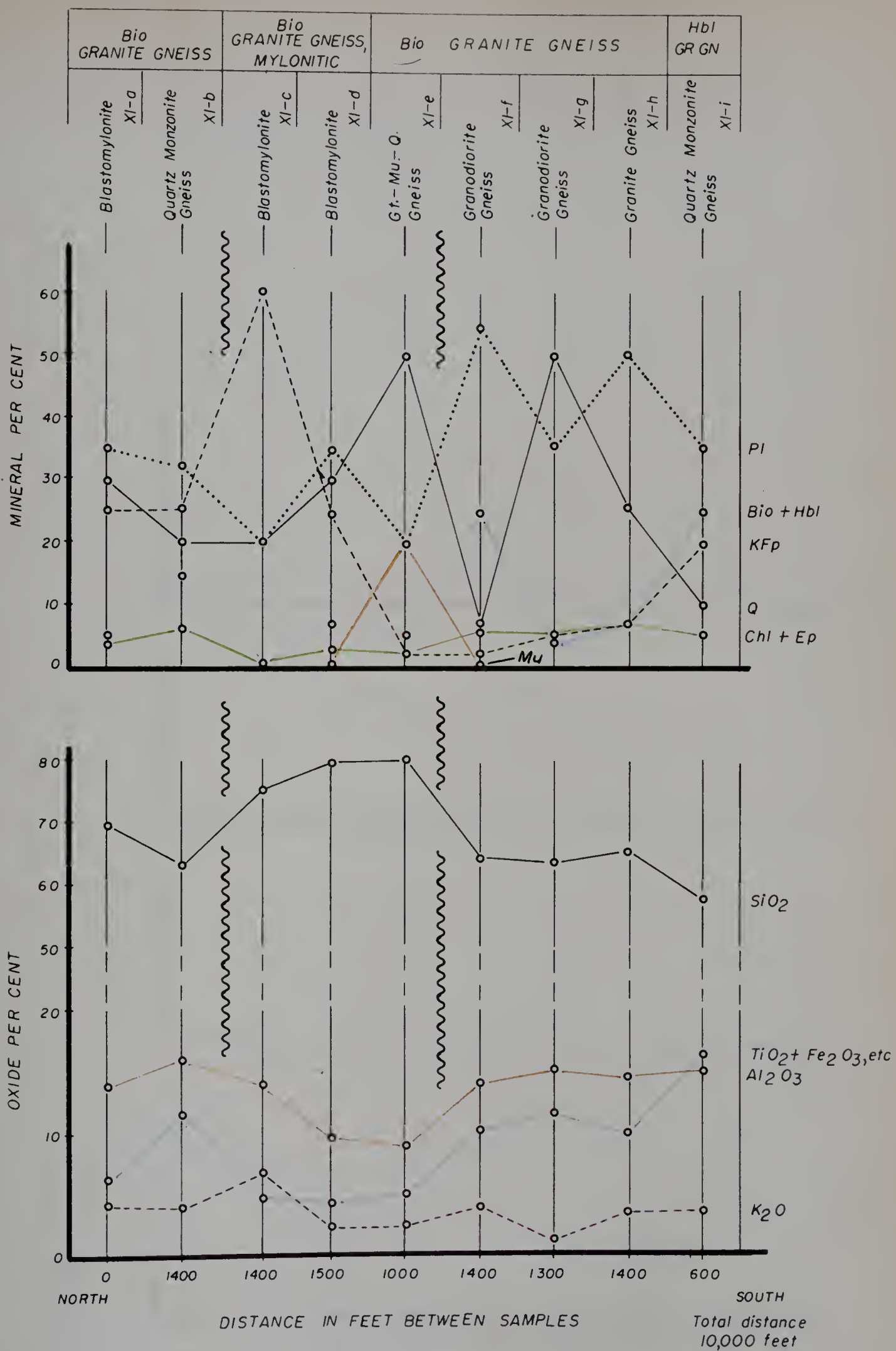


Figure 17. Petrologic profiles for samples from area XI, Ashton Lake.

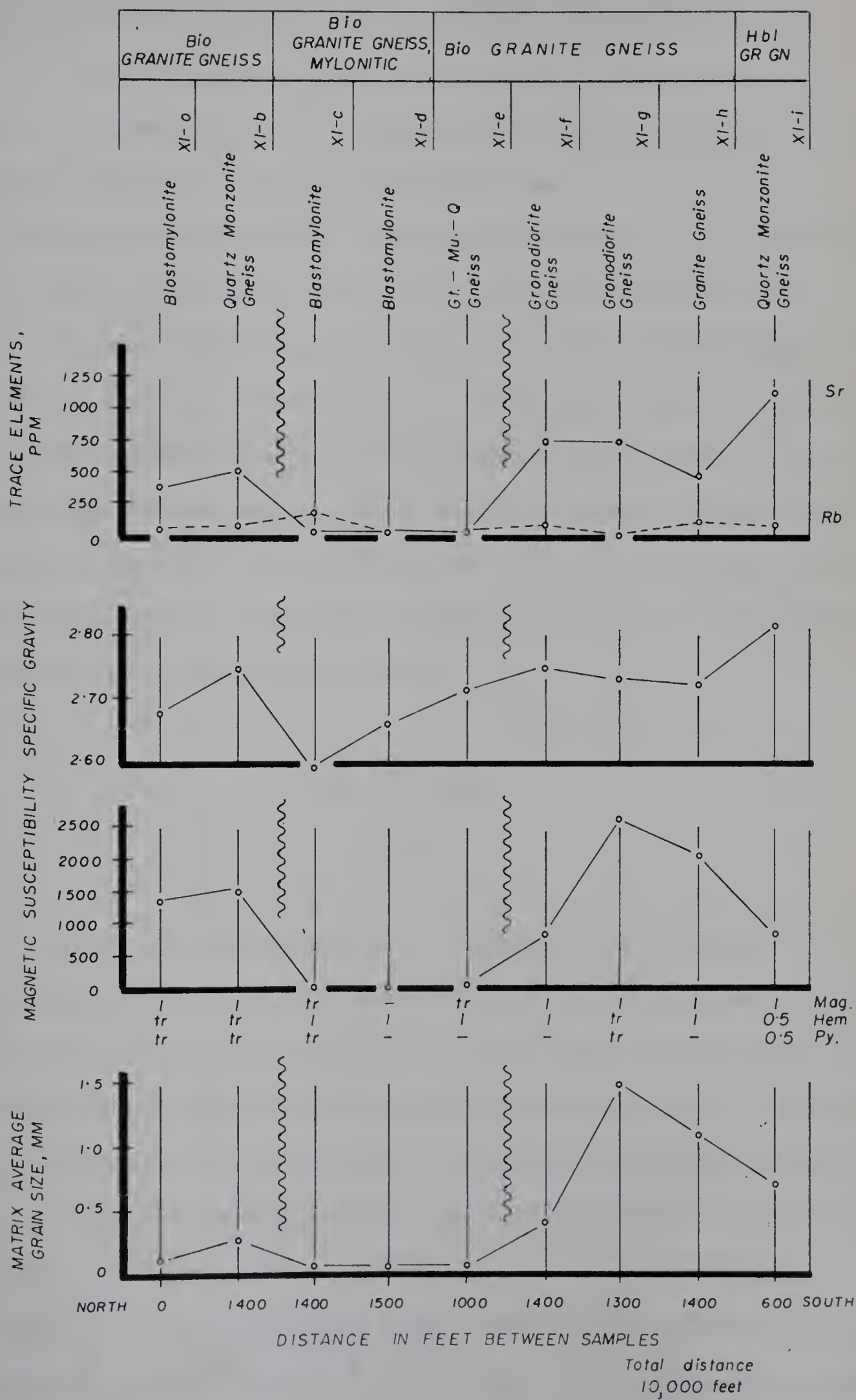


Figure 17. (Continued)

ples within the fault zone that result from hematization of magnetite by fault solutions give very low susceptibility values, and rocks outside the fault zone have high susceptibility values which decrease with increasing alteration of magnetite to hematite and rare pyrite. Apparently, the fault solutions were most readily introduced and reaction with magnetite was promoted in the finer-grained rocks.

The geologic history of the Ashton Lake area includes an early cataclastic event and a later period of fault activity. Early cataclasis produced mylonites in a one-quarter to one-half mile zone, with extensive leaching of mafic minerals, silicification, and local potash metasomatism within the mylonite zone. Recrystallization of the mylonites in a deep-seated environment produced blastomylonites. A second deformation under shallow-seated conditions caused brecciation and local mylonitization along two parallel faults, and hydrothermal solutions caused extensive sericitization and saussuritization of plagioclase, chloritization of biotite, and hematization of magnetite, chiefly in the finer-grained rocks.

Collins Lake Study

Area XII

A composite mylonite band comprising mylonites M and O extends northward from Collins Lake and continues beyond the Northwest Territories boundary. The distinction between mylonite M and mylonite O is complicated by the dark grey to black colour of both rocks and the lack of diagnostic features of each rock. A sequence of 18 samples were selected for detailed study in an attempt to investigate the genetic affinity of mylonite M to the adjacent granite gneiss, and to define differences that serve to distinguish mylonite M from mylonite O.

Chloritic biotite granite gneiss grades transitionally into mylonite M along the west and east sides of the composite mylonite band. The majority of the samples from the western band of mylonite M have a dissimilar chemical and mineral compos-

ition compared to biotite granite gneiss. Mylonite M may be derived chiefly from hornblende granite gneiss as suggested by the high content of calcic chemical constituents, particularly CaO (Table 36, Appendix A), in both the chloritized hornblende granite gneiss sample and most of the mylonite M samples. In contrast, along the margin of the eastern band of mylonite M, chlorite granite gneiss represents chloritized biotite granite gneiss, and the composition of chlorite granite gneiss and the adjacent mylonite M compares very well. Thus, samples from the western mylonite M band are likely derived from chiefly hornblende granite gneiss, whereas samples from the eastern mylonite M band are likely derived from biotite granite gneiss. High Sr content in the western mylonite M body, and low Sr in the eastern body further substantiates the belief that the two bands are derived from different parent rocks.

The diagnostic feature that distinguishes mylonite O from mylonite M is the large amount of white mica (15 to 40 per cent) seen in both hand specimens and thin sections of mylonite O. A high Al_2O_3 content relates to the abundant mica and indicates a substantial amount of argillaceous material in the original sedimentary rock. The chemical composition of mylonite O is similar to Tyrrell's average greywacke (from Pettijohn, 1957, p. 307) and resembles the chemical composition of a siliceous argillite from the Precambrian of Michigan (Pettijohn, 1957, p. 345). Mineral and chemical data indicate that sample XII-o is significantly dissimilar to the other mylonite O samples, and thin section study shows that uncommon minor brecciation with vein quartz and calcite fillings is responsible for the change in composition. Sample XII-j is also brecciated, but the powder for X-ray fluorescence analysis was prepared from an unfractured phase of the sample. Tourmaline in samples XII-m, XII-n, and XII-o occurs as euhedral porphyroblasts that are commonly broken, the segments are displaced (Plate 11, g) and rarely sericitized (Plate 11, h).

The metamorphic history in area XII is complex, but three distinct deformation episodes can be distinguished. (i) The earliest cataclastic event took place at

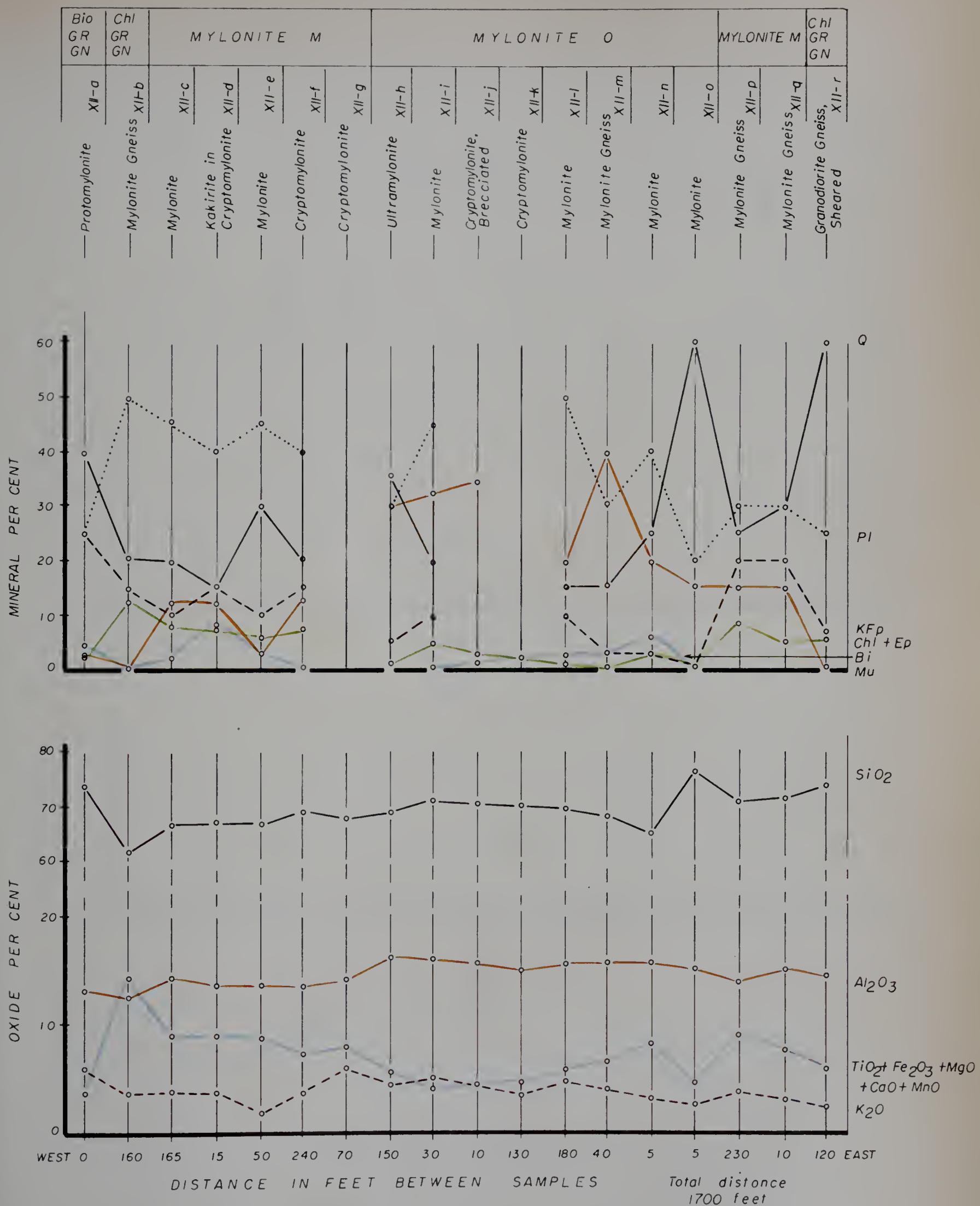


Figure 18. Petrologic profiles for samples from area XII,

Collins Lake.

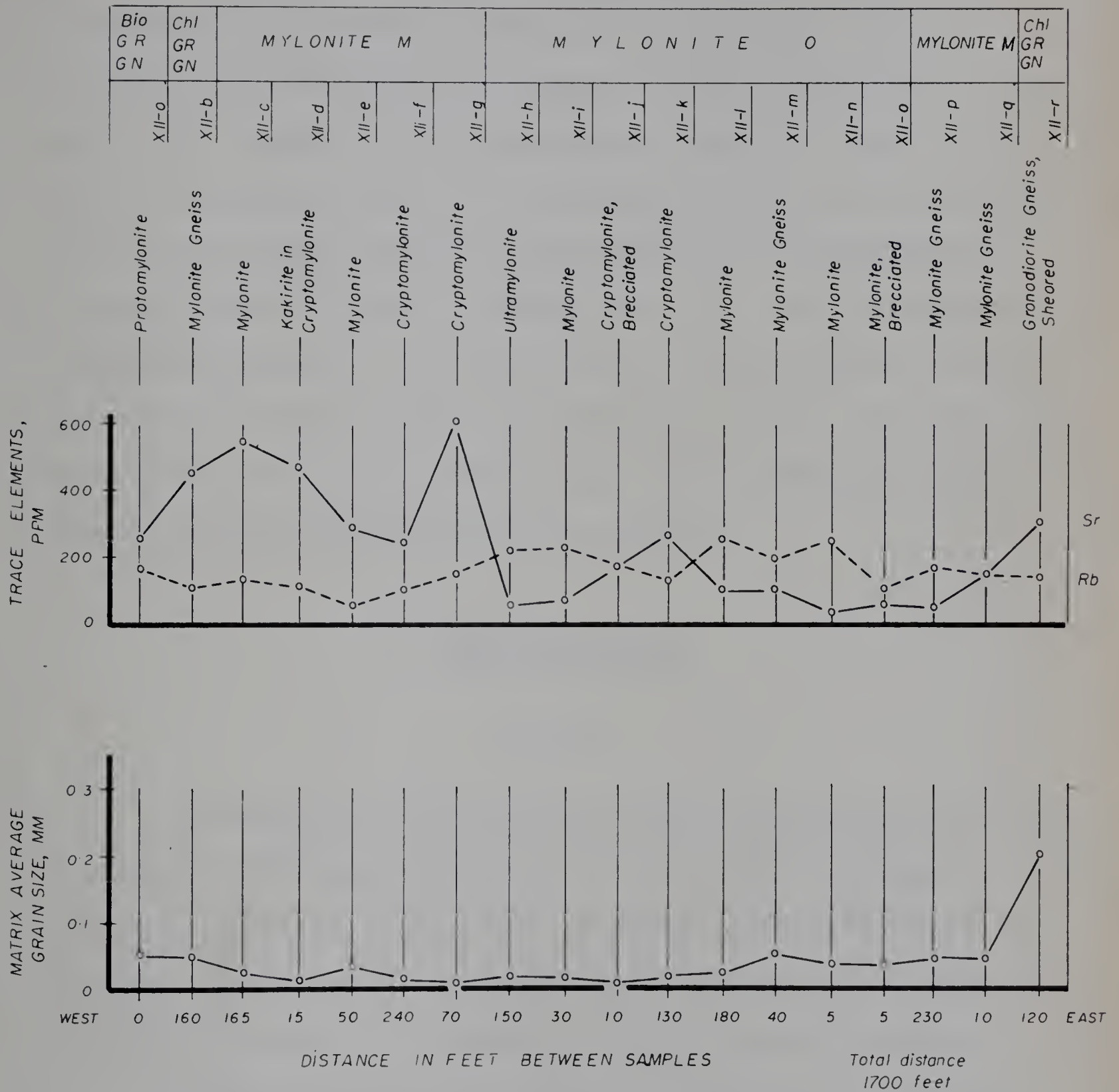


Figure 18. (Continued)

the synkinematic stage and produced a wide, composite band of mylonites M and O derived from granite gneiss and impure metasedimentary rocks, respectively. Recrystallization of the mylonites accompanied waning deformation. (ii) Renewed cataclasis in the late-kinematic stage produced cryptomylonite and kakirite in the western band of mylonite M, and cryptomylonite in mylonite O. Rare, rounded mylonite fragments are enclosed within another mylonite (Plate 11, c) and prove the existence of two ages of cataclasis in parts of area XII. Recrystallization after the second cataclastic episode was relatively minor. (iii) The third deformation caused local megascopic brecciation of mylonite O, and examination of polished rock slabs and thin sections reveal a quartz stockwork with drusy quartz and calcite partially filling residual cavities (Plate 11, e, f). This last deformation is post-orogenic in age and took place under shallow conditions.

Bayonet Lake Study

Area XIII

An elongate lens of mylonite O about one mile north of Bayonet Lake shows a transitional relationship across strike to impure quartzite. Six samples were collected through the contact zone to demonstrate the petrologic changes that may arise from shearing. A seventh sample from another metasedimentary lens 400 feet farther east is included for comparison of composition with the main band of metasedimentary rock.

Average matrix grain size decreases in a westerly direction, and sample XIII-a is too fine-grained (cryptomylonite) for estimation of the plagioclase and quartz content.

The profiles for samples XIII-a to XIII-f show considerable variation in mineral content but relatively slight changes in chemistry. These samples may be representative of a single sedimentary lithology where differences in mineral content arise from varied degrees of cataclasis and superimposed neomineralization. The effect

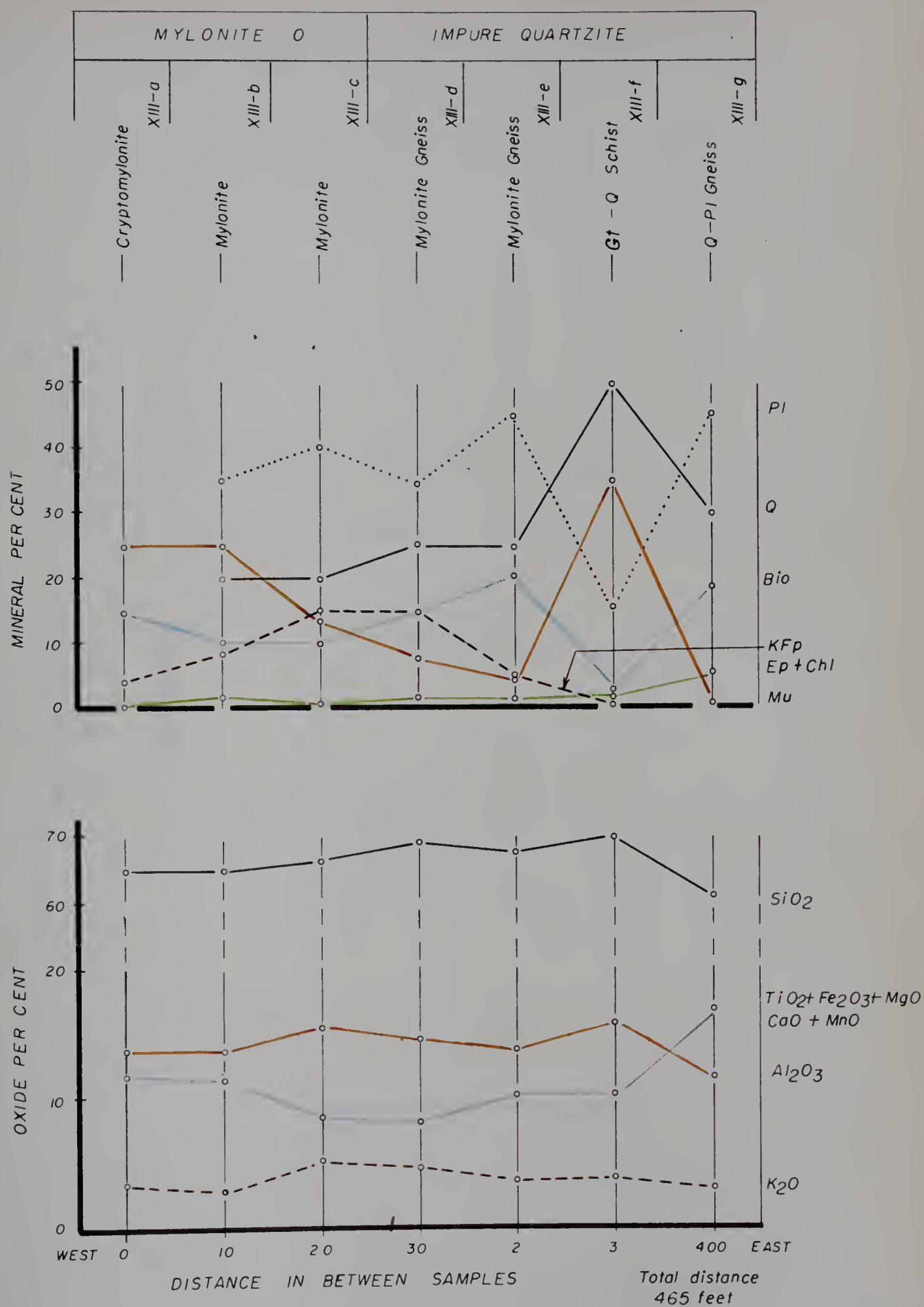


Figure 19. Petrologic profiles for samples from area XIII, Bayonet Lake.

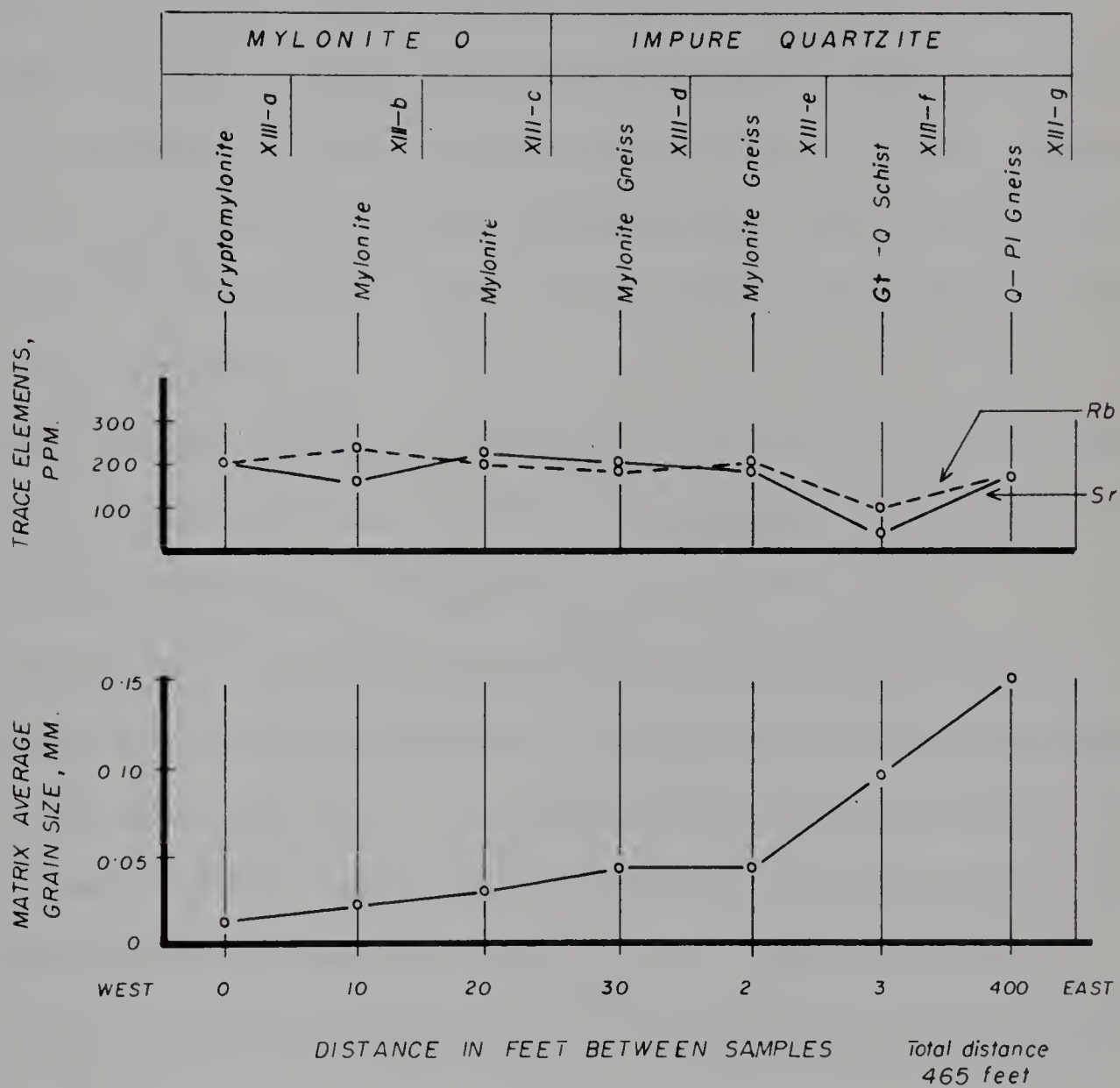


Figure 19. (Continued)

of increasing degree of cataclasis from sample XIII-f to XIII-a is seen by (i) a decrease in quartz, and (ii) the increase of white mica at the expense of plagioclase and probably garnet. Potash feldspar is seen as only megacrysts that were probably chiefly formed by neomineralization during the waning stages of deformation. Quartz forms irregular blebs and layers in sample XIII-f and appears to be intruded, but the silica profile shows negligible enrichment; the development of white mica from plagioclase releases silica which results in quartz, provided that potash feldspar does not crystallize, as shown in sample XIII-f. Thus, quartz enrichment without appreciable increase in SiO_2 is explained.

The chemical composition of mylonite O and impure quartzite from area XIII are similar to mylonite O from area XII, and resembles an analysis of siliceous argillite from the Precambrian of Michigan (Pettijohn, 1957, p. 345).

Detailed study of samples from area XIII show that different proportions of the same mineral assemblage may arise from homogeneous rocks with varying degree of cataclasis and neomineralization. The presence of relict garnet streaks enclosed by alteration mats of white mica and biotite in sample XIII-f shows that the metamorphic grade of the metasedimentary rocks was at least amphibolite facies and cataclasis has caused retrogressive metamorphism or took place under declining metamorphic conditions.

Area XIV

The mylonite zone along the east side of Bayonet Lake is structurally and lithologically complex. Major bands of mylonites K, L, and M are enclosed by hornblende and biotite granite gneisses, and the whole complex is disrupted by late transverse and longitudinal faults. The six samples used in this study represent a cross section through the mylonite bands and the enclosing granite gneiss (Fig. 6), and are examined in an attempt to show petrologic changes that accompany development of mylonites in granite gneiss. These samples were also used in the magnetic susceptibility

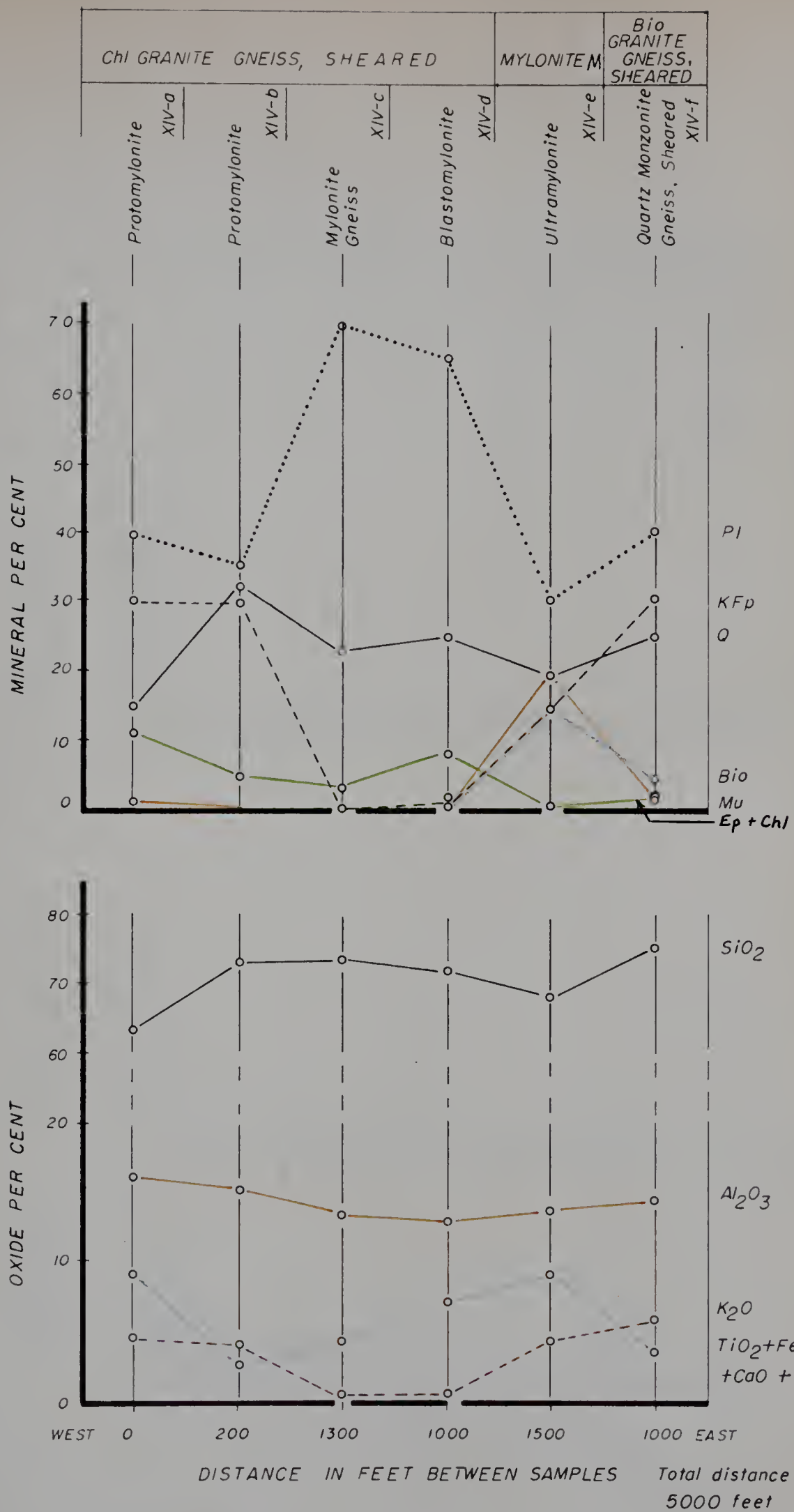


Figure 20. Petrologic profiles for samples from area XIV,
Bayonet Lake.

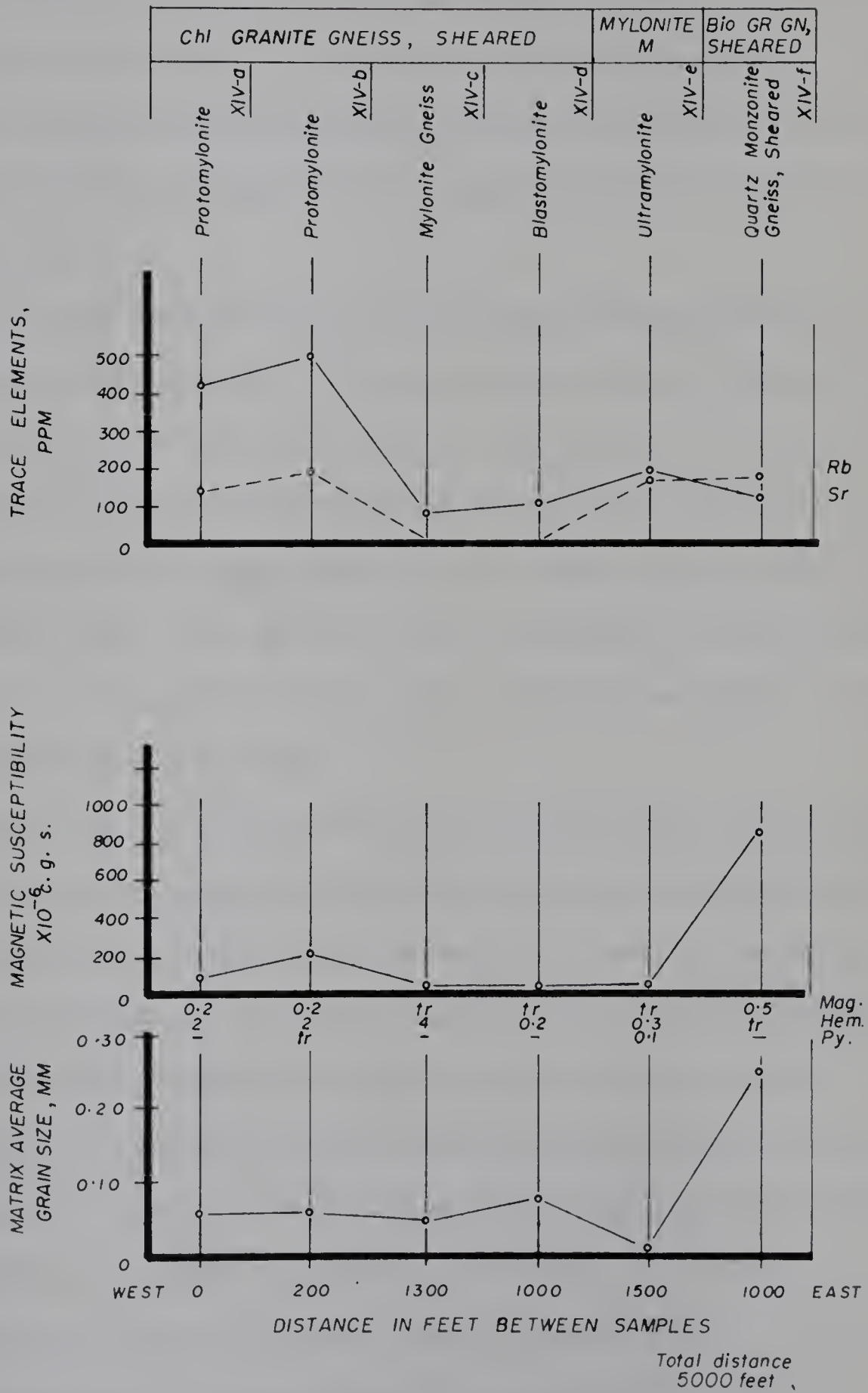


Figure 20. (Continued)

study discussed in chapter three.

Examination of hand specimens shows sample XIV-e as the only typical mylonite, and thin section study verifies this observation. Samples XIV-a and XIV-b are highly recrystallized protomylonites which are slightly sheared by a subsequent deformation. Samples XIV-c and XIV-d are former mylonites that have been extensively recrystallized to produce mylonite gneiss and blastomylonite, and are proximal to observed mylonite bands. Sample XIV-f is a quartz monzonite gneiss that shows incipient granulation.

The mineral and chemical profiles show several distinct features, and indicate considerable chemical adjustment. The virtual absence of potash feldspar and potash in samples XIV-c and XIV-d is extraordinary for acidrocks, and is interpreted as a leaching effect in a zone of intense cataclasis during an early deformation episode. A corresponding increase of plagioclase in the same samples indicates that plagioclase replaced potash feldspar. The absence of white mica suggests that potash migrated from the zone of intense mylonitization leaving a chemical environment unsuitable for the crystallization of white mica.

Samples XIV-a and XIV-e have a high content of TiO_2 , Fe_2O_3 , MgO , CaO , and MnO , and low SiO_2 compared to the other samples, and are likely derived from hornblende granite gneiss. The proximity of sample XIV-e to hornblende granite gneiss (see map-sheet 5) supports the hypothesis. Sample XIV-e (standard sample 79) is mapped as mylonite M and has a composition similar to mylonite M from area XII. The prolific white mica content in sample XIV-e may have developed during a second cataclastic event that produced local mylonite bands from existing highly recrystallized mylonite. Intense cataclasis in a moderate temperature environment and in the presence of water probably produced white mica from plagioclase and potash feldspar. Alternatively, the prolific development of white mica may be due to different chemical composition.

The absence of biotite in samples XIV-a, XIV-b, XIV-c is likely due to chloritization associated with post-crystalline fault activity predominantly in the

western part of the study area.

Magnetic susceptibility measurements apparently reflect the cataclastic history of the rocks, with lowest values from samples that have undergone intense cataclasis, regardless of the degree of recrystallization.

The tectonic history of area XIV includes two episodes of mylonite development, and a third deformation episode that produced faults without pronounced mylonite development. The first deformation episode was intense and widespread with the formation of a wide mylonite and protomylonite zone, and probably occurred during the synkinematic stage of orogenesis. Waning stress and high but declining temperatures promoted recrystallization of the crushed material. A second episode of cataclasis during the late-kinematic stage developed relatively narrow mylonite bands. The third deformation is post-crystalline in age and is responsible for the observed fault pattern and extensive hydrothermal alteration in the western part of area XIV.

Area XV

Seven samples were collected along a westerly traverse in an attempt to show the petrologic changes that accompany cataclasis of hornblende granite gneiss that results in the production of mylonite M. In addition, the relationship of mylonite M to mylonite L is examined. Area XV may be regarded as a detailed study of the eastern segment of area XIV as the traverse lines are nearly colinear.

Thin sections show that samples XV-a, XV-b, and XV-e are highly recrystallized mylonites, whereas samples XV-c and XV-d are less recrystallized mylonites, and the profile showing average matrix grain size forms a smooth, steep valley.

Samples XV-f and XV-g are typical hornblende granite gneisses with a low silica, and a high iron, manganese, magnesia, and lime content. The mineralogy is similar in the two samples, with abundant plagioclase, biotite, and hornblende, and

high plagioclase to potash feldspar ratio. Sample XV-g has at least one per cent relict diopside grains enclosed within uraltite and pale green hornblende. Where hornblende and diopside are intimately intergrown, it is commonly impossible to distinguish one from the other. The mineral association indicates upper amphibolite or hornblende granulite facies of metamorphism, with diaphoresis of the granite gneisses proximal to mylonite zones.

The change to mylonite M from hornblende granite gneiss takes place through a migmatite zone about 300 feet wide. Samples XV-d, and XV-e have uniform chemical composition, and are similar to mylonite M from areas XII and XIV. The apparent transition from hornblende granite gneiss to mylonite M in area XV entails an appreciable increase in SiO_2 , and a corresponding loss in mafic oxides which correspond to an increase in quartz and decrease in mafic minerals, respectively, as shown by the profiles. Sr follows Ca geochemically, and both show a sharp decrease in mylonite M samples which suggests that Ca was likely released during albitization of intermediate plagioclase and removed in fault solutions.

Sample XV-a is similar to many mylonite L samples with a low MgO and CaO content, although SiO_2 is also appreciably lower than average. The chemical composition of the mixed mylonite is similar to mylonite L except for anomalously high Al_2O_3 which may be due to diffusion from adjacent rocks or inherited from the parent rock. Sr is disproportionately enriched in samples XV-a and XV-b compared to CaO increase, and may be due to preferential migration of Sr from adjacent rocks.

The tectonic history of area XV is analogous to area XIV. Severe synkinematic cataclasis produced a wide zone of mylonites which was thoroughly recrystallized under conditions of relaxed shearing stress and high temperature. Reactivated shearing within the existing mylonite zone during the late-kinematic phase produced secondary mylonites in an environment that allowed plastic flowage of the matrix into spaces between fragmented porphyroclasts. Slight recrystallization of the secondary mylonites succeeded cataclasis and caused differentiation of quartz into granoblastic lenticles.

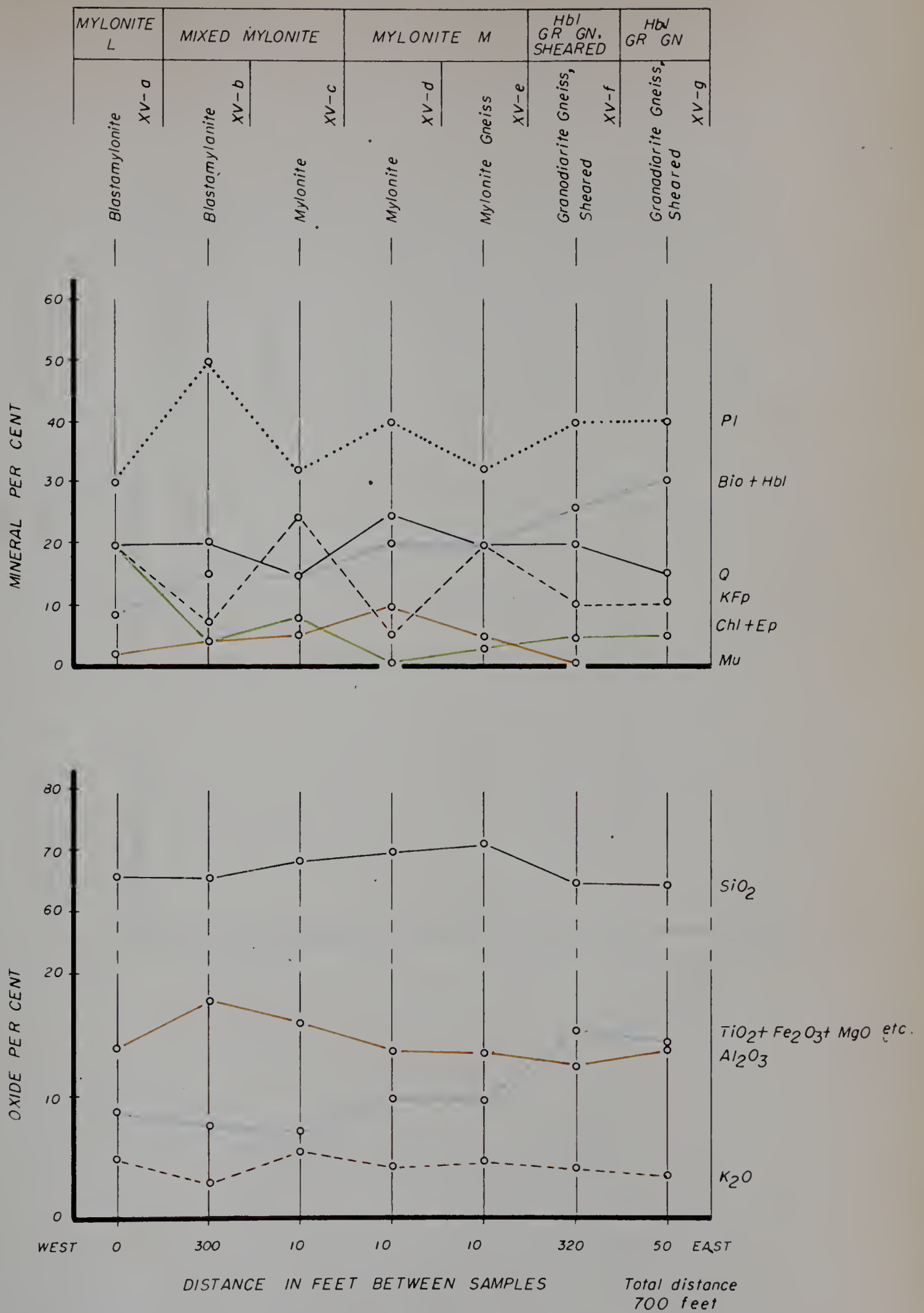


Figure 21. Petrologic profiles for samples from area XV,

Bayonet Lake.

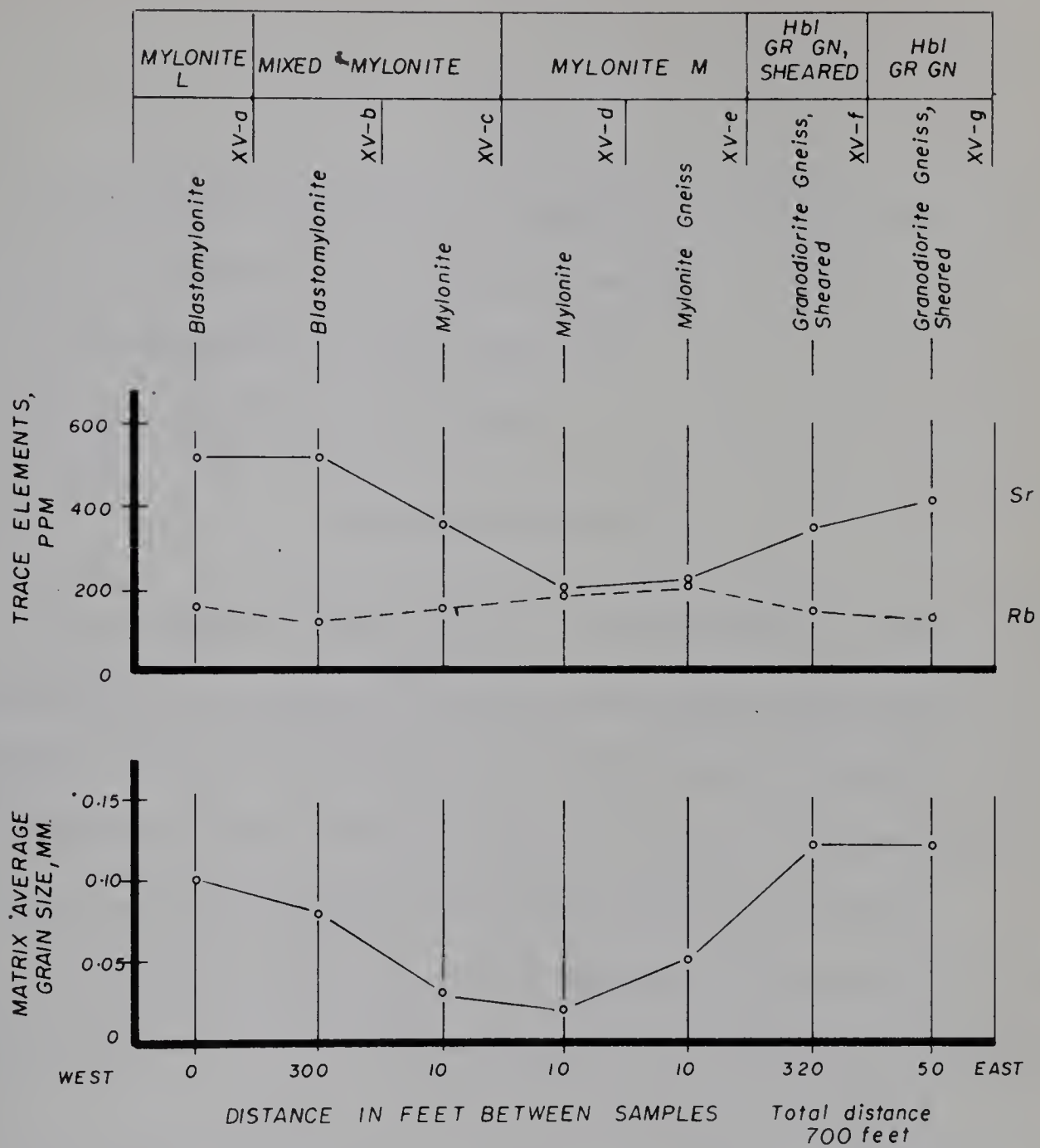


Figure 21. (Continued)

CHAPTER FIVE

STRUCTURE

Faults

Extreme cataclastic effects are exceptionally well developed in northeastern Alberta, and are attributed to two periods of faulting:

- (i) paracrystalline or early faults, and
- (ii) post-crystalline or late faults.

Paracrystalline Faults

The root region of mountain belts is characterized by an intimate interaction of recrystallization and deformation during the synorogenic phase of mountain building. The Precambrian Shield is regarded as the denuded remains of extensive orogenic belts, and the observation of deformational features in the field, hand specimen, and thin section, may be used to reconstruct the tectonic history of such areas.

In northeastern Alberta, the chief deep-seated deformational effect has been the development of wide mylonite zones which are referred to as paracrystalline faults.

Three northerly trending paracrystalline fault zones are found in the study area and are designated as (i) the Charles Lake zone, (ii) the Treasure Loch zone, and (iii) the Bayonet Lake zone. These early fault zones are recognized by the development of wide bands of cataclastic rocks composed of aphanitic to fine-grained rocks that are generally resistant to weathering and hence stand out as ridges. These fault zones parallel the major lithologic and foliation trends.

Granite gneiss is the prevalent rock-type in map-areas 5 and 9 and which also contain an abundance of mylonites K and L, whereas the presence of major, con-

tinuous bands of relatively easily deformed granite F in map-areas 5, 10, and 11 has accommodated much of the deformation in the Charles Lake and Treasure Loch fault zones with common development of mylonite P.

Strike-slip separation cannot be deciphered from these early mylonite zones due to the paucity of suitable markers along the longitudinal faults; however, the steeply dipping, straight, continuous cataclastic rock zones are indicative of transcurrent faulting. Further, the highly recrystallized nature of the mylonites, plastic folding within the mylonite bands, and biotite neomineralization shows that cataclasis took place at considerable depth and high temperature. Suggested oscillatory lateral movement along the paracrystalline fault zones is based upon:

- (i) field data; on-strike changes in uncrushed rock-types proximal to the fault zones are accompanied by the development of the corresponding cataclastic rock-types, and the juxtaposition of dissimilar mylonite-types is accompanied by very little mechanical mixing;
- (ii) petrographic data; thin sections commonly show fractured porphyroclasts with only slight displacement of the segments and flowage of the matrix into the interstices;
- (iii) petrologic data; cataclastic rocks can be traced gradationally across strike into the corresponding parent rock even in wide mylonite bands, whereas this would be impossible if considerable movement brought dissimilar rocks in juxtaposition;
- (iv) aeromagnetic data; the Charles Lake crush zone beyond the southern margin of the study area apparently does not displace a major aeromagnetic-high ridge that trends obliquely through the crush zone.

Field and petrographic observations indicate that rocks of the three cataclastic rock bands are the result of a major synkinematic phase of faulting followed by moderate to intense recrystallization and a less severe late-kinematic phase with slight re-

crystallization. Post-crystalline cataclasis has produced negligible quantity of cataclastic rock.

Post-crystalline Faults

Numerous longitudinal and transverse, post-crystalline faults are observed in the study area. Longitudinal faults trend from north 0 to 20 degrees east, whereas most transverse faults are related to either the north 30 to 45 degrees west direction, or the north 30 to 45 degrees east direction. Criteria for the recognition of late faults are based upon (i) field observations, (ii) air photo interpretation, (iii) aeromagnetic map interpretation, and (iv) thin section and polished rock slab examination.

In many cases late faults are detected by field observations such as a narrow, straight valley, with breccia developed in rocks within the valley and along the valley walls, commonly accompanied by an alteration zone containing abundant chlorite and red feldspar. Fault-line scarps with minor relief are also commonly observed. Mylonitic rock may be present as narrow bands several inches to tens of feet wide. The Bonny Fault trending northwesterly past the northern tip of Bayonet Lake shows most of the above-mentioned features. However, the trace of late faults is generally the locus of differential weathering, and the rocks are commonly obscured by muskeg, sand, or both, and supplementary criteria are required to determine whether the valley is due to (i) faulting, (ii) jointing, (iii) differential erosion along the contact of dissimilar rocks, (iv) preferential erosion of a narrow metasedimentary rock band, or (v) glacial erosion.

Map compilation provides an effective means of recognizing faults where major rock bands are truncated or displaced. In such cases, aerial photographs show a linear, coincident with the fault.

Major late faults that transect hornblende granite gneiss (high aeromagnetic relief) may be expressed by an aeromagnetic trough ("demagnetization" of granite

gneiss) coincident with the fault trace. The prime example is the Bonny fault located predominantly in map-area 1 with an extension into the northeast quadrant of map-area 5, discussed by Godfrey (Godfrey and Baadsgaard, 1962). A second sample is seen northeast of Ashton Lake (Map 1) where a northeasterly fault transects granite gneiss. However, aeromagnetic data only corroborate the field evidence, and should not be used as a single criterion to indicate faulting.

Thin sections supplemented by polished rock slabs provide definite evidence for late faulting, with the development of breccia, micro-shears, quartz, calcite, and epidote fracture fillings, and chloritization of mafic minerals. These features are particularly evident in reactivated shears within an existing mylonite zone; thus, post-crystalline faulting is shown to have been operative along the axis of the Charles Lake and Bayonet Lake mylonite zones. Allanite, and magnetite-sphene euhedra are commonly present in the rocks proximal to late faults.

The precise nature of the movement along the fault planes could not be determined owing to the low relief of the glaciated outcrops. However, horizontal separation can be measured where the faults cut the steep foliation at a high angle, and two examples of sinistral strike separation are seen: (i) in the northwest quadrant of map-sheet 9 with about 1,000 feet separation, and (ii) east of Bayonet Lake, map-sheet 5 with at least 3,000 feet separation along the Bonny fault.

Joints

Joints were observed in all major rock types but were not systematically measured due to their sparse development. However, one of the distinctive features of hornblende cataclasite in the Charles Lake, North map-area is the development of a northerly trending and steeply westerly to vertical dipping joint system, parallel to the foliation of the enclosing mylonite L. The joints are spaced about three inches apart and give rise to tabular fracture blocks forming talus slopes along the east side of the two northernmost peninsulas in Charles Lake. This type of sheeting

has developed within hornblende cataclasite only and may be due to elastic expansion as the cover rocks are removed by erosion. The absence of similar joint pattern in the adjacent rocks may be due to relatively less elastic strain energy. Hornblende cataclasite in map-area 11 shows similar, incipient development of jointing.

Foliation and Lineation

Foliation is well developed in most rock-types from the study area and is expressed in the alignment of mica flakes, quartz lenticles, and feldspar megacrysts, singly or in combination. Layering (gneissosity) may be regarded as the extreme development of foliation as exemplified by biotite and hornblende granite gneisses. The foliation is virtually always steeply dipping with values within 20 degrees of vertical, and it has a northerly regional trend. Massive structure is typical of hornblende cataclasite, grey hornblende granite, leucocratic granite, and phases of both biotite "q" granite and granite F. The typical lamination of mylonites results from granulation and streaking and is regarded as one type of foliation. The foliation trends of the major cataclastic bands are conformable with those of the enclosing rocks, and therefore likely resulted from the same stress system.

Lineation observations in the study area are lacking due to: (i) the planar, polished surfaces of glaciated outcrops, (ii) the steeply dipping foliation which makes the distinction between lineation from foliation difficult, and (iii) the paucity of prismatic minerals. Feldspar megacrysts in granite F and Arch Lake granite appear to be lineated in outcrop, but splitting of the rock along the foliation showed that the feldspar megacrysts tend to be tabular and irregularly aligned in the plane of foliation. The plunge of minor folds is difficult to measure due to isoclinal folding, although a steep plunge is indicated by the absence of shallow dips around the nose of such folds.

Folds

Major folds are not observed in the study area, although numerous minor folds larger than outcrop scale are shown on the map-sheets, and progressively smaller-scale folding is seen in outcrop, hand specimen, and thin section.

Minor folds in all major rock-types are recognized from field readings on adjacent easterly traverse lines on a 1/4 mile spacing, and show development of rheomorphic (Hills, 1963, pp. 245-246) and saddle-shaped folds. These features are particularly evident in biotite and hornblende granite gneisses.

Two granite gneiss areas exhibit folding which contrasts with the predominantly northerly structural trend throughout the study area; (i) a large, bulbous area of hornblende granite gneiss in the northeast quadrant of map-area 9 is intricately folded and shows a swirled foliation. This area is enclosed within the bifurcation of the Charles Lake cataclastic band and represents a wedge that was likely deformed between the two zones of mylonitization. (ii) Biotite granite gneiss and quartzite east and southeast of Bayonet Lake (map-area 5) show rheomorphic folding that may be related to the stresses which caused mylonitization of the Bayonet Lake fault zone.

The mylonite bands show predominantly straight foliation and lithologic trends, although plastic flowage effects are seen on all scales of observation. Mylonite P bands are commonly folded in the Treasure Loch (map-area 5, east and north of the lake), and Charles Lake (map-area 10, center band at the bottom of the map-sheet) areas. The folded nature of these bands, and the commonly ungranulated nature of the enclosing rocks indicates that mylonite P is partly intrusive, with intrusion taking place during plastic deformation of the host rocks. Plastic flowage after the main phase of mylonitization is shown by the minor folds, commonly seen in mylonite P and more rarely in mylonite K, corroborated by small-scale folds in both hand specimen and thin section.

CHAPTER SIX

DISCUSSION AND SUMMARY

Faulting

Deep-seated movement zones have produced three main cataclastic rock bands. Field, hand specimen, and thin section observations indicate two periods of paracrystalline, longitudinal faulting associated with cataclastic bands up to one mile wide in a single orogenic event. The early, synkinematic pulse was responsible for the main development of the mylonite bands. Prevailing high temperatures subsequently promoted recrystallization of the crushed rocks with most extensive recrystallization in the Bayonet Lake bands. The late-kinematic phase of cataclasis produced a new generation of cataclastic rocks within the existing cataclastic bands with only slight recrystallization under conditions of decreased temperature. Lateral movement along these paracrystalline faults was likely oscillatory.

Post-crystalline, steeply dipping faults are both longitudinal and transverse, and horizontal separation is observed along a few of the transverse faults. Microscopic breccia, kakirite, and some cryptomylonite may represent an early phase of post-crystalline faulting, whereas megascopic breccia with partial to complete infilling of interstices by quartz and calcite may represent a late phase of post-crystalline faulting at a shallow level in the crust.

Tension fractures may be related to relief of the stresses that produced post-crystalline faults, or they may have formed in response to the release of load pressure by denudation of the cover rocks.

The paracrystalline faults are major in magnitude and probably represent zones of crystal weakness where renewed movement has recurred throughout the tectonic history of the study area. It is likely that earlier episodes of mylonitization have acted along these crush zones but the cataclastic textures are oblit-

erated by thorough recrystallization during subsequent plutonic metamorphism.

Magnetic Susceptibility

The low relief of the major cataclastic bands on the aeromagnetic map is shown to be due to both (i) a parent rock (area V) of initially low magnetic susceptibility, and (ii) "demagnetization" accompanying mylonitization of initially high magnetic susceptibility rocks (area XIV).

The results of magnetic susceptibility and petrographic studies of sample suites from cataclastic areas of low aeromagnetic relief show that high susceptibility values correlated with a high magnetite content, and "demagnetization" of rocks corresponds to the hematization of magnetite. Hydrothermal solutions in the fault zones caused extensive hematization of magnetite, chloritization of the mafic minerals, and sericitization of feldspar. The most pronounced alteration has occurred in the finest grain-size fraction by virtue of the larger surface area available for reaction, and the high strain energy of the extensively comminuted grains.

Specific Gravity

Specific gravity profiles of samples from selected traverses across parental and cataclastically-derived rocks (areas III, V, VIII, X, and XI) generally show good correlation with corresponding cationic oxides profiles. The effect of variations in SiO_2 , Al_2O_3 , K_2O , and the degree of crushing (average matrix grain size) on specific gravity changes cannot be accurately assessed in the scope of this study, although their effects are considered to be secondary.

Mineralogical and Chemical Changes with Cataclasis

Likely and established mineralogical and chemical changes that accompany cataclasis are indicated in Table 24, and some general observations are listed below.

where β is the slope, α is the intercept, σ^2 is the variance of the error term.

Regression Analysis

The first step in the regression analysis is to determine the relationship between the dependent variable and the independent variable. This is done by plotting the data points and visually inspecting the relationship. If the relationship appears to be linear, then a simple linear regression model can be fitted to the data. If the relationship is non-linear, then a non-linear regression model may be more appropriate.

The second step in the regression analysis is to estimate the parameters of the regression model. This is done by using the method of least squares, which minimizes the sum of the squared residuals. The residuals are the differences between the observed values and the predicted values from the regression model. The third step in the regression analysis is to test the significance of the regression coefficients. This is done by using the t-test, which compares the estimated coefficient to zero. If the t-statistic is large in absolute value, then the coefficient is significantly different from zero. The fourth step in the regression analysis is to calculate the coefficient of determination, R^2 , which measures the proportion of the variance in the dependent variable that is explained by the independent variable. The fifth step in the regression analysis is to use the regression model to make predictions about the dependent variable for given values of the independent variable.

Linear Regression

Linear regression is a statistical method for modeling the relationship between a continuous dependent variable and one or more independent variables. The most common form of linear regression is simple linear regression, which models the relationship between a single independent variable and a continuous dependent variable. The equation for simple linear regression is $y = \beta_0 + \beta_1 x + \epsilon$, where y is the dependent variable, x is the independent variable, β_0 is the intercept, β_1 is the slope, and ϵ is the error term. The parameters β_0 and β_1 are estimated using the method of least squares, which minimizes the sum of the squared residuals. The residuals are the differences between the observed values of y and the predicted values from the regression model.

Multiple Regression and Logistic Regression

Multiple regression is a statistical method for modeling the relationship between a continuous dependent variable and two or more independent variables. The equation for multiple regression is $y = \beta_0 + \beta_1 x_1 + \beta_2 x_2 + \dots + \beta_k x_k + \epsilon$, where y is the dependent variable, x_1, x_2, \dots, x_k are the independent variables, $\beta_0, \beta_1, \beta_2, \dots, \beta_k$ are the regression coefficients, and ϵ is the error term. Logistic regression is a statistical method for modeling the relationship between a binary dependent variable and one or more independent variables. The equation for logistic regression is $\text{logit}(p) = \beta_0 + \beta_1 x_1 + \beta_2 x_2 + \dots + \beta_k x_k$, where p is the probability of the event occurring, x_1, x_2, \dots, x_k are the independent variables, $\beta_0, \beta_1, \beta_2, \dots, \beta_k$ are the regression coefficients, and $\text{logit}(p)$ is the log of the odds of the event occurring.

A. Mineralogical Changes

- (i) White mica develops during shearing and sericitization of chiefly potash feldspar and plagioclase.
- (ii) During the early phase of paracrystalline deformation biotite was the stable ferromagnesian mineral and hornblende was largely altered to biotite.
- (iii) During the late phase of paracrystalline deformation chlorite was the stable ferromagnesian mineral and biotite was largely altered to chlorite.
- (iv) During post-crystalline faulting quartz, epidote, chlorite, and calcite, singly or in combination, were introduced into the cataclastic rock zones as interstitial cement in breccia, and fracture fillings.

B. Chemical Changes

- (i) The comparison of chemical analyses of parent and derived rocks shows an appreciable increase of loss on ignition in the sheared rocks that indicates an increase in chemically combined water. Abundant sericite and chlorite in the sheared rocks reflects the pronounced hydrothermal activity that accompanies cataclasis.
- (ii) Potash tends to be mobilized during cataclasis and commonly shows an irregular distribution in the cataclastic rocks. Nevertheless, the systematic enrichment of K_2O in mylonite L as compared to mylonite K serves to distinguish these rocks.
- (iii) SiO_2 may be locally either enriched, or depleted during paracrystalline cataclasis. Such changes are likely due to a contrast in SiO_2 content between the parent and adjacent rock-type, with ionic diffusion of silica taking place during shearing in an attempt to establish chemical equilibrium.

Post-crystalline cataclasis commonly entails introduction of considerable SiO_2 in the form of free quartz as breccia infilling.

- (iv) Boron metasomatism during the late phase of paracrystalline cataclasis is likely responsible for the abundant tourmaline in metasedimentary mylonite O of area XII.

Metamorphism

Grade of Metamorphism

The granite gneisses in the thesis area typically contain hornblende and biotite, with minor amounts of diopside and cordierite indicating a metamorphic grade ranging from upper amphibolite to granulite facies. Metasedimentary rocks, which are more sensitive indicators of metamorphic grade, are intimately associated with the granite gneisses within and just east of the thesis area (Godfrey and Watanabe, in press). They commonly show the mineral assemblage muscovite-garnet-cordierite-sillimanite that is transitional between the sillimanite-almandine subfacies of the almandine amphibolite facies and the hornblende granulite facies (Fyfe, Turner, and Verhoogen, 1958, p. 211).

Mineral transformations with decreasing metamorphism tend to be infinitesimally slow, such that high-grade mineral assemblages persist in a metastable state after the termination of metamorphism. However, shearing and hydrothermal solutions promote crystallization of new minerals that are stable under the existing pressure-temperature conditions (Turner and Verhoogen, 1960, p. 481 and 484).

Textural and mineralogical data show two phases of paracrystalline cataclasis. The cataclastic rocks produced during the early phase of paracrystalline cataclasis typically have abundant biotite which indicates that deformation and neomineralization took place under upper to middle greenschist facies conditions, whereas the prevalence of chlorite and epidote in the rocks affected by the late phase of paracrystalline cataclasis indicates that deformation and neomineralization took place under lower greenschist facies conditions. Post-crystalline cataclasis took place under essentially non-metamorphic (very shallow) conditions as evidenced by the lack of neomineralization and recrystallization in the affected rocks.

Large-size Feldspar Megacrysts

Large-size microcline megacrysts have been described from mylonite P and the granite F parent rock (Chapter Two). Augen-shaped to euhedral megacrysts in the former are up to 4 inches, and subhedral to euhedral porphyroblasts in the latter are up to 6 inches. Mylonite P and granite F form composite elongate bands that are almost invariably sheathed with metasedimentary rocks and contain numerous meta-sedimentary rock inclusions, a situation which is compatible with the hypothesis of a metasomatic origin for granite F. The garnet-biotite-microcline-plagioclase mineral association and the general lack of muscovite indicates that granitization took place under conditions represented by the middle to upper almandine amphibolite facies. Granite F crystallization was essentially complete before cataclasis was initiated, as evidenced by the textural gradation with mylonite P, and granite F rock fragments in mylonite P. The large-size microcline megacrysts in mylonite P, however, have a complex growth history.

The critical features of the microcline megacrysts that serve to unravel the history of mylonite P are: (i) megacryst shape - augen to euhedra, with all intermediate gradations, and (ii) nature of inclusions - sigmoidal and zonal arrangement of biotite inclusions, and zonal arrangement of plagioclase inclusions.

The large-size porphyroblasts in granite F likely grew under static conditions thereby promoting maximum development of the plagioclase and microcline porphyroblasts with relatively few inclusions. Under conditions of declining temperature, the early phase of paracrystalline cataclasis caused severe crushing of the matrix minerals and peripheral granulation and streaking of the feldspar megacrysts giving rise to numerous feldspar augen. Decrease of differential stress and availability of K_2O in mylonite P (chemical analyses show that K_2O is consistently appreciably higher in mylonite P than in granite F) promoted renewed growth of microcline, commonly as a shell around the microcline megacrysts core. Biotite and

plagioclase may or may not be enclosed at the interface of new growth and pre-existing microcline. Locally, slight differential stress caused rotation of the microcline megacrysts which responded by bodily rotation and development of rare "snowball" structure.

Thus, an essentially static growth environment with slight pulses of differential stress and plastic flowage accommodates the presence of subhedral microcline megacrysts with streaks of microcline fragments extending from the ends of the crystals, and the common euhedral microcline. These features show that crystallization outlasted deformation.

The late phase of paracrystalline cataclasis in mylonite P caused local stretching and granulation of feldspar, and extensive chloritization of biotite. No evidence of renewed microcline growth is observed.

Massive Texture of Hornblende Cataclasite

Hornblende cataclasite is typically very fine grained (0.03 to 0.09 mm), massive, inequigranular, and crystalloblastic, and can be recognized as a cataclastic rock only with considerable difficulty. Mylonites derived from a single parent rock generally can be arranged in a sequence of increasing cataclasis or decreasing grain size, whereas the cataclasites form a sequence of increasing grain size due to recrystallization.

In the Charles Lake area, the intimate association of cataclasite with mylonite L of the same metamorphic grade (middle to upper greenschist facies) shows that the genesis of cataclasite is coeval with the main phase of mylonitization, and the cataclasite texture is likely due to physical and chemical properties peculiar to its parent rock. That is, biotite and hornblende granite gneiss parent rocks have responded to cataclasis differently under essentially the same temperature and load pressure conditions during the early phase of paracrystalline cataclasis; mylonite L is the product of intense comminution contemporaneous with flowage in the rock, whereas hornblende cataclasite is the product of intense comminution without flowage.

Attempts to explain the unlaminated texture of cataclasite have been made in other studies: Sutton and Watson (1959, p. 11) suggest a mechanism involving post-crystalline cataclasis in a deep-seated environment; Christie (1960, p. 87) relates the formation of cataclasite (secondary mylonitic rock) to post-crystalline cataclasis of competent quartzo-feldspathic rocks and mylonites representative of an earlier generation of cataclasis (primary mylonitic rocks); and Reed (1964, p. 682) relates the formation of the cataclasite group and the mylonite group to paracrystalline deformation during two orogenies, with the mylonite group formed during the earlier orogeny. Thus, cataclasite may develop in different environments.

Hornblende cataclasite grades to grey hornblende granite by increase of grain size. The thermal energy required to promote this anomalously thorough recrystallization needs explanation. Where cataclasis and plastic flow (recrystallization) were largely contemporaneous, as in mylonite L, the strain energy of the comminuted grains was largely dissipated, whereas cataclasis without plastic flow in cataclasite permitted strain energy to accumulate. Under hydrostatic metamorphic conditions prior to the second phase of paracrystalline cataclasis, cataclasite underwent thorough recrystallization with local development of grey hornblende granite.

Lithologic Correlation

During detailed field mapping, it was possible to distinguish several cataclastic rock-types. Subsequent detailed mineralogical and chemical studies show that the field classification of the cataclastic rocks is valid, and the distinctiveness of a single rock-type is maintained over a large area.

Petrologic relationships of cataclastic rocks to their parent rocks are shown to be relatively consistent in different parts of the map-area, and a similar observation has been stated or implied in other studies, (e.g. Waters and Campbell, 1935, p. 481; Hsu, 1955, p. 264). An important stratigraphic implication is that a single distinctive parent rock-type gives rise to a correspondingly distinctive cataclastic

rock-type, and either parent rock or derived rock may be used in a regional correlation.

Different cataclastic rock-types are commonly located in juxtaposition but they can be clearly mapped separately. Field observations indicate that only slight mechanical mixing of the different adjacent rocks has accompanied cataclasis, and mineralogical and chemical data suggest that the main effect is ionic diffusion where the adjacent rock-types have appreciably different compositions.

Rocks of markedly different composition may respond to shearing in a dissimilar manner under the same pressure-temperature conditions. The same conclusion has been drawn by others, including Hsu (1955, p. 312), and Johnson (1961, p. 421). In the study area, the common occurrence of migmatitic mafic gneiss proximal to felsic cataclastic rock bands shows that plastic flow and ruptural deformation may take place contemporaneously.

Geologic History

The following sequence of events is based primarily upon observations made during the course of this study, and as such deals only with the events that followed the formation of the basement gneiss complex.

- (i) A thick column of sedimentary rocks accumulated upon an existing basement complex and became involved in the Hudsonian Orogeny (Godfrey and Baadsgaard, 1962).
- (ii) The rocks at the base of the sedimentary column were subjected to conditions equivalent to the upper amphibolite to lower granulite facies of metamorphism.
- (iii) Granite F was formed during the granitization of part of the sedimentary rocks which likely took place during and shortly after the peak phase of metamorphism.
- (iv) Metamorphic conditions slowly subsided, and cataclastic effects became predominant over plastic deformation and recrystallization under conditions equivalent to the upper to middle greenschist facies.
- (v) An early phase of paracrystalline cataclasis under upper to middle greenschist fac-

ies conditions produced the major bands of cataclastic rocks.

(vi) Intrusion of porphyritic quartz diorite (raisin granite) and Arch Lake granite likely took place between the first and second phases of paracrystalline cataclasis.

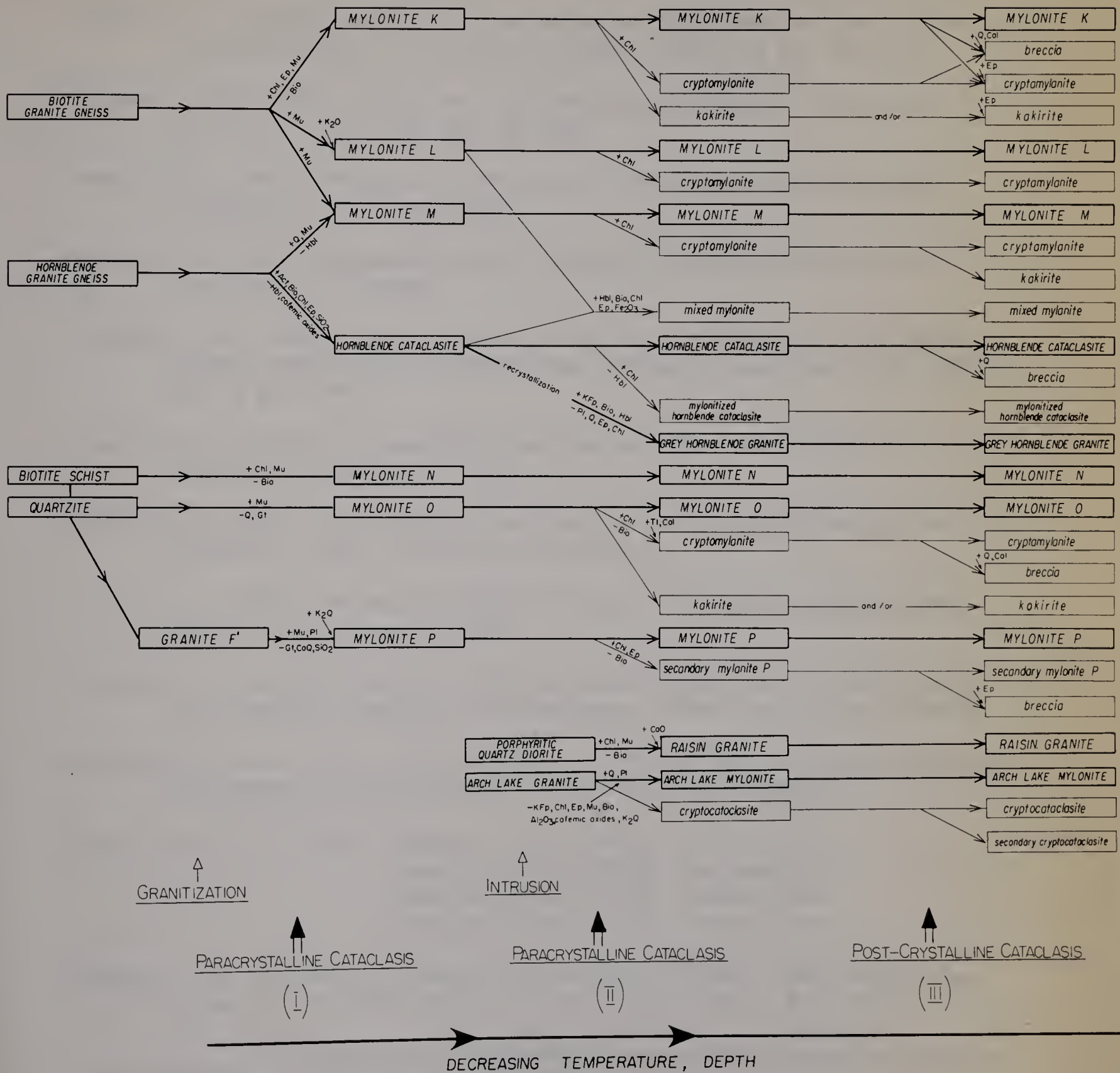
(vii) Subsequent recrystallization of the cataclastic rocks under middle greenschist facies conditions resulted in an increase of grain size, which however, did not obliterate the cataclastic textures.

(viii) A second phase of paracrystalline cataclasis under lower greenschist facies conditions locally produced secondary cataclastic rocks within the existing cataclastic bands.

(ix) Subsequent recrystallization was slight, and thereafter, the rocks behaved in a brittle manner under conditions equivalent to the zeolite facies or under essentially non-metamorphic conditions.

(x) Post-crystalline cataclasis produced mainly breccia which is typical of near-surface conditions.

TABLE 24 PETROGENESIS OF THE CATACLASTIC ROCKS



REFERENCES CITED

- Alf, R.M. (1948): A mylonite belt in the southeastern San Gabriel Mountains, California; *Bull. Geol. Soc. Amer.*, vol. 59, pp. 1101-1120.
- Armstrong, Elizabeth (1941): Mylonitization of hybrid rocks near Philadelphia, Pennsylvania; *Bull. Geol. Soc. Amer.*, vol. 52, pp. 667-694.
- Backlund, H. (1918): Petrogenetische studien an taimyrgesteine; *Geol. Fören. Stockholm Förh.*, vol. 40, pp. 101-203, especially pp. 195-199.
- Bateman, J.D. (1940): An Archean mylonite from northwestern Ontario; *Am. Jour. Sci.*, vol. 238, pp. 742-750.
- Beavis, F.C. (1961): Mylonites of the Upper Kiewa Valley; *Proc. Roy. Soc. Victoria*, vol. 74, pp. 55-66.
- Chayes, F. (1956): Petrographic modal analysis; John Wiley and Sons, Inc., New York, 113 pages.
- Christie, J.M. (1960): Mylonitic rocks of the Moine thrust-zone in the Assynt region, North-west Scotland; *Trans. Edinburgh Geol. Soc.*, vol. 18, pt. 1, pp. 79-93.
- Clough, C.T. (1888): The geology of the Cheviot Hills; *Mem. Geol. Surv. England and Wales*, pp. 1-60.
- Elliott, R.B. (1952): The 'Superposition Error' in the micrometric analysis of rocks; *Min. Mag.*, vol. 29, pp. 833-837.
- _____ (1956): An effect of depth of focus on micrometric analysis; *Min. Mag.*, vol. 31, pp. 272-275.
- Fleischer, M., and Stevens, R.E. (1962): Summary of new data on rock samples G-1 and W-1; *Geochim. et Cosmochim. Acta*, vol. 26, pp. 525-543.
- Fyfe, W.S., Turner, F.J., and Verhoogen, J. (1958): Metamorphic reactions and metamorphic facies; *Geol. Soc. Am. Mem.* 73, 259 pages.
- Geol. Surv. Can. (1964): Geophysics Map 2892G, Colin Lake;
Geophysics Map 2893G, Cornwall Lake;
Geophysics Map 2903G, Charles Lake;
Geophysics Map 2904G, Andrew Lake.
- Godfrey, J.D. (in press): Geology of the Bayonet, Ashton, Potts, and Charles Lakes Districts, Alberta; *Res. Coun. Alberta Prelim. Rept.* 65-6.
- _____ (in preparation): The chemical composition of an area of the Precambrian Shield in northeastern Alberta.
- Godfrey, J.D., and Baadsgaard, H. (1962): Structural pattern of the Precambrian Shield in northeastern Alberta and mica age-dates from the Andrew Lake district; *Roy. Soc. Can., Spec. Publ.* IV, pp. 30-39.

- Godfrey, J.D., and Watanabe, R.Y. (in press): The mineralogical composition of an area of the Precambrian Shield in northeastern Alberta; Rept. 22nd Inter. Geol. Congr., New Delhi.
- Grubenmann, U., and Niggli, P. (1924): *Die Gesteinsmetamorphose*; Borntraeger, Berlin, 467 pages, especially pp. 219-223.
- Hall, A.L., and Molengraaf, G.A.F. (1925): The Vredefort Mountain Land in the southern Transvaal and Orange Free State; Shaler Memorial Series, K. Akad. Wetensch. Amsterdam Verh., Series 2, vol. 24, No. 3, pp. 93-113.
- Harker, A. (1950): *Metamorphism*; Methuen and Co. Ltd., London, 3rd ed., 362 pages.
- Hills, E.S. (1963): *Elements of structural geology*; John Wiley and Sons, Inc., New York, 483 pages.
- Hsu, K.J. (1955): Granulites and mylonites of the region about Cucamonga and San Antonio Canyons, San Gabriel Mountains, California; Univ. Calif. Publ. Geol. Sci., vol. 30, pp. 223-352.
- Johannsen, A. (1932): A descriptive petrography of the igneous rocks, vol. II: the quartz-bearing rocks; The Univ. of Chicago Press, Chicago, 438 pages.
- Johnson, M.R.W. (1961): Polymetamorphism in movement zones in the Caledonian thrust belt of northwest Scotland; Jour. Geol., vol. 69, pp. 417-432.
- King, W., Jr., and Foote, R.B. (1864): On the geological structure of portions of Madras; Mem. Geol. Surv. India, vol. 4, pp. 223-379, especially p. 271.
- Knopf, E.B. (1931): Retrogressive metamorphism and phyllonitization; Am. Jour. Sci., vol. 21, pp. 1-27.
- Lapworth, C. (1885): The Highland controversy in British geology: its causes, course, and consequences; Nature, vol. 32, pp. 558-559.
- Michel-Lévy, A. (1928): Sericitoschistes des chaînes du Mont-Blanc et des Aiguilles Rouges qui sont des mylonites recristallisées postérieures au granite; Bull. Soc. Géol. du France, Series 4, vol. 28, pp. 255-260.
- Moorhouse, W.W. (1959): *The study of rocks in thin section*; Harper and Brothers, New York, 514 pages.
- Nockolds, S.R. (1954): Average chemical compositions of some igneous rocks; Bull. Geol. Soc. Am., vol. 65, pp. 1007-1032.
- Peach, B.N., and Horne, J. (1930): *Chapters on the geology of Scotland*; Oxford Univ. Press, London, 232 pages.
- Pettijohn, F.J. (1957): *Sedimentary Rocks*; Harper and Brothers, New York, 2nd ed., 718 pages.

- Quensel, P. (1916): Zur Kenntnis der Mylonitbildung, erläutert an material aus dem Kebnekaisegebiet; Univ. Upsala, Bull. Geol. Inst., vol. 15, pp. 91-116.
- Raquin, E. (1925): Au sujet de divers de 'mylonites granitiques' le long des lignes de dislocation de l'Quest du Plateau Central; Bull. des Serv. Carte Geol. de la France et des Topog., vol. 29, No. 261, Paris, pp. 1-18.
- Reed, J.J. (1964): Mylonites, cataclasites, and associated rocks along the Alpine Fault, South Island, New Zealand; New Zealand Jour. Geol. Geophys., vol. 7, No. 4, pp. 645-684.
- Reynolds, R.C. (1963): Matrix correction in trace element analysis by X-ray fluorescence: estimation of mass absorption co-efficients by Compton scattering; Am. Min., vol. 48, pp. 1133-1143.
- Sander, B. (1911): Über Zusammenhänge zwischen Teilbewegung und Gefüge in Gesteinen; Tschermak's Miner. u. Petr. Mitt., vol. 30, pp. 281-314.
- _____. (1912): Über einige Gesteinsgruppen des Tauernwestendes; Geol. Reichsanst. Jahrb., vol. 62, pp. 249-257.
- Scott, J.S., and Drever, H.I. (1953): Frictional fusion along a Himalayan thrust; Proc. Roy. Soc. Edinburgh, Sect. B, vol. 65, pt. 2, pp. 121-142.
- Shand, S.J. (1916): The pseudotachylite of Parijs (Orange Free State); Quart. Jour. Geol. Soc. London, vol. 72, pp. 198-220.
- Staub, R. (1915): Petrographische Untersuchungen im westlichen Berninagebirge; Vjschr. naturf. Ges. Zurich, vol. 60, pp. 71-91.
- Sutton, J., and Watson, J. (1959): Metamorphism in deep-seated zones of trans-current movement at Kungwe Bay, Tanganyika Territory; Jour. Geol., vol. 67, pp. 1-13.
- Termier, P., and Boussac, J. (1911): Sur les mylonites de la region de Savonne; Compt. Rend. Ac. des Sci., vol. 152, pp. 1550-1556.
- Turner, F.J., and Verhoogen, J. (1960): Igneous and metamorphic petrology; McGraw-Hill Book Company, Inc., New York, 694 pages.
- Tyrrell, G.W. (1926): The principles of petrology; Methuen and Co. Ltd., 349 pgs.
- Watanabe, R.Y. (1961): Geology of the Waugh Lake metasedimentary complex, northeastern Alberta; unpublished M.Sc. thesis, Univ. Alberta, 89 pages.
- Waters, A.C., and Campbell, C.D. (1935): Mylonites from the San Andreas fault zone; Am. Jour. Sci., vol. 29, pp. 473-503.
- Watkins, N.D. (1961): Studies in paleomagnetism; unpublished M.Sc. thesis, Univ. Alberta, 140 pages.

Winchell, A.N., and Winchell, H. (1951): Elements of optical mineralogy. Part II: Descriptions of minerals; John Wiley and Sons, Inc., London, 551 pages.

Yoder, H.S., and Eugster, H.P. (1954): Phlogopite synthesis and stability range; *Geochim. et Cosmochim. Acta*, vol. 6, pp. 157-185.

APPENDIX A

TABLES 25 TO 39

TABLE 25

MINERALOGY AND CHEMISTRY OF SAMPLES FROM AREA I, CHARLES LAKE

MINERALOGY (estimated percentages)							
	I-a	I-b	I-c	I-d	I-e	I-f	I-g
Q	20	20	15	23	20	20	18
KFp	5	15	15	20	6	.10	5
Pl	45	50	60	45	68	55	65
Hbl	14	-	-	-	-	-	-
Bio	-	1	1	7	5	8	5
Chl	15	1	0.5	1	-	1	2
Mu	-	12	7	4	0.5	-	0.2
Ep	tr	tr	0.5	-	-	3	3
Cal	tr	0.5	0.2	0.1	-	-	-
Zr	tr	tr	tr	tr	0.1	tr	tr
Ap	0.3	tr	-	-	-	0.5	tr
Sph	tr	-	-	-	-	-	-
Mag	1	0.3	0.2	tr	tr	1	1.5
Hem	-	0.2	0.3	tr	-	1	0.5
Py	-	tr	-	-	-	0.2	tr
TOTAL	100.3	100.0	99.7	100.1	99.6	99.7	100.2

CHEMISTRY (X-ray fluorescence)							
	Trace, ppm	Major and minor oxides, per cent					
SiO ₂		62.90	72.35	74.00	72.71	75.21	68.76
TiO ₂		0.58	0.37	0.29	0.29	0.13	0.25
Al ₂ O ₃		14.43	14.40	14.81	14.15	13.08	15.17
Fe ₂ O ₃		5.36	2.29	1.80	2.07	1.23	2.49
MnO		.029	.028	.020	.031	.024	.061
MgO		2.23	1.01	0.61	0.51	0.31	0.71
CaO		3.47	1.12	0.90	0.98	1.23	2.43
K ₂ O		1.74	4.73	5.23	4.77	3.35	2.95
Rb	59	226	249	258	138	62	37
Sr	495	167	155	156	297	948	1,030
TOTAL		90.80	96.30	97.66	95.51	94.56	92.82

TABLE 26

MINERALOGY AND CHEMISTRY OF SAMPLES FROM AREA II, CHARLES LAKE

MINERALOGY (estimated percentages)								
	II-a	II-b	II-c	II-d	II-e	II-f	II-g	II-h
Q	x						x	
KFp	30						10	
Pl	x						x	
Hbl	-						-	
Bio	x						3	
Chl	15						2	
Mu	x						20	
Ep	15						tr	
Cal	-						0.2	
Zr	tr	Too Fine Grained	Too Fine Grained	Too Fine Grained	Too Fine Grained	Too Fine Grained	0.1	Too Fine Grained
Ap	1						0.8	
Al	tr						-	
Sph	1						-	
Lx	2						-	
Mag	tr						0.2	
Hem	1						1	
Py	-						-	
TOTAL	-	-	-	-	-	-	-	-

CHEMISTRY (X-ray fluorescence)									
Trace, ppm	Major and minor oxides, per cent								
	SiO ₂	TiO ₂	Al ₂ O ₃	Fe ₂ O ₃	MnO	MgO	CaO	K ₂ O	
	56.40	0.72	16.79	5.77	.121	2.33	4.47	4.43	
	63.13	0.42	13.78	5.50	.128	2.63	5.28	2.85	
	52.52	0.82	16.82	6.07	.119	2.84	6.75	5.92	
	61.56	0.74	13.28	7.26	.145	5.17	4.32	0.62	
	63.26	0.31	17.97	2.18	.036	0.91	1.47	5.83	
	76.76	0.23	13.75	1.58	.019	0.91	0.42	4.23	
	68.01	0.56	14.81	3.78	.037	1.62	1.82	3.79	
	73.40	0.28	14.63	2.04	.027	0.71	1.06	5.20	

x Mineral present

Table 26 (cont'd.)

MINERALOGY (estimated percentages)

	II-i	II-j	II-k	II-l	II-m	II-n	II-o
Q	15	17	15	20	20	20	15
KFp	7	8	6	8	20	20	20
Pl	60	55	60	53	48	50	45
Hbl	0.2		-	0.2	-	-	-
Bio	3	5	5	7	2	1	4
Chl	6	5	2	3	4	2	-
Mu	-	2	-	-	3	7	15
Ep	8	7	10	7	1	-	-
Cal	0.1	tr	-	-	-	tr	-
Zr	tr	tr	tr	tr	tr	tr	tr
Ap	tr	tr	tr	0.5	0.2	tr	-
Al	-	-	-	-	tr	-	-
Sph	tr	-	-	-	0.4	-	-
Lx	-	-	-	-	0.1	-	-
Mag	0.5	0.5	1	1	0.5	0.5	0.2
Hem	0.1	0.2	0.3	tr	1	-	0.5
Py	-	0.2	0.2	tr	-	-	-
TOTAL	99.9	99.9	99.5	99.7	100.2	100.5	99.7

CHEMISTRY (X-ray fluorescence)

Trace, Major and minor oxides,
ppm per cent

SiO ₂	66.31	65.53	67.73	65.87	73.04	75.78	74.00
TiO ₂	0.30	0.32	0.24	0.21	0.29	0.24	0.29
Al ₂ O ₃	15.78	15.30	14.98	16.36	14.99	14.30	14.04
Fe ₂ O ₃	2.98	3.40	3.54	2.36	1.56	1.40	1.91
MnO	.077	.088	.078	.073	.019	.017	.020
MgO	1.32	1.72	0.91	1.01	0.61	0.61	0.71
CaO	3.01	4.07	4.48	3.90	0.98	0.78	1.08
K ₂ O	2.29	1.79	1.68	2.07	4.47	5.20	5.00
Rb	68	248	22	25	161	211	271
Sr	986	1,174	1,223	1,252	259	163	156
TOTAL	92.07	92.22	93.56	91.85	95.96	98.33	97.05

TABLE 27

MINERALOGY AND CHEMISTRY OF SAMPLES FROM
AREA III, CHARLES LAKE

MINERALOGY (estimated percentages)

	III-a	III-b	III-c	III-d	III-e	III-f	III-g	III-h	III-i
Q	42.1	25	35	30	30	24	20	25	24
KFp	37.4	45	40	45	35	30	25	20	19
Pl	7.6	10	15	10	20	30	35	30	42
Di	-	-	-	-	-	-	-	-	-
Hbl	7.4	15	10	8	14	13	-	-	-
Bio	5.3	4	-	7	1	2	tr	1	2
Chl	-	-	-	-	-	-	1	1	1
Mu	-	-	-	-	-	-	18	23	12
Ep	-	tr	-	-	-	0.5	tr	-	tr
Cal	-	-	-	-	-	-	-	-	-
Zr	0.1	-	tr	tr	tr	tr	tr	-	-
Ap	-	tr	tr	-	-	tr	-	-	-
Al	-	0.5	-	-	0.5	-	-	-	-
Sph	0.3	tr	tr	-	tr	-	tr	-	-
Lx	-	-	-	-	-	-	1	-	-
Mag	0.1	tr	0.3	tr	tr	0.5	-	-	-
Hem	-	tr	-	tr	tr	tr	0.2	0.4	0.2
Py	-	-	-	tr	-	-	-	-	-
TOTAL	100.3	99.5	100.3	100.0	100.5	100.0	100.2	100.4	100.2

CHEMISTRY (X-ray fluorescence)

Trace, Major and minor oxides,
ppm per cent

SiO ₂	74.44	74.28	74.51	70.80	75.96	67.57	70.00	75.39	70.80
TiO ₂	0.25	0.21	0.28	0.29	0.25	0.35	0.22	0.09	0.33
Al ₂ O ₃	11.21	11.93	10.59	12.24	10.80	13.46	14.57	14.79	14.92
Fe ₂ O ₃	3.94	3.79	4.56	4.39	4.68	5.55	1.80	0.76	2.41
MnO	.046	0.043	.059	.066	.063	0.094	.032	.012	.039
MgO	0.10	.20	0.20	0.20	0.20	0.20	0.51	0.30	0.61
CaO	1.15	1.4	1.41	1.35	1.19	1.87	1.13	0.64	1.07
K ₂ O	4.20	5.22	4.54	5.30	4.52	5.36	5.33	4.74	5.40
Rb	95	98	80	99	88	90	271	277	345
Sr	7	207	188	-	19	72	135	62	113
TOTAL	95.34	95.47	96.10	94.64	97.66	94.45	93.59	96.72	95.58

Table 27 (cont'd.)

MINERALOGY (estimated percentages)									
	III-j	III-k	III-l	III-m	III-n	III-o	III-p	III-q	93*
Q	20	15	25	10	17.3	15	15	10	8.6
KFp	10	5	10	7	11.6	15	20	8	13.7
Pl	50	49	49	60	59.1	54	49	55	48.7
Di	-	-	-	-	-	-	-	5	-
Hbl	-	10	tr	20	0.4	4	7	3	3.2
Bio	16	10	3	-	4.4	8	7	15	15.5
Chl	2	5	9	-	1.5	-	tr	tr	-
Mu	-	2	-	-	-	-	-	-	-
Ep	2	3	2	3	4.7	3	1	tr	4.1
Cal	-	-	0.5	tr	0.1	tr	-	-	-
Zr	tr	tr	tr	-	tr	-	tr	-	0.1
Ap	tr	tr	tr	0.5	0.5	tr	tr	0.1	1.5
Al	tr	-	-	-	-	-	-	-	0.2
Sph	-	tr	tr	tr	tr	tr	tr	-	1.3
Lx	-	-	-	-	-	-	-	-	-
Mag	tr	0.7	0.5	tr	0.5	1	1	3	3.3
Hem	-	0.2	1	tr	-	-	tr	-	0.1
Py	0.5	0.1	-	tr	-	-	-	-	-
TOTAL	100.5	100.0	100.0	100.5	100.1	100.0	100.0	99.3	100.3

CHEMISTRY (X-ray fluorescence)										
Trace, ppm	Major and minor oxides, per cent									
	SiO ₂	66.38	64.04	67.00	62.28	64.86	65.92	66.31	61.72	53.25
	TiO ₂	0.48	0.68	0.39	0.22	0.22	0.21	0.21	0.60	1.27
	Al ₂ O ₃	13.47	13.88	14.30	14.04	16.20	16.47	15.07	13.88	15.46
	Fe ₂ O ₃	4.29	4.89	3.82	4.05	2.42	2.29	2.83	4.89	5.23
	MnO	.097	.082	.113	.137	.078	.093	.084	0.071	0.123
	MgO	2.23	1.82	1.92	2.33	1.01	0.91	1.22	2.22	1.90
	CaO	3.64	3.38	3.29	5.46	3.55	3.58	3.25	4.15	5.27
	K ₂ O	2.42	2.82	1.78	1.57	2.15	2.06	2.47	2.72	3.85
	Rb	140	147	21	16	21	25	15	56	65
	Sr	492	365	924	1.077	1.261	1.346	1.347	724	869
	TOTAL	93.01	91.59	92.61	90.09	90.49	91.53	91.49	90.25	84.35

* Standard rock sample

TABLE 28

MINERALOGY AND CHEMISTRY OF SAMPLES FROM AREA IV, CHARLES LAKE

MINERALOGY (estimated percentages)						
	84	IV-a	IV-b	IV-c	IV-d	91
Q	25.7	35	25	30	25	24.5
KFp	9.2	6	8	5	20	2.7
Pl	49.8	44	39	42	40	64.3
Bio	-	1	8	6	11	2.9
Chl	9.3	10	7	4	0.5	1.4
Mu	2.2	3	12	10	3	3.6
Ep	3.2	tr	0.3	0.1	tr	-
Cal	0.1	0.2	tr	tr	tr	0.6
Gt	-	-	-	2	-	-
Ar	0.1	tr	tr	tr	tr	-
Ap	0.3	0.2	-	tr	-	-
Al	-	-	-	-	-	tr
Sph	0.1	-	-	-	-	-
Lx	-	1	-	0.2	0.2	0.2
Mag	-	-	-	tr	tr	0.2
Hem	-	-	0.2	0.2	-	-
Py	-	-	tr	0.1	-	-
Total	100.0	100.4	99.5	99.6	99.1	100.4

CHEMISTRY (X-ray fluorescence)									
				Major and minor oxides, per cent					
Trace, ppm			SiO ₂	-	67.54	67.35	73.74	71.60	-
			TiO ₂	-	0.49	0.60	0.38	0.38	-
			Al ₂ O ₃	-	12.93	13.69	12.14	14.41	-
			Fe ₂ O ₃	-	4.34	4.31	4.86	3.47	-
			MnO	-	0.075	0.073	0.187	0.044	-
			MgO	-	1.90	2.01	2.01	1.69	-
			CaO	-	1.75	1.79	0.93	0.99	-
			K ₂ O	-	3.41	4.32	3.41	5.42	-
			Rb	-	95	174	122	166	-
			Sr	-	286	210	126	221	-
		Total	-	92.44	94.14	97.66	98.00	-	

TABLE 29

MINERALOGY AND CHEMISTRY OF SAMPLES FROM
AREA V, CHARLES LAKE

MINERALOGY (estimated percentages)							
	V-a	V-b	V-c	V-d	V-e	V-f	V-g
Q	10		20	20	25	30	30
KFp	25		5	7	2	5	10
Pl	55		45	43	47	40	40
Bio	-		10	25	20	20	15
Chl	3		5		1	2	1
Mu	-		15	5	5	3	4
Ep	6	Too Fine Grained	0.1	-	-	tr	-
Cal	0.1		-	-	-	tr	-
Zr	-		tr	tr	tr	tr	tr
Ap	-		-	tr	tr	tr	-
Al	-		-	-	-		-
Sph	0.1		tr	tr	tr	tr	-
Lx	tr		0.1	tr	tr	tr	-
Mag	-		tr	-	-		tr
Hem	1		0.1	tr	tr	tr	tr
TOTAL	100.2		100.3	100.0	100.0	100.0	100.0

CHEMISTRY (X-ray fluorescence)							
	Trace, ppm	Major and minor oxides, per cent					
SiO ₂	68.86	80.06	67.36	65.95	65.66	68.58	70.00
TiO ₂	0.29	0.13	0.83	0.39	0.74	0.58	0.56
Al ₂ O ₃	14.52	12.33	15.52	14.85	14.65	13.70	14.43
Fe ₂ O ₃	3.22	2.06	7.28	4.74	5.25	4.75	4.51
MnO	0.060	0.0[9	.081	.074	.056	.069	.079
MgO	1.80	0.40	2.43	1.52	2.13	1.52	1.22
CaO	1.78	0.34	0.47	2.55	1.86	2.59	1.83
K ₂ O	4.14	3.62	3.75	4.03	2.79	3.17	4.08
Rb	129	154	136	175	79	119	180
Sr	351	79	80	295	286	268	163
TOTAL	94.67	98.97	97.72	94.10	93.14	94.96	96.71

TABLE 30

MINERALOGY AND CHEMISTRY OF SAMPLES FROM
AREA VI, CHARLES LAKE

		VI-a	VI-b	VI-c	VI-d	VI-e	VI-f
MINERALOGY (estimated percentages)	Q		20	20	20	15	25
	KFp		7	5	15	10	10
	Pl		43	53	25	28	32
	Di		-	-	-	17	-
	Act+ Hbl		-	-	-	8	10
	Bio		5	20	8	5	7
	Chl		20	2	7	11	5
	Mu		5		20	5	7
	Ep	Too Fine Grained	tr	tr	-	-	0.5
	Cal		tr	-	-	-	-
	Gt		0.5	-	3	-	-
	Ct		-	-	2	-	-
	Zr		tr	-	tr	tr	tr
	Ap		tr	0.5	-	0.5	0.5
	Sph		-	tr	-	-	-
	Mag		tr	tr	tr	0.5	3
	Hem		tr	-	tr	-	-
	TOTAL		100.5	100.5	100.0	100.0	100.0

		VI-a	VI-b	VI-c	VI-d	VI-e	VI-f
CHEMISTRY (X-ray fluorescence)	SiO ₂	63.05	69.53	68.60	65.27	60.50	64.50
	TiO ₂	0.57	0.59	0.55	0.59	0.60	0.59
	Al ₂ O ₃	15.28	13.49	14.70	16.70	12.30	13.14
	Fe ₂ O ₃	4.81	5.17	4.06	6.94	5.76	5.10
	MnO	.070	.071	.067	.095	.114	.104
	MgO	1.42	1.62	1.42	2.23	5.77	4.86
	CaO	2.56	1.89	2.56	0.73	5.57	0.36
	K ₂ O	4.25	2.52	3.02	4.73	3.41	2.47
	Rb	112	76	199	205	155	71
	Sr	298	164	293	107	726	872
	TOTAL	92.01	94.88	94.98	97.29	94.02	91.12

Trace, Major and minor oxides,
ppm per cent

TABLE 31

MINERALOGY AND CHEMISTRY OF SAMPLES FROM
AREA VII, CHARLES LAKE

MINERALOGY (estimated percentages)					
	VII-a	VII-b	VII-c	150	152
Q	30	30	25	13.8	21.3
KFp	15	20	18	22.9	01
Pl	41	35	45	54.4	56.0
Di	-	-	-	-	29
Hbl	-	-	2	3.9	7.8
Bio	6	1	7	1.4	8.5
Chl	1	8	0.5	-	21
Mu	1	-	-	-	-
Ep	4	5	1	1.5	0.7
Cal	-	tr	-	-	-
Zr	tr	tr	tr	-	tr
Ap	tr	0.1	0.1	0.3	0.3
Al	-	tr	-	0.3	-
Sph	tr	tr	tr	-	-
Lx	0.3	-	-	-	-
Mag	0.5	1	1	0.7	0.7
Hem	0.2	0.5	-	-	-
Py	tr	-	-	-	-
TOTAL	100.0	100.6	99.6	99.2	100.4

CHEMISTRY (X-ray fluorescence)						
Trace, ppm		Major and minor oxides, per cent				
SiO ₂		68.45	71.55	68.76	68.47	61.81
TiO ₂		0.21	0.19	0.20	0.24	0.55
Al ₂ O ₃		15.27	15.75	15.82	16.62	14.60
Fe ₂ O ₃		2.12	1.98	2.14	2.38	4.69
MnO		.093	.075	.073	.088	0.096
MgO		0.71	0.91	0.91	0.71	2.85
CaO		2.83	2.34	3.43	3.26	5.39
K ₂ O		2.49	3.70	1.90	2.53	1.25
Rb	36	74	31	54	24	
Sr	1,434	1,032	1,119	1,156	465	
TOTAL		92.17	96.50	93.23	94.30	91.24

TABLE 32

MINERALOGY AND CHEMISTRY OF SAMPLES FROM
AREA VIII, CORNWALL LAKE

MINERALOGY (estimated percentages)	VIII-a VIII-b VIII-c VIII-d VIII-e VIII-f					
Q	25	30	30	35		
KFp	30	25	20	20		
Pl	27	30	40	40		
Bio	4	-	-	-		
Chl	1	7	4	3	1	2
Mu	10	8	6	2	1	1
Ep	2	-	-	-	-	-
Zr	tr	-	-	tr	-	-
Ap	-	-	tr	-	-	-
Al	-	-		tr	-	-
Sph	0.1		tr	0.1	tr	-
Lx	0.1	0.4	tr	0.1	tr	tr
Mag	0.5	-	-	tr	-	-
Hem	tr	tr	tr	0.5	tr	tr
TOTAL	99.7	100.4	100.0	100.7	-	-

CHEMISTRY (X-ray fluorescence)							
Trace, ppm	Major and minor oxides, per cent						
	SiO ₂	69.79	72.29	74.18	50.00	83.34	90.15
	TiO ₂	0.43	0.29	0.35	0.18	0.24	0.17
	Al ₂ O ₃	14.63	14.54	12.34	10.70	8.83	8.35
	Fe ₂ O ₃	2.84	1.95	2.04	1.78	1.87	1.62
	MnO	.021	.019	.023	0.019	0.020	0.017
	MgO	1.11	1.01	0.91	0.81	0.51	0.61
	CaO	1.60	0.32	0.55	0.43	0.57	0.35
	K ₂ O	4.67	5.46	2.71	3.02	2.66	2.63
	Rb	277	247	156	136	162	143
Sr	232	112	83	85	108	70	
<hr/>							
TOTAL	95.09	95.88	93.10	96.94	98.04	103.90	

TABLE 33

MINERALOGY AND CHEMISTRY OF SAMPLES FROM
AREA IX, CORNWALL LAKE

MINERALOGY (estimated percentages)

	IX-a	IX-b	IX-c	IX-d	IX-e	IX-f	IX-g	IX-h
Q	25	15	15	15	22	20	20	20
KFp	25	30	10	15	13	2	10	15
Pl	30	40	40	45	45	63	35	45
Bio	10	4	28	15	17	8	8	-
Chl	1	8	-	0.5	1	2	tr	tr
Mu	-	1	-	-	1	2	20	14
Ep	4	1.5	5	7	1	3	7	0.5
Cal	-	0.5	-	0.5	tr	tr	-	-
Zr	tr	tr	tr	tr	tr	tr	tr	tr
Ap	1.5	tr	0.5	1	tr	tr	tr	tr
Al	tr	-	tr	-	-	-	-	-
Sph	1.5	tr	1.5	-	-	-	-	tr
Lx	-	-	-	1	-	-	-	0.2
Mag	1	tr	-	-	-	-	-	tr
Hem	1	0.2	tr	tr	tr	tr	tr	0.2
Py	0.1	-	tr	-	-	-	-	tr
TOTAL	100.1	99.7	100.0	100.0	100.0	100.0	100.0	99.9

CHEMISTRY (X-ray fluorescence)

Trace, Major and minor oxides,
ppm per cent

SiO ₂	63.96	67.91	58.36	64.47	68.37	64.50	64.09	70.77
TiO ₂	0.91	0.28	1.26	0.44	0.60	0.41	0.57	0.34
Al ₂ O ₃	12.57	15.57	13.54	14.05	12.64	14.27	14.89	13.80
Fe ₂ O ₃	5.91	3.23	7.52	4.35	5.03	4.28	6.74	4.12
MnO	.096	.082	.141	.089	.079	.082	.201	.104
MgO	2.43	1.52	3.65	2.43	2.63	2.74	2.63	1.42
CaO	2.32	1.99	4.02	4.06	1.78	2.57	2.68	1.13
K ₂ O	4.71	5.07	3.25	2.90	2.92	2.22	5.00	4.48
Rb	76	134	246	173	156	129	191	195
Sr	166	359	393	414	351	445	245	235
TOTAL	92.91	95.65	91.74	92.79	94.05	91.07	96.80	96.16

Table 33 (cont'd.)

	IX-i	IX-j	IX-k	IX-l	IX-m	IX-n	IX-o
Q	15	18	20	25	25	30	30
KFp	10	20	15	20	15	6	15
Pl	55	45	45	30	35	43	35
Bio	15	8	13	20	20	15	13
Chl	1	2	2	1	1	0.5	2
Mu	3	7	3	2	2	5	4
Ep	1	-	2	2	2	-	1
Cal	-	-	tr	-	-	0.5	tr
Zr	tr	tr	tr	tr	tr	tr	tr
Ap	tr	tr	tr	0.1	tr	tr	tr
Al	tr	0.3	-	-	tr	-	-
Sph	-	-	-	tr	-	-	-
Lx	-	-	tr	-	-	tr	-
Mag	-	tr	-	tr	tr	tr	-
Hem	tr	tr	tr	tr	tr	tr	0.2
Py	tr	tr	-	-	-	-	-
TOTAL	100.0	100.3	100.0	100.1	100.0	100.0	100.2

CHEMISTRY (X-ray fluorescence)

Trace, Major and minor oxides,
ppm per cent

SiO ₂	67.67	72.55	67.15	64.68	63.83	66.07	67.73
TiO ₂	0.62	0.56	0.60	0.70	0.73	0.61	0.62
Al ₂ O ₃	14.33	13.28	13.91	14.46	14.24	14.44	13.99
Fe ₂ O ₃	4.97	3.58	4.58	5.44	5.76	4.51	4.81
MnO	.081	.064	.076	.092	.098	.091	.079
MgO	1.92	1.32	1.72	1.62	1.82	1.72	1.62
CaO	2.04	1.30	2.03	3.21	2.96	2.34	2.40
K ₂ O	3.10	3.58	3.64	2.88	3.18	4.30	3.07
Rb	163	81	152	174	203	166	181
Sr	266	152	242	325	300	259	223
TOTAL	94.73	96.23	95.71	93.08	92.62	94.08	94.32

TABLE 34

MINERALOGY AND CHEMISTRY OF SAMPLES FROM
AREA X, TREASURE LOCH

MINERALOGY (estimated percentages)

	X-a	X-b	X-c	X-d	X-e	X-f	X-g
Q	30	25	25	20	15	10	40
KFp	20	8	7	8	4	4	5
Pl	43	50	55	50	63	65	20
Bio	7	12	10	20	15	12	7
Chl	tr	0.1	0.5	-	-	-	-
Mu	-	3	3	1	-	8	25
Ep	-	-	-	-	-	-	-
Cal	-	-	tr	tr	-	-	tr
Gt	-	1	-	-	-	-	3
Zr	tr	0.1	tr	tr	-	tr	tr
Ap	0.2	0.5	-	0.5	2	0.3	-
Al	-	-	-	-	-	-	-
Sph	-	-	-	-	-	-	-
Lx	-	-	0.2	-	-	0.1	tr
Mag	tr	tr	tr	0.5	0.2	0.2	tr
Hem	tr	tr	tr	0.5	0.5	0.5	tr
Py	tr	-	tr	tr	-	-	-
TOTAL	100.2	99.8	100.7	100.5	99.7	100.1	100.0

CHEMISTRY (X-ray fluorescence)

Trace, Major and minor oxides,
ppm per cent

SiO ₂	66.20	61.61	68.78	61.27	63.47	68.91	57.30
TiO ₂	0.49	0.42	0.57	0.63	0.80	0.56	0.98
Al ₂ O ₃	15.01	16.94	14.65	16.72	15.59	15.41	16.44
Fe ₂ O ₃	3.40	2.99	3.64	4.08	4.16	4.27	10.39
MnO	.043	.044	.073	.052	.043	.063	.255
MgO	2.03	1.62	1.72	2.03	2.23	2.03	3.34
CaO	1.88	1.98	2.24	2.58	2.58	2.98	0.46
K ₂ O	4.28	6.32	3.60	5.33	3.98	2.16	4.12
Rb	152	186	152	185	173	121	200
Sr	467	524	353	476	503	455	67
TOTAL	93.33	91.92	95.27	92.64	92.85	96.38	93.29

Table 34 (cont'd.)

MINERALOGY (estimated percentages)

	X-h	X-i	X-j	X-k	X-l	X-m	X-n
Q	30	40	25	25	35	35	30
KFp	1	0.2	1	7	30	30	12
Pl	32	20	45	35	23	22	41
Bio	tr	1	7	15	8	3	8
Chl	10	8	3		0.5	5	2
Mu	25	30	15	15	3	3	1
Ep	tr	-	-	-	-	1	3
Cal	-	-	-	-	-	0.1	-
Gt	0.2	tr	4	-	-	-	-
Zr	tr	tr	tr	tr	tr	tr	tr
Ap	-	-	-	tr	-	tr	0.3
Al	-	-	-	-	-	tr	tr
Sph	-	-	-	-	-	tr	1
Lx	0.2	-	-	-	-	tr	-
Mag	0.1	tr	0.1	-	tr	0.1	1.5
Hem	1	0.2	0.2	3	0.5	1	-
Py	-	-	-	-	-	tr	-
TOTAL	99.5	99.4	99.3	100.0	100.0	100.2	99.8

CHEMISTRY (X-ray fluorescence)

Trace, Major and minor oxides,
ppm per cent

SiO ₂	64.37	73.66	63.08	69.15	75.06	74.85	68.16
TiO ₂	0.58	0.39	0.77	0.88	0.23	0.24	0.64
Al ₂ O ₃	17.47	15.97	14.73	16.81	13.40	13.34	14.78
Fe ₂ O ₃	7.69	3.69	8.61	6.27	1.81	1.89	4.75
MnO	.092	.074	.235	.046	.037	.035	.101
MgO	2.53	1.42	2.83	2.43	0.61	0.61	1.52
CaO	0.37	0.88	1.96	6.85	0.74	1.26	2.98
K ₂ O	3.49	2.88	3.32	4.27	5.71	4.37	3.65
Rb	127	107	193	229	228	122	133
Sr	53	248	170	97	97	193	330
TOTAL	96.59	98.96	95.54	100.71	97.60	96.60	96.58

TABLE 35

MINERALOGY AND CHEMISTRY OF SAMPLES FROM
AREA XI, ASHTON LAKE

MINERALOGY (estimated percentages)

	XI-a	XI-b	XI-c	XI-d	XI-e	XI-f	XI-g	XI-h	XI-i
Q	30	20	20	30	50	7	50	25	10
KFp	25	25	59	25	2	2	5	7	21
Pl	35	33	20	34	20	56	35	52	36
Hbl	-	-	-	-	-	-	-	-	15
Bio	5	15	-	7	5	26	4	7	10
Chl	1	1	tr	1	2	2	1	5	tr
Mu	-	-	-	-	20	-	-	-	-
Ep	3	5	-	2	-	4	4	2	5
Cal	tr	tr	-	-	-	-	-	-	-
Gt	-	-	-	-	0.5	-	-	-	-
Ct	-	-	-	-	-	-	-	-	0.3
Zr	tr	tr	-	tr	tr	-	tr	tr	tr
Ap	tr	tr	-	-	-	1	-	tr	tr
Al	tr	-	-	-	-	-	-	-	-
Sph	tr	-	-	tr	-	tr	-	tr	tr
Mag	1	1	tr	-	tr	1	1	1	1
Hem	tr	tr	1	1	1	1	tr	1	0.5
Py	tr	tr	tr	-	-	-	tr	-	0.5
TOTAL	100.0	100.0	100.0	100.0	100.5	100.0	100.0	100.0	99.3

CHEMISTRY (X-ray fluorescence)

Trace, Major and minor oxides,
ppm

SiO ₂	69.40	63.24	75.57	79.31	80.14	64.19	63.57	65.51	57.40
TiO ₂	0.43	0.72	0.03	0.21	0.46	0.57	0.68	0.62	0.74
Al ₂ O ₃	13.94	15.89	13.92	9.45	8.89	14.18	15.24	14.53	14.72
Fe ₂ O ₃	2.94	5.23	4.44	2.72	3.62	4.97	5.37	5.07	6.57
MnO	.042	.091	.008	.034	.052	.067	.041	.080	.144
MgO	0.91	1.82	0.10	0.61	0.81	2.03	2.03	2.13	3.14
CaO	2.29	3.80	0.16	0.78	0.21	2.62	3.48	6.97	5.51
K ₂ O	4.33	4.01	6.92	2.40	2.23	4.07	1.24	3.75	3.68
Rb	70	82	166	54	70	97	31	132	88
Sr	417	531	44	85	47	751	764	468	1,145
TOTAL	94.28	94.80	101.15	95.51	96.41	92.70	91.65	93.65	71.96

TABLE 36

MINERALOGY AND CHEMISTRY OF SAMPLES FROM
AREA XII, COLLINS LAKE

MINERALOGY (estimated percentages)									
	XII-a	XII-b	XII-c	XII-d	XII-e	XII-f	XII-g	XII-h	XII-i
Q	40	20	20	15	29	20		34	20
KFp	25	15	10	15	10	15		5	10
Pl	25	50	45	40	44	40		29	45
Bio	5	-	2	8	3	-		-	tr
Chl	2	8	4	4	4	7		1	5
Mu	3	tr	12	12	3	13		30	20
Ep	0.2	5	4	3	2	1	2	-	-
Cal	-	-	tr	-	1	1	tr	0.5	-
Zr	tr	-	tr	tr	tr	tr	tr	tr	tr
Ap	tr	tr	0.2	tr	tr	0.1	tr	-	tr
Al	tr	tr	0.5	0.5	tr	-	0.2	-	tr
Sph	-		0.2	1	tr	-	-	-	-
Lx	-	0.2	1	0.2	2	1	1	0.5	0.5
Tl	-	-	-	-	-	-	-	-	-
Mag	0.2	1	1	1	-	0.2	0.3	-	-
Hem	0.3	1	0.5	0.2	2	2	1	tr	tr
Py	tr	-	0.1	tr	0.2	tr	tr	-	-
Gf	-	-	-	-	-	-	-	-	-
TOTAL	100.7	100.2	100.5	99.9	100.2	100.3	-	100.0	100.3

CHEMISTRY (X-ray fluorescence)										
Trace, ppm		Major and minor oxides, per cent								
	SiO ₂	73.80	61.82	66.87	66.80	66.69	69.22	67.70	68.68	70.72
	TiO ₂	0.24	0.59	0.56	0.59	0.66	0.43	0.36	0.30	0.24
	Al ₂ O ₃	13.07	12.56	14.47	13.37	13.62	13.13	14.11	16.31	15.81
	Fe ₂ O ₃	1.92	6.47	4.01	4.24	4.02	3.92	5.53	1.85	2.44
	MnO	.031	.073	.057	.062	.064	.038	.033	.035	.025
	MgO	0.61	5.37	1.82	1.92	1.62	2.03	1.01	0.81	1.01
	CaO	0.72	1.92	2.35	1.96	2.38	0.71	1.15	2.53	0.03
	K ₂ O	6.03	3.61	3.98	3.77	1.72	3.81	5.93	4.50	4.86
	Rb	172	110	136	110	51	102	144	215	233
	Sr	264	456	549	482	296	235	624	55	71
	TOTAL	96.42	92.41	94.12	92.71	90.77	93.83	95.82	95.02	95.41

Table 36 (cont'd.)

MINERALOGY (estimated percentages)									
	XII-j	XII-k	XII-l	XII-m	XII-n	XII-o	XII-p	XII-q	XII-r
Q	*		15	15	25	60	25	30	60
KFp	T.F.G.		10	3	3	1	20	20	7
Pl			50	30	40	20	30	30	25
Bio			3	3	6	-	-	-	-
Chl	3		tr	tr	3	1	8	5	5
Mu	35		20	40	20	15	15	15	-
Ep	-		1	-	-	-	1	tr	0.5
Cal	-		1	2	-	3	-	-	0.5
Zr	tr	Too Fine Grained	tr	tr	tr	tr	tr	tr	tr
Ap	tr		-	-	-	tr	-	-	-
Al	-		-	-	-	-	-	-	-
Sph	-		-	-	1	-	-	-	-
Lx	1		0.2	0.2	tr	-	1	0.2	-
Tl	-		-	6	2	0.2	-	-	-
Mag	-		tr	0.2	-	-	tr	tr	-
Hem	1		tr	0.5	-	tr	tr	tr	2
Py	-		-	0.1	tr	-	-	-	-
Gf	-		-	0.2	0.5	-	-	0.2	-
TOTAL	-	-	100.2	100.2	100.5	100.2	100.0	100.4	100.0

CHEMISTRY (X-ray fluorescence)	Trace, ppm	Major and minor oxides, per cent							
		SiO ₂	TiO ₂	Al ₂ O ₃	Fe ₂ O ₃	MnO	MgO	CaO	K ₂ O
		69.71	69.27	68.27	64.14	75.91	70.54	71.52	73.30
		0.31	0.41	0.34	0.89	0.06	0.64	0.54	0.10
		14.88	15.57	15.57	15.43	14.33	13.67	14.72	14.24
		2.37	3.59	3.51	6.73	1.22	5.59	4.72	2.36
		.034	.043	.043	.071	.025	.071	.049	.041
		0.81	1.22	1.22	2.33	0.61	2.33	1.92	1.42
		1.03	0.78	1.41	0.58	2.44	0.28	0.28	1.92
		3.50	4.67	4.02	3.40	2.56	3.64	3.18	2.47
		129	259	186	252	114	170	151	140
		273	102	103	42	60	48	120	295
TOTAL		92.64	95.55	94.38	93.57	97.16	96.76	96.93	15.85

* Too Fine grained

TABLE 37

MINERALOGY AND CHEMISTRY OF SAMPLES FROM
AREA XIII, BAYONET LAKE

MINERALOGY (estimated percentages)	XIII-a XIII-b XIII-c XIII-d XIII-e XIII-f XIII-g						
Q	-	20	20	25	25	48	30
KFp	4	8	15	15	5	tr	-
Pl	-	35	40	35	44	15	45
Bio	15	10	10	15	20	2	18
Chl	-	0.5	tr	1	tr	1	tr
Mu	25	25	13	8	4	33	-
Ep	0.1	0.5	0.5	0.2	1	-	5
Cal	0.1	0.2	tr	-	-	-	-
Gt	-	-	-	-	-	1	-
Zr	0.1	tr	tr	tr	tr	tr	tr
Ap	-	-	-	-	-	-	tr
Sph	0.2	0.3	0.5	0.5	1	-	tr
Lx	0.2	0.1	0.5	0.5	1	tr	-
Mag	0.2	-	0.5	0.1	-	1	2
Hem	tr	tr	0.1	0.2	0.1	-	-
Py	0.2	0.5	0.1	0.5	-	-	-
TOTAL	-	100.1	99.7	100.5	100.1	100.0	100.0

CHEMISTRY (X-ray fluorescence)							
SiO ₂	64.86	64.50	66.25	68.60	67.24	70.00	60.99
TiO ₂	0.50	0.53	0.60	0.39	0.63	0.72	1.87
Al ₂ O ₃	13.83	13.59	15.20	14.49	13.54	15.75	11.33
Fe ₂ O ₃	5.34	6.05	4.38	4.10	5.40	7.30	10.21
MnO	.074	.062	.058	.058	.072	.033	.111
MgO	3.85	3.24	1.92	2.03	2.53	1.72	1.92
CaO	2.00	1.47	1.46	1.39	1.59	0.27	2.31
K ₂ O	3.22	2.78	5.22	4.73	3.71	3.68	2.90
Rb	199	227	201	178	200	98	164
Sr	207	162	215	195	184	42	164
TOTAL	92.72	92.22	95.09	95.79	94.71	99.67	91.64

Trace, Major and minor oxides,
ppm per cent

TABLE 38

MINERALOGY AND CHEMISTRY OF SAMPLES FROM
AREA XIV, BAYONET LAKE

MINERALOGY (estimated percentages)	XIV-a XIV-b XIV-c XIV-d XIV-e XIV-f					
Q	15	32	23	25	20	25
KFp	30	30	-	1	15	30
Pl	40	35	70	65	29	40
Bio	tr	-	-	-	15	4
Chl	10	0.5	3	8	tr	1
Mu	1	tr	-	-	20	-
Ep	1	tr	-	tr	tr	tr
Zr	tr	tr	tr	tr	tr	tr
Ap	tr	tr	tr	tr	-	tr
Al	-	tr	-	tr	tr	-
Sph	-	tr	-	tr	-	-
Lx	-	-	tr	0.3	-	-
Mag	0.2	0.2	tr	tr	tr	0.5
Hem	2	2	4	0.2	1	tr
Py	-	tr	-	-	-	-
TOTAL	99.2	99.7	100.0	99.5	100.0	100.5

CHEMISTRY (X-ray fluorescence)	XIV-a XIV-b XIV-c XIV-d XIV-e XIV-f					
SiO ₂	63.65	73.02	73.58	71.65	67.80	75.57
TiO ₂	0.67	0.11	0.29	0.50	0.53	0.29
Al ₂ O ₃	16.23	15.20	13.22	12.91	13.70	13.76
Fe ₂ O ₃	4.57	1.05	2.66	3.41	4.94	1.76
MnO	.082	.028	.019	.035	.076	.026
MgO	1.82	0.51	0.81	2.53	2.03	0.51
CaO	2.04	0.71	0.36	0.64	1.57	0.96
K ₂ O	4.55	6.40	0.40	0.47	4.55	5.81
Rb	152	196	-	-	174	178
Sr	411	501	68	108	197	108
TOTAL	93.61	97.03	91.34	92.15	95.20	98.69

Trace, Major and minor oxides,
ppm per cent

TABLE 39

MINERALOGY AND CHEMISTRY OF SAMPLES FROM
AREA XV, BAYONET LAKE

MINERALOGY (estimated percentages)

	XV-a	XV-b	XV-c	XV-d	XV-e	XV-f	XV-g
Q	20	20	15	25	20	20	15
KFp	20	7	25	5	20	10	10
Pl	30	50	32	40	32	40	40
Hbl + Di	-	-	-	-	-	6	15
Bio	8	15	15	20	20	20	15
Chl	15	1	5	tr	1	-	3
Mu	2	4	5	10	5	tr	-
Ep	5	3	3	0.2	2	4	2
Cal	tr	tr	tr	tr	-	tr	-
Zr	tr	tr	tr	tr	-	tr	-
Ap	tr	tr	tr	tr	tr	tr	-
Al	-	tr	tr	-	-	-	-
Sph	0.3	-	tr	-	-	-	-
Lx	0.2	-	tr	-	tr	-	-
Mag	tr	-	-	-	-	tr	tr
Hem	tr	tr	tr	0.5	0.2	tr	tr
Py	-	tr	-	tr	-	0.1	0.5
TOTAL	100.5	100.0	100.0	100.7	100.2	100.1	100.5

CHEMISTRY (X-ray fluorescence)

Trace, Major and minor oxides,
ppm per cent

SiO ₂	65.22	65.22	67.86	69.09	70.44	64.34	64.14
TiO ₂	0.48	0.31	0.43	0.50	0.54	0.57	0.58
Al ₂ O ₃	13.89	17.57	15.92	13.41	13.47	12.34	13.67
Fe ₂ O ₃	4.04	2.33	2.98	4.88	4.56	6.05	5.20
MnO	.065	.046	.046	.073	.065	.112	.083
MgO	1.42	1.22	1.01	1.92	2.53	5.06	3.24
CaO	2.72	3.62	2.30	1.99	1.74	3.34	4.95
K ₂ O	4.72	2.71	5.32	3.80	4.29	3.91	3.44
Rb	164	116	155	184	206	140	116
Sr	516	525	353	197	212	337	402
TOTAL	92.56	93.03	95.87	95.66	97.64	95.72	95.30

APPENDIX B

X-RAY FLUORESCENCE ANALYSIS:

Technique
 Operating conditions
 Chemical analyses of calibration standards
 Standard deviation and precision
 Comparison of X-ray Fluorescence and wet chemical analyses
 Calibration curves

Technique

X-ray fluorescence equipment was used to determine the major and minor oxides SiO_2 , TiO_2 , Al_2O_3 , Fe_2O_3 , MnO , MgO , CaO , and K_2O , and the trace elements Rb and Sr. Only Na_2O , P_2O_5 , and loss on ignition are lacking for a normal silicate rock analysis.

About 2 ml of rock powder with a small amount of cellulose powder (about 40:1 dilution) added for binding strength, were blended for 10 minutes in a Pica Blender. The blended powders were pressed at 15,000 p.s.i. into briquettes backed and rimmed with cellulose.

Measurements were made with a Norelco Type 12215/0 unit, using Cr, W, and Mo radiation sources. The operating conditions for measurement of each chemical constituent are shown in Table 40.

Briquettes of 3 unknowns and a single standard were placed in the sample holder. Continued use of the standard with each new group of 3 unknowns served to detect instrument drift where a large number of samples were involved. The count on the K alpha peak and background position of each element were measured in turn for 10 seconds, and the difference in the two readings provided a measure of the chemical constituent.

The conversion of counting rate to weight per cent was accomplished using calibration curves (Figures 22 to 29) for each element, with the major and minor elements reported as oxides. The chemical analyses (Table 41) used in the construction of these calibration curves represent rocks petrologically similar to the study samples. These range in composition from intermediate to acid with the exception of W-1, which is basic. The conversion of Rb and Sr counting rates to parts per million was accomplished using the matrix correction method of Reynolds (1963). Here, the unknown is corrected for variation in mass absorption relative to G-1 by the counting rate on the Compton peak. G-1 has 220 ppm Rb, and 250 ppm Sr (Fleischer and

RESULTS

The first experiment was designed to determine the effect of the amount of information presented on the response time.

Subjects were presented with a series of stimuli consisting of a number of letters and digits. The number of stimuli was varied from 1 to 10. The response time was measured for each stimulus. The results are shown in Table 1.

The second experiment was designed to determine the effect of the amount of information presented on the accuracy of the response.

Subjects were presented with a series of stimuli consisting of a number of letters and digits. The number of stimuli was varied from 1 to 10. The response time was measured for each stimulus. The results are shown in Table 2.

The third experiment was designed to determine the effect of the amount of information presented on the consistency of the response.

Subjects were presented with a series of stimuli consisting of a number of letters and digits. The number of stimuli was varied from 1 to 10. The response time was measured for each stimulus. The results are shown in Table 3.

The fourth experiment was designed to determine the effect of the amount of information presented on the speed of the response.

Subjects were presented with a series of stimuli consisting of a number of letters and digits. The number of stimuli was varied from 1 to 10. The response time was measured for each stimulus. The results are shown in Table 4.

The fifth experiment was designed to determine the effect of the amount of information presented on the accuracy of the response.

Subjects were presented with a series of stimuli consisting of a number of letters and digits. The number of stimuli was varied from 1 to 10. The response time was measured for each stimulus. The results are shown in Table 5.

The sixth experiment was designed to determine the effect of the amount of information presented on the consistency of the response.

Stevens, 1961).

The standard deviation and precision (Table 42) of each chemical constituent were calculated from a series of six measurements made on the "running" standard following every three unknown samples from area XII.

Comparison of X-ray fluorescence analyses with chemical analyses is shown in Table 43, and percentage differences are indicated.

TABLE 40. OPERATING CONDITIONS FOR X-RAY FLUORESCENCE ANALYSES

Element	Tube	Analysing Crystal	Peak	Background	Detector	Detector Voltage	Pulse Height Analyser	
							Level	Window
Si	Cr	EDDT	77.80°	77.10°	Flow	1560	7.0	5.5
Ti	W	LiF	86.22°	85.00°	Flow	1480	5.0	10.0
Al	Cr	EDDT	112.45°	111.50°	Flow	1650	12.5	14.0
Fe	Mo	LiF	57.55°	56.75°	Sc	940	1.5	0.0
Mn	W	LiF	62.95°	61.65°	Flow	1490	12.5	7.5
Mg	Cr	ADP	106.54°	105.58°	Flow	1630	10.5	12.0
Ca	W	EDDT	14.85°	14.00°	Flow	1510	7.5	8.0
K	W	EDDT	20.22°	19.20°	Flow	1570	11.7	10.0
Rb	Mo	LiF	26.53°	26.00°	Sc	850	1.5	0.0
Sr	Mo	LiF	25.08°	24.37°	Sc	870	1.5	0.0

TABLE 41. CHEMICAL ANALYSES USED FOR CALIBRATION CURVES

	32	33	56	60	76	170	179	Comb. 8	Comb. 16	G-1	W-1
SiO ₂	75.26	62.85	73.98	66.63	71.02	69.30	76.40	60.76	69.16	72.48	52.55
TiO ₂	0.33	0.59	0.10	0.51	0.50	0.04	0.01	0.96	0.41	0.26	1.08
Al ₂ O ₃	12.43	14.99	13.58	15.49	13.58	15.20	14.11	16.14	11.52	14.20	14.98
Fe ₂ O ₃	3.06	5.77	0.70	3.70	3.25	0.39	0.37	8.12	5.33	1.86	11.08
MnO	0.03	0.12	0.01	0.06	-	0.03	0.14	0.11	0.09	0.025	0.161
MgO	1.08	3.06	0.43	2.37	0.65	0.41	0.34	3.77	4.76	0.37	6.59
CaO	0.09	3.34	0.76	1.92	1.68	1.33	0.31	2.80	3.97	1.35	10.98
Na ₂ O	0.22	2.36	2.99	3.51	2.83	1.88	7.09	3.16	1.29	3.29	2.14
K ₂ O	5.47	3.69	6.13	3.40	5.60	9.75	1.76	2.26	2.07	5.52	0.62
L.O.I.	1.68	1.25	0.84	1.20	0.50	0.30	0.12	1.83	1.29	0.34	0.52
P ₂ O ₅	0.09	0.17	0.03	0.25	0.18	0.66	0.06	0.09	0.11	0.08	0.12
Total	99.74	98.33	99.55	99.04	99.79	99.29	100.70	100.00	100.00	99.78	100.82

All analyses except G-1 and W-1 by H.A. Wagenbauer

32	Felsic porphyroclastic phyllonite	179	Aplite
33	Biotite microgranite (Granodiorite)	Comb. 8	Combination sample (Metasedimentary rock band)
56	Biotite granite gneiss (Quartz monzonite)	Comb. 16	Combination sample (Metasedimentary rock band)
60	Biotite granite D (Granodiorite)	G-1	Granite (U.S.G.S. Standard)
76	Biotite 'g' granite (Quartz monzonite)	W-1	Diabase (U.S.G.S. Standard)
170	Aplite		

TABLE 42. STANDARD DEVIATION AND PRECISION FOR
X-RAY FLUORESCENCE ANALYSES*

Constituent	Standard	Amount Present	Standard Deviation	Precision
SiO ₂	G-1	72.48 %	<u>±</u> 0.63 %	<u>±</u> 0.87 %
TiO ₂	W-1	1.08	0.002	0.19
Al ₂ O ₃	G-1	14.20	0.05	0.51
Fe ₂ O ₃	32	3.06	0.009	0.30
MnO	W-1	0.161	0.001	0.65
MgO	W-1	6.59	0.24	3.60
CaO	W-1	10.98	0.04	0.32
K ₂ O	G-1	5.52	0.018	0.32
Rb	G-1	220 ppm	3 ppm	1.36
Sr	G-1	250 ppm	2 ppm	0.97

* Standard deviation and precision for each constituent are calculated from a series of six measurements made on a standard sample following every three unknown samples.

TABLE 43. COMPARISON OF X-RAY FLUORESCENCE DATA WITH CHEMICAL ANALYSES

67 (Mylonite O)			
	Chem.	X.R.F.	% Diff.
SiO ₂	70.26	69.71	- 0.36
TiO ₂	0.31	0.31	0.00
Al ₂ O ₃	14.86	14.88	+ 0.14
Fe ₂ O ₃	2.11	2.37	+12.32
MnO	0.04	0.034	\pm
MgO	0.88	0.81	- 7.95
CaO	1.57	1.03	-34.39
Na ₂ O	3.94		-
K ₂ O	3.69	3.50	- 5.15
L.O.I.	1.05		-
P ₂ O ₅	0.11		-
Total	98.82	92.64	-

85 (Mylonite L)		
Chem.	X.R.F.	% Diff.
71.91	72.50	+ 0.82
0.31	0.35	12.90
14.40	14.30	- 0.69
1.91	2.12	+11.00
0.03	0.028	\pm
0.82	0.71	-13.42
1.37	1.10	-19.71
2.91		-
5.22	5.22	0.00
1.01		-
0.13		-
100.02	96.35	-

89 (Foliated hornblende granite)			
SiO ₂	74.37	74.44	+ 0.09
TiO ₂	0.26	0.25	- 3.85
Al ₂ O ₃	11.42	11.21	- 1.84
Fe ₂ O ₃	3.98	3.94	- 1.00
MnO	0.05	0.046	\pm
MgO	0.30	0.10	-66.67
CaO	1.43	1.15	-21.18
Na ₂ O	2.51		-
K ₂ O	4.55	4.20	- 7.69
L.O.I.	0.26		-
P ₂ O ₅	-		-
Total	99.13	95.34	-

94 (Hornblende cataclasite)		
66.95	64.86	- 3.12
0.21	0.22	+ 4.76
17.28	16.20	- 7.41
2.26	2.42	+ 7.08
0.08	0.078	<u>+</u>
1.09	1.01	- 7.34
3.84	3.55	- 7.55
5.09		-
2.41	2.15	-10.79
0.69		-
0.09		-
99.99	90.49	-

TABLE 43 (Continued)

127 (Granite F)			
	Chem.	X.R.F.	% Diff.
SiO ₂	67.95	70.13	+ 3.21
TiO ₂	0.50	0.41	-18.00
Al ₂ O ₃	15.51	14.02	- 9.61
Fe ₂ O ₃	4.28	3.63	-15.19
MnO	0.07	0.061	\pm
MgO	1.39	2.13	+53.24
CaO	2.30	2.90	+26.09
Na ₂ O	3.05		-
K ₂ O	2.93	3.42	+17.41
L.O.I.	1.16		-
P ₂ O ₅	0.12		-
Total	99.28	96.70	-

133 (Granite F)		
Chem.	X.R.F.	% Diff.
	69.94	-
0.44	0.43	- 2.27
	14.37	-
3.35	3.59	+ 7.16
0.05	0.052	\pm
	1.01	-
	1.75	-
3.01		-
3.82	4.00	+ 2.09
0.78		-
0.16		-
-	98.84	-

150 (Grey hornblende granite)			
SiO ₂	66.16	68.47	+ 3.49
TiO ₂	0.23	0.24	+ 4.35
Al ₂ O ₃	17.14	16.62	- 3.03
Fe ₂ O ₃	2.26	2.38	+ 5.31
MnO	0.09		-
MgO	1.06	0.71	-33.02
CaO	3.60	3.26	- 9.44
Na ₂ O	5.29		-
K ₂ O	2.53	2.53	0.00
L.O.I.	0.37		-
P ₂ O ₅	0.11		-
Total	98.84	94.30	-

Abbreviations

Chem. = Chemical analysis

X.R.F. = X-ray Fluorescence
analysis

Diff. = Difference

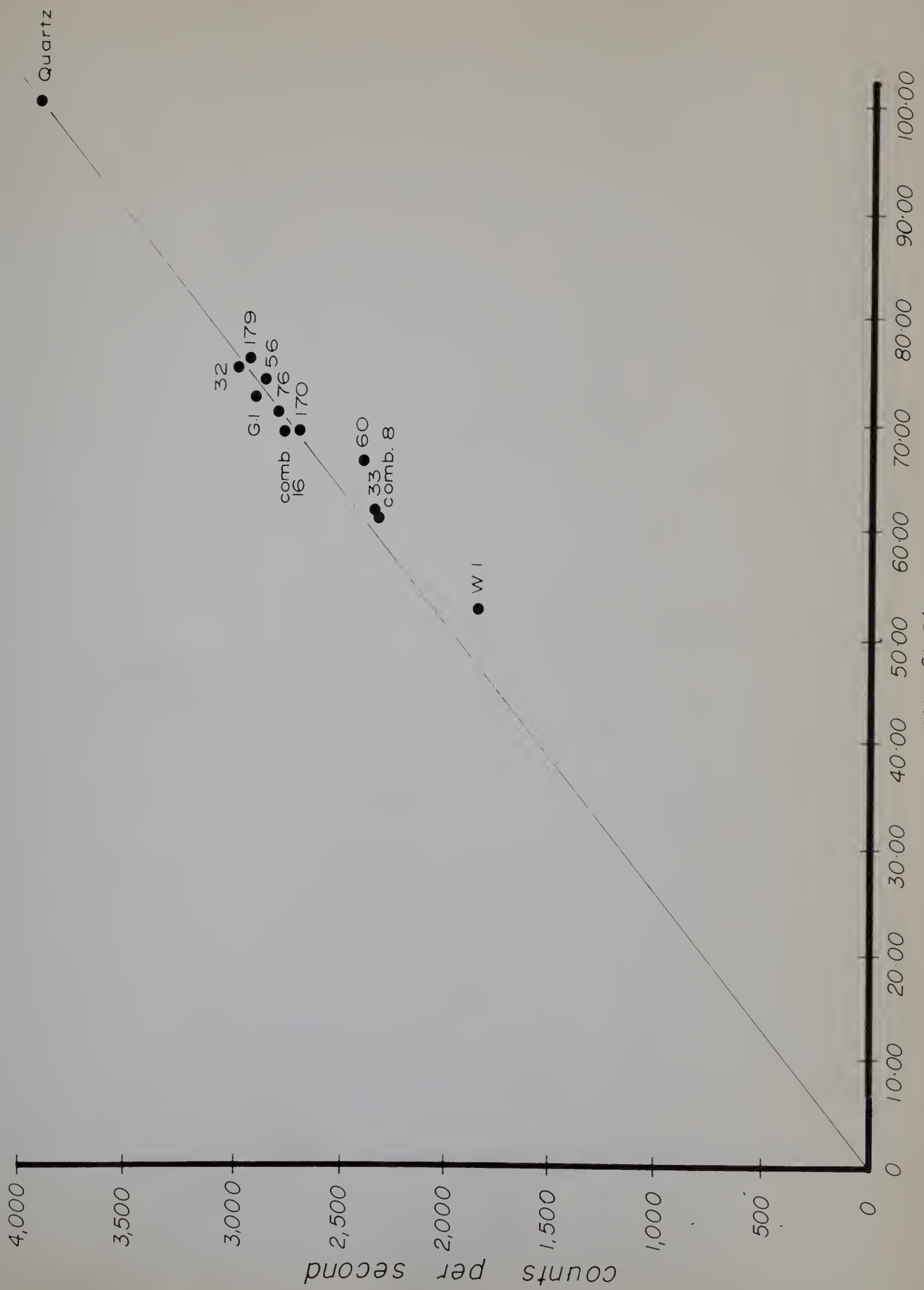


Fig.22. X-Ray fluorescence calibration curve for SiO₂

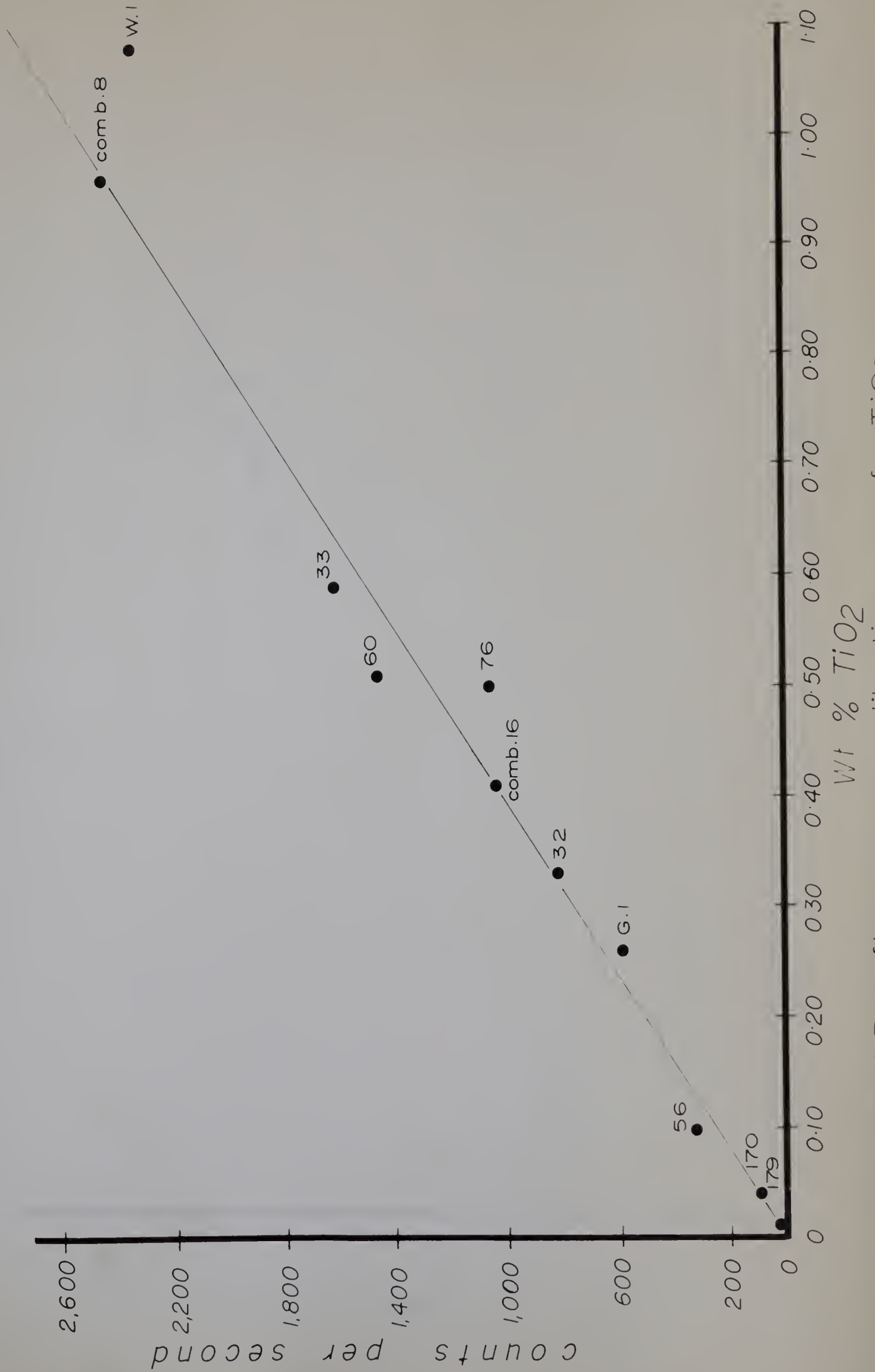


Fig.23. X-Ray fluorescence calibration curve for TiO_2

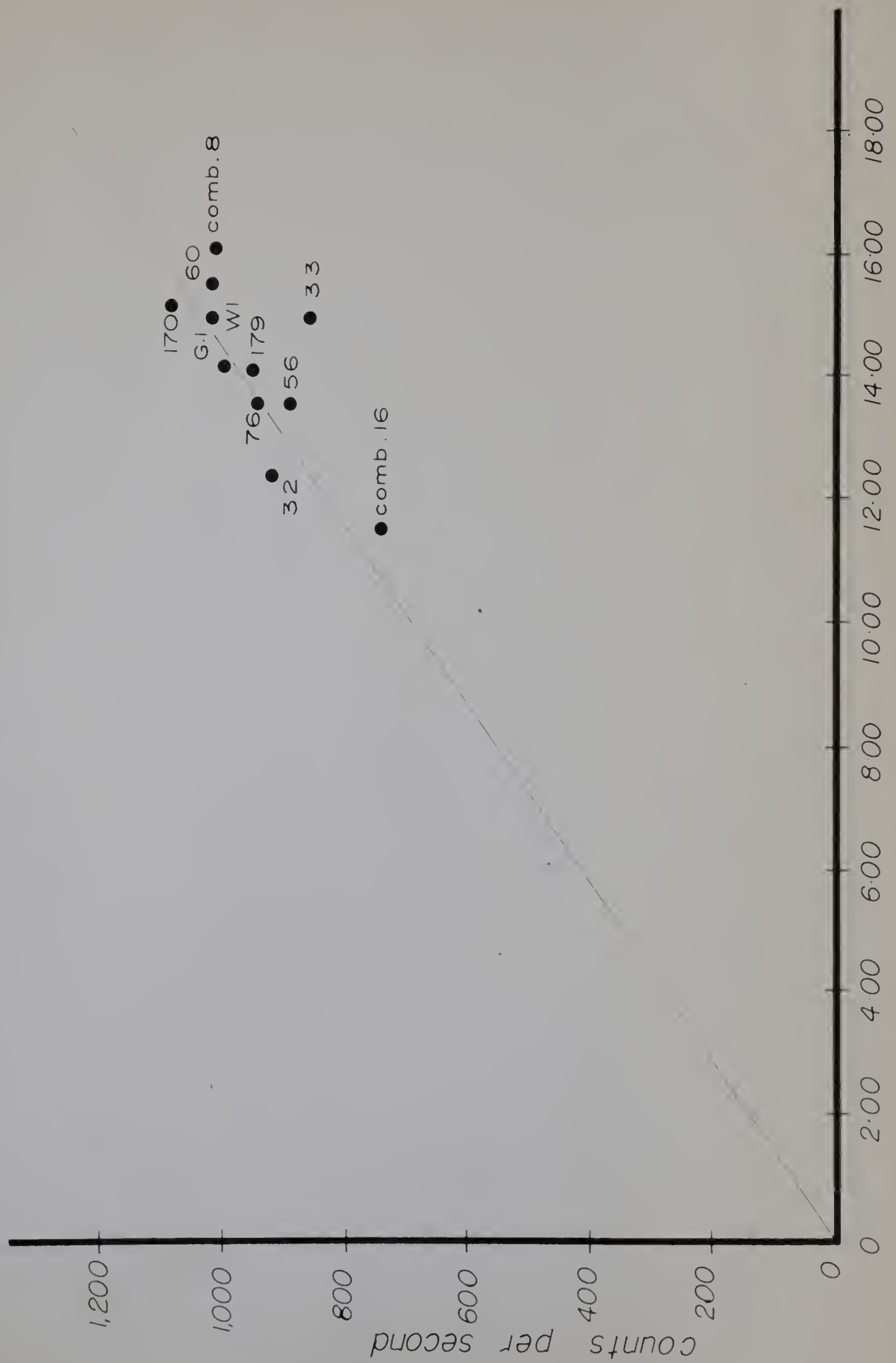


Fig. 24. X-Ray fluorescence calibration curve for Al_2O_3

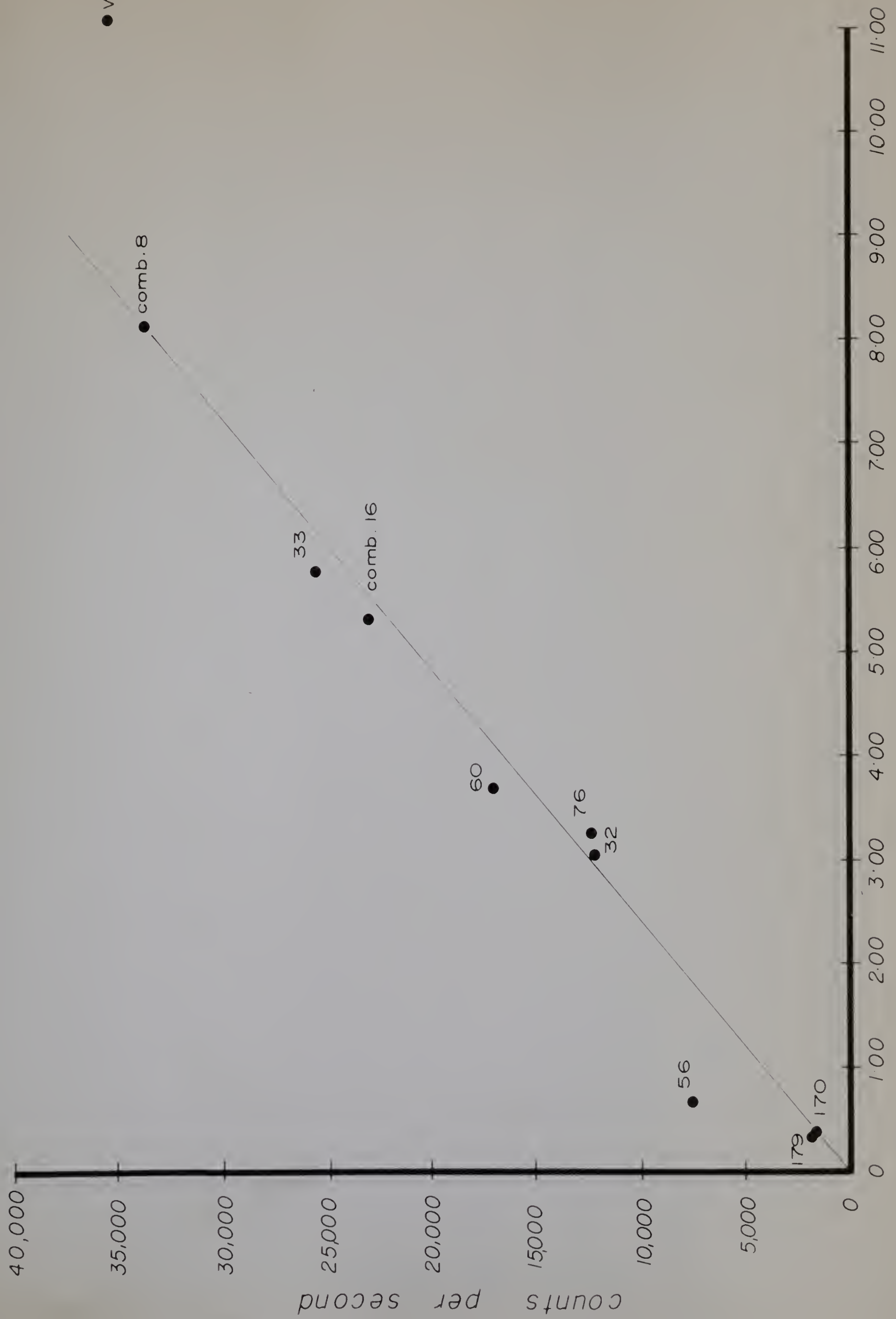


Fig.25. X-Ray fluorescence calibration curve for Fe₂O₃

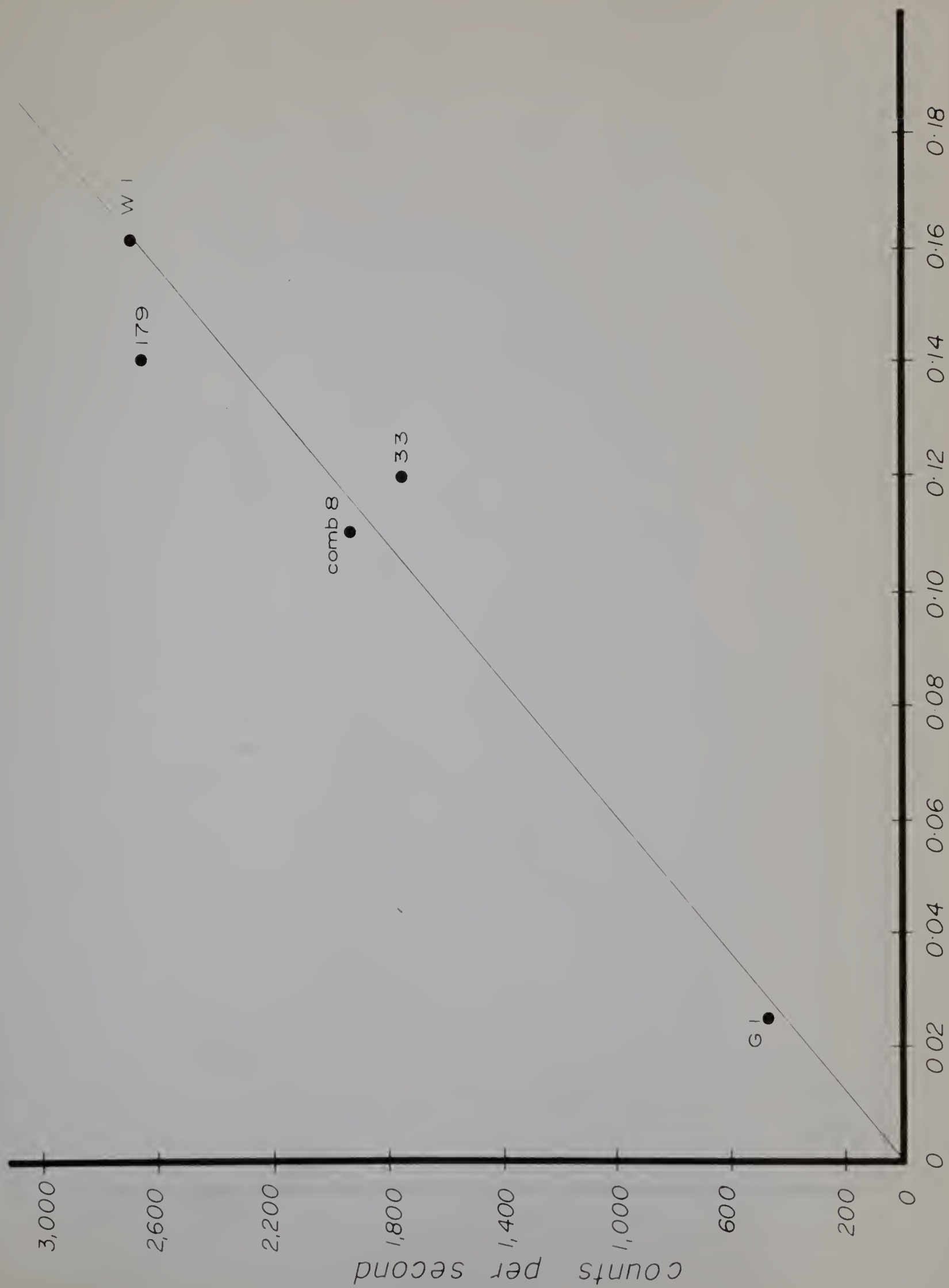


Fig.26. X-Ray fluorescence calibration curve for MnO

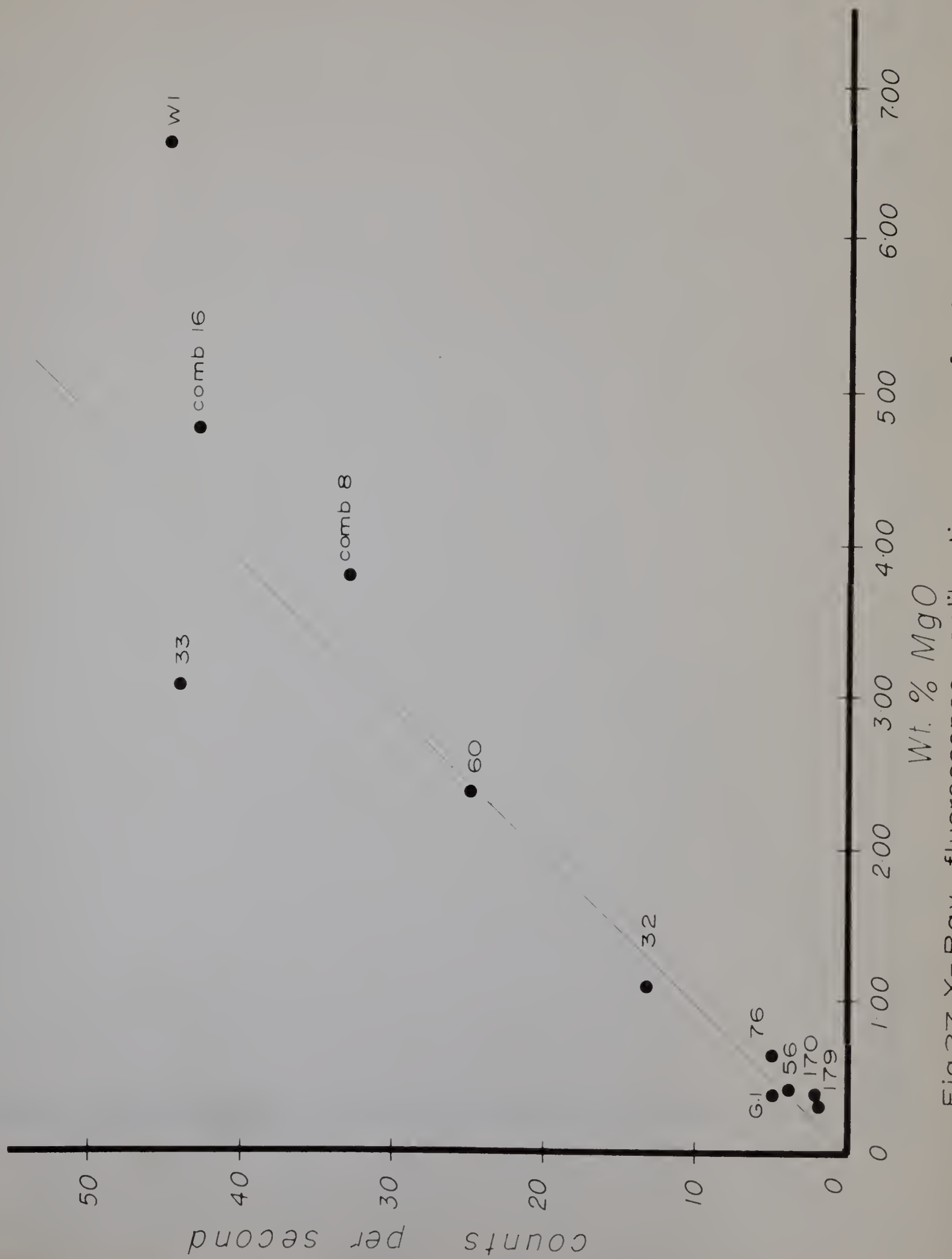


Fig.27 X-Ray fluorescence calibration curve for MgO

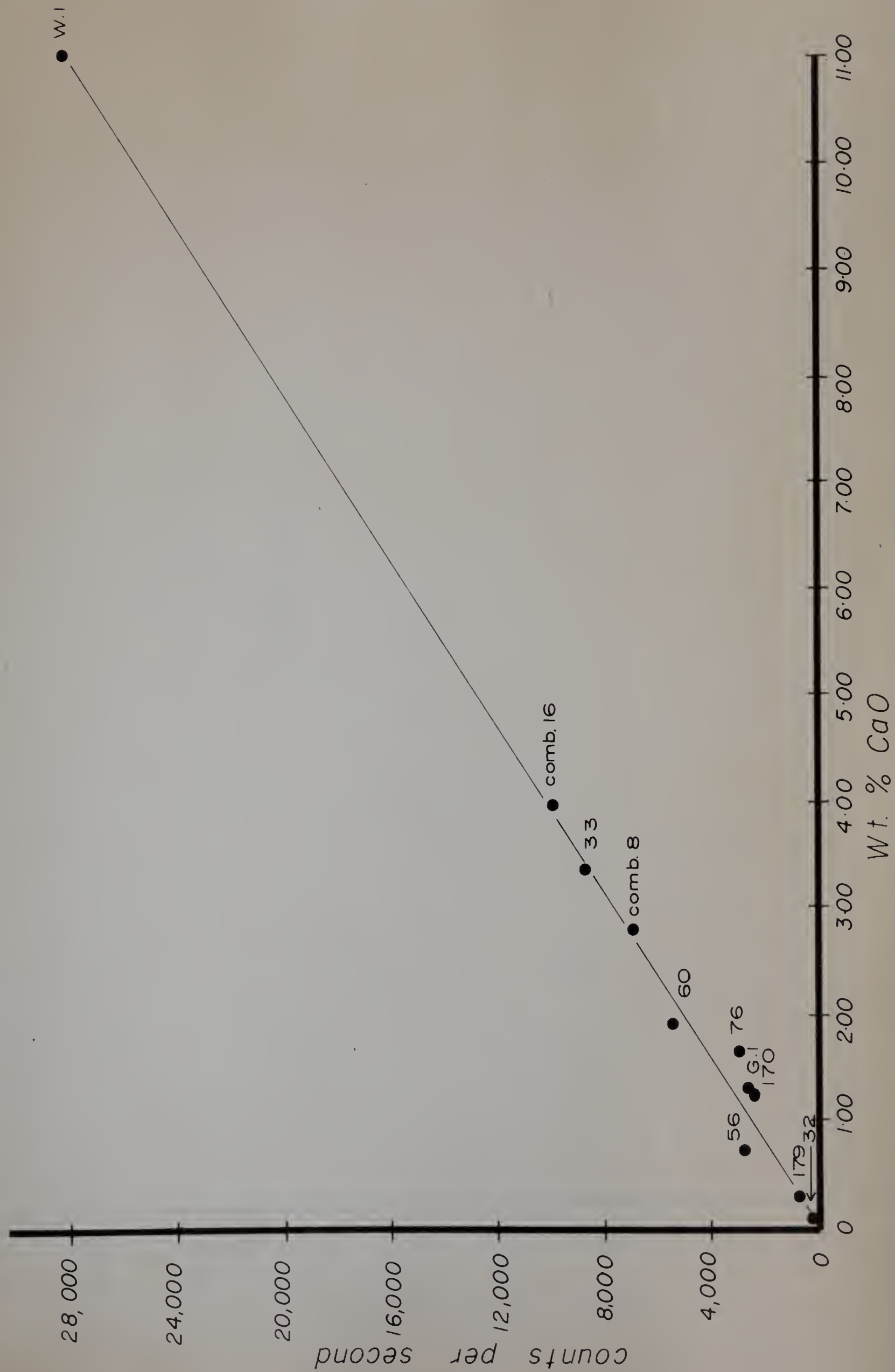


Fig. 28. X-ray fluorescence calibration curve for CaO

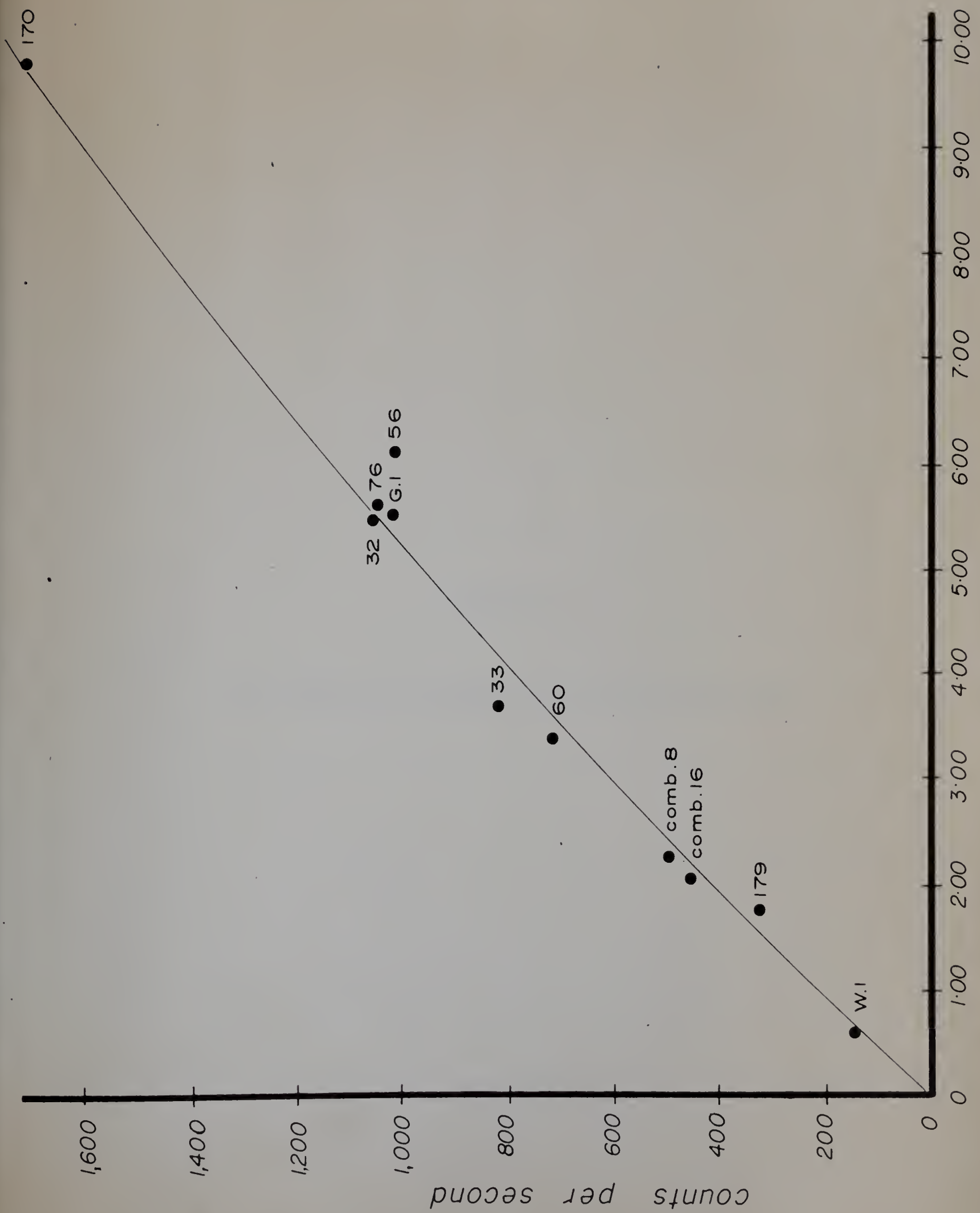


Fig 2a X-Ray fluorescence calibration curve for K₂O

APPENDIX C

THE LOWER LIMIT OF GRAIN SIZE IN MODAL ANALYSIS

The Lower Limit of Grain Size in Modal Analysis

Quantitative modal analysis of finely crushed rocks is difficult and commonly impossible. As the matrix grain size approaches the thickness of the rock slice in thin section (0.03 mm) or smaller, it becomes increasingly difficult to confine observations to the upper surface of the rock slice, and grain contacts become diffuse due to overlap of adjacent grains.

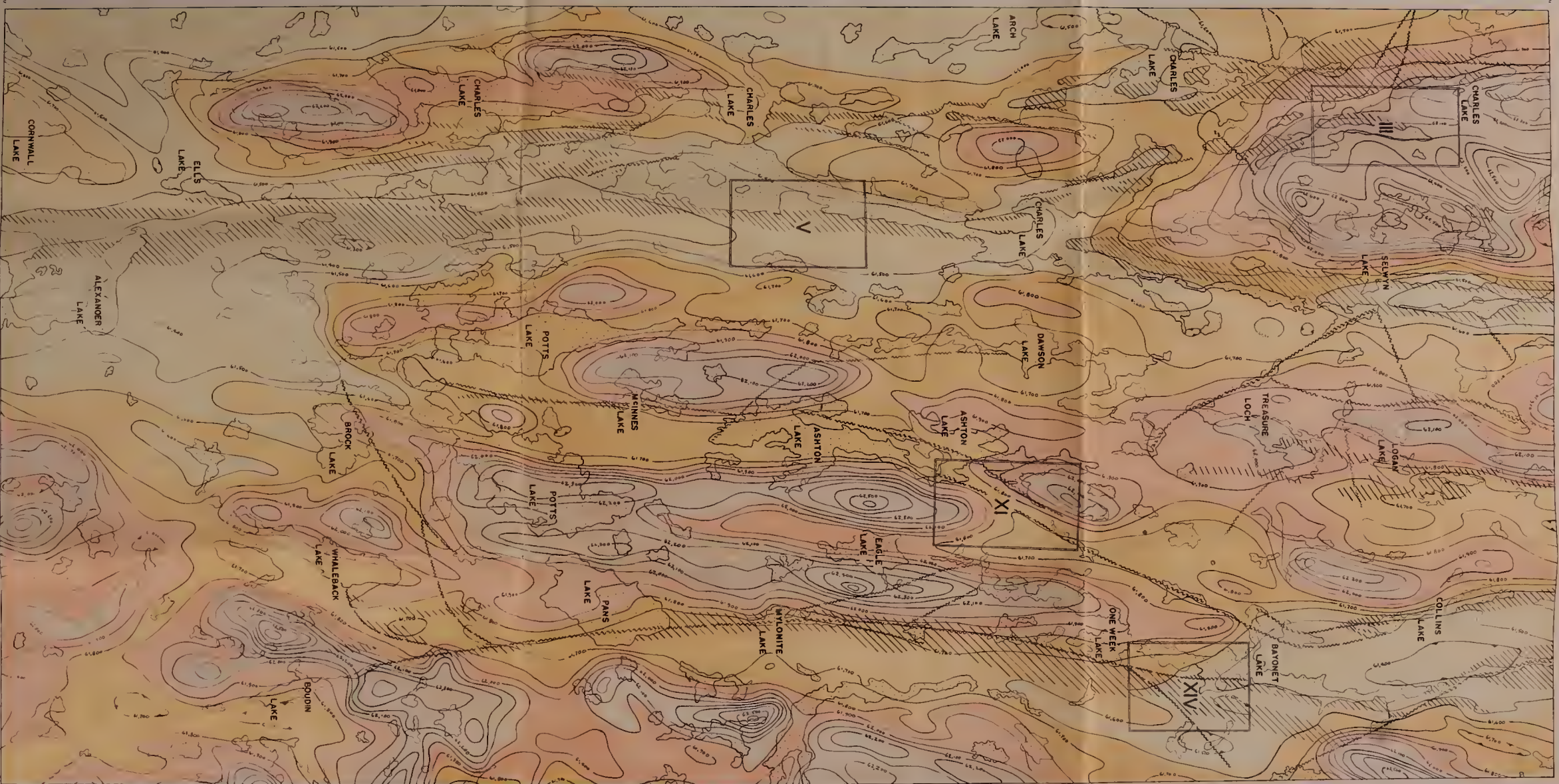
Chayes (1956, pp. 96-100) experimentally evaluated the errors in estimating the volume of opaque spheres in a transparent medium by transmitted light. The volume of opaque spheres is always overestimated (Holmes effect), and the error increases with decreasing radius of the opaque spheres. However, samples from the study area have only accessory amounts of opaque minerals, so that the Holmes effect is not an important consideration.

Elliott (1952) discusses fine-grained rocks containing transparent minerals of contrasting relief and inclined grain contacts, thereby giving rise to a "superposition error". This error is relevant in the study of cataclastic rocks, and the use of untreated thin sections introduces a systematic bias in the volume estimation of the major minerals. However, the error can be diminished by: -

- (i) the use of thin sections about 0.02 mm thick which decreases the overlap effect of adjacent grains,
- (ii) a strong hydrofluoric acid etch which frosts the feldspars and helps to restrict observations to the upper surface of the rock section, and
- (iii) sodium cobaltinitrite staining of potash feldspar which also is a surface feature that aids in restricting observations to the upper surface of the rock slice.

In this thesis, it was found that point counting on treated thin sections of standard rock specimens became extremely difficult where the average matrix grain size was less than about 0.03 mm. In such cases, a supplementary thin section with a stronger hydrofluoric acid treatment was prepared, and a visual estimate made of the minerals.

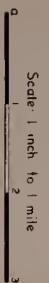
Where the average matrix grain size was about 0.01 mm and less, the contacts of adjoining grains became so diffuse that even volume estimates of minerals was too inaccurate.



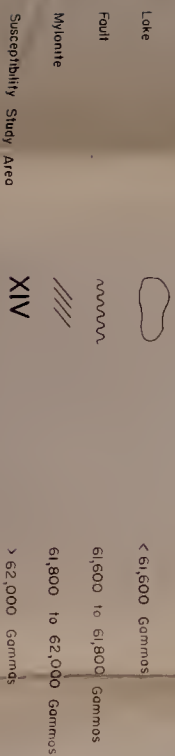
MAP 1

AEROMAGNETIC MAP OF THE STUDY AREA

Compiled from Geophysics Maps 2892G, 2893G, 2903G, 2904G, Geological Survey of Canada.
Contour Interval 100 Gamma

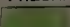
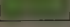
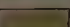
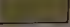
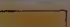
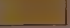



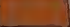
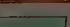
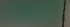
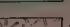

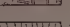

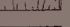

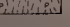
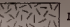



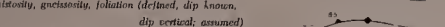
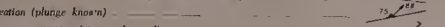


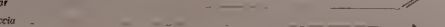


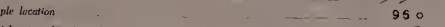
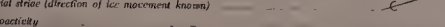


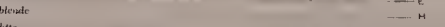
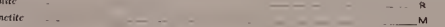
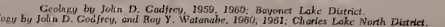

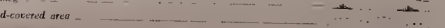

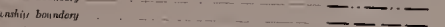
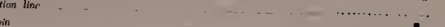
LEGEND



LEGEND

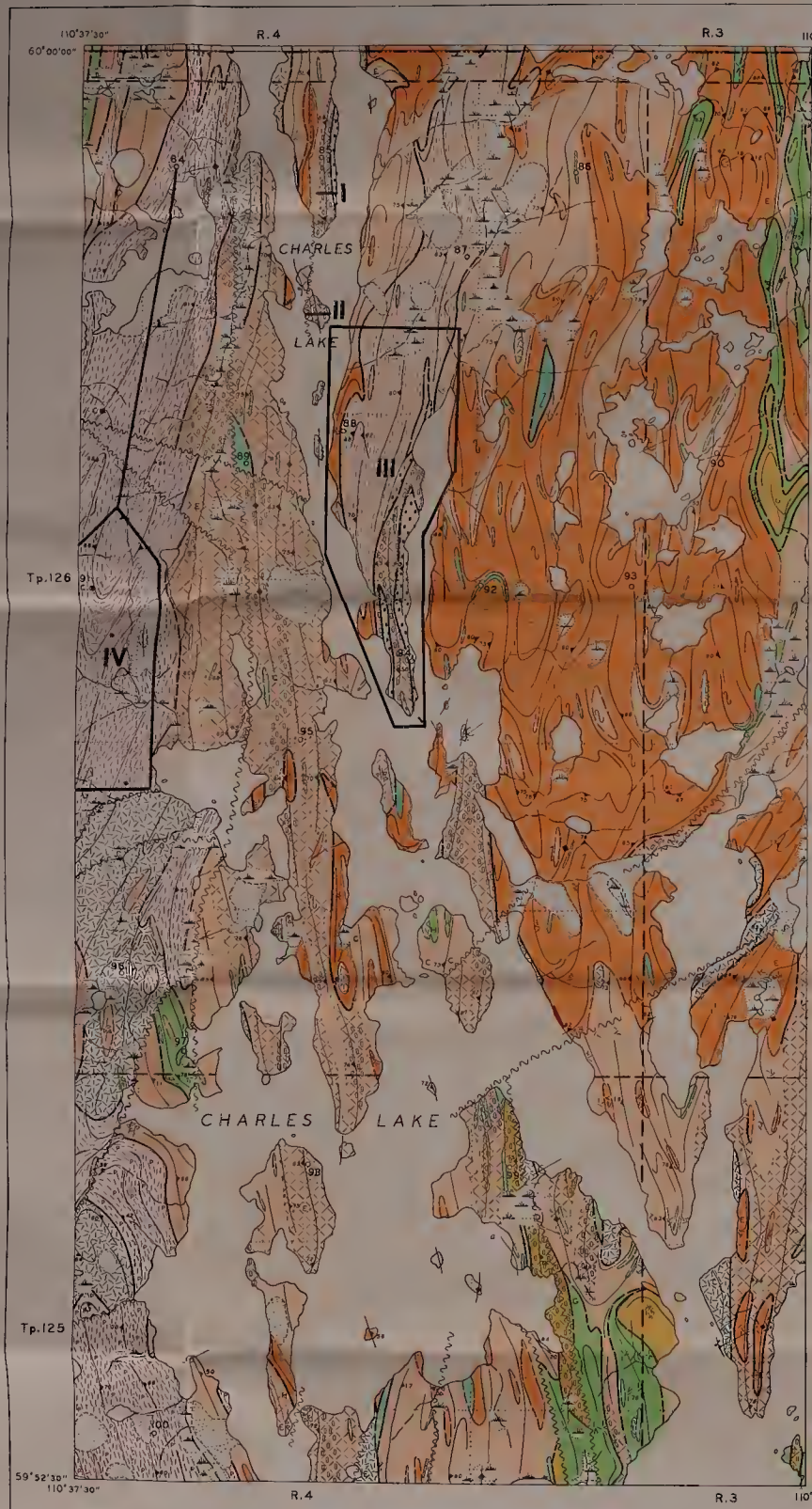
PRECAMBRIAN*

-  Quartzite, pure and impure, white, grey, green, pink and blue, including biotite, sericite, minor milky quartz, feldspar, augen, granite and pegmatite lenses, ferruginous and garnetiferous zones.
-  Biotite schist, with abundant quartz, some sericite, including phyllite, plagioclase, quartzite, minor milky quartz, feldspar, augen, granite and pegmatite lenses, ferruginous and garnetiferous zones.
-  Biotite granite F with white to grey subbedded to columnar feldspar megacrysts, one to four inches in size, averaging two inches, in a coarse-grained, massive matrix of quartz, feldspar and biotite, including minor sphile and pegmatite.
-  Biotite granite gneiss, with some hornblende, chlorite, megacrystic feldspar phases, including minor massive to foliated granite - some megacrystic, hornblende, chlorite, lenses of biotite, quartzite, amphibolite, garnetiferous zones.
-  Hornblende granite gneiss, with some biotite, chlorite, megacrystic feldspar phases, including minor massive to foliated granite - some megacrystic, hornblende and in folio.
-  Amphibolite, including biotite amphibolite, hornblende, mainly massive, little banded.
-  Biotite 'A' granite, with white to pink to red abundant feldspar megacrysts one-quarter inch in size, minor sericite, in medium-grained, massive to foliated matrix of biotite, feldspar and quartz.
-  Raita granite, mottled, with abundant white to red, rounded, feldspar one-tenth to one-quarter inch in size, in a sheared green chloritic foliated matrix with lenticular quartz and mica, rare white to pink feldspar augen up to one-half inch in size.
-  Arch Lake granite, with white to pink subbedded elongate feldspar megacrysts from one-half to one inch in size subparallel aligned, in a medium-grained, streaky to foliated matrix of blue quartz, biotite and feldspar.
-  Leucocratic granite, with pink to red anhedral feldspars, equigranular, massive, locally foliated, including minor microgranite and pegmatite.
-  Granitic material, biotite, and muscovite granite and pegmatite, some leucocratic phases, intermixed with host rock; typically massive, generally equigranular.
-  Foliated hornblende granite, pink to grey, with pink feldspar, quartz, and streaky patches of hornblende aggregates; texture equigranular, medium to coarse-grained, typically foliated.
-  Recrystallized porphyroclastic hornblende calcicite, light greyish green, with hornblende porphyroclasts up to one-tenth inch in size, and local feldspar porphyroclasts from one-half to three-quarters inch in size in a crushed, foliated, fine-grained matrix, some indistinct banding. Locally mixed with and transitional to minor grey hornblende granite, (see legend map 65-6F).
-  Recrystallized mylonite K, light colored, with minor white to pink feldspar porphyroclasts, one-quarter to three-quarters inch in size, constituting up to 2 per cent of rock, in a foliated, finely banded, aphanitic matrix, including recrystallized mylonites L, M, N, and O.
-  Recrystallized mylonite L, light colored, with white to pink feldspar porphyroclasts, one-quarter to three-quarters inch in size, constituting about 5 per cent of rock, in a foliated, finely banded, aphanitic matrix, including recrystallized mylonites K, M, N, and O.
-  Recrystallized mylonite M, dark colored, with white to pink feldspar porphyroclasts, one-quarter to three-quarters inch in size, constituting about 5 per cent of rock, in a foliated, finely banded, aphanitic matrix, including recrystallized mylonites K, L, N, and O.
-  Recrystallized mylonite N, green to black, schistose to slaty, with biotite, sericite, and some chlorite, feldspar and minor quartz porphyroclasts in a foliated, finely banded, aphanitic matrix, including minor recrystallized mylonite O.
-  Recrystallized mylonite O, green to black, allanitic, with biotite, chlorite, sericite, and minor feldspar porphyroclasts in a banded, aphanitic matrix, massive to foliated, including minor recrystallized mylonite N.
-  Recrystallized mylonite P, dark colored, with white to grey anhedral porphyroclasts and columnar feldspar porphyroclasts, one-half to two inches in size, foliated, locally granitic, in an aphanitic locally medium-grained, matrix, including minor sphile and pegmatite.
-  Basic dyke, massive, locally sheared with chlorite.

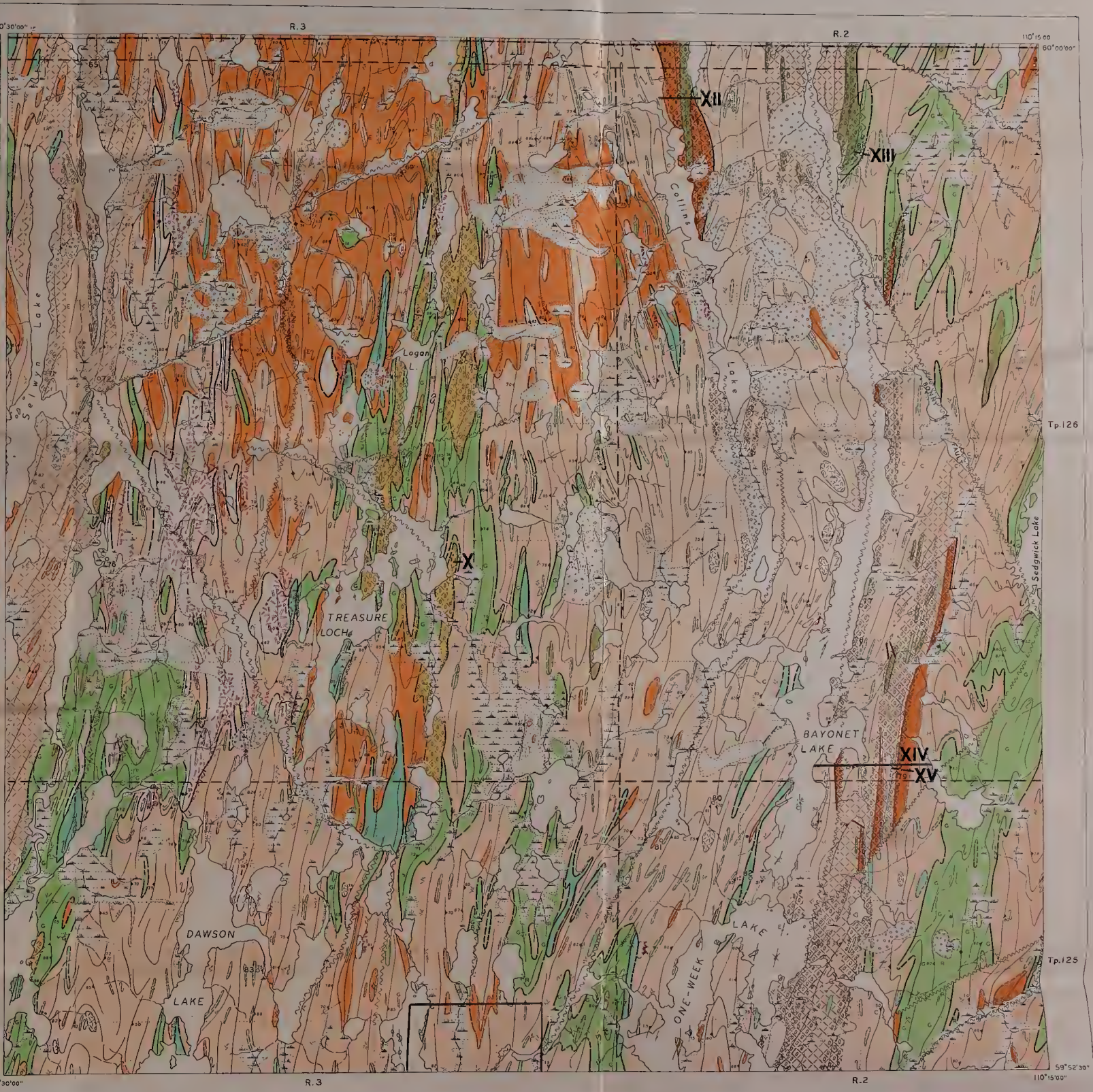
- *Note: Rock units are not arranged chronologically.
-  Geological boundary (defined, approximate, assumed)
-  Schistosity, gneissosity, foliation (defined, dip known, dip vertical; assumed)
-  Lineation (plunge known)
-  Extreme contortion (structural trend)
-  Tight folds (structural trend)
-  Fault (defined, approximate, assumed)
-  Shear
-  Breccia
-  Mylonite
-  Quartz vein
-  Joint (dip known, unknown)
-  Sample location
-  Glacial striae (direction of ice movement known)
-  Radioactivity
-  Garnet
-  Chlorite, abundant
-  Epidote, abundant
-  Hornblende
-  Graphite
-  Magnetite

Geology by John D. Godfrey, 1959, 1960; Bayonet Lake District.
Geology by John D. Godfrey, and Roy Y. Watanabe, 1960, 1961; Charles Lake North District.
Drainage (permanent, intermittent)
Mudflow
Sand-covered area
Sand- and boulder-covered area
Provincial boundary
Township boundary
Section line
Cabin

Base maps compiled from planimetric sheets 74¹⁴ NW and 74¹⁵ NE published by Government of Alberta, Department of Lands and Forests, Edmonton.
Air photographs covering this area are obtainable from the Technical Division, Department of Lands and Forests, Government of Alberta, Edmonton, and the National Air Photographic Library, Topographical Survey, Ottawa.
Approximate magnetic declination 25° 40' East in 1965, decreasing 6' annually.



MAP 65-6B
CHARLES LAKE, NORTH DISTRICT
WEST OF FOURTH MERIDIAN
Scale: Two Inches to One Mile



MAP 65-6A
BAYONET LAKE DISTRICT
WEST OF FOURTH MERIDIAN
Scale: Two Inches to One Mile



LEGEND

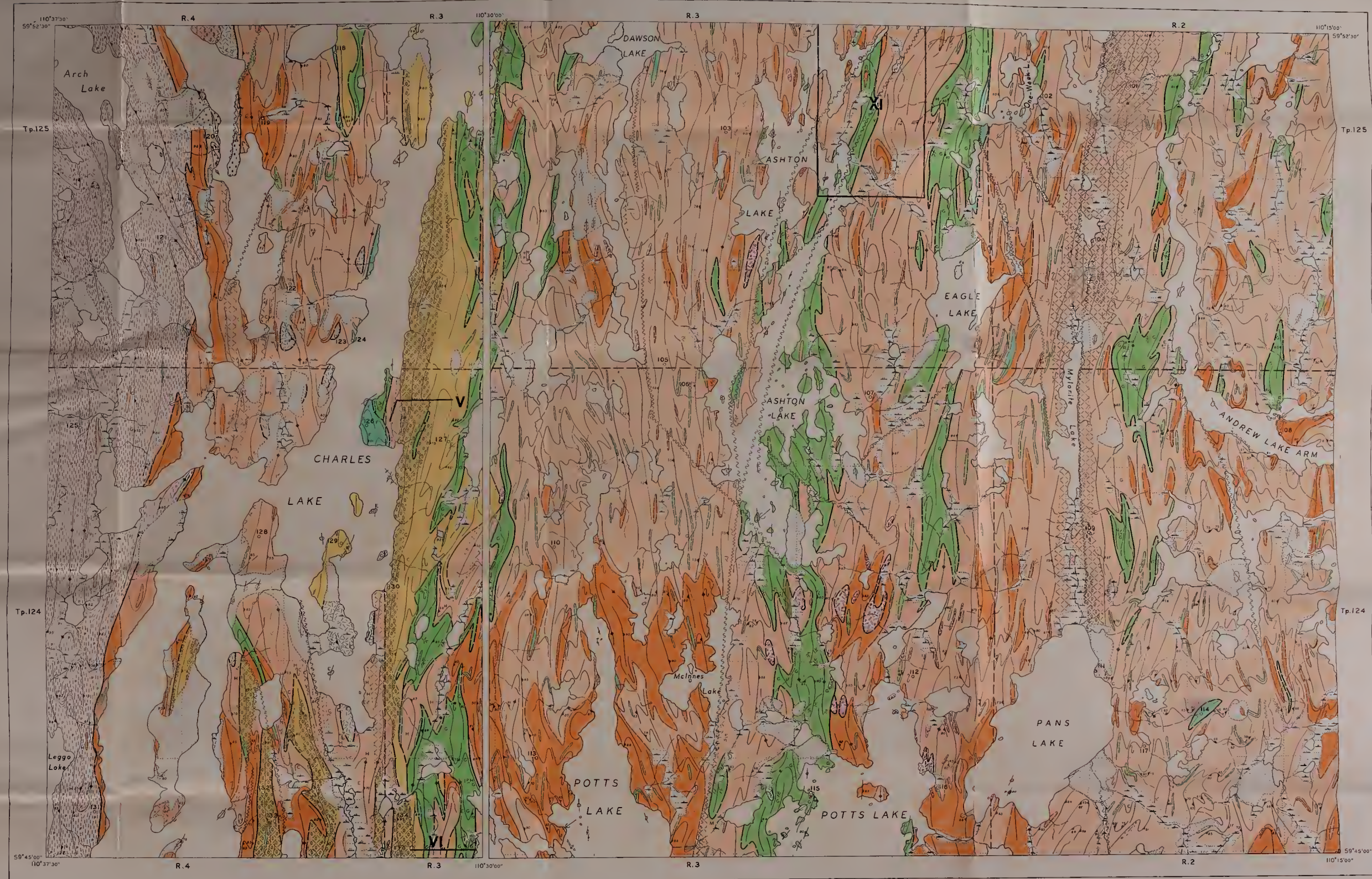
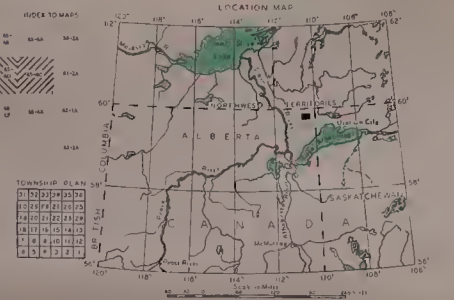
- PRECAMBRIAN***
- Quartzite, pure and impure, white, grey, green, pink and blue, including biotite, sericite, schist, minor milky quartz, pods, feldspar, augen, garnet and pegmatite lenses, ferruginous and garnetiferous zones.
 - Biotite schist, with abundant quartz, some sericite, including phyllite, phyllonite, quartzite, minor milky quartz, pods, feldspar, augen, garnet and pegmatite lenses, ferruginous and garnetiferous zones.
 - Biotite granite F, with white to grey subhedral to euhedral feldspar megacrysts, up to four inches in size, averaging two inches, in a coarse-grained, massive matrix of quartz, feldspar and biotite, including minor apite and pegmatite.
 - Biotite granite gneiss, with some hornblende, chlorite, megacrystic feldspar phases, including minor massive to foliated granite - some megacrystic, granoblastic, alkali, leucite of biotite, quartz, amphibolite, garnetiferous zones.
 - Hornblende granite gneiss, with some biotite, chlorite, megacrystic feldspar phases, including minor massive to foliated granite - some megacrystic, granoblastic and amphibolite.
 - Amphibolite, including biotite amphibolite, hornblende, mainly massive, little banded. Feldspar - rich type F.
 - Biotite 'q' granite, with white to pink to red abundant feldspar megacrysts one-half to one inch in size, minor crystals in medium-grained, massive to foliated matrix of biotite, feldspar and quartz.
 - Arch Lake granite, with white to pink subhedral elongate feldspar megacrysts from one-half to one inch in size subparallel aligned, in a medium-grained, streaky to foliated matrix of blue quartz, biotite and feldspar.
 - Leucocratic granite, with pink to red anhedral feldspars, equigranular; massive, locally foliated, including minor microgranite and pegmatite.
 - Granitic material, biotite- and muscovite-granite and pegmatite, some leucocratic phases, intermixed with host rock, typically massive, generally equigranular.
 - Grey hornblende granite, buff to grey, with dark specks of hornblende and local feldspar porphyroclasts from one-quarter to one-half inch in size in a quartz-feldspar matrix, texture fine to medium grained, massive to slightly foliated. Locally mixed with and gradational to recrystallized porphyroclastic hornblende cataclastic.
 - Recrystallized porphyroclastic hornblende cataclastic, light greyish-green, with hornblende porphyroclasts up to one-half inch in size, and local feldspar porphyroclasts from one-half to three-quarters inch in size, in a crushed, foliated, fine-grained matrix, some radiating banding. Locally mixed with and transitional to minor grey hornblende granite.
 - Recrystallized mylonite K, light colored, with minor white to pink feldspar porphyroclasts, one-quarter to three-quarters inch in size, constituting up to 2 per cent of rock, in a foliated, finely banded, aphanitic matrix, including recrystallized mylonites L, M, N, and O.
 - Recrystallized mylonite L, light colored, with white to pink feldspar porphyroclasts, one-quarter to three-quarters inch in size, constituting about 5 per cent of rock, in a foliated, finely banded, aphanitic matrix, including recrystallized mylonites K, M, N, and O.
 - Recrystallized mylonite P, dark colored, with white to grey anhedral porphyroclasts and euhedral feldspar porphyroclasts, one-half to two inches in size, foliated, locally gneissic, in an anhydrous, locally medium-grained, matrix, including minor apite and pegmatite.

*Note: Rock units are not arranged chronologically.

- Geological boundary (defined, approximate) ————
Schistosity, gneissosity, foliation (defined, dip known, dip vertical; assumed) ————
Extreme contortion (structural trend) ————
Tight folds (structural trend) ————
Fault (defined, approximate, assumed) ————
Shear ————
Breccia ————
Mylonite ————
Joint (dip known, vertical, unknown) ————
Sample location ————
Glacial striae (direction of ice movement known) ————
Mineral occurrence (molybdenite) ————
Radioactivity ————
Carnet ————
Chlorite, abundant ————
Epidote, abundant ————
Hornblende ————
Graphite ————
Magnetite ————

- Geology by John D. Godfrey, 1958, 1960, 1961; Ashton Lake District.
Geology by John D. Godfrey and Roy Y. Watanabe, 1961; Charles Lake Central District.
Drainage (permanent, intermittent) ————
Muskeg ————
Sand-covered area ————
Sand- and boulder-covered area ————
Township boundary ————
Section line ————

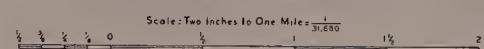
Base maps compiled from planimetric sheets 74M₁₆W and 74M₁₅E, published by Government of Alberta, Department of Lands and Forests, Edmonton.
Air photographs covering this area are obtainable from the Technical Division, Department of Lands and Forests, Government of Alberta, Edmonton, and the National Air Photographic Library, Topographical Survey, Ottawa.
Approximate magnetic declination 25° 40' East in 1965, decreasing 6' annually.



Maps to Accompany Preliminary Report 65-6

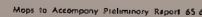
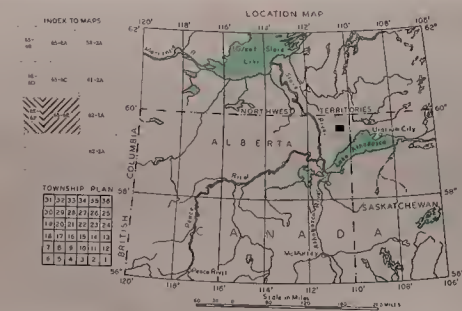
Published 1966

MAP 65-6D
CHARLES LAKE, CENTRAL
WEST OF FOURTH MERIDIAN



MAP 65-6C
ASHTON LAKE DISTRICT
WEST OF FOURTH MERIDIAN





Scale: Two Inches to One Mile = $\frac{1}{31,680}$

Scale: Two Inches to One Mile: $\frac{1}{31.680}$

/ University of Alberta Library



0 1620 1066 9677

B29850